LBL-24359 c.2

Lawrence Berkeley Laboratory
UNIVERSITY OF CALIFORNIA

Materials & Chemical Sciences Division

LAWRENCE
BERKELEY LABORATORY

FEB 1 1988

LIBRARY AND
DOCUMENTS SECTION

Reactive Intermediates in Organometallic Chemistry

P.O. Stoutland
(Ph.D. Thesis)

August 1987

TWO-WEEK LOAN COPY

This is a Library Circulating Copy which may be borrowed for two weeks.

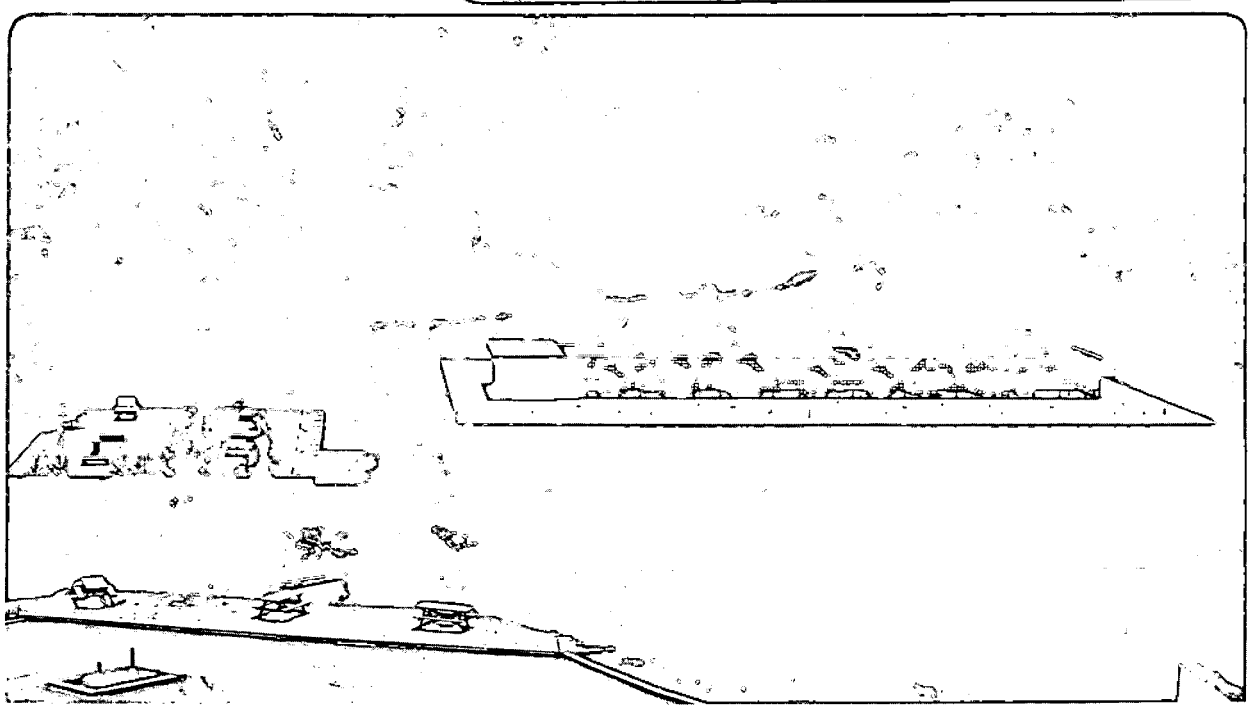

LBL-24359 c.2

Prepared for the U.S. Department of Energy under Contract DE-AC03-76SF00098

DISCLAIMER

This document was prepared as an account of work sponsored by the United States Government. While this document is believed to contain correct information, neither the United States Government nor any agency thereof, nor the Regents of the University of California, nor any of their employees, makes any warranty, express or implied, or assumes any legal responsibility for the accuracy, completeness, or usefulness of any information, apparatus, product, or process disclosed, or represents that its use would not infringe privately owned rights. Reference herein to any specific commercial product, process, or service by its trade name, trademark, manufacturer, or otherwise, does not necessarily constitute or imply its endorsement, recommendation, or favoring by the United States Government or any agency thereof, or the Regents of the University of California. The views and opinions of authors expressed herein do not necessarily state or reflect those of the United States Government or any agency thereof or the Regents of the University of California.

Reactive Intermediates in Organometallic Chemistry

Page Oliver Stoutland

Ph.D. Thesis

Lawrence Berkeley Laboratory
University of California
Berkeley, California 94720

August 1987

This work was supported by the U.S. Department of Energy
under Contract Number DE-AC03-76SF00098.

Reactive Intermediates in Organometallic Chemistry

Page Oliver Stoutland

Abstract

Chapter 1. Experiments involving (η^5-Me_5C_5)(PMe_3)Ir(R)(H) from which thermodynamic information has been obtained are discussed. Included in the discussion are kinetic experiments which placed as upper limit on the sum of the Ir-C_6H_{11} and Ir-H bond dissociation enthalpies (BDE's), an equilibrium study which provided estimates for relative Ir-C BDE's (R = C_6H_{11}, C_5H_{11}, C_5H_9, $CH_2C(CH_3)_3$, $CH_2CH(CH_3)CH(CH_3)_2$), and calorimetric experiments which allowed determination of relative Ir-X bond dissociation enthalpies for a series of ligands (R = H, C_6H_5, C_6H_{11}, $CHCH_2$, and CH_3).

Chapter 2. Thermolysis of (η^5-Me_5C_5)(PMe_3)Ir(C_6H_{11})(H) at 130 - 160°C in cyclohexane in the presence of ethylene results in formation of (η^5-Me_5C_5)(PMe_3)Ir(HC=CH_2)(H) **1**, and (η^5-Me_5C_5)(PMe_3)Ir(H_2C=CH_2) **2** in a ratio of 2:1. Thermolysis of **1** in cyclohexane or benzene above 180°C results in quantitative conversion to **2**. Thermolysis of (η^5-Me_5C_5)(PMe_3)Ir(C_6H_{11})(H) in the presence of ethylene-d_2 results in insertion into both the C-H and the C-D bonds, and allows determination of an intramolecular isotope effect: $k_H/k_D = 1.18 \pm 0.03$. Competition experiments involving ethylene and ethylene-d_4 allows determination of an intermolecular isotope effect for insertion into a C-H(D) bond: $k_H/k_D = 1.49 \pm 0.08$. The isotope effect for formation of **2** was found to be 0.82 ± 0.05. The different intra and intermolecular isotope effects require an intermediate on the reaction pathway leading to **1**.

Chapter 3. Thermolysis or irradiation of (η^5-Me_5C_5)(PMe_3)Ir(R)(H) (R = C_6H_5, C_6H_{11}, H, C_5H_{11}, $CHCH_2$, CH_3) in the presence of acetylene results in insertion of acetylene into the Ir-H bond and formation of (η^5-Me_5C_5)(PMe_3)Ir(R)(HC=CH_2). Chemical oxidation of (η^5-Me_5C_5)(PMe_3)Ir(R)(HC=CH_2) (R = C_6H_5 and $CHCH_2$) results

in reductive elimination of $RHC{=}CH_2$ and formation of $[(\eta^5\text{-}Me_5C_5)(PMe_3)Ir(NCCH_3)_2][X]_2$. Electrochemical experiments were conducted in an attempt to understand the sensitivity of the reductive elimination reactions to the R group on the metal.

Chapter 4. Flash photolysis of several metal carbonyl species ($CpMn(CO)_3$, $CpRe(CO)_3$, $W(CO)_6$, $Cp(CO)_2Re(CH_3)_2$, $Mn(NO)(CO)_4$) results in production of unsaturated, highly reactive species. The use of time resolved infrared spectroscopy allowed observation of those having lifetimes of 500 ns or greater.

Acknowledgements

It is now time to thank the many wonderful people with whom I have had the pleasure of working over the last several years. First, I wish to thank all of my friends at St. Olaf College. If it were not for the enthusiasm of the St. Olaf Chemistry Department, I might have pursued something else. I am particularly grateful to Prof. Gary L. Miessler, my undergraduate advisor, for giving me the freedom to pursue my interests, even when I was inexperienced.

Here at Berkeley, I am indebted to my graduate advisor Robert G. Bergman for allowing me to follow my interests, and for providing an example of a fine scientist. I am particularly thankful that he allowed me to spend my last year here doing something neither of us knew too much about: time resolved infrared spectroscopy.

The Bergman Group is fortunate to have many talented students and post doctoral associates; I wish to thank them collectively for stimulating discussions in the lab, and for diversions outside of lab. I would especially like to acknowledge Jeff Hayes for teaching me the techniques of organometallic chemistry, and Eric Wasserman who was particularly patient in explaining physical chemistry to me. For diversions outside of the lab, I wish to thank Colin Schaverien and Eric Jacobsen (for showing me how to nearly die mountain climbing), and John Freudenberger (for showing me how to have a successful mountain climbing trip).

Finally, I wish to thank my wife Sue Rossi for always being encouraging, and for being such a joy to be with. Thank you for everything. It is to her that this Thesis is dedicated.

Abbreviations

[Ir]	$(\eta^5\text{-}Me_5C_5)(PMe_3)Ir$
BDE	bond dissociation enthalpy
bipy	bipyridine
br	broad (NMR)
d	doublet (NMR)
dmpe	dimethylphosphinoethane
dppe	diphenylphosphinoethane
hv	light
IR	infrared spectroscopy
m	multiplet (NMR), medium intensity (IR)
MS	mass spectroscopy
NMR	nuclear magnetic resonance spectroscopy
ppm	parts per million
py	pyridine
R	alkyl or aryl group
S	solvent
s	singlet (NMR), strong intensity (IR)
saloph	N,N'-disalicylidene-o-phenylenediamine
THF	tetrahydrofuran
TRIR	time resolved infrared spectroscopy
w	weak intensity (IR)

Table of Contents

Chapter 1 The Thermodynamic Driving Force for C-H Activation at Iridium 1

Introduction 2

Thermodynamics of C-H activation/functionalization 3

Metal-Carbon and Metal-Hydrogen Bond Strengths 9

Ir-X BDE's for $Cp^*(PMe_3)IrX_2$ 11

Predictions Of Reactivity 20

The Origin of Metal-Carbon and Metal-Hydrogen Bond Strengths 22

Conclusion 27

Experimental 28

References 29

Chapter 2 Activation of Ethylene by Iridium: Inter and Intramolecular Isotope Effects 33

Introduction 34

Activation of Ethylene 37

Thermolysis of $(\eta^5\text{-}Me_5C_5)(PMe_3)Ir(HC{=}CH_2)(H)$ 40

Irradiation of $(\eta^5\text{-}Me_5C_5)(PMe_3)Ir(H_2C{=}CH_2)$ 47

Synthesis and Structure 47

Intermolecular Isotope Effects 53

Intramolecular Isotope effects 60

Discussion of Isotope Effects 65

Comparison of Inter- and Intramolecular Isotope Effects 66

The Nature of the Intermediate 75

Conclusions 79

Experimental 87

General 87

Thermolysis of $(\eta^5\text{-}Me_5C_5)(PMe_3)Ir(HC{=}CH_2)(H)$ 89

Photolysis of (η^5-Me_5C_5)(PMe_3)Ir(H_2C=CH_2). 90

Intermolecular Isotope Effects. 90

Intramolecular Isotope Effects. 91

Relative Solubilities of Ethylene and Ethylene-d_4. 92

(η^5-Me_5C_5)(PMe_3)Ir(HC=CH_2)(Br). 93

(η^5-Me_5C_5)(PMe_3)Ir(HC=CH_2)(H). 94

X-ray Data Collection 94

References 99

Chapter 3 Stoichiometric Functionalization of Benzene and Ethylene: Attempts to Understand Potential Alkane Functionalization Processes 103

Introduction. 104

Insertion reactions. 106

Independent syntheses. 109

Other acetylenes and metal complexes. 111

Discussion of insertion reactions. 111

Reductive elimination of H_2C=CHR 120

Thermolysis. 120

Chemical oxidation. 125

Electrochemical oxidation. 130

Discussion 132

Experimental. 136

General. 136

Insertion reactions. 138

Crossover experiment 138

Thermolysis of (η^5-Me_5C_5)(PMe_3)Ir(C_6H_5)($HCCH_2$). 138

Thermolysis of other (η^5-Me_5C_5)(PMe_3)Ir(R)($HCCH_2$) compounds. 139

Oxidation of (η^5-Me_5C_5)(PMe_3)Ir(C_6H_5)($HCCH_2$) 139

Oxidation of (η^5-Me_5C_5)(PMe_3)Ir($HC{=}CH_2$)$_2$ 140

Oxidation of (η^5-Me_5C_5)(PMe_3)Ir(n-C_5H_{11})($CHCH_2$) 140

Electrochemistry 141

Independent synthesis and characterization 141

(η^5-Me_5C_5)(PMe_3)Ir($HC{=}CH_2$)$_2$ 141

(η^5-Me_5C_5)(PMe_3)Ir(C_6H_5)($HCCH_2$) 142

[(η^5-Me_5C_5)(PMe_3)Ir($NCCH_3$)$_2$][PF_6]$_2$ 142

(η^5-Me_5C_5)(PMe_3)Ir(CH_3)($HCCH_2$) 143

(η^5-Me_5C_5)(PMe_3)Ir(n-C_5H_{11})($HCCH_2$) 143

References 145

Chapter 4 Study of Organometallic Transients by Time-Resolved Infrared Spectroscopy: An Exploratory Study 148

Introduction 149

Matrix techniques 149

Flash photolysis in solution 150

Fast infrared and Raman techniques 151

Experimental Setup 154

UV light source 155

Infrared sources 157

Principles of operation 157

Detectors 158

Experimental procedure 159

Solution handling 160

Results 163

Background: Relative stabilities of S-M(CO)$_n$ 163

$CpMn(CO)_3$ 165

$CpRe(CO)_3$ 173

$W(CO)_6$ 173

Study of $Cp(CO)_2Re(CH_3)_2$ 177

Study of $Mn(NO)(CO)_4$ 184

Conclusion 196

Experimental 197

References 198

Tables

Table 1.1 Enthalpies for selected insertion reactions (kcal/mol) 8

Table 1.2 Selected first row metal-carbon bond dissociation enthalpies..... 9

Table 1.3 Selected metal-carbon and metal-hydrogen bond dissociation enthalpies for third row transition metals and actinides..... 10

Table 1.4 Relative Ir-X bond dissociation enthalpies for $(PMe_3)_2(CO)Ir(Cl)(I)(X)$..... 12

Table 1.5 Relative Iridium-Carbon BDE's in $(\eta^5\text{-}Me_5C_5)(PMe_3)Ir(R)(H)$..... 13

Table 1.6 Ir-X bond dissociation enthalpies for $(\eta^5\text{-}Me_5C_5)(PMe_3)Ir(X)_2$..... 19

Table 1.7 Enthalpies for selected reductive elimination/oxidative addition reactions..... 21

Table 1.8 Calculated enthalpies of oxidative addition for selected species to "$(\eta^5\text{-}Me_5C_5)(PMe_3)Ir$"..... 22

Table 2.1 Selected Intramolecular Bond Distances (A) and esd's for $(\eta^5\text{-}Me_5C_5)(PMe_3)Ir(HC{=}CH_2)(H)$ **1** 52

Table 2.2 Selected Intramolecular Bond Angles for **1**..... 53

Table 2.3 Table of Torsional Angles for **1**..... 53

Table 2.4 Intramolecular isotope effects for formation of **1**..... 65

Table 2.5 A summary of the individual isotope effect for Mechanisms A and B..... 75

Table 2.6 Intermolecular isotope effect data..... 91

Table 2.7 Crystal and Data Collection Parameters for **1**..... 97

Table 2.8 Positional Parameters and Their Estimated Standard Deviations..... 98

Table 3.1 Enthalpies for $[Ir](R)(CHCH_2) + C_6H_6$ ----> $[Ir](Ph)(H) + RHC{=}CH_2$..... 124

Table 3.2 Electrochemical Potentials of $[Ir](R)(CHCH_2)$..... 132

Table 4.1 Rates of reaction of $CpMn(CO)_2(S)$ with P-nBu_3 in selected solvents..... 172

Table 4.2 Selected rate constants for the flash photolysis of $Mn(NO)(CO)_4$ with $P(C_6H_{11})_3$..... 191

Table of Figures

Figure 1.1 Reaction coordinate diagram for the reductive elimination of RH from $(\eta^5\text{-}Me_5C_5)(PMe_3)Ir(R)(H)$ 16

Figure 1.2 Plot of Ir-X bond dissociation enthalpies in $(\eta^5\text{-}Me_5C_5)(PMe_3)Ir(X)(H)$ vs. the respective hydrogen carbon BDE's 20

Figure 2.1 First order kinetic plot of the thermolysis of $(\eta^5\text{-}Me_5C_5)(PMe_3)Ir(HC{=}CH_2)(H)$ in C_6D_{12} at 185°C 45

Figure 2.2 Plot of ln(k/T) vs 1/T for the thermolysis of the the vinyl complex **1** in cyclohexane-d_{12} at five temperatures between 180 and 220°C 46

Figure 2.3 Molecular geometry and labeling for $(\eta^5\text{-}Me_5C_5)(PMe_3)Ir(HC{=}CH_2)(H)$ **1** 50

Figure 2.4 Molecular geometry and labeling for $(\eta^5\text{-}Me_5C_5)(PMe_3)Ir(HC{=}CH_2)(H)$ **1** 51

Figure 2.5 ^{31}P NMR of the reaction mixture resulting from thermolysis of $(\eta^5\text{-}Me_5C_5)(PMe_3)Ir(C_6H_{11})(H)$ in the presence of $H_2C{=}CH_2$ and C_6H_6 56

Figure 2.6 ^{31}P NMR of the reaction mixture resulting from thermolysis of $(\eta^5\text{-}Me_5C_5)(PMe_3)Ir(C_6H_{11})(H)$ in the presence of $D_2C{=}CD_2$ and C_6H_6 57

Figure 2.7 Apparatus used to measure the relative solubilities of $H_2C{=}CH_2$ and $D_2C{=}CD_2$ 61

Figure 2.8 The vinyl region of the ^2H NMR of a reaction mixture resulting from the thermolysis of $(\eta^5\text{-}Me_5C_5)(PMe_3)Ir(C_6H_{11})(H)$ in the presence of ethylene-1,1-d_2 63

Figure 2.9 Proposed approximate reaction coordinate diagram for the reaction of "$(\eta^5\text{-}Me_5C_5)(PMe_3)Ir$" with ethylene, and the conversion of **1** to **2** 76

Figure 2.10 Possible structures for the intermediate on the pathway leading to C-H bond insertion 78

Figure 3.1 Apparatus used to add acetylene to NMR tubes 137

Figure 4.1 Schematic of experimental setup 156

Figure 4.2 A selected kinetic trace showing the temporal behavior of a signal due to $W(CO)_5(S)$ produced by the laser pulse to 50μs 161

Figure 4.3 A selected transient spectrum taken at 8 μs after the flash photolysis of $CpMn(CO)_3$ in cyclohexane 162

Figure 4.4 Kinetic trace taken at 1959 cm^{-1} showing the temporal behavior to 200 µs of $CpMn(CO)_2(S)$ in a 3 x 10^{-3} M solution of P-*n*Bu_3 in cyclohexane 166

Figure 4.5 Kinetic trace at 1907 cm^{-1} showing the appearance of a new product (rate = 6.1 x 10^3 s^{-1}) over 200 µs. This is thought to be $CpMn(CO)_2$(P-*n*Bu_3) formed upon reaction of $CpMn(CO)_2(S)$ with P-*n*Bu_3 167

Figure 4.6 Spectra assembled at 8, 72, and 152 µs after the laser pulse showing the reaction of $CpMn(CO)_2(S)$ with P-*n*Bu_3 168

Figure 4.7 Comparison of the rates of reaction of $Cp(CO)_2Mn(S)$ with P-*n*Bu_3 in cyclohexane and in hexane 172

Figure 4.8 A kinetic trace taken at 1955 cm^{-1} showing the temporal behavior of a transient produced upon flash photolysis of $W(CO)_6$ in the presence of 0.005 M P-*n*Bu_3 174

Figure 4.9 A kinetic trace taken at 1921 cm^{-1} showing the appearance of a new band over 50 µs in the flash photolysis of $W(CO)_6$ in the presence of 0.005 M P-*n*Bu_3 175

Figure 4.10 Comparison of the rates of reaction of $W(CO)_5(S)$ with P-*n*Bu_3 and with $P(C_6H_{11})_3$ in cyclohexane 176

Figure 4.11 A kinetic trace taken at 1888 cm^{-1} showing the temporal behavior to 50 µs after the photolysis of $CpRe(CO)_2(CH_3)_2$ in cyclohexane 180

Figure 4.12 A kinetic trace taken at 1981 cm^{-1} showing the temporal behavior to 50 µs after the photolysis of $CpRe(CO)_2(CH_3)_2$ in cyclohexane 181

Figure 4.13 A kinetic trace taken at 1903 cm^{-1} showing the temporal behavior to 50 µs after the photolysis of $CpRe(CO)_2(CH_3)_2$ in cyclohexane 182

Figure 4.14 Spectra assembled at 4, 12, and 36 µs after the laser pulse of $CpRe(CO)_2(CH_3)_2$ in cyclohexane 183

Figure 4.15 Spectra assembled at 5, 10, and 20 µs after the laser pulse of $CpRe(CO)_2(CH_3)_2$ in a cyclohexane solution 9.3 x 10^{-3} M in $P(C_6H_{11})_3$ 185

Figure 4.16 Spectra assembled at 1 and 2 µs after the laser pulse of $CpRe(CO)_2(CH_3)_2$ in a cyclohexane solution 8.0 x 10^{-3} M in P-*n*Bu_3 186

Figure 4.17 Kinetic trace at 1951 cm^{-1} over 100 µs of a transient resulting from flash photolysis of $Mn(NO)(CO)_4$ 189

Figure 4.18 Spectra assembled at 5, 20, and 45 µs after the laser pulse of $Mn(NO)(CO)_4$ in cyclohexane 190

Figure 4.19 A spectrum assembled at 5 µs after the laser pulse of $Mn(NO)(CO)_4$ in a 3 x 10^{-3} M solution of $P(C_6H_{11})_3$ in cyclohexane 192

Figure 4.20 A kinetic trace taken at 1951 cm^{-1} showing the temporal behavior of a transient produced upon flash photolysis of $Mn(NO)(CO)_4$ in the presence of 1.4×10^{-3} M $P(C_6H_{11})_3$ 193

Figure 4.21 A kinetic trace taken at 1907 cm^{-1} showing the appearance of a new band over 10 μs in the flash photolysis of $Mn(NO)(CO)_4$ in the presence of 1.4×10^{-3} M $P(C_6H_{11})_3$ 194

Figure 4.22 Spectra assembled at 0.4, 2.8, and 7.6 μs after the laser pulse of $Mn(NO)(CO)_4$ in a 1.4×10^{-3} M solution of $P(C_6H_{11})_3$ in cyclohexane 195

Chapter 1

The Thermodynamic Driving Force for C-H Activation at Iridium

Introduction

Catalytic, selective functionalization of hydrocarbons has been one of the enduring goals of chemistry. While we may still be years from realizing this goal, recently we have witnessed a blossoming of exploration in this field from which many important results have emerged.[1] This goal of hydrocarbon functionalization consists of two fundamental problems, that of activation or bonding to the hydrocarbon, and that of functionalization once it has been activated. Of course central to both problems is the necessity for selectivity.

Non-selective functionalization of alkanes has, of course, been known for quite some time. Not all of these processes require the use of a transition metal , and many have been shown to have free radical mechanisms (e.g. photochlorination, autoxidation).[2] In addition to requiring harsh conditions, they typically suffer from a lack of selectivity. It has been the hope of chemists that the use of transition metal complexes might allow activation to proceed under mild conditions, as well as providing the necessary selectivity. The first attempts at using metals to functionalize alkanes, were mildly successful but left much to be desired in the areas of selectivity and efficiency.[3] These difficulties led chemists to concentrate on stoichiometric reactions between hydrocarbons and transition metals; it is this approach which has proven most fruitful in recent years.

At the outset, however, it was not clear that this approach was the proper one. For while no one doubted that the overall thermodynamics for many possible alkane functionalization processes were favorable, many believed that a possible intermediate in any functionalization scheme, a cis-transition metal alkyl hydride, would not be isolable due to some intrinsic weakness of the metal-carbon and metal-hydrogen bonds. This belief was not unfounded, for at the time the few known cis-alkyl hydrides reductively eliminated alkane at low temperatures.[4]

In the last twenty years however, and particularly the last five, tremendous advances have been made in the area of C-H bond activation. Today, there are numerous

examples of transition metal fragments that will insert intermolecularly into the C-H bonds of hydrocarbons forming stable cis-alkyl hydrides. This has raised the hopes for functionalization of alkanes in at least a stoichiometric manner from the alkyl hydrides, perhaps by using insertion reactions followed by reductive elimination.

Fundamental to this questions of C-H activation and functionalization is the knowledge of the strength of the metal-carbon and the metal-hydrogen bonds, the driving force for C-H bond activation. Very little is known about such bond strengths,[5] but clearly systems capable of C-H activation are special in this regard. It is this uniqueness which has spurred our interest in these systems.

Thermodynamics of C-H activation/functionalization

The isolation of stable alkyl hydrides resulting from C-H insertion reactions is significant because such insertions constitute the first step in simple functionalization cycles (e.g., Scheme 1.1). The latter steps, insertion and reductive elimination, are well precedented in organometallic chemistry.[6] Limited homogeneous catalytic functionalization of hydrocarbons has been achieved using organometallic complexes, and may or may not require the intermediacy of alkyl hydrides.[7] For example, several polyhydrides have been shown to convert alkanes into alkenes in the presence of a hydrogen atom acceptors (Scheme 1.2).[8] Aromatic hydrocarbons appear to be easier to functionalize (presumably because they are easier to activate). In this area several reports of functionalization have appeared (Scheme 1.3 - 1.4).[9] Unfortunately, these appear to be special cases and will not be suitable for hydrocarbons such as methane.[10]

Consider the general C-H activation and functionalization sequence in Scheme 1.1 which would be suitable for a wide variety of hydrocarbons substrates. If such a sequence is to be successful, each step must have a free energy close to, or less than, zero. For the first step, this means that the sum of the M-C and M-H bond dissociation energies must be greater than or comparable to the strength of the carbon hydrogen bond being broken.

Scheme 1.1

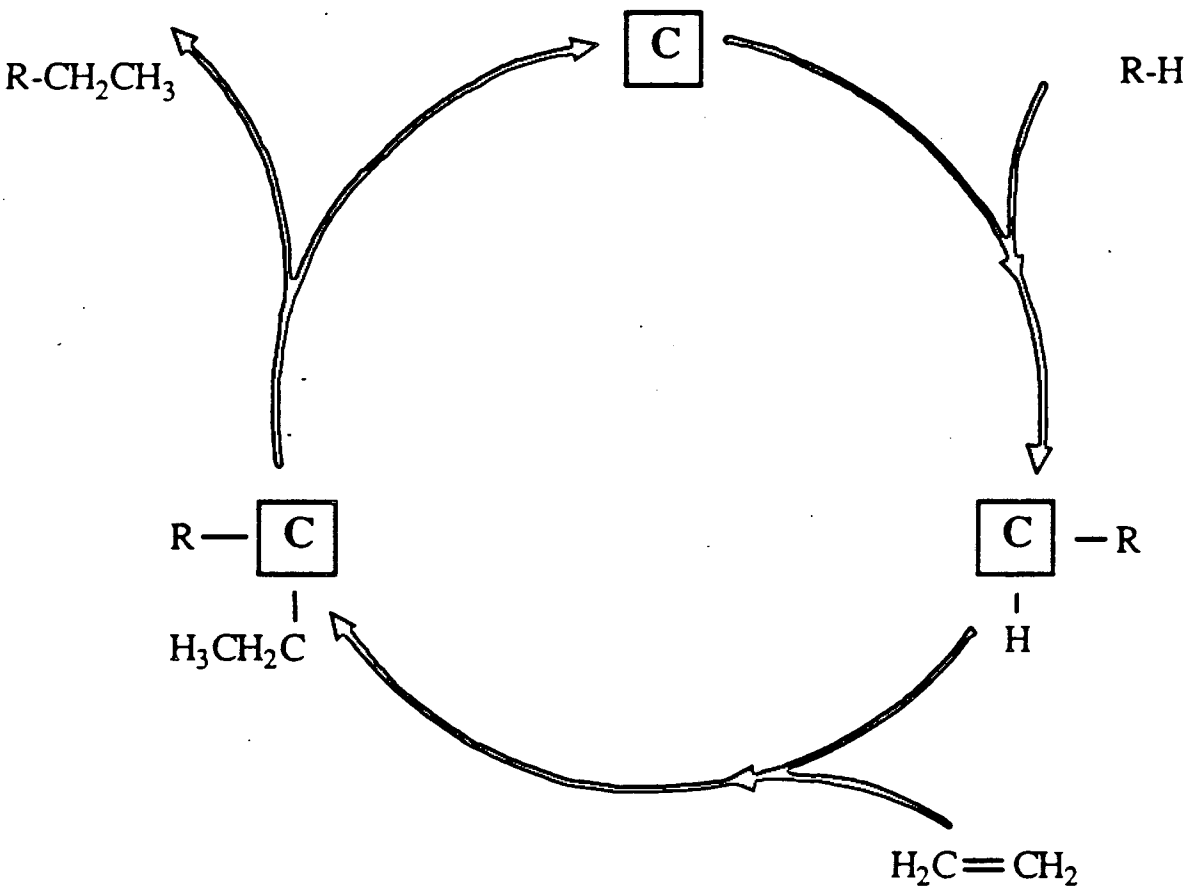

Scheme 1.2

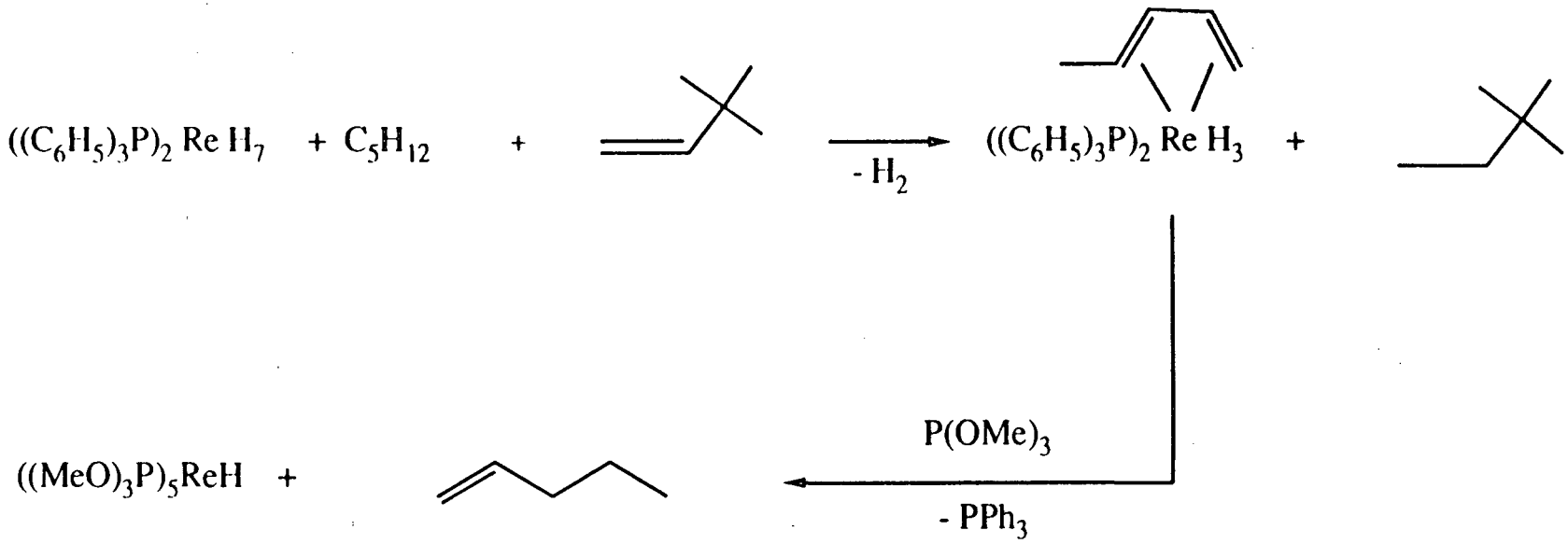

Scheme 1.3

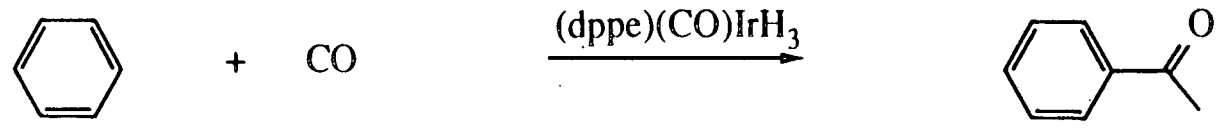

Scheme 1.4

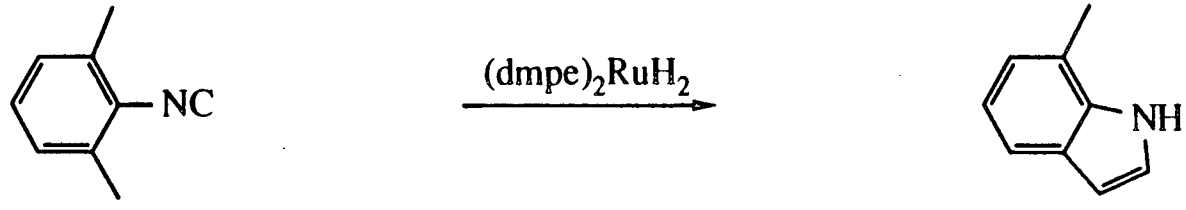

Furthermore, for reactions such as those shown the entropy of activation (ΔS) at room temperature can be estimated to be close to -30 e.u. This leads to a $T\Delta S$ contribution to $\Delta G_{reaction}$ of approximately 9 kcal/mol at 25 °C.[11] Thus with typical C-H bond enthalpies on the order of 95-110 kcal/mol, the sum of the M-C and the M-H bond dissociation enthalpies must be greater than 104-119 kcal/mol for insertion to be thermodynamically favored.

For the second step, it is desirable that the reagent to be inserted into either the metal-carbon or the metal-hydrogen bond be one that would be amenable to large scale processes. Such a reagent should be inexpensive, abundant, and easy to handle; fitting these categories are simple olefins, acetylene, and carbon monoxide. The enthalpies of these insertion reactions can be approximated by starting with the known enthalpies of similar reactions.

For example, consider the insertion of ethylene into the M-H bond of an alkyl hydride. In order to estimate the enthalpy of the ethylene insertion reaction, one can start with the experimental enthalpy of ethylene hydrogenation (-32.3 kcal/mol) and then: (1) subtract the H-H BDE (104 kcal/mol), (2) add the C-H bond strength in ethane (98 kcal/mol), and finally (3) add the M-CH_2CH_3 BDE and subtract the M-H BDE (unknown), thus arriving at an estimate of the enthalpy of the insertion reaction. This type of analysis is expected to be reasonably accurate, except in cases where the metal affects the strengths of the bonds in the alkyl chain.

Scheme 1.5

$H_2C{=}CH_2 + H_2$	------->	$H_3C\text{-}CH_3$ (ΔH = -32.3 kcal/mol)
$H\cdot + \cdot H$	------->	H_2 (ΔH = -104 kcal/mol)
$H_3C\text{-}CH_3$	------->	$H_3C\text{-}CH_2\cdot + \cdot H$ (ΔH = 98 kcal/mol)
$\cdot M(R)$	------->	$\cdot M + R\cdot$ ($\Delta H = D_{M\text{-}R}$)
$M(R)(H)$	------->	$\cdot M(R) + H\cdot$ ($\Delta H = D_{M\text{-}H}$)
$M(R)(H) + H_2C{=}CH_2$	------->	$M(CH_2CH_3)(R)$ ($\Delta H_{insertion}$)

In this case, $\Delta H_{insertion} = D_{(M-C)} - D_{(M-H)} - 38.3$ kcal/mol. Estimates for the heats of this and two other insertion reactions are given in Table 1.1.

Table 1.1. Enthalpies for selected insertion reactions (kcal/mol)

Reagent	ΔH (insertion into M-H bond)	ΔH (insertion into M-R bond)
CO	$D_{(M-H)} - D_{(M-C=O)} - 15$	$D_{(M-C)} - D_{(M-C=O)} - 10$
$H_2C=CH_2$	$D_{(M-H)} - D_{(M-C)} - 38$	-25
HCCH	$D_{(M-H)} - D_{(M-C=C)} - 44$	$D_{(M-C)} - D_{(M-C=C)} - 40$

From Table 1.1 it is apparent that all the insertion reactions are thermodynamically possible unless the M-H bond energy is much larger than the M-C bond energy. It is important to remember however, that $T\Delta S$ will contribute ca. 10 kcal/mol to $\Delta G_{reaction}$. Later we will return to the thermodynamics of such insertion reactions after considering the magnitudes of M-H and M-C bond dissociation energies.

The thermodynamics of the last step in such a functionalization scheme, reductive elimination, can also be estimated if metal-carbon and metal-hydrogen bond strengths are known. However, it is clear that such reactions will not be facile, as complexes which form stable alkyl hydrides will also form very stable dialkyls, alkyl acyls, and vinyl alkyls. There is thus the need to couple this step with one that is sufficiently exothermic so that the overall free energy of the reaction is close to zero. A particularly attractive couple is shown in the Scheme, again the knowledge of the metal-carbon and metal-hydrogen bond strengths are of the utmost importance in the evaluation of such a cycle. It is important to remember, however, that success of these reactions will also depend on the kinetic barriers involved.

Systems that are amenable to this are very special indeed. Note particularly the requirements for forming stable alkyl hydrides and the various insertion reactions. If one is to observe alkyl hydrides one must seek to maximize the strength of the metal-carbon and

the metal-hydrogen bonds; this however, lessens the propensity of the alkyl hydrides to undergo further reaction. Later we will try to understand what affects these bond strengths, and how modifications in the electronic and steric nature of the ligands can change them.

Metal-Carbon and Metal-Hydrogen Bond Strengths

Despite recent interest in determining M-C and M-H bond strengths, there is still a paucity of information, especially for metals of the second and third rows of the transition series. Somewhat more information is available on the strengths of bonds formed with first row transition metals. Halpern, for example, has extensively studied cobalt alkyl compounds similar in structure to Coenzyme B_{12}. For these complexes he has found that the metal-carbon bond strengths typically lie in the range of 18-25 kcal/mol. The steric requirements of the alkyl group are one of the most important factors controlling where in this range a particular bond dissociation energy may lie.[12] Connor has determined metal-carbon bond dissociation enthalpies for X-$Mn(CO)_5$.[13] The similarity of these BDE's is evident (Table 1.2). The available data on other first row organometallic compounds indicate that their metal-carbon bond dissociation enthalpies are also under 30 kca/mol.[14]

Table 1.2. Selected first row metal-carbon bond dissociation enthalpies.

ML_n	R	D_{Co-R} (kcal/mol)
[R-Co(saloph)(py)]	$CH_2C(CH_3)_3$	18
	$CH(CH_3)_2$	20
	$CH_2C_6H_5$	22
	$CH_2CH_2CH_3$	25
R-$Mn(CO)_5$	$CH_2C_6H_5$	29
	$(CO)CH_3$	39
	CH_3	44
	C_6H_5	49

Extensive information is now accumulating from experiments done in ICR spectrometers on the strength of metal-carbon and metal-hydrogen bonds in simple cationic metal hydrides and alkyls.[15] Although the transferability of these values to organometallic compounds in solution is at best tenuous, the relative metal-carbon bond strengths between a given metal and a variety of alkyl groups are certainly valuable. The strength of metal-hydrogen bonds appear to be similar to that found in solution, ranging from 35-60 kcal/mol. Metal-methyl bond strengths, however, are strengthened relative to the metal-hydrogen bond in the gas phase when the metal is positively charged. Even for first row metals, metal-methyl bond dissociation enthalpies are typically 60-70 kcal/mol. Metal alkyl bond strengths are also well known for a variety of homoleptic metal alkyls. Most of these, however, are average bond dissociation energies, and are of limited utility in predicting reactivity. These compounds typically have strong metal-carbon bonds ranging from slightly less than 80 kcal/mol for $Hf(CH_3)_4$ to 35 kcal/mol for $W(CH_3)_6$.[16]

Bond dissociation enthalpies for late, third row transition metal complexes appear to be much less well known. The available data, however, indicate that we may expect significantly stronger metal-carbon bonds than found for complexes of the first row metals. Summarized in Table 1.3 are metal-hydride and metal-carbon bond dissociation enthalpies for a variety of third row transition metals, as well as for the actinide element thorium.[17] Both the tungsten and the thorium compounds are capable of C-H bond activation.

Table 1.3. Selected metal-carbon and metal-hydrogen bond dissociation enthalpies for third row transition metals and actinides.

X	$(PMe_3)_2Cl(CO)Ir(I)(X)$	Cp_2WX_2	Cp^*ThX_2
H	60	72.9	97.5
CH_3	35.4	50.2	82.4
C_6H_5	--	--	90.6
C_6H_{11}	--	--	74.9

Information concerning the strength of the metal-hydrogen bond is more readily available, but is similarly sparse for the third row transition metals. Most of the information is for first row metals and indicates that metal-hydrogen bond strengths hover around 60 kcal/mol.[18] Studies of a wide variety of diatomic metal hydrides carried out in the gas phase show no convincing trends; few are over 60 kcal/mol, the notable exceptions being Au-H and Pt-H at 74 and 80 kcal/mol, respectively.[19] The few determinations of third row metal-hydrogen bond strengths support the belief that stronger bonds are formed to third row metals. For example, the Os-H bond strength in $H_2Os(CO)_4$ has been estimated to be 78 kcal/mol.[20] The metal-hydrogen BDE's of some other heavier transition metals are listed in Table 3, and are also significantly stronger than the 60 kcal/mol found for many first row metal hydrides.

Ir-X BDE's for $Cp^*(PMe_3)IrX_2$

We felt particularly frustrated by this lack of information concerning the strength of metal-carbon and metal-hydrogen bonds, as it increased the difficulty of rationally designing an alkane functionalization sequence using $(\eta^5\text{-}Me_5C_5)(PMe_3)Ir(R)(H)$. For large organometallic molecules such as those of interest to us, the determination of relative BDE's is much easier than the determination of absolute BDE's. Several techniques allow one to determine relative bond strengths accurately. For example, in the equilibrium technique, measuring the temperature dependence of the equilibrium constant allows determination of ΔH for the reaction. In simple equilibria such as that shown in Equation 1.1, $\Delta H_{reaction}$ is equal to the difference in the BDE's of M-X and M-Y.

$$L_n\text{-}M\text{-}X + Y \;\text{---->}\; L_n\text{-}M\text{-}Y + X \qquad (1.1)$$

The equilibrium method does suffer from several weaknesses. First, well behaved equilibria for many compounds do not exist; in others the strengths of the other bonds in

the molecule may change upon substitution of Y for X, masking the significance of ΔH. Even when complexes are amenable to such studies, it is only useful for reactions with limited K_{eq} values, meaning that only nearly thermoneutral reactions can be studied for reactions with small ΔS values. The only way one can obtain relative BDE's for ligands with significantly different BDE's is by using the "ladder" technique, where one measures a series of equilibrium constants.

Another way to determine relative bond strengths is by using calorimetry, a technique in which one measures relative ΔH values directly. This approach to determining relative BDE's typically consists of determining ΔH for reactions which differ by only a single ligand. The study by Yoneda and Blake[21] illustrated in Table 1.4 is an example of this. By measuring the enthalpy of the reaction shown in Equation 1.2,

$$(PMe_3)_2(CO)Ir(Cl) + XI \quad \text{---->} \quad (PMe_3)_2(CO)Ir(Cl)(X)(I) \qquad (1.2)$$

the relative Ir-X BDE's could be found knowing only the enthalpy of the reaction and the appropriate X-I BDE's. Using this technique, Yoneda and Blake were able to determine the relative bond dissociation enthalpies for a variety of metal-carbon bonds.

Table 1.4. Relative Ir-X bond dissociation enthalpies for $(PMe_3)_2(CO)Ir(Cl)(I)(X)$.

X	$D_{Ir-X} - D_{Ir-I}$
H	14
CH_3	0
$CH(CH_3)_2$	-7
$CH_2(C_6H_5)$	-17
$CO(CH_3)$	0

Our first attempt at understanding the factors controlling the strengths of the metal-carbon bonds in $(\eta^5\text{-}Me_5C_5)(PMe_3)Ir(R)(H)$ consisted of an equilibrium study. In these experiments an alkyl hydride was heated in mixtures of alkanes in varying proportions.

Observation of the final amounts of the two C-H insertion products, allowed us to determine equilibrium constants for reactions such as that shown in Equation 1.3.

$$Cp^*(PMe_3)Ir(C_6H_{11})(H) + C_5H_{12} \text{ -----> } Cp^*(PMe_3)Ir(C_5H_{11})(H) + C_6H_{12} \quad (1.3)$$

This in turn allowed calculation of ΔG^o for the reaction. Since the magnitudes of the C-H bond dissociation enthalpies in the hydrocarbons are known, the origin of $\Delta G_{reaction}$ lies entirely in the difference of the free energy contributions from the metal-carbon bonds.[22] Derivation of relative iridium-carbon bond dissociation enthalpies from the equilibrium constants (and thus $\Delta G^o_{reaction}$) requires separation of the enthalpic and entropic components of $\Delta G^o_{reaction}$. Normally this is done by measuring the temperature dependence of the equilibrium constant. In this case, however, the range of temperatures under which the reactions could be carried out would have led to large errors in ΔH^o values. We instead made the assumption that the $T\Delta S$ contribution to ΔG^o_{rxn} was close to zero.[23] The resulting relative iridium-carbon bond dissociation enthalpies are given in Table 1.5.

Table 1.5. Relative Iridium-Carbon BDE's in $(\eta^5\text{-}Me_5C_5)(PMe_3)Ir(R)(H)$.

Compound	$\Delta D_{Ir\text{-}C}$ (kcal/mol)
[Ir](neopentyl)	-4
[Ir](cyclohexyl)	0
[Ir](cyclopentyl)	0
[Ir](2,3-dimethylbutyl)	4
[Ir](pentyl)	6

In this case, the equilibrium method for determining relative bond strengths suffered from several weaknesses. For example, highly volatile hydrocarbons such as methane and ethane could not be used for practical reasons. Hydrocarbons with several types of C-H bond could not be used due to the difficulty in interpreting the resulting

mixtures of alkyl hydrides. Finally, the method we choose for analysis, ^{31}P NMR, is subject to uncertainties on the order of 5-10% and is not particularly sensitive, being useful only for reactions with K_{eq} values between 0.005 and 200. Despite these disadvantages, the qualitative trends are clear. Perhaps most striking is that the strongest iridium-carbon bonds were formed by breaking the strongest C-H bonds; also evident is the dependence on the steric requirements of the alkyl group.

Absolute bond dissociation enthalpies are typically much more difficult to determine experimentally than relative values. This is especially true for large organometallic molecules, as they are difficult to decompose in a clean manner to complexes for which we know the heats of formation. Alternative techniques exist, but have not been demonstrated to be generally applicable. One can, for example, determine the upper limit of a bond dissociation enthalpy by determining the threshold wavelength for the photolytic dissociation of a metal-ligand bond. Values found in this manner may be up to 20 kcal/mol too high.[24]

Another technique for determining an <u>upper</u> limit for a bond dissociation enthalpy involves determination of $\Delta H^{\neq}$ for a process such as that shown in Equation 1.4.

$$L_n\text{-M-R} \;\text{---->}\; L_n\text{-M}\cdot + \cdot\text{R} \qquad (1.4)$$

If the barrier for the back reaction is sufficiently low, this provides a reasonable estimate for the BDE. Thermolysis of $(\eta^5\text{-Me}_5\text{C}_5)(\text{PMe}_3)\text{Ir(R)(H)}$ does not result in simple Ir-R or Ir-H bond homolysis, but reductive elimination of R-H. Since the appropriate R-H bond strengths are known, we can use $\Delta H^{\neq}$ to determine an upper limit for the <u>sum</u> of the Ir-R and the Ir-H bond dissociation enthalpies (Equations 1.5 - 1.7).

$$(\eta^5\text{–}Me_5C_5)(PMe_3)Ir(R)(H) \;\text{---->}\; (\eta^5\text{–}Me_5C_5)(PMe_3)Ir + R\text{-}H \qquad (1.5)$$

$$R\text{-}H \;\text{---->}\; R\cdot + \cdot H \qquad (1.6)$$

$$(\eta^5\text{–}Me_5C_5)(PMe_3)Ir(R)(H) \;\text{---->}\; (\eta^5\text{–}Me_5C_5)(PMe_3)Ir + R\cdot + \cdot H \qquad (1.7)$$

This is shown schematically in the energy diagram in Figure 1.1. By measuring the temperature dependence of the rate constants for the reaction shown in Equation 1.5, we determined that $\Delta H^{\neq} = 35.6$ kcal/mol for the reductive elimination of cyclohexane. This is thus an upper limit for ΔH_5. On the basis of the low kinetic selectivity of the unsaturated intermediate, we estimate the barrier for oxidative addition to be between 2 and 5 kcal/mol. Using a value of 95.5 kcal/mol (ΔH_6) for the C-H bond strength in cyclohexane leads to a value of 127 to 130 kcal/mol ($\Delta H_7 = \Delta H_5 + \Delta H_6$ - (2 to 5 kcal/mol)) for the sum of the iridium-carbon and iridium-hydrogen bond strengths.

Although this gives us an estimate for the sum of the iridium-carbon and iridium-hydrogen bond dissociation enthalpies, as well as for some relative iridium-carbon bond BDE's, we still did not know the relative strengths of the iridium-carbon and iridium-hydrogen bonds, nor any absolute BDE's. We thus undertook calorimetric studies to determine the difference in the iridium-carbon and iridium-hydrogen bond dissociation enthalpies, which when combined with the kinetic studies resulted in accurate values for the *absolute* iridium-carbon and iridium-hydrogen bond strengths.[25]

Reaction of either $(\eta^5\text{-}Me_5C_5)(PMe_3)Ir(C_6H_{11})(H)$ or $(\eta^5\text{-}Me_5C_5)(PMe_3)Ir(H)_2$ with anhydrous HCl in toluene at 25 °C resulted in quantitative production of $(\eta^5\text{-}Me_5C_5)(PMe_3)Ir(Cl)_2$ as shown in Equation 1.8 and Equation 1.9. Subtraction of these two equations leads directly to the heat of hydrogenation of the iridium-cyclohexyl bond as shown in Equation 1.10. Using the well-established bond strengths for H-H (104 kcal/mol) and Cy-H (96 kcal/mol) we calculated that the difference in the iridium-

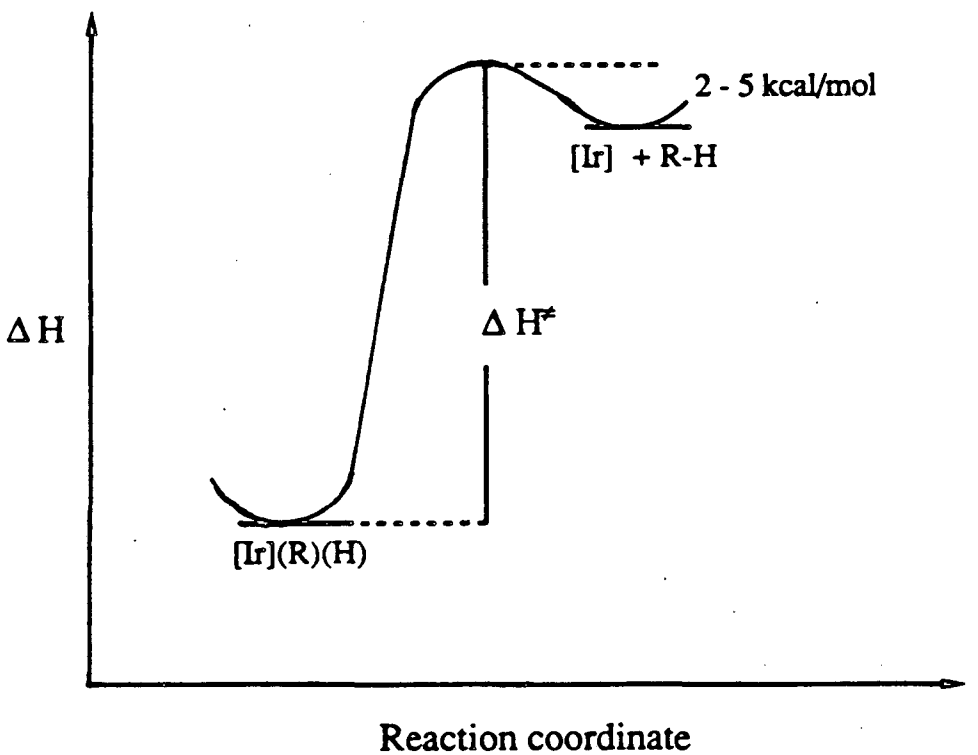

$$D_{(Ir-R)} + D_{(Ir-H)} < D_{(R-H)} + \Delta H^{\neq}$$

Figure 1.1. Reaction coordinate diagram for the reductive elimination of RH from (η^5-Me_5C_5)(PMe_3)Ir(R)(H).

cyclohexyl and the iridium-hydrogen bond strengths is 23.5 kcal/mol.[26] Using the lower value for the sum of the iridium-cyclohexyl and the iridium-hydrogen bond strengths allowed us to estimate that the absolute bond strengths are at least 75 and 52 kcal/mol respectively.[27]

$$Cp^*(PMe_3)Ir(C_6H_{11})(H) + 2HCl \text{ -----> } Cp^*(PMe_3)Ir(Cl)_2 + C_6H_{12} + H_2 \quad \Delta H = -45.5 \pm 0.5 \quad (1.8)$$

$$Cp^*(PMe_3)Ir(H)_2 + 2HCl \text{ -----> } Cp^*(PMe_3)Ir(Cl)_2 + 2H_2 \quad \Delta H = -30.0 \pm 1.3 \quad (1.9)$$

$$Cp^*(PMe_3)Ir(C_6H_{11})(H) + H_2 \text{ -----> } Cp^*(PMe_3)Ir(H)_2 + C_6H_{12} \quad \Delta H = -15.5 \pm 1.8 \quad (1.10)$$

In a similar manner we were able to determine other iridium-carbon bond strengths. Reaction of the phenyl hydride with two moles of anhydrous HCl resulted in production of the dichloride and a mole of benzene and hydrogen (Equation 1.11). Subtraction of Equation 1.9 shows that hydrogenation of the phenyl hydride is virtually thermoneutral (Equation 1.12). Transferring the Ir-H bond strength from above allows us to calculate an iridium-phenyl bond dissociation enthalpy of 82 kcal/mol.

$$Cp^*(PMe_3)Ir(C_6H_5)(H) + 2HCl \text{ -----> } Cp^*(PMe_3)Ir(Cl)_2 + C_6H_6 + H_2 \quad \Delta H = -30.6 \pm 2.7 \quad (1.11)$$

$$Cp^*(PMe_3)Ir(C_6H_5)(H) + H_2 \text{ -----> } Cp^*(PMe_3)Ir(H)_2 + C_6H_6 \quad \Delta H = -0.6 \pm 4.0 \quad (1.12)$$

Calorimetric studies also allow us to obtain estimates for metal-carbon bond dissociation enthalpies derived from hydrocarbons which were not suitable for equilibration studies. Reaction of $(\eta^5\text{-}Me_5C_5)(PMe_3)Ir(CH_3)_2$ with two moles of HCl results in production of $(\eta^5\text{-}Me_5C_5)(PMe_3)Ir(Cl)_2$ and two moles of methane (Equation 1.13). This allows us to determine the strength of the metal methyl bond strength (here an average) to be 56 kcal/mol. Similarly, reaction of $(\eta^5\text{-}Me_5C_5)(PMe_3)Ir(HC{=}CH_2)(Br)$ with HCl results in production of ethylene and $(\eta^5\text{-}Me_5C_5)(PMe_3)Ir(Cl)(Br)$, and leads to a metal-vinyl bond strength of 71 kcal/mol (Equation 1.14).

$$Cp^*(PMe_3)Ir(CH_3)_2 + 2HCl \text{ -----> } Cp^*(PMe_3)Ir(Cl)_2 + 2CH_4 \quad \Delta H = -68.0 \pm 1.3 \quad (1.13)$$

$$Cp^*(PMe_3)Ir(C_2H_3)(Br) + HCl \text{ -----> } Cp^*(PMe_3)Ir(Cl)(Br) + C_2H_4 \quad \Delta H = -19.3 \pm 1.2 \quad (1.14)$$

In order to test the transferability of the iridium-hydride bond strength to molecules with different alkyl groups, the following reactions were carried out (Equations 1.15 - 1.18). Within experimental error, the enthalpies of reaction are the same in all cases, indicating that changing the ancillary ligand has a negligible effect on the metal-hydrogen bond.

$$Cp^*(PMe_3)Ir(H)_2 + 2CCl_4 \text{ -----> } Cp^*(PMe_3)Ir(Cl)_2 + 2CHCl_3 \quad \Delta H = -83.0 \pm 0.6 \quad (1.15)$$

$$Cp^*(PMe_3)Ir(H)(Cl) + CCl_4 \text{ -----> } Cp^*(PMe_3)Ir(Cl)_2 + CHCl_3 \quad \Delta H = -41.8 \pm 0.7 \quad (1.16)$$

$$Cp^*(PMe_3)Ir(C_6H_5)(H) + CCl_4 \text{ -----> } Cp^*(PMe_3)Ir(C_6H_5)(Cl) + CHCl_3 \quad \Delta H = -40.9 \pm 1.4 \quad (1.17)$$

$$Cp^*(PMe_3)Ir(C_6H_{11})(H) + CCl_4 \text{ -----> } Cp^*(PMe_3)Ir(C_6H_{11})(Cl) + CHCl_3 \quad \Delta H = -43.1 \pm 1.5 \quad (1.18)$$

The calorimetric studies thus confirmed our belief that the iridium-carbon and iridium-hydrogen bonds were significantly stronger than those determined for other systems. The calorimetric studies also allowed us assign absolute values to the bond strengths for which we only had relative values from the equilibrium studies. The combined results are shown in Table 1.6.

Table 1.6. Ir-X bond dissociation enthalpies for $(\eta^5\text{-}Me_5C_5)(PMe_3)Ir(X)_2$.

X	$D_{Ir\text{-}X}$ (kcal/mol)
$CH_2C(CH_3)_3$	48
C_6H_{11}	52
C_5H_9	52
CH_3	56
$CH_2CH(CH_3)CH(CH_3)_2$	56
C_5H_{11}	58
$CH{=}CH_2$	71
H	75
C_6H_5	82

It is interesting to compare the relative metal-carbon/hydrogen bond dissociation enthalpies found here with those recently considered by Bryndza, Bercaw, and their coworkers.[28] When studying the relative metal-carbon, metal-oxygen and metal-nitrogen bonds in (DPPE)(Me)Pt-X and $(\eta^5\text{-}Me_5C_5)(PMe_3)_2Ru\text{-}X$, a 1:1 correlation to the analogous H-X bond dissociation enthalpies was found. A similar correlation was noted for $(\eta^5\text{-}Me_5C_5)_2(OCMe_3)Th\text{-}X$. The ruthenium and platinum systems were also surprisingly insensitive to steric effects. Our relative metal-carbon bond strengths, however, do <u>not</u> correlate well with H-X bond strengths. The metal-neopentyl bond is too weak, most likely due to steric reasons. The metal-methyl bond also deviates substantially, being weaker than the H-X bond strength would predict. Correlation of M-X and H-X bond strengths would predict that metal-methyl and metal-hydrogen bonds strengths should be about equal; the strength of the iridium-methyl bond, however, is approximately 20 kcal/mol weaker than the iridium-hydrogen bond, consistent with early studies of first row metal complexes. The remainder of the bond strengths do lie in a straight line when plotted against the H-X bond strengths. However, the slope of the line (0.5) is significantly smaller than that observed in the earlier work (Figure 1.2).

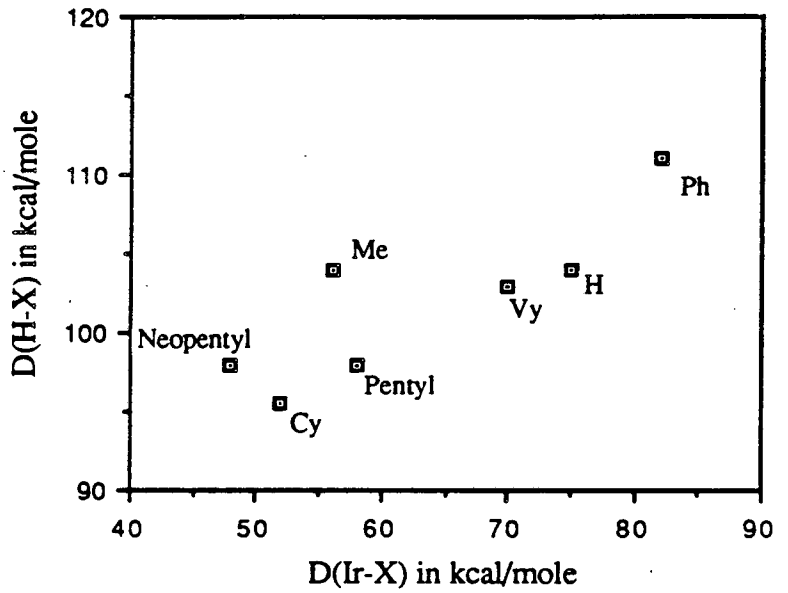

Figure 1.2. Plot of Ir-X bond dissociation enthalpies in (η^5-Me_5C_5)(PMe_3)Ir(X)(H) vs. the respective H-X BDE's.

Predictions Of Reactivity

We are now in a position to make some predictions concerning the reactivity of (η^5-Me_5C_5)(PMe_3)Ir(R)(H) as well as reactions of the reactive intermediate (η^5-Me_5C_5)(PMe_3)Ir with other substrates. Specifically, we can make reasonable thermochemical estimates for some insertion reactions involving (η^5-Me_5C_5)(PMe_3)Ir(R)(H). Having good estimates for the Ir-R and Ir-H BDE's, we can now refer back to Table 1.1. Assuming the strength of a metal-acyl bond to be approximately 5 kcal/mol weaker than a metal-pentyl bond,[29] we find that insertion of CO into a metal-pentyl bond has an enthalpy of reaction of -5 kcal/mol, while insertion into the metal-hydrogen bond has an enthalpy of reaction of +10 kcal/mol. Assuming the reactions would have to be carried out at ambient temperature or above, the $T\Delta S$ contribution to ΔG is at least 10 kcal/mol. Insertion reactions involving CO, not driven by addition of a ligand, are not thermodynamically favored.

Insertion of ethylene into the metal-hydrogen bond can be seen to have an enthalpy of reaction of -21 kcal/mol, while insertion into the metal-carbon bond has an enthalpy of reaction of -25 kcal/mol, independent of the strength of the metal-carbon and metal-hydrogen bonds. Despite the unfavorable entropy of reaction, both insertions will be favored at common reaction temperatures. Insertion of acetylene into either the metal-carbon or metal-hydrogen bond is favorable with enthalpies of reaction of -52 kcal/mol and -39 kcal/mol, respectively. The negative entropies of reaction will have little effect on such exothermic reactions, and indeed insertion into the metal-hydrogen bond has been observed with acetylene.[30]

Knowing that insertion reactions are thermodynamically feasible leads us to consider the last step in a stoichiometric functionalization scheme, reductive elimination. Since reductive elimination of R_2 or RH would result in production of the highly energetic fragment $(\eta^5\text{-}Me_5C_5)(PMe_3)Ir$, we must couple this reaction with one that will result in favorable energetics as well as being compatible with our catalytic cycle. Reaction of $(\eta^5\text{-}Me_5C_5)(PMe_3)Ir$ with RH is such a reaction. The enthalpies of reaction are calculated below (Table 1.7).

Table 1.7. Enthalpies for selected reductive elimination/oxidative addition reactions.

Reactions	ΔH (kcal/mol)
$[Ir](CH_2CH_3)(R) + RH \text{ ----> } [Ir](R)(H) + CH_3CH_2\text{-}R$	-4
$[Ir](CH_2CH_2R)(H) + RH \text{ ----> } [Ir](R)(H) + RCH_2CH_3$	0
$[Ir](CH{=}CH_2)(R) + RH \text{ ----> } [Ir](R)(H) + H_2C{=}CHR$	4
$[Ir](CH{=}CHR)(H) + RH \text{ ----> } [Ir](R)(H) + H_2C{=}CHR$	21
$[Ir](COR)(H) + RH \text{ ----> } [Ir](R)(H) + HCOR$	10

$[Ir] = (\eta^5\text{-}Me_5C_5)(PMe_3)Ir$.

Reaction of the ethylene insertion products with an alkane are very attractive from a thermodynamic standpoint. Particularly interesting is that the product is one which could again react with ethylene, completing a catalytic cycle. The reductive elimination reactions

with the acetylene or carbon monoxide insertion products are not promising due to their endothermicity. Unfortunately, a significant kinetic barrier exists for ethylene insertion. We due not see any insertion products up to temperatures where reductive elimination of the alkane takes place.[31] Such problems will most likely be commonplace in these coordinatively saturated complexes. If insertion could be managed, there are significant problems to overcome before reductive elimination will be observed, not the least of which is competing lower energy pathways such as metal-carbon bond homolysis.

We can now also evaluate reactions involving (η^5-Me_5C_5)(PMe_3)Ir other than C-H insertion reactions. The enthalpies of some of the most interesting, along with some C-H insertion enthalpies, are shown in Table 1.8. It should be noted that only C-H insertion reactions have been observed, pointing to significant kinetic barriers for the other types of reactions.

Table 1.8. Calculated enthalpies of oxidative addition for selected species to "(η^5-Me_5C_5)(PMe_3)Ir".

A-B	ΔH (kcal/mol)
C_6H_{11}-C_6H_{11}	-12
C_6H_{11}-H	-29
H-H	-44
C_6H_5-H	-45
C_6H_5-C_6H_5	-61
C-Cl	-63
H_3C-CH_3	-22

The Origin of Metal-Carbon and Metal-Hydrogen Bond Strengths

The previous section highlighted the importance of having good estimates for bond dissociation energies: if we know the bond energies in a particular system we can make accurate predictions of reactivity. Unfortunately, the myriad of combinations of different metals and ligands makes it extremely difficult to have experimental values for all possible bond dissociation enthalpies. Organic chemists have for years had a large amount of

thermodynamic information available, and from this have been able to generate the "group additivity tables" which allow accurate calculation of ΔH_f for many organic molecules.[32] This in turn allows accurate estimation of enthalpies of reaction. This approach is particularly successful in organic chemistry as only a limited number of elements is involved, and there are only three stable geometries (sp, sp^2, and sp^3 hybridized) about carbon. The many geometries possible for transition metal complexes, and the many different ligands used, will preclude this from being a practical approach for organotransition metal chemistry. There is thus the need to identify and quantify the key factors responsible for the strengths of metal-ligand bonds so that some reasonable estimates can be made for unknown metal-ligand bond strengths.

Estimation of the various factors which contribute to a metal-ligand bond dissociation energy would have been more difficult a few years ago. The experimental work reported here, along with what is known about other systems, now makes it possible to comment in a qualitative way on the various elements which contribute to a bond strength. As the reader will note, there are many gaps in our understanding of how changes in a metal complex will affect bond dissociation enthalpies; we hope the ensuing discussion will stimulate new investigations in these areas.

In many cases organic chemists have been able to identify the primary factors responsible for the stability of a molecule. For example, the electronic properties of a substituted benzyl group can be changed without changing its steric requirements.[33] Similarly, changes in the branching of a hydrocarbon chain will change its steric requirements while only slightly changing the electronics of the molecule. Similar experiments can be done in many cases with organometallic molecules; however, we need to introduce other factors which affect metal-ligand BDE's. Among the factors which influence bond strengths are: the steric demand of a ligand, the metal involved, the ligand involved, and the geometry and oxidation state about the metal. Although many of the

ideas discussed have wider implications, the factors which govern the strength of metal-carbon and metal-hydrogen bonds are of particular interest to us.

The effect of changing the steric requirements of an alkyl group has been studied for several systems. For example, Halpern[4] examined the effect that the steric demand of an alkyl group had on the Co-R bond strength (Table 1.2). In this system the metal-carbon BDE could be predicted by considering the steric requirements of the alkyl group. While not studied as extensively, the metal-alkyl bond dissociation enthalpies in $(PMe_3)_2(CO)Ir(Cl)(I)(alkyl)$ also decrease as the steric demand of the alkyl group increases. In our investigations as well, the relative strengths of the metal-alkyl bonds seemed to be controlled to a large extent by the steric demand of the ligand. In each of these cases, the difference between the strongest and the weakest metal-alkyl bonds was approximately 7 kcal/mol, indicating that this may be typical of compounds of this type. The metal-hydrogen bonds are usually stronger; hydrogen's smaller steric demand is undoubtedly one of the reasons for this.

The effect of changing the metal in a particular transition metal complex is less well understood than the effect which arises from changing a ligand. The existing evidence, however, indicates that metal-ligand bond dissociation enthalpies increase as one descends a column in the transition series of the periodic table. This behavior contrasts with non-transition metal systems, where bond energies typically decrease as one descends a column in the periodic table. Most first row metal-carbon bond dissociation enthalpies are between 20 and 30 kcal/mol, while several recent studies of complexes containing third row metals indicate that metal-carbon bonds formed with these metals may be significantly stronger. This trend does not extend, however, to simple metal alkyls in the gas phase. For example, the metal-carbon bond dissociation energy of M^+-CH_3 is 68 ± 4 kcal/mol for M=Fe while that for M=Ru is 54 ± 5 kcal/mol. Similarly, the M^+-CH_3 bond dissociation energies for M=Co and M=Rh are 61 ± 4 and 47 ± 5 kcal/mol, respectively.

In an attempt to more fully understand periodic trends in bond strengths vis-a-vis metal-methyl and metal-hydrogen bond strengths, Ziegler et al.[34] have recently performed calculations using a modified Hartree-Fock-Slater method (also known an the Xα method) on molecules as large as X-M(CO)$_n$. Their calculations are able to accurately reproduce known bond dissociation enthalpies, and successfully model the increase in metal-carbon bond strengths that occurs as one descends a column in the periodic table. For example, the calculated M-C bond dissociation enthalpy in $(CO)_5Mn\text{-}CH_3$ is 37 kcal/mol (Exp. value: 37 kcal/mol), rising to 48 kcal/mol for M=Re. Similarly, the value calculated for the M-C bond dissociation enthalpy is 38 kcal/mol in $(CO)_4Co\text{-}CH_3$ and 51 kcal/mol for the corresponding iridium complex. Two key factors were identified as responsible for this behavior. Firstly, the overlap of the ligand orbitals with the (p,d)-hybrid on the metal increases as one descends the periodic table. The second factor responsible for the particularly strong bonds formed to the third row metals is a relativistic effect which may contribute up to 10 kcal/mol. Systematic studies are clearly required if we hope to be able to quantitatively predict how changing the metal in a complex will affect the BDE's.

The effect arising from changing the alkyl/aryl group on the metal-carbon bond dissociation enthalpy is more predictable than the effect from changing the metal. As first noted by Bercaw and Bryndza[28] many metal-carbon BDE's parallel the analogous carbon-hydrogen BDE's. They noted that if the C-H BDE's are plotted against M-H BDE's and a line drawn through the points, a line of slope of 1.0 results. This trend was observed for several different systems. One can do the same thing for the relative BDE data presented earlier, and find that this observation is generally valid. Deviations from the line occur when the alkyl/aryl group is particularly bulky, and when the alkyl group is methyl. Many of the slopes of the lines are less than one, indicating that hydrocarbons which have strong C-H bonds (such as ethylene and benzene), form particularly strong M-C bonds, perhaps enhanced by π-effects involving empty metal p or d orbitals of the appropriate symmetry. Studies involving $(PMe_3)_2(CO)Ir(Cl)(I)(X)$,

(η^5-Me_5C_5)(PMe_3)Ir(R)(H), and $(CO)_5$Mn-R suggest that the difference between the strongest and the weakest metal-carbon bonds (between a metal-phenyl and a metal-benzyl or a metal-alkyl bond for example) can be as large as 20 to 30 kcal/mol.

The effects of changing ancillary ligands on the metal, and of changing the coordination geometry about the metal on the rates of reactions are well understood in many cases,[35] but the effect of such changes on the BDE's are understood in only a qualitative sense. This is particularly relevant to the field of intermolecular C-H bond activation, as we would like to be able to make systematic modifications to systems known to insert into the C-H bonds of hydrocarbons, so as to improve the selectivity of the activation process, and to modify the stability of the resulting alkyl hydrides. Changing the size of the ancillary ligands seems to have the effect predicted from steric arguments, but the electronic nature of the ligand is not as well understood. It is believed that the electronic nature of ligand exhibits only a small effect on C-H oxidative addition/reductive elimination reactions, as oxidative addition of alkanes to a metal center is oxidizing only in a formal sense.[36] This is indeed reasonable, as the electronegativities of carbon, hydrogen and late transition metals are similar.

Changing the coordination geometry about the metal by using rigid ligands, or by using very bulky ligands, also affects the bond strengths in the molecule. Unfortunately, this effect is presently difficult to quantify. Theoretical papers have addressed this question,[37] and reasonably suggest that molecules which will lead to highly unstable fragments upon reductive elimination, for example, will not tend to reductively eliminate (i.e. the metal-carbon and metal-hydrogen bonds will be stronger). Experimental evidence is difficult to interpret as there have been no studies specifically directed towards trying to understand the magnitude of this effect. As an illustration, consider an octahedral iridium(III) complex such as [Ir(H)(Cl)(p-C_6H_4Me)(CO)$(PPh_3)_2$],and one of the molecules studied by us, (η^5-Me_5C_5)(PMe_3)Ir(C_6H_{11})(H). Upon reductive elimination of RH from either complex,the resulting metal fragment is one containing iridium(I) which is

known to prefer a square planar geometry.[38] The intermediate formed by reductive elimination from the octahedral complex can easily isomerize to one of square planar geometry. In contrast, "(η^5-Me_5C_5)(PMe_3)Ir",formed by reductive elimination of cyclohexane from (η^5-Me_5C_5)(PMe_3)Ir(C_6H_{11})(H), cannot exist in a square planar form. This results in a very unstable, reactive iridium(I) intermediate. This reactive intermediate thus has a lower kinetic barrier for the back reaction, insertion into a C-H bond, as it does not have to undergo a prior isomerization in order to be in the proper geometry for insertion. Of more relevance here however, is that the bonds formed are also much stronger for a molecule which does not have to undergo this reorganization prior to bond formation. While it is difficult to assign differences in kinetic stability solely to differences in geometry, the relative stabilities of these compounds are consistent with this. The octahedral complex, [Ir(H)(Cl)(p-C_6H_4Me)(CO)(PPh_3)$_2$], will reductively eliminate at ca. 100 °C, while (η^5-Me_5C_5)(PMe_3)Ir(C_6H_5)(H) is stable to above 200 °C.[39]

Conclusion

Efficient and general methods for the catalytic activation and functionalization of alkanes are not yet available. We also do not yet fully understand the C-H activation process. Thermodynamic studies are a small but important step toward understanding what is necessary for C-H activation and functionalization. These studies have contributed to the small but growing body of information concerning metal-hydrogen and metal-carbon bond strengths.

Accurate absolute bond strengths in complicated organometallic systems are rare due to the errors incurred in converting the species of interest to those for which the heat of formation is known. The use of a combination of techniques (kinetic, equilibration studies, calorimetric experiments), however, is now leading to reasonable estimates for some of these values. The relative strengths of the metal-carbon bonds found here are as expected with C_6H_5 > $CHCH_2$ > CH_3 > n-alkyl > c-alkyl. The absolute values, however, are much

larger than those found for first row metals, and the difference between the strengths of the iridium-phenyl and the iridium-methyl bonds is also much greater than found earlier.[40] We continue to investigate these and related compounds in the hope of more fully understanding the factors which affect metal-carbon and metal-hydrogen bond dissociation enthalpies.

Experimental

General experimental procedures are described in Chapter 2 of this Thesis. $(\eta^5\text{-}Me_5C_5)(PMe_3)Ir(C_6H_{11})(H)$, $(\eta^5\text{-}Me_5C_5)(PMe_3)Ir(H)_2$, $(\eta^5\text{-}Me_5C_5)(PMe_3)Ir(C_6H_5)(H)$, $(\eta^5\text{-}Me_5C_5)(PMe_3)Ir(CH_3)_2$, $(\eta^5\text{-}Me_5C_5)(PMe_3)Ir(HC{=}CH_2)(Br)$, and $(\eta^5\text{-}Me_5C_5)(PMe_3)Ir(Cl)(H)$ were synthesized and purified as previously described in our laboratories.[41] Calorimetric measurements were carried out at the University of Miami by Carl D. Hoff and Steven P. Nolan using previously reported procedures.[42]

References

[1] For recent reviews of C-H activation see: (a) Halpern, J. *Inorg. Chim. Acta.* **1985**, *100*, 41. (b) Aktogu, N.; Baudry, D.; Cox, D.; Ephritikhine, M.; Felkin, H.; Holmes-Smith, R.; Zakrzewski, J. *Bull. Soc. Chim. France* **1985**, 381. (c) Green, M.L.H.; O'Hare, D. *Pure & Appl. Chem.* **1985**, *57*, 1897. (d) Crabtree, R.H. *Chem. Rev.* **1985**, *85*, 245.

[2] (a) Walling, C. *Free Radicals in Solution*; Wiley: New York, 1957. (b) Huyser, E.S. *Free Radical Chain Reactions*; Wiley: New York, 1970. (c) Pryor, W.A. *Free Radicals*; McGraw-Hill: New York, 1966. See also: (d) Beckwith, A.L.J.; Duong, T.*J. Chem. Soc., Chem. Comm.* **1978**, 413. (e) Cohen, Z.; Keinan, E.; Mazur, Y.; Haim Varkony, T. *J. Org. Chem.* **1975**, *40*, 2141 and references therein. (f) Meyer, M.D.; Stroud, S.G.; Tomezsko, E.S. *Tetrahedron* **1977**, *33*, 2503. (g) Rozen, S.; Gal, C.; Faust, Y. *J. Am. Chem. Soc.* **1980**, *102*, 6861 and references therein. (h) Olah, g.A.; Parker, D.G.; Yoneda, N. *Angew. Chem., Int. Ed. Engl.* **1978**, *17*, 909.

[3] (a) Hanotier, J.; Camerman, P.; Hanotier-Bridoux, M.; De Radzitzky, P. *J. C. S. Perkin II* **1972**, 2247. (b) Barton, D.H.R.; Hay-Motherwell, R.S.; Motherwell, W.B. *Tett. Lett.* **1983**, *24*, 1979. (c) Barton, D.H.R.; Gustiger, M.J.; Motherwell, W.B. *J.C.S. Chem. Comm.* **1983**, 41. (c) Smegal, J.A.; Hill, C.L. *J. Am. Chem. Soc.* **1983**, *105*, 3515. (d) Hill, C.J.; Smegal, J.A.; Henley, T.J. *J. Org. Chem.* **1983**, *48*, 3277. (e) Groves, J.T.; Nemo, T.E. *J. Am. Chem. Soc.* **1983**, *105*, 6243. (f) Tabushi, I.; Yazaki, A. *J. Am. Chem. Soc.* **1981**, *103*, 7371. (g) Mansuy, D.; Fontecave, M.; Bartoli, J.F. *J.C.S. Chem. Comm.* **1983**, 253.

[4] (a) Abis, L.; Sen, A.; Halpern, J. *J. Am. Chem. Soc.* **1978**, 100, 2915. (b) Michelin, R.A.; Faglia, S.; Uguagliati, P. *Inorg. Chem.* **1983**, *22*, 1831 and references therein. (c) Abis, L.; Santi, R.; Halpern, J. *J. Organomet. Chem.* **1981**, 215, 263 and references therein.

[5] See for example: (a) Connor, J.A. *Top. Curr. Chem.* **1977**, *71*, 71. (b) Halpern, J. *Acc. Chem. Res.* **1982**, *15*, 238. (c) Halpern, J. *Inorg. Chem.* Acta. **1985**, *100*, 41.

[6] Collman, J.P.; Hegedus, L.S.; Norton, J.R.; Finke, R.G. *Principles and Applications of Organotransition Metal Chemistry* ; University Science Books: Mill Valley, CA, 1987.

[7] (a) Crabtree, R.H.; Mihelcic, J.M.; Quirk, J.M. *J. Am. Chem. Soc.* **1979**, *101*, 7738. (b) Crabtree, R.H.; Mellea, M.F.; Mihelcic, J.M.; Quirk, J.M. *J. Am. Chem. Soc.* **1982**, *104*, 107. (c) Crabtree, R.H.; Parnell, C.P. *Organometallics* **1984**, *3*, 1727. (d) Crabtree, R.H.; Demou, P.C.; Eden, D.; Mihelcic, J.M.; Parnell, C.P.; Quirk, J.M.; Morris, G.E. *J. Am. Chem. Soc.* **1982**, *104*, 6994. (e) Baudry, D.; Ephritikine, M.; Felkin, H. *J. Chem. Soc., Chem. Comm.* **1980**, 1243. (f) Baudry, D.; Ephritikine, M.; Felkin, H.; Holmes-Smith, R. *J. Chem. Soc., Chem. Comm.* **1983**, 788. (g) Baudry, D.; Ephritikine, M.; Felkin, H.; Zakrzewski J. *J. Chem. Soc., Chem. Comm.* **1982**, 1235. (h) Baudry, D.; Ephritikine, M.; Felkin, H.; Zakrzewski, J. *Tetrahedron Lett.* **1984**, 1283. (i) Gol'dshleger, N.F.; Tyabin, M.B.; Shilov, A.E.; Shteinman, A.A. *Zh. Fiz. Khim.* **1969**, *43*, 2174. (j) Khrushch, L.A.;Lavrushko,V.V.; Misharin, Y.S.; Moravsky, A.P.; Shilov, A.E. *Nouv. J. Chim.* **1983**, *7*, 729. (k) Shulpin, G.B.; Nizova, G.V.; Shilov, A.E. *J. Chem. Soc., Chem. Comm.* **1983**, 761.

[8] (a) Burchard, T.; Felkin, H. *Nouv. J. Chim.* **1986**, *10*, 673. (b) Aktogu, N.; Baudryt, D.; Cox, D.; Ephritikhine, M.; Felkin, H.; Holmes-Smith, R.; Zakrzewski, J. *Bull. Soc. Chim. Fr.* **1985**, 381. (c) Felkin, H.; Fillebeen-Khan, T.; Holmes-Smith, R.; Lin, Y. *Tett. Lett.* **1985**, 1999. (d) Baudry, D.; Ephritikhine, M.; Felkin, H.; Zakrzewski, J. *Tett. Lett.* **1984**, 1283. (e) Felkin, H.; Fillebeen-Khan, T.; Gault, Y.; Holmes-Smith, R.; Zakrzewski, J. *Tett. Lett.* **1984**, 1279.

[9] (a) Fisher, B.J.; Eisenberg, R. *Organometallics* **1983**, *2*, 764. (b) Jones, W.D.; Kosar, W.P. *J. Am. Chem. Soc.* **1986**, *108*, 5640.

[10] Well established methane to synthesis gas technology exists; this process is extremely energy intensive. (a) Witcoff, H.A.; Reuben, B.G. *Industrial Organic Chemicals in Perspective*; Wiley: New York, 1980; Part 1, pp 108-119. (b) Dybkjaer, I. *CEER Chem. Econ. Eng. Rev.* **1981**, *13*, 17-25. (c) Weissermel, K.; Arpe, H.-J. *Industrial Organic Chemistry*; Verlag Chemie: Weinheim, 1978. (d) Haggin, J. *Chem. & Eng. News* **1987**, June 1, pp 22-28. There have also been recent reports describing other routes leading to higher hydrocarbons: (a) Labinger, J.A.; Ott, K.C. *J. Phys. Chem.* **1987**, *91*, 2682 and references therein. (b) Gesser, H.D.; Hunter, N.R.; Prakash, C.B. *Chem. Rev.* **1985**, *85*, 235.

[11] Page, M.I. *Angew. Chem., Int. Ed. Engl.*, **1977**, *16*, 449.

[12] (a) Halpern, J.; Ng, F.T.T.; Rempel, G.L. *J. Am. Chem. Soc.* **1979**, 101, 7124. (b) Ng, F.T.T.; Rempel, G.L.; Halpern, J. *J. Am. Chem. Soc.* **1982**, 104, 621. (c) Tsou, T.T.; Loots, M., Halpern, J. *J. Am. Chem. Soc.* **1982**, 104, 623. (d) Ng, F.T.T., Rempel, G.L.; Halpern, J. *Inorg. Chim. Acta*, **1983**, 77, L165.

[13] Connor, J.A.; Zafarani-Moattar, M.T.; Bickerton, J.; El Saied, N.I.; Suradi, S.; Carson, R.; Al Takhin, G.; Skinner, H.A. *Organometallics* **1982**, *1*, 1166. BDE's were adjusted upwards from those listed in this paper, due to a more accurate determination of the BDE of the Mn-Mn bond in $Mn_2(CO)_{10}$: Goodman, J.L.; Peters, K.S.; Vaida, V. *Organometallics* **1986**, *5*, 815.

[14] (a) Brown, D.L.S.; Connor, J.A.; Skinner, H.A. *J. Organomet. Chem.* **1974**, *81*, 403. (b) Nappa, M.J.; Santi, R.; Diefenbach, S.P.; Halpern, J. *J. Am. Chem. Soc.* **1982**, *104*, 619.

[15] See, for example: (a) Halle, L.F.; Armentrout, P.B.; Beauchamp, J.L. *Organometallics* **1982**, *1*, 963. (b) Armentrout, P.B.; Halle, L.F.; Beauchamp, J.L. *J. Am. Chem. Soc.* **1981**, *103*, 6501. (c) Armentrout, P.B.; Beauchamp, J.L. *J. Am. Chem. Soc.* **1981**, *103*, 784.

[16] Connor, J.A. *Top. Curr. Chem.* **1977**, 71, 71 and references therein.

[17] (a) Bruno, Joseph W., Marks, Tobin J., Morss, Lester R. *J. Am. Chem. Soc.* **1983**, 105, 6824. (b) Calado, J.C.G., Dias, A.R., Salem, M.S., Marthinho Simoes, J.A. *J. Chem. Soc., Dalton Trans.* **1981**, 1174 and references therein. (c) Yoneda, G., Blake, D.M. *Inorg. Chem.* **1981**, 20, 67.

[18] Pearson, R.G. *Chem. Rev.* **1985**, *85*, 41 and references therein.

[19] Halpern, J. *Inorg. Chim. Acta.* **1985**, *100*, 41 and references therein.

[20] Calderazzo, R. *Ann. N. Y. Acad. Sci*, **1983**, 415, 37.

[21] Yoneda, G.; Blake, D.M. *Inorg. Chem.* **1981**, *20*, 67.

[22] This assumes that the strengths of the other bonds in (η^5-Me_5C_5)(PMe_3)Ir(R)(H) do not change upon substitution of the R group. We feel that such changes would be slight, considering the similarities of the R groups used.

[23] Because of the similarity of the forward and reverse reactions, the translational component of ΔS^o is almost certainly close to zero. Estimation of the rotational and vibrational components is more complicated, but the contributions of $T\Delta S^o_{rot}$ and $T\Delta S^o_{vib}$ to ΔG^o are likely to be less than our uncertainty in ΔG^o.

[24] (a) Halpern, J. *Acc. Chem. Res.* **1982**, *15*, 238 and references therein.

[25] Nolan, S.P., Hoff, C.D., Stoutland, P.O., Newman, L.J., Buchanan, J.M., Bergman, R.G., Yang, G.K., Peters, K.S. *J. Am. Chem. Soc.* **1987**, *109*, 3143.

[26] It is possible that the cyclohexyl ligand is bulky enough to destabilize other metal-ligand bonds in the molecule. This would make the iridium-cyclohexyl bond dissociation enthalpy proportionally larger.

[27] The strength of the iridium hydride bond has been confirmed by photoacoustic measurements. Nolan, S.P., Hoff, C.D., Stoutland, P.O., Newman, L.J., Buchanan, J.M., Bergman, R.G., Yang, G.K., Peters, K.S. *J. Am. Chem. Soc.* **1987**, *109*, 3143.

[28] Bryndza, Henry E., Fong, Lawrence K., Paciello, Rocco A., Tam, Wilson, Bercaw, John E. *J. Am. Chem. Soc.* **1987**, 109, 1444.

[29] There are few experimental numbers to base this on, but the Mn-acyl bond is ca. 5 kcal/mol weaker than the Mn-methyl bond in $(CO)_5$Mn-R. Connor, J.A.; Zafarani-Moattar, M.T.; Bickerton, J.; El Saied, N.I.; Suradi, S.; Carson, R.; Al Takhin, G.; Skinner, H.A. *Organometallics* **1982**, *1*, 1166.

[30] Stoutland, P.O.; Bergman, R.G. manuscript in preparation.

[31] Stoutland, P.O; Bergman, R.G. *J. Am. Chem. Soc.* **1985**, *107*, 4581.

[32] Benson, S.W. *Thermochemical Kinetics*; Wiley: New York, 1968.

[33] Lowry, T.H.; Richardson, K.S. *Mechanism and Theory in Organic Chemistry*; Harper & Row: New York, 1981.

[34] Ziegler, T.; Tschinke, V.; Becke, A. *J. Am. Chem. Soc.* **1987**, *109*, 1351.

[35] Langford, C.H.; Gray, H.B. *Ligand Substitution Processes*, W.A. Benjamin, Inc.: Reading, Mass., 1974.

[36] (a) Crabtree, R.H. *Chem. Rev.* **1985**, *85*, 245. (b) Crabtree, R.H.; Hlatky, G.G. *Inorg. Chem.* **1980**, *19*, 57.

[37] Saillard, J-Y.; Hoffmann, R. *J. Am. Chem. Soc.* **1984**, *106*, 2006.

[38] (a) Cotton, F.A.; Wilkinson, G. *Advanced Inorganic Chemistry*; Wiley: New York, 1980. (b) *Comprehensive Organometallic Chemistry*; Vol. 5, Wilkinson, G.; Stone, F.G.A.; Abel, E.W., Ed., Pergamon: New York, 1982.

[39] (a) Dahlenburg, L.; Nast, R. *J. Organomet. Chem.* **1976**, *110*, 395. (b) Behrens, U.; Dahlenburg, L. *J. Organomet. Chem.* **1976**, *116*, 103.

[40] Feher, F.J.; Jones, W.D. *J. Am. Chem. Soc.* **1984**, *106*, 1650.

[41] (a) Buchanan, J.M.; Stryker, J.M.; Bergman, R.G. *J. Am. Chem. Soc.* **1986**, *108*, 1537. (b) Stoutland, P.O.; Bergman, R.G. chapter 2 of this Thesis.

[42] Hoff, C.D. *J. Organomet. Chem.* **1985**, *282*, 201.

Chapter 2

Activation of Ethylene by Iridium: Inter and Intramolecular Isotope Effects

Introduction

For many years it has been known that transition metals are able to catalyze organic reactions such as those involving saturated and unsaturated hydrocarbons, which in the absence of a metal have either very high activation barriers or are not seen due to competing lower energy processes. Chemists have hoped that an understanding of how hydrocarbons are activated towards further reaction by metals would enable improvements to be made in processes presently in use, as well as aid in the development of new processes. Mechanistic studies of the ways in which hydrocarbons are activated have been vigorously pursued, and indeed have constituted one of the major driving forces behind the development of organometallic chemistry.[1] Heterogeneous catalytic processes are often of most interest due to their commercial importance, but have proven to be very difficult to study.[2] Because of these difficulties, many of the mechanistic details of heterogeneous catalytic reactions have been gained from homogeneous model systems, where compounds possibly similar to important intermediates in catalytic cycles are at least transiently stable, and can be identified by common spectroscopic techniques. These studies have encouraged the development of homogeneous catalytic processes which often have increased selectivities.[3]

Of key importance in understanding both heterogeneous and homogeneous reactions is an understanding of the primary interaction between the transition metal and the hydrocarbon; it is this which may control the selectivity of these reactions. This undoubtedly is dependent on a variety of factors including: whether the metal is present as a complex or as a surface, the steric environment and the electronic nature of the metal, and the type of hydrocarbon involved. In addition to this, one can envision at least three different ways in which a hydrocarbon can interact with transition metals: through its σ-electrons, through the loosely held π-electrons of an unsaturated hydrocarbon, and by a bond breakage reaction where a single bond in a hydrocarbon is actually broken, resulting

in formation of two new σ-bonds to the transition metal (C-H or C-C bond activation). All of these have now been identified, and some of them are quite well understood.

Hydrocarbons with double or triple bonds are able to interact through their π-electrons with d or p-type orbitals on the metal of the appropriate symmetry. Starting with the discovery of Ziese's salt[4], $K[Pt(C_2H_4)Cl_3]$, in 1827, many transition metal olefin and acetylene complexes have been isolated.[5] Recently, η^2-arene complexes have been identified as well.[6] Studies of many of these reactions have indicated that there are often low activation barriers for formation of π-complexes, as expected for a reaction in which no σ-bonds are being broken. π-Complexes are particularly sensitive to steric factors; less substituted olefins typically form much more stable complexes.[5] Mechanisms for many processes include formation of a π-complex as the first step, including: olefin/arene hydrogenation, olefin polymerization, olefin metathesis, and nucleophilic addition to an olefin.[7]

Until recently, very little was understood about the way in which saturated hydrocarbons interact with metals. Recent evidence, however, has demonstrated that there are at least two modes possible by which saturated hydrocarbons can interact with metals. Kinetic evidence obtained in solution indicates that σ-complexes can exist as discrete intermediates. In these cases, there is thought to be an interaction with the metal involving electrons in the σ-bonds of the hydrocarbon. For example, solvates of the type $Cr(CO)_5$-S are much more stable in hydrocarbon solvents than in solvents such as perfluoromethylcyclohexane.[8] This suggests a stabilizing interaction with a hydrocarbon, perhaps through the C-H bonds. This evidence is further supported by several recent structure determinations of organometallic complexes, where weak interactions between C-H bonds and unsaturated metal centers are evident.[9]

The second way in which saturated hydrocarbons can interact with metals is through bond breakage reactions which results in formation of metal-carbon and/or metal-hydrogen bonds. Many metal surfaces have been shown to be capable of this, and a

variety of species have been identified using ultra-high-vacuum (UHV) techniques and the associated spectroscopic techniques.[10] Clean metal surfaces, such as those used under UHV conditions, are extremely reactive; many products are typically formed, making it difficult to identify the primary mode of interaction. It has recently been observed that some transition metal complexes are also capable of insertion into the C-H bonds of alkanes, frequently resulting in formation of transition metal alkyl hydrides. These discoveries have particularly excited chemists, as they have raised the hopes for alkane functionalization processes starting from the alkyl hydrides. Research in this area has been intense, and has recently been reviewed.[11] These results, and the well known instability of many alkyl hydrides, suggest that C-H insertion reactions are most likely not seen more often for thermodynamic, rather than kinetic reasons. Many first and second row metal alkyl hydrides, for example, would not be expected to be stable at room temperature.[12] In this light it is interesting to ask if unsaturated hydrocarbons form π-complexes upon reaction with metals because the C-H insertion products are unstable to the reaction conditions, or because formation of a π-complex is kinetically favored. The discovery of systems capable of inserting into the C-H bonds of hydrocarbons, resulting in formation of stable alkyl hydrides, now makes it possible to address this question.

We have recently been investigating the reaction of $(\eta^5\text{-}Me_5C_5)(PMe_3)Ir(C_6H_{11})(H)$ with ethylene under conditions where the species capable of insertion into unactivated C-H bonds, "$(\eta^5\text{-}Me_5C_5)(PMe_3)Ir$", is generated. Our initial report[13] described the formation of $(\eta^5\text{-}Me_5C_5)(PMe_3)Ir(HC{=}CH_2)(H)$ (**1**) and $(\eta^5\text{-}Me_5C_5)(PMe_3)Ir(H_2C{=}CH_2)$ (**2**), and the isomerization of **1** to **2** at higher temperatures. This system is unique in that both a C-H insertion product and a π-complex are formed, both of which are completely stable to the reaction conditions. Hoping to understand the initial interaction of unsaturated hydrocarbons with metals, we have studied this system in detail. We now wish to report the results of our mechanistic studies, including the effect that isotopic substitution has on the course of the reaction.

Activation of Ethylene

Thermolysis of (η^5-Me_5C_5)(PMe_3)Ir(C_6H_{11})(H) in cyclohexane-d_{12} at 130 - 160 °C results in reversible formation of "(η^5-Me_5C_5)(PMe_3)Ir" and cyclohexane.[14] In the presence of ethylene the reactive intermediate can be trapped. This results in formation of (η^5-Me_5C_5)(PMe_3)Ir(HC=CH_2)(H) (**1**) and (η^5-Me_5C_5)(PMe_3)Ir(H_2C=CH_2) (**2**) in a ratio of 66 : 34, independent of the reaction temperature, and invariant during the reaction when monitored by ^{1}H NMR (Scheme 2.1). This is a kinetic product ratio (vide post). The temperature independence of the ratio of **1** to **2** suggests that the two products are formed via two different transition states and that $\Delta\Delta H^{\neq}$ is near zero.

Reactions with other olefins are typically more complicated. Use of 2-methyl propene under photochemical conditions results only in C-H bond activation products.[15] Propene appeared to behave similarly to ethylene, but several products were seen, and isolation was not attempted. Use of cis- or trans-2-butene resulted in a complicated mixture of products and isomerization of the olefin.[16]

Before our initial report, several examples were known in which mononuclear transition metal complexes inserted into the C-H bonds of activated alkenes.[17] In at least one case,[18] changes in olefin substitution resulted in the complete suppression of vinyl hydride formation, and formation of a π-complex (Scheme 2.2). The effect of an electron withdrawing substituent on the double bond was believed to be two-fold. First, the substituents all had lone pairs of electrons available, which could coordinate to the metal in a first step, allowing the C-H bond of the olefin to then come into the proper configuration for insertion. This is consistent with the many observations of arene cyclometallation. Second, the electron withdrawing substituent is believed to strengthen the metal-carbon bond, so as to make the product less prone to reductive elimination of the olefin. Polynuclear systems are known to insert into the C-H bond of even unactivated alkenes.[19]

Scheme 2.1

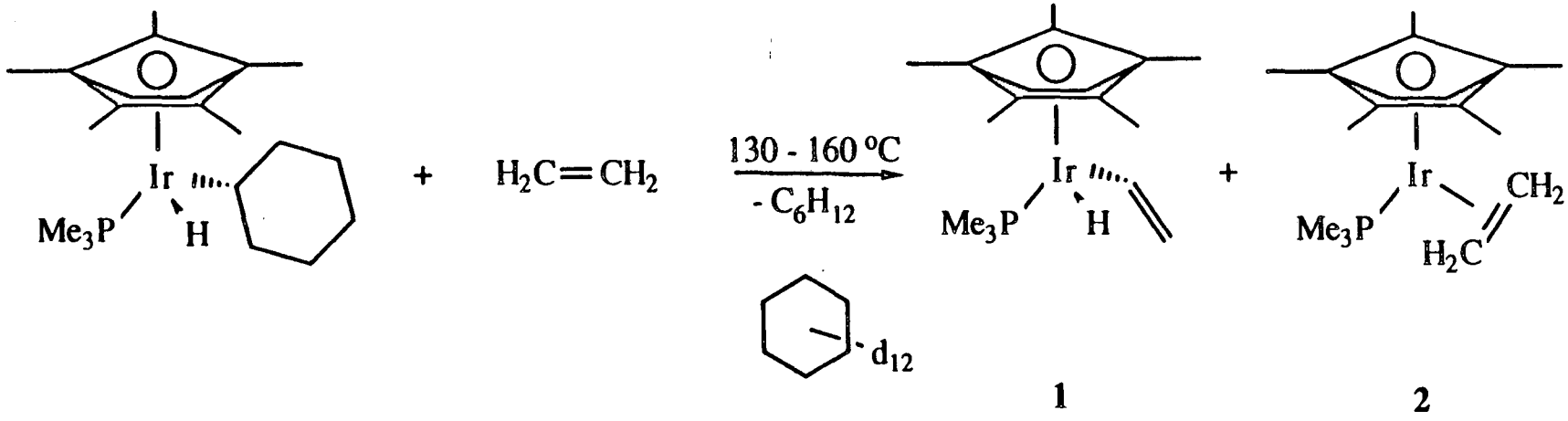

Scheme 2.2

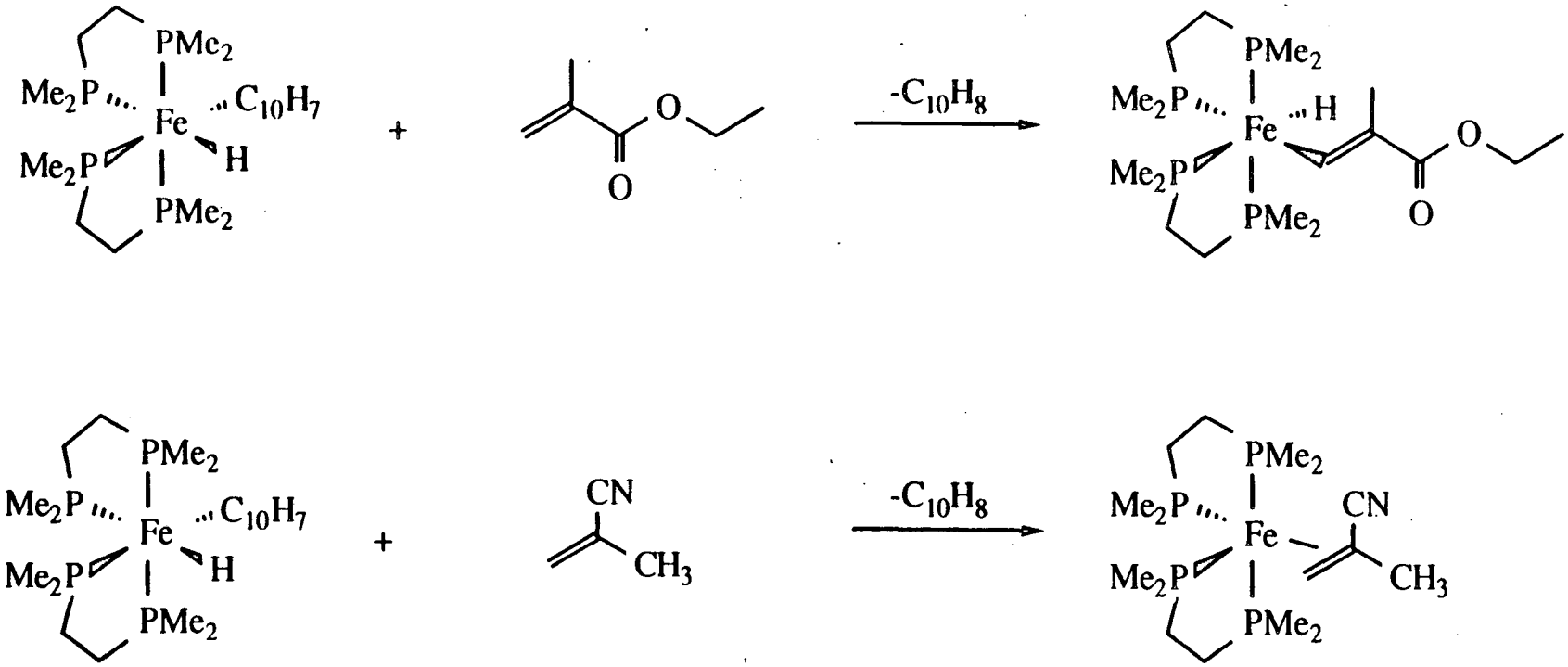
PMe2
Me2P
Fe
C10H7
H
Me2P
PMe2
+
O
O
-C10H8
PMe2
Me2P
Fe
H
Me2P
PMe2
O
O
PMe2
Me2P
Fe
C10H7
H
Me2P
PMe2
+
CN
CH3
-C10H8
PMe2
Me2P
Fe
CN
Me2P
CH3
PMe2

Here it is believed that coordination to one metal center through the π-electrons "activates" the alkene so that a second metal center can insert into a C-H bond (Scheme 2.3).

Since our initial report, several other mononuclear systems have been discovered which are capable of insertion into the C-H bonds of unactivated alkenes (Schemes 2.4 and 2.5). When "$(DEPE)_2Fe$" is generated photochemically (at -80 °C) in the presence of ethylene, both the vinyl hydride and the π-complex are formed in a ratio of 90 : 10.[20] When the intermediate is generated thermally (- 28 °C), by reductive elimination of methane, the ratio is 95 : 5. In this case the reaction is performed at temperatures at which the vinyl hydride exists as a mixture of cis and trans isomers. Raising the temperature to ambient, in either case, results in conversion of the vinyl hydride to the π-complex. Some products arising from C-H activation of the solvent are observed, indicating that some reductive elimination of ethylene is taking place. Irradiation of the π-complex results in a mixture of the vinyl hydride and the π-complex in a ratio of 90 : 10, indicating that this may be a photostationary state.

Generation of "$(\eta^5\text{-}C_5H_5)(PMe_3)_2Re$" at 20 °C in the presence of ethylene results in a 10 : 1 mixture of the vinyl hydride and the olefin complex.[21] At this temperature, however, the vinyl hydride slowly isomerized to the π-complex, indicating that the vinyl hydride may have been the sole kinetic product. Irradiation of the olefin complex resulted in a 1 : 6 mixture of it and the vinyl hydride.

Thermolysis of $(\eta^5\text{-}Me_5C_5)(PMe_3)Ir(HC{=}CH_2)(H)$

In our system as well, the η^2-olefin complex is more stable than the vinyl hydride. Thermolysis of pure $(\eta^5\text{-}Me_5C_5)(PMe_3)Ir(HC{=}CH_2)(H)$ in cyclohexane or benzene solvent at temperatures above 180 °C results in quantitative conversion to $(\eta^5\text{-}Me_5C_5)(PMe_3)Ir(H_2C{=}CH_2)$ (Scheme 2.6). This confirms that the initially observed product mixture arising from activation of ethylene is indeed a kinetic, not a thermodynamic, product mixture. Since $(\eta^5\text{-}Me_5C_5)(PMe_3)Ir(C_6H_5)(H)$ is stable under

Scheme 2.3

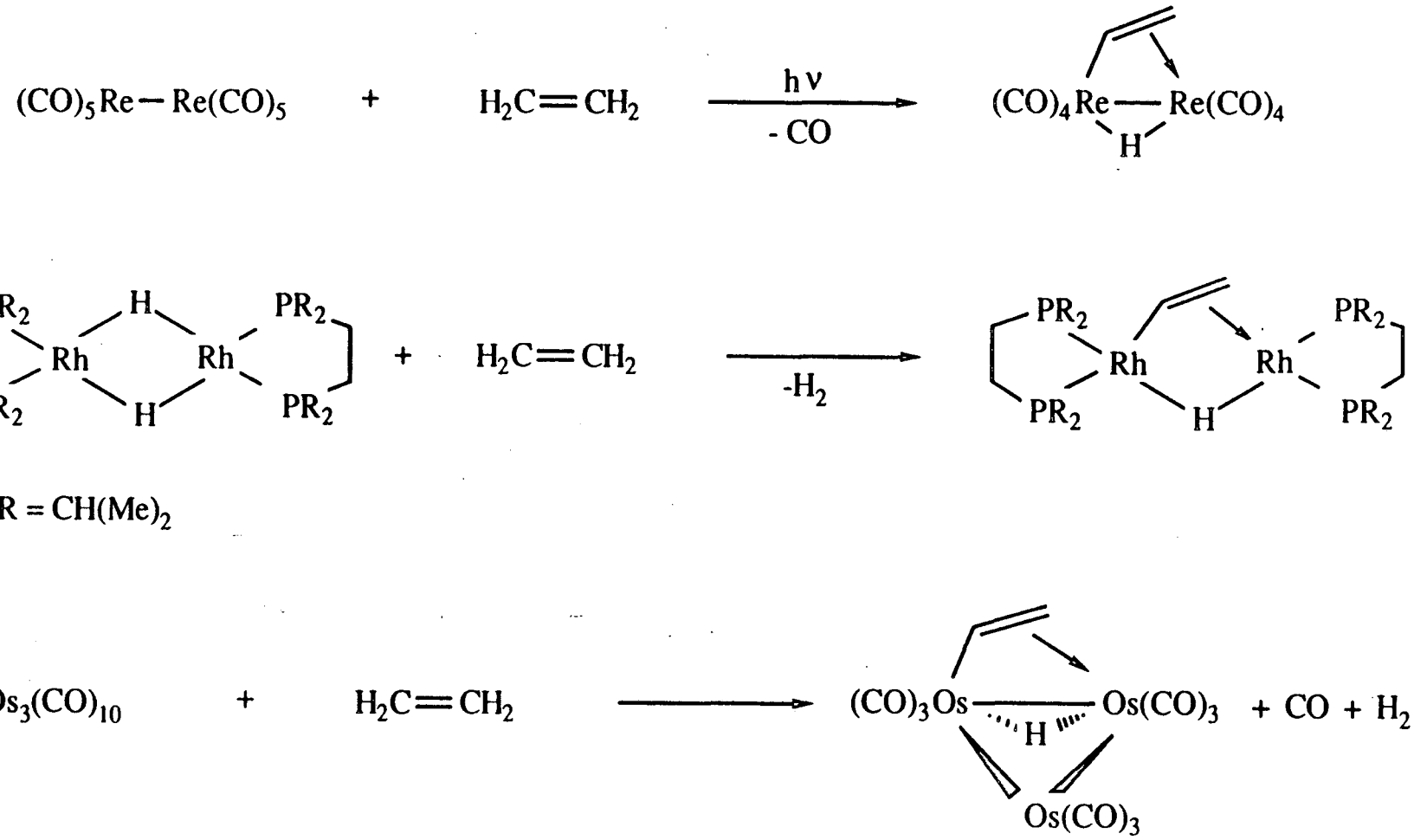
(CO)5Re—Re(CO)5
+
H2C=CH2
hν
- CO
(CO)4Re—Re(CO)4
H
PR2
H
PR2
Rh
Rh
PR2
H
PR2
+
H2C=CH2
-H2
PR2
PR2
Rh
Rh
PR2
H
PR2
R = CH(Me)2
H2Os3(CO)10
+
H2C=CH2
(CO)3Os
Os(CO)3
H
Os(CO)3
+ CO + H2

Scheme 2.4

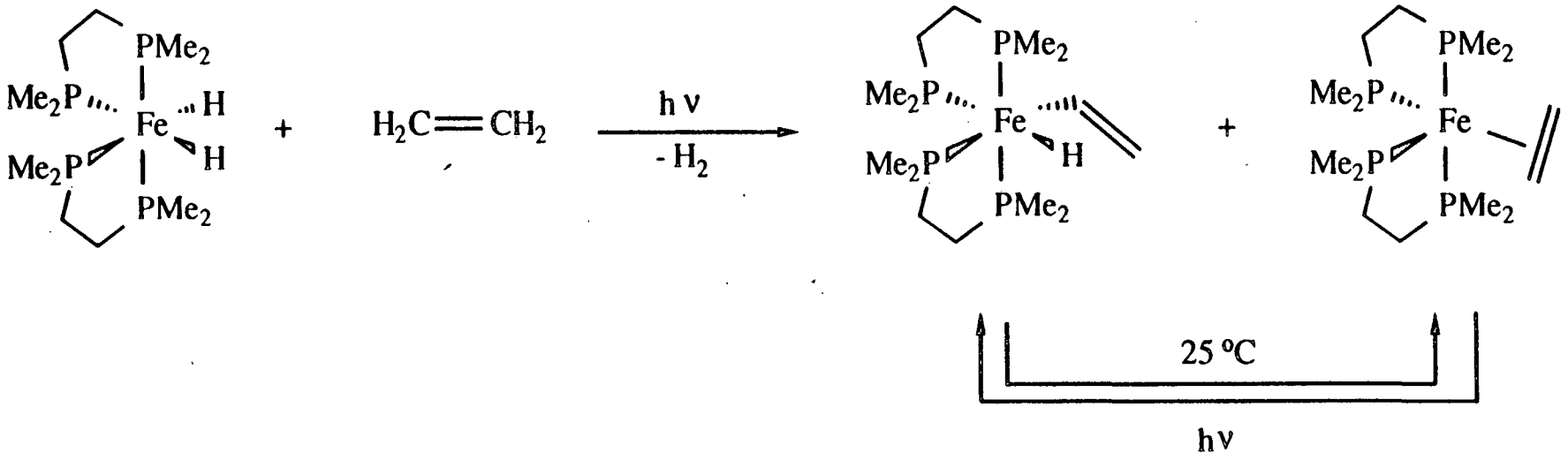
PMe2
Me2P
Fe
H
H
PMe2
+
H2C=CH2
h ν
- H2
25 °C
hν

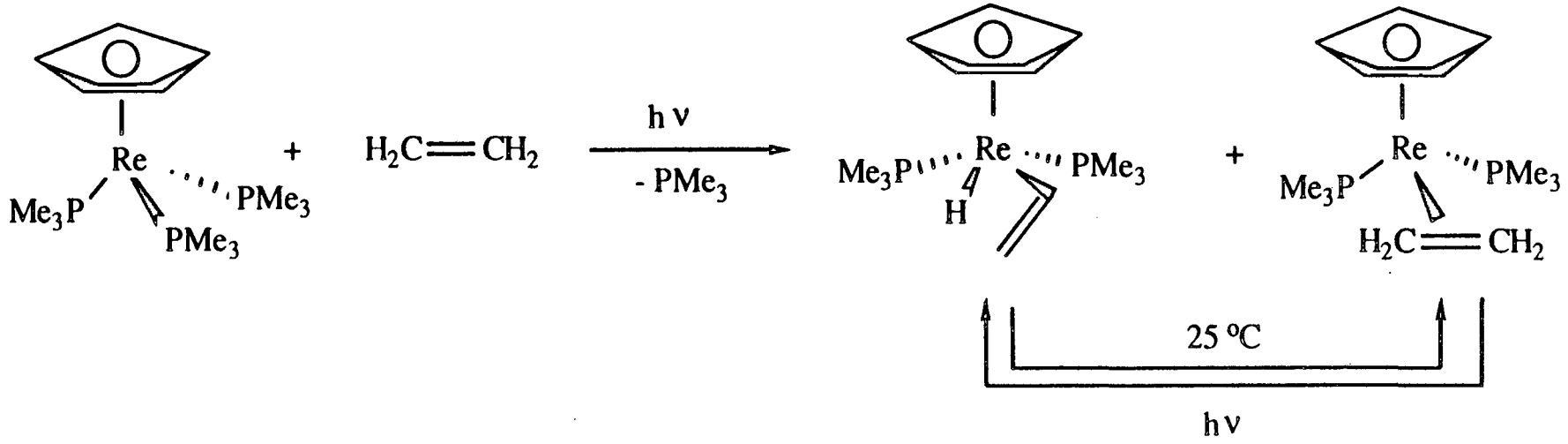
Re
Me3P
PMe3
PMe3
+
H2C=CH2
h ν
- PMe3
H
25 °C
hν

Scheme 2.5

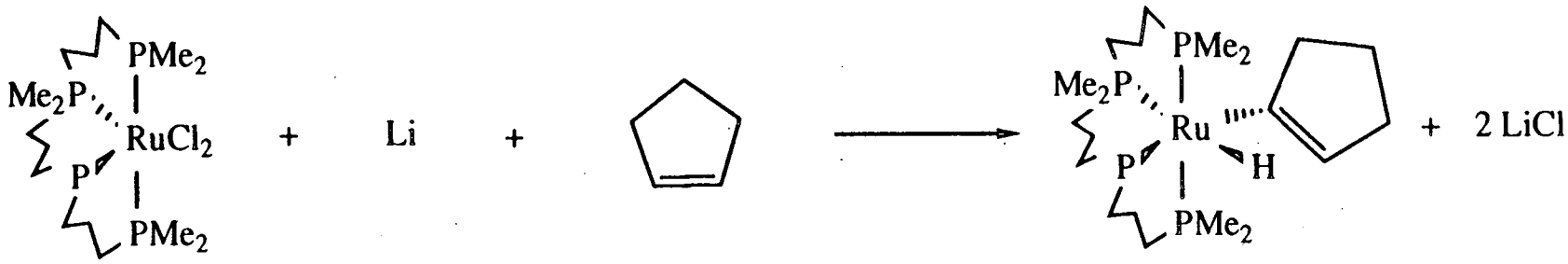

Scheme 2.6

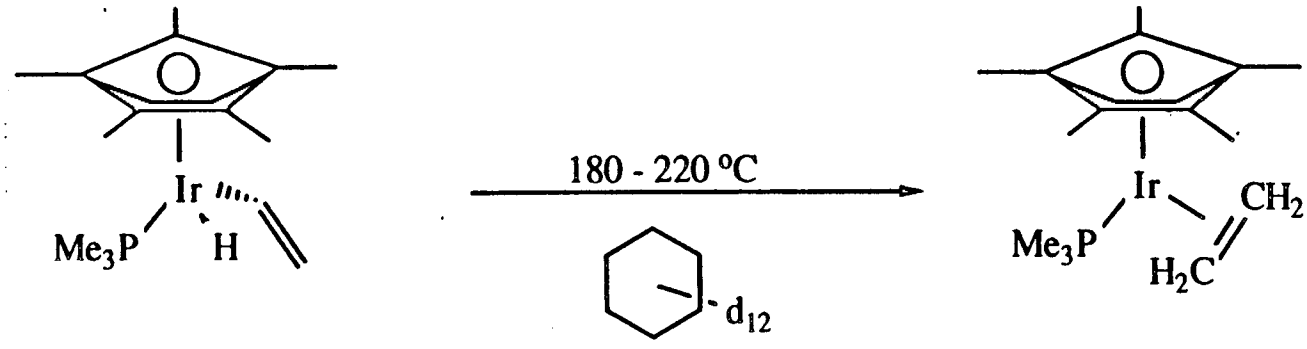

1 **2**

the thermolysis conditions, its absence when the reaction is performed in benzene indicates that the conversion of **1** to **2** does not occur by reductive elimination to generate free (i.e. non-caged) (η^5-Me_5C_5)(PMe_3)Ir and ethylene, followed by addition to the unsaturated metal fragment: if this were occurring, the unsaturated intermediate would be expected to activate benzene.[22] This isomerization can be conveniently followed by ^{1}H NMR in cyclohexane-d_{12} (Figure 2.1).

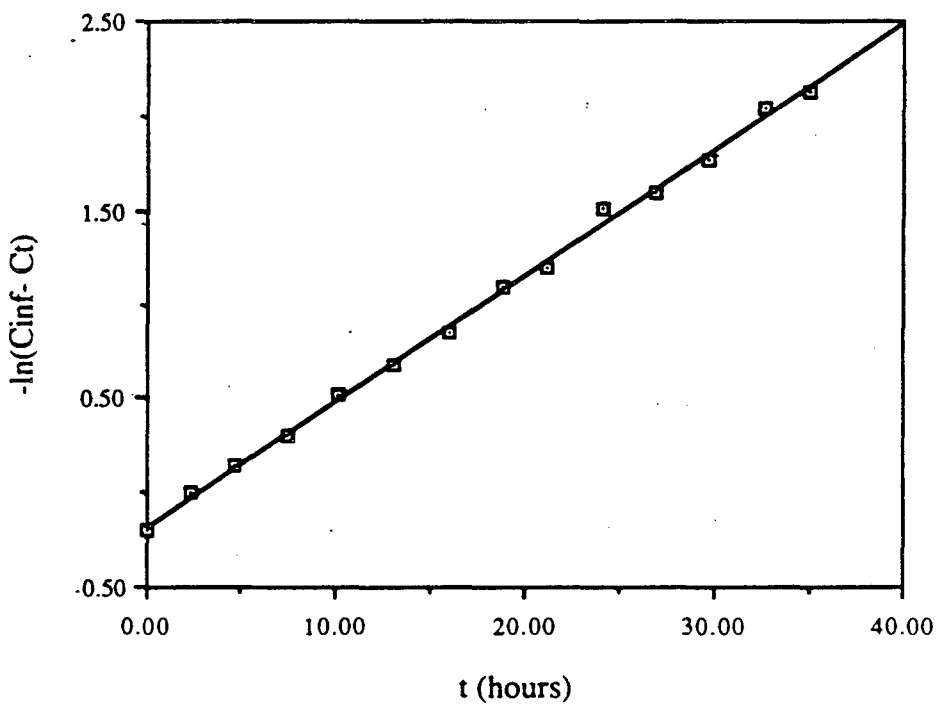

Figure 2.1. First order kinetic plot of the thermolysis of (η^5-Me_5C_5)(PMe_3)Ir(HC=CH_2)(H) in C_6D_{12} at 185°C.

Using the rates found at five temperatures between 180 and 220 °C allowed us to determine that $\Delta H^{\neq} = 34.6 \pm 1.2$ kcal/mol and $\Delta S^{\neq} = 2.6 \pm 2.6$ e.u. (Figure 2.2). While **1** is quite stable thermally, exposure to small amounts of oxygen resulted in isomerization to **2**.[23] Similarly, if **1** was left in the "gum phase" (the oily residue remaining after removal of the

volatile materials from the crude reaction mixture), isomerization to **2** was occasionally observed.

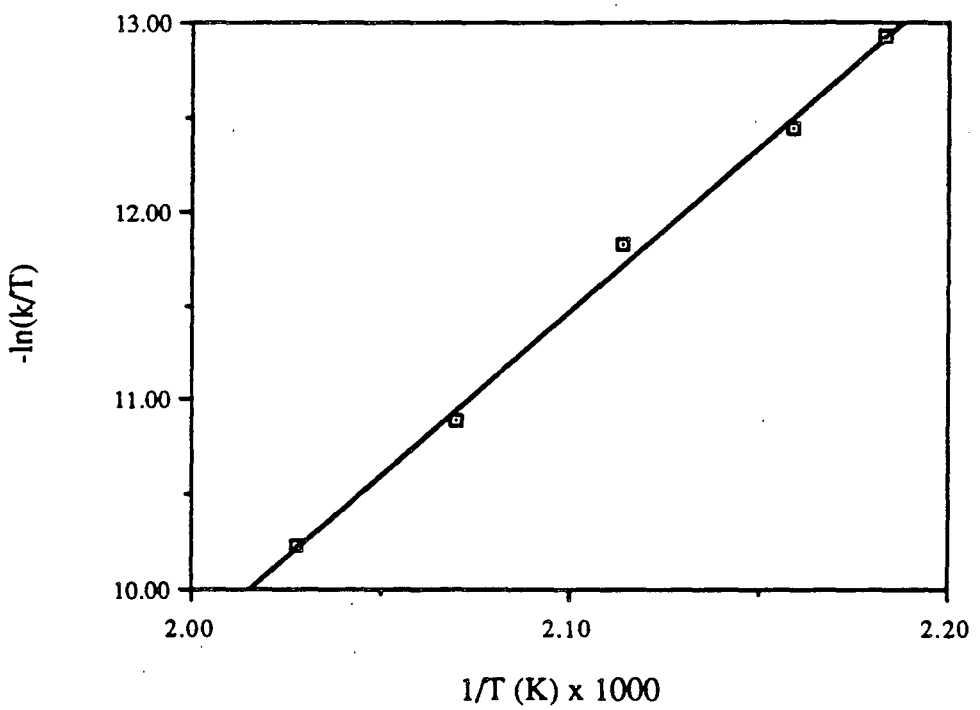

Figure 2.2. Plot of ln(k/T) vs 1/T for the thermolysis of the vinyl complex **1** in cyclohexane-d_{12} at five temperatures between 180 and 220°C.

From separately conducted calorimetric studies,[24] we can estimate ΔH for the unobserved reductive elimination reaction leading to the unsaturated iridium species and free ethylene. In those studies the bond dissociation enthalpies (BDE) of the iridium-hydrogen, and the iridium-vinyl bonds were found to be 76 kcal/mol and 71 kcal/mol, respectively. Knowing the C-H BDE in ethylene (103 kcal/mol) allows us to calculate a ΔH of 44 kcal/mole for the reaction. Previously, we estimated that the barrier for the reverse reaction, oxidative addition of (η^5-Me_5C_5)(PMe_3)Ir to a C-H bond, is 2 - 5 kcal/mol; this leads to a value of $\Delta H^{\neq}$ between 2 and 5 kcal/mol larger than ΔH.[25] The isomerization of **1** to **2** is thus taking

place a full 10 kcal/mol lower in energy than would be required to fully dissociate ethylene from **1**, and then bring it back to form the π-complex. It is likely that the π-electrons of the vinyl group participate in some way, lowering this barrier. This is consistent with the general observation that vinyl-alkyl and divinyl transition metal complexes typically undergo reductive elimination more rapidly than the analogous dialkyl and alkyl-aryl complexes.[26]

Irradiation of $(\eta^5\text{-}Me_5C_5)(PMe_3)Ir(H_2C{=}CH_2)$

Irradiation of a pure solution of the olefin complex **2**, resulted in nearly quantitative regeneration of **1**. Similar cycles have been observed in organic and organometallic systems, and formally constitute an energy storage cycle.[27] Analogous cycles have been observed for $(DEPE)_2Fe(HC{=}CH_2)(H)$ and for $(\eta^5\text{-}C_5H_5)(PMe_3)_2Re(HC{=}CH_2)(H)$.[21] Irradiation of $(\eta^5\text{-}C_5H_5)Ir(H_2C{=}CH_2)_2$ results in isomerization of only one of the olefin ligands yielding $(\eta^5\text{-}C_5H_5)(H_2C{=}CH_2)Ir(HC{=}CH_2)(H)$.[28]

Synthesis and Structure

In order to confirm the identification of the products from the reactions with ethylene, and to allow the synthesis of larger quantities of material, we sought independent routes to these compounds. Reaction of $(\eta^5\text{-}Me_5C_5)(PMe_3)Ir(Cl)_2$ with 1.2 equivalents of $H_2C{=}CHMgBr$ in THF results in the formation of $(\eta^5\text{-}Me_5C_5)(PMe_3)Ir(HC{=}CH_2)(Br)$ as a yellow/orange, air-stable solid in 67.4 % yield. Reaction of $(\eta^5\text{-}Me_5C_5)(PMe_3)Ir(HC{=}CH_2)(Br)$ with $NaBH_4$ in isopropyl alcohol at temperature slightly above ambient for several hours yields a white, mildly air-sensitive compound. $(\eta^5\text{-}Me_5C_5)(PMe_3)Ir(HC{=}CH_2)(H)$ was isolated in 82.8 % yield after chromatography at -80 to -100 °C on Alumina (III) under air-free conditions (Scheme 2.7). Alternatively, **1** may be recrystallized from highly concentrated solutions of pentane or hexamethyldisiloxane. The corresponding deuteride may be made easily by using $NaBD_4$.

Scheme 2.7

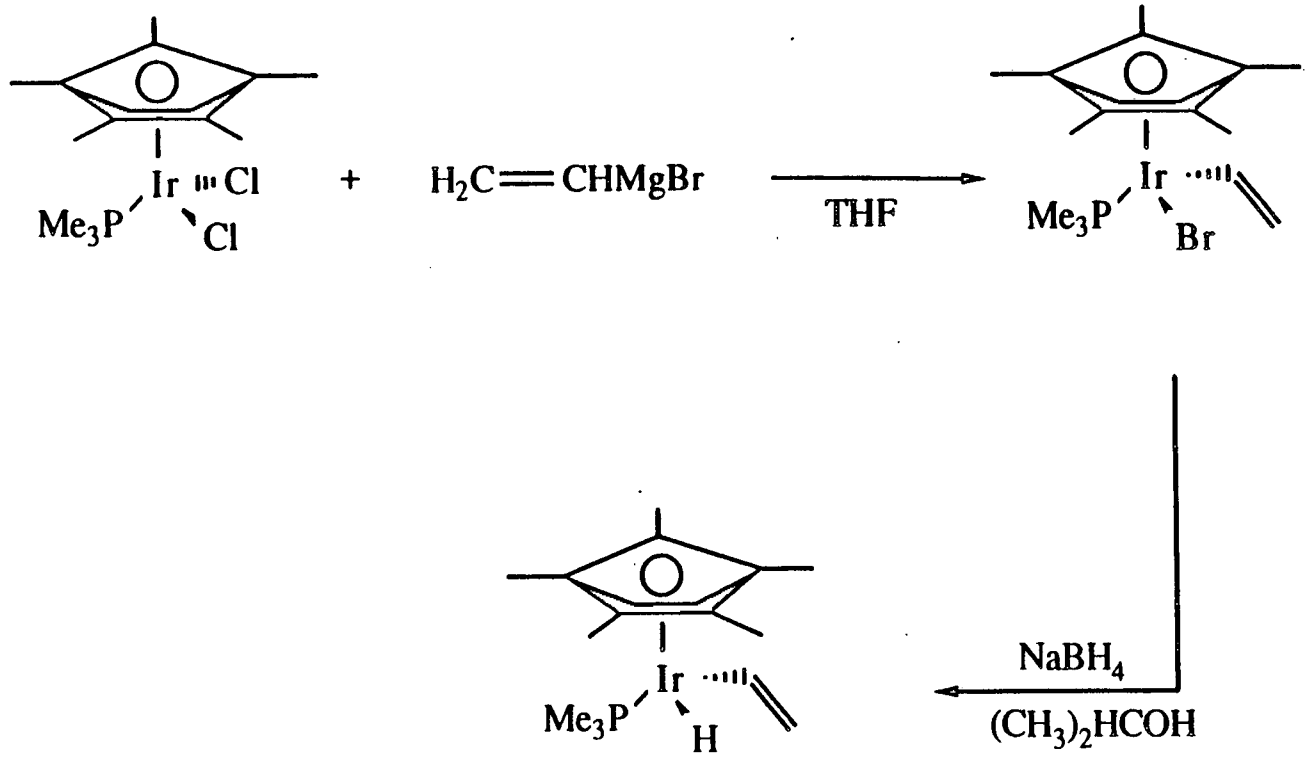
Ir
Cl
Me3P
Cl
+
H2C=CHMgBr
THF
Ir
Me3P
Br
NaBH4
(CH3)2HCOH
Ir
Me3P
H

We attempted to synthesize (η^5-Me_5C_5)(PMe_3)Ir(H_2C=CH_2) in a manner analogous to that mentioned by Maitlis et al.[29] for the synthesis of (η^5-Me_5C_5)(PPh_3)Ir(H_2C=CH_2). Bubbling ethylene through a refluxing ethanol solution of (η^5-Me_5C_5)(PMe_3)Ir$(Cl)_2$ in the presence of Na_2CO_3 for 9 hours resulted in a low yield of (η^5-Me_5C_5)(PMe_3)Ir(H_2C=CH_2), the major side product being (η^5-Me_5C_5)(PMe_3)Ir$(H)_2$. We have been unable, however, to separate these two compounds cleanly.

We have also carried out an X-ray structure determination of (η^5-Me_5C_5)(PMe_3)Ir(HC=CH_2)(H). Clear, yellow needles suitable for diffraction were obtained by slowly cooling a solution of **1** in hexamethyldisiloxane to -40 °C. Fragments cleaved from these crystals were suitable for diffraction, and were found to belong to the space group $P2_1/n$. In order to avoid excess thermal motion in the crystal, the data were acquired at -118 °C. In a difference Fourier map, calculated after refinement of all non-hydrogen atoms with anisotropic thermal parameters, peaks corresponding to the expected position of most of the hydrogen atoms were found. A difference Fourier map calculated after inclusion of all other hydrogen atoms clearly showed the position of the hydride. All hydrogen atoms were then allowed to refine with isotropic thermal parameters. The final residuals were R = 2.04 % and wR = 2.53 %.

The structure shows the expected three-legged piano stool, pseudooctahedral geometry with the cyclopentadienyl ligand occupying three sites, and the phosphine, vinyl, and hydride ligands occupying the others (Figures 2.3 and 2.4). The Ir-H bond length of 1.61(5) A is typical of M-H bond lengths, as is the Ir-C bond length (2.054(4) A) which is slightly shorter than that found in (η^5-Me_5C_5)(PMe_3)Ir(C_6H_{11})(H) (2.125 A), as expected for a bond to an sp^2 carbon. The length of the C=C bond in the vinyl group (1.296 A) is slightly shorter than that of a typical double bond. The pentamethylcyclopentadienyl ligand is nearly planar, but there is a small, but statistically significant, variation (6 σ) in the C-C bond lengths. The shortest C-C bond (1.418 A), C_1-C_5, is opposite the hydride ligand.

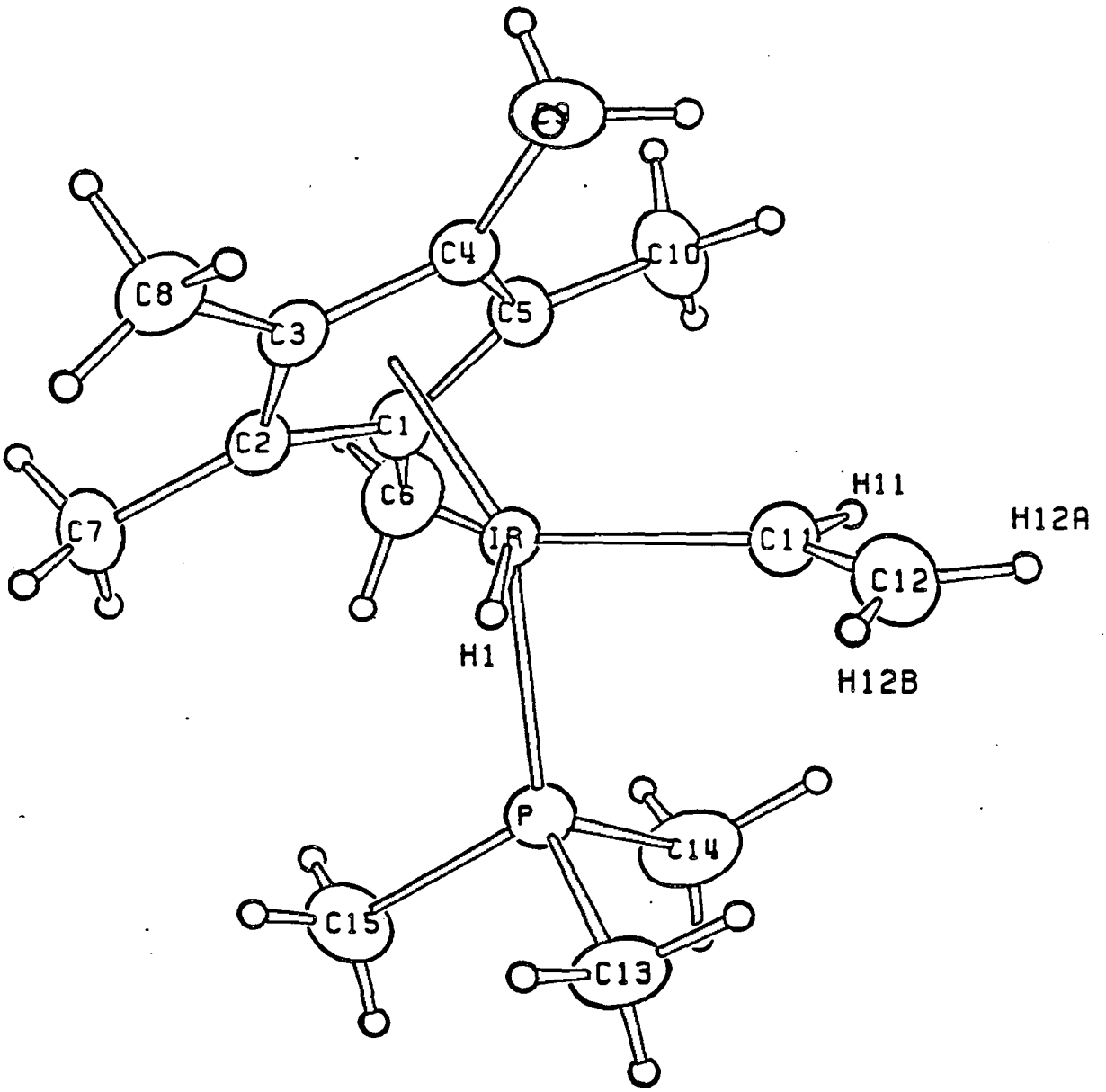

Figure 2.3. Molecular geometry and labeling for (η^5-Me_5C_5)(PMe_3)Ir($HC{=}CH_2$)(H) (**1**). The ellipsoids are scaled to represent the 50 % probability surface. Hydrogen atoms are given as arbitrarily small spheres for clarity.

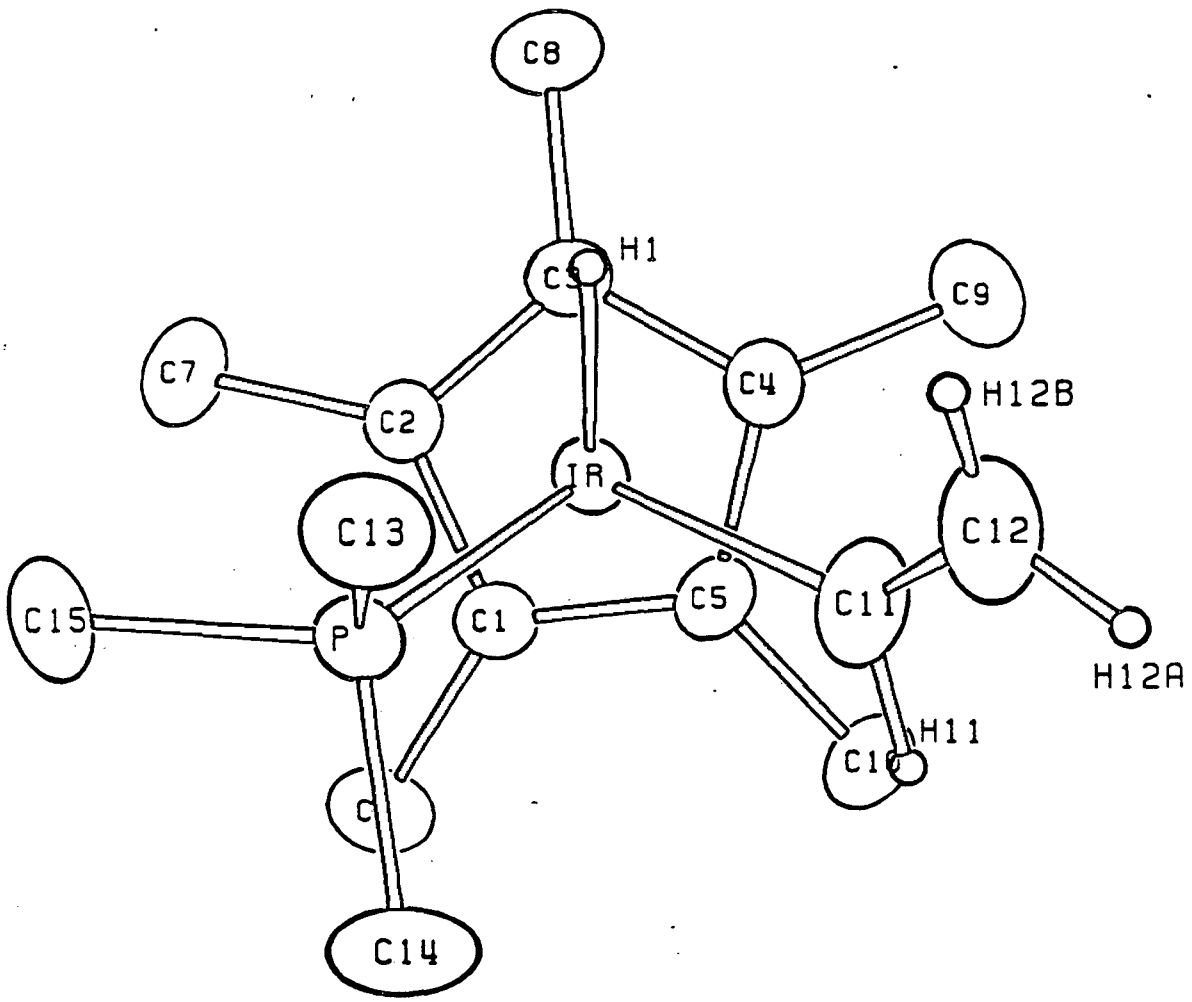

Figure 2.4. Molecular geometry and labeling for (η^5-Me_5C_5)(PMe_3)Ir($HC{=}CH_2$)(H) (**1**). The ellipsoids are scaled to represent the 50 % probability surface. Hydrogen atoms are given as arbitrarily small spheres for clarity.

Adjacent to it are the two longest bonds, C_1-C_2 and C_4-C_5, at 1.445 and 1.453 A, respectively. The remaining C-C bonds, C_2-C_3 and C_3-C_4, are of intermediate length at 1.427 A. Selected bond lengths and angles are given in Tables 2.1 and 2.2. Selected torsional angles are given in Table 2.3. These data suggest a significant contribution from an allyl-ene resonance structure. Similar, but larger, deviations have been observed for $(\eta^5\text{-}Me_5C_5)Rh(CO)_2$[30] and $(\eta^5\text{-}Me_5C_5)Co(CO)_2$.[31] It is thought that this is caused by a localization of the p_π electron density on the cyclopentadienyl ligand, believed to arise from a breakdown of the doubly degenerate e_1 ring orbital degeneracy caused by interaction with nondegenerate metal-based atomic orbitals.

Table 2.1. Selected Intramolecular Bond Distances (A) and esd's for **1**.

atoms	distance	atoms	distance
Ir-C_1	2.279(3)	P-C_{14}	1.818(4)
Ir-C_2	2.266(3)	P-C_{15}	1.814(4)
Ir-C_3	2.250(3)	C_1-C_2	1.445(4)
Ir-C_4	2.225(3)	C_2-C_3	1.427(5)
Ir-C_5	2.263(3)	C_3-C_4	1.427(5)
Ir-P	2.226(1)	C_4-C_5	1.453(5)
Ir-C_{11}	2.054(4)	C_5-C_1	1.418(5)
Ir-H_1	1.61(5)	C_1-C_6	1.495(5)
C_{11}-C_{12}	1.296(6)	C_2-C_7	1.496(5)
C_{11}-H_{11}	1.06(5)	C_3-C_8	1.500(5)
C_{12}-H_{12a}	0.96(5)	C_3-C_8	1.500(5)
C_{12}-H_{12b}	0.92(4)	C_4-C_9	1.491(5)
P-C_{13}	1.815(4)	C_5-C_{10}	1.489(5)

Table 2.2. Selected Intramolecular Bond Angles for **1**.

atom 1	atom 2	atom 3	angle (deg)	atom 1	atom 2	atom 3	angle (deg)
Cp_1	Ir	P	135.2	C_5	C_1	C_2	107.9(3)
Cp_1	Ir	C_{11}	123.6	C_1	C_2	C_3	107.6(3)
Cp_1	Ir	H_1	127.4	C_2	C_3	C_4	109.0(3)
P	Ir	C_{11}	85.8(1)	C_3	C_4	C_5	106.9(3)
P	Ir	H_1	82.8(17)	C_4	C_5	C_1	108.5(3)
C_{11}	Ir	H_1	86.2(17)	C_6	C_1	C_2	125.3(3)
Ir	C_{11}	C_{12}	132.8(4)	C_6	C_1	C_5	126.5(3)
Ir	C_{11}	H_{11}	113.7(28)	C_7	C_2	C_1	126.0(3)
H_{11}	C_{11}	C_{12}	113.3(28)	C_7	C_2	C_3	125.7(3)
C_{11}	C_{12}	H_{12a}	117.3(32)	C_8	C_3	C_2	126.0(3)
C_{11}	C_{12}	H_{12b}	121.5(26)	C_8	C_3	C_4	124.8(3)
H_{12a}	C_{12}	H_{12b}	121.1(41)	C_9	C_4	C_3	127.4(3)
Ir	P	C_{13}	116.7(2)	C_9	C_4	C_5	125.5(3)
Ir	P	C_{14}	114.7(2)	C_{10}	C_5	C_1	126.3(3)
Ir	P	C_{15}	117.2(2)	C_{10}	C_5	C_4	125.1(3)

Cp_1 = centroid of the cyclopentadienyl ring.

Table 2.3. Table of Torsional Angles for **1**.

atom 1	atom 2	atom 3	atom 4	angle (deg)
H_1	Ir	C_{11}	C_{12}	-1.9
P	Ir	C_{11}	C_{12}	-84.9
Cp_1	Ir	C_{11}	C_{12}	131.5
C_{11}	Ir	P	C_{15}	-176.1
H_1	Ir	P	C_{13}	-22.8
Cp_1	Ir	P	C_{13}	-160.7
H_1	Ir	Cp_1	C_3	-5.8
H_1	Ir	Cp_1	C_4	65.7
C_{11}	Ir	Cp_1	C_4	-48.3
C_{11}	Ir	Cp_1	C_5	24.6
P	Ir	Cp_1	C_1	-27.1
P	Ir	Cp_1	C_2	45.4

Cp_1 = centroid of the cyclopentadienyl ring.

Intermolecular Isotope Effects

By measuring the relative rates of reaction of $(\eta^5\text{-}Me_5C_5)(PMe_3)Ir(C_6H_{11})(H)$ with ethylene and with deuterium labeled ethylenes, one can determine the intermolecular isotope

effect for both C-H insertion and π-complex formation. Normally this is done by directly comparing the rate of reaction of a non-deuterated substrate, with that of a deuterium-containing substrate. To measure the intermolecular isotope effect we first allowed the iridium species to compete for ethylene and ethylene-d_n in the same tube and attempted to measure the final relative concentrations of **1** and **1**-d_n in order to calculate relative rates. This required making a comparison between the cyclopentadienyl or the PMe_3 resonances and the vinyl resonances. Unfortunately, the errors incurred in determining the relative amounts of **1** and **1**-d_n in this manner were unacceptably large. Attempts to take advantage of the splitting in the ^{31}P NMR spectrum caused by a deuterium on the metal were similarly unsuccessful.

A further complication should be noted here. While experimenting with reactions where ethylene and ethylene-d_4 were heated in the same tube in the presence of $(\eta^5\text{-}Me_5C_5)(PMe_3)Ir(C_6H_{11})(H)$, it was found that the ethylenes underwent H/D exchange with each other. Mass spectral analysis of the volatile materials showed a nearly statistical mixture of d_0, d_1, d_2, d_3, and d_4. Later experiments (vide post) revealed that this scrambling process was also observed with ethylene-d_2. Addition of a small amount of PMe_3 (> 0.05 M) to the reaction mixture effectively inhibited this (4 - 20 % scrambled) so that any scrambling had a negligible effect on the isotope effects.[32] Interestingly $P(C_6H_5)_3$ was not effective at stopping this scrambling process. All experiments aimed at determining isotope effects (both intra and intermolecular competition experiments) were thus done in the presence of at least 0.05 M PMe_3.

To circumvent this problem we sought a reagent which could be mixed with ethylene and ethylene-d_n in separate tubes, compete with ethylene for the metal center, and lead to a product with a signal in the NMR spectrum sufficiently different from those of $(\eta^5\text{-}Me_5C_5)(PMe_3)Ir(HC{=}CH_2)(H)$ and $(\eta^5\text{-}Me_5C_5)(PMe_3)Ir(H_2C{=}CH_2)$ so that accurate integrations could be made. In this way, the relative rates of reaction of ethylene and of ethylene-d_n with this reagent could be measured, thus allowing us to directly compare the

rates of reaction with ethylene and with ethylene-d_n, as if they were competing for the iridium center in the same tube. Benzene proved to be suitable for this as it was stable to the reaction conditions, and reacts with the iridium center forming the stable phenyl hydride which has a distinct ^{31}P NMR shift.

We thus made up a standard solution of (η^5-Me_5C_5)(PMe_3)Ir(C_6H_{11})(H) and C_6H_6 in cyclohexane-d_{12}, and split this between two NMR tubes so that the volume of solution in each tube was the same. We condensed $H_2C{=}CH_2$ into one of the tubes, and into the other an equal amount of $D_2C{=}CD_2$. In order to be sure that the pressure of ethylene (and thus the concentration in solution) was the same in each tube, the tubes were sealed so that the lengths were equal (within 3 mm, total length ca. 25 cm). Side-by-side thermolysis at 145 °C of these tubes resulted in the first containing (η^5-Me_5C_5)(PMe_3)Ir(C_6H_5)(H), (η^5-Me_5C_5)(PMe_3)Ir($HC{=}CH_2$)(H), and (η^5-Me_5C_5)(PMe_3)Ir($H_2C{=}CH_2$), and the second containing (η^5-Me_5C_5)(PMe_3)Ir(C_6H_5)(H), (η^5-Me_5C_5)(PMe_3)Ir($DC{=}CD_2$)(D), and (η^5-Me_5C_5)(PMe_3)Ir($D_2C{=}CD_2$). In Figures 2.5 and 2.6 are shown representative ^{31}P NMR spectra of the reaction mixtures at the end of the reaction.

Since the concentration of benzene is the same in both tubes, the rate of formation of (η^5-Me_5C_5)(PMe_3)Ir(C_6H_5)(H) is the same is both tubes. This allowed us to normalize the concentrations of the products in each tube to the amount of (η^5-Me_5C_5)(PMe_3)Ir(C_6H_5)(H) formed, and to compare the relative amounts (and thus the relative rates of formation) of (η^5-Me_5C_5)(PMe_3)Ir($HC{=}CH_2$)(H) with (η^5-Me_5C_5)(PMe_3)Ir($DC{=}CD_2$)(D), and of (η^5-Me_5C_5)(PMe_3)Ir($H_2C{=}CH_2$) with (η^5-Me_5C_5)(PMe_3)Ir($D_2C{=}CD_2$) (Scheme 2.8).

In this way we were able to determine the intermolecular isotope effect for insertion into a C-H bond, and for formation of the π-complex. Finding the intermolecular isotope effect for formation of **1** is straightforward when $H_2C{=}CH_2$ is compared to $D_2C{=}CD_2$, as there are no statistical corrections to make. When the rate of insertion into any of the

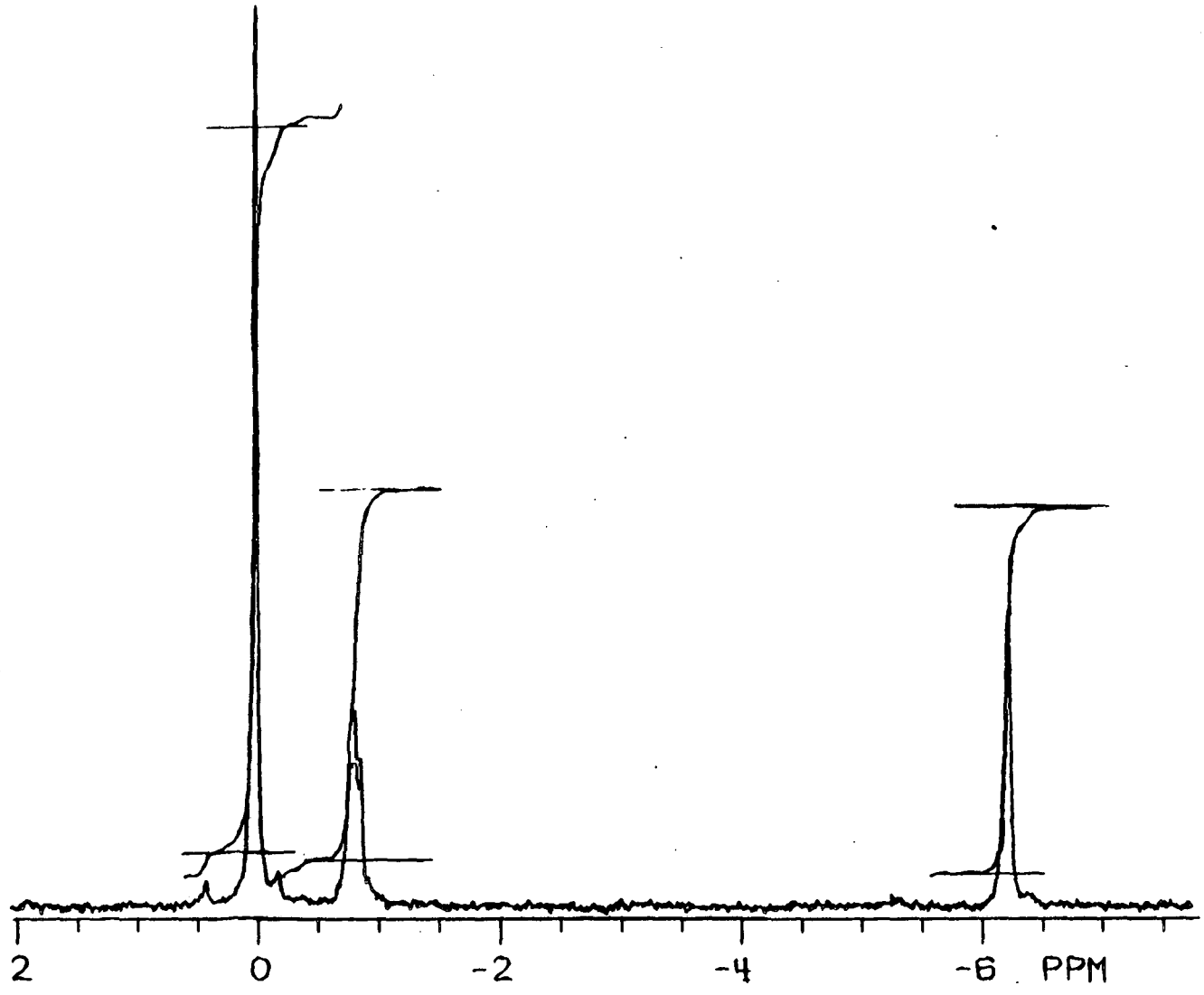

Figure 2.5. ^{31}P NMR of the reaction mixture resulting from thermolysis of $(\eta^5\text{-}Me_5C_5)(PMe_3)Ir(C_6H_{11})(H)$ in the presence of $H_2C{=}CH_2$ and C_6H_6, from left to right is $(\eta^5\text{-}Me_5C_5)(PMe_3)Ir(C_6H_5)(H)$, $(\eta^5\text{-}Me_5C_5)(PMe_3)Ir(HC{=}CH_2)(H)$, and $(\eta^5\text{-}Me_5C_5)(PMe_3)Ir(H_2C{=}CH_2)$.

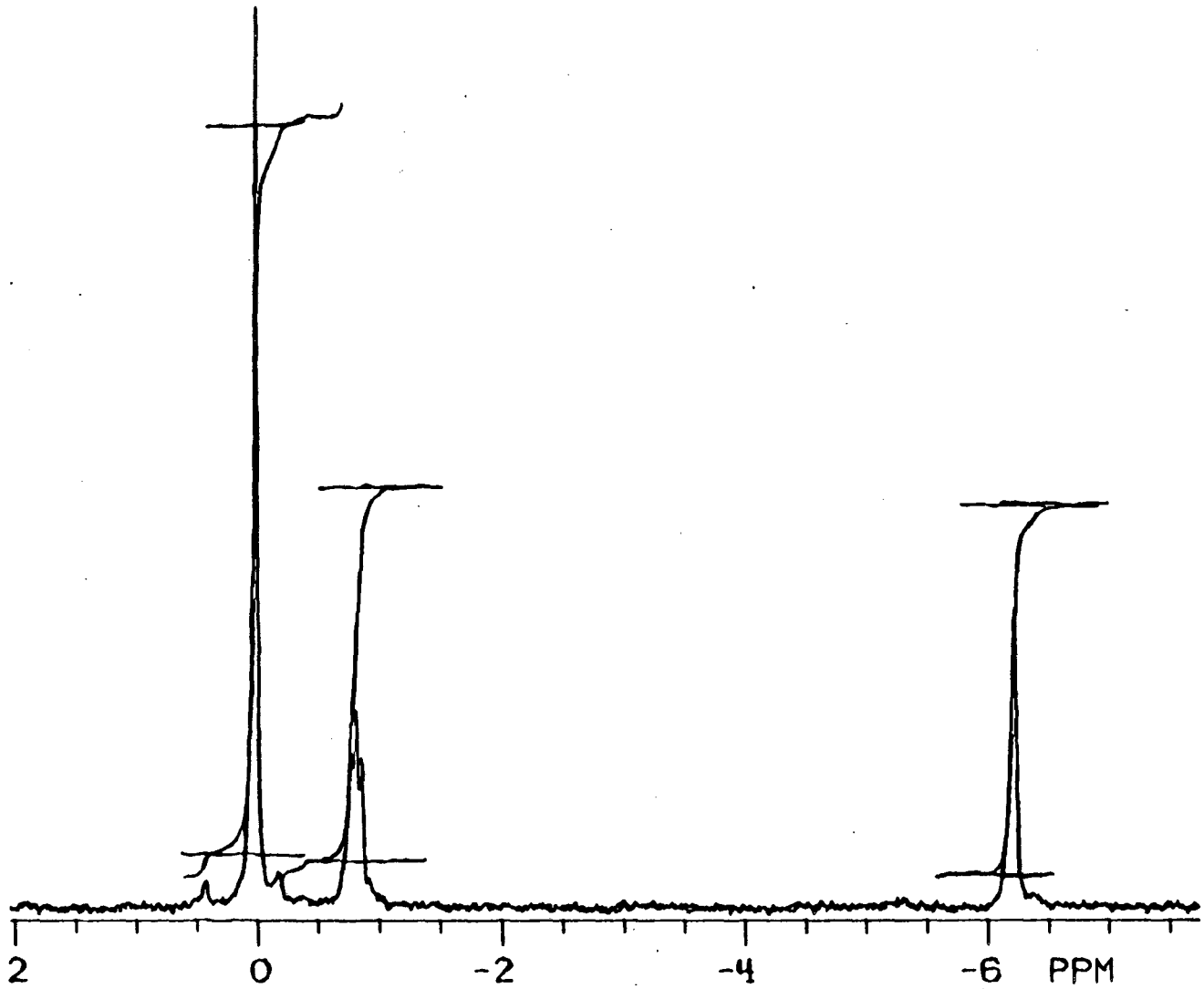

Figure 2.6. ^{31}P NMR of the reaction mixture resulting from thermolysis of $(\eta^5\text{-}Me_5C_5)(PMe_3)Ir(C_6H_{11})(H)$ in the presence of $D_2C{=}CD_2$ and C_6H_6, from left to right is $(\eta^5\text{-}Me_5C_5)(PMe_3)Ir(C_6H_5)(H)$, $(\eta^5\text{-}Me_5C_5)(PMe_3)Ir(DC{=}CD_2)(D)$, and $(\eta^5\text{-}Me_5C_5)(PMe_3)Ir(D_2C{=}CD_2)$.

Scheme 2.8

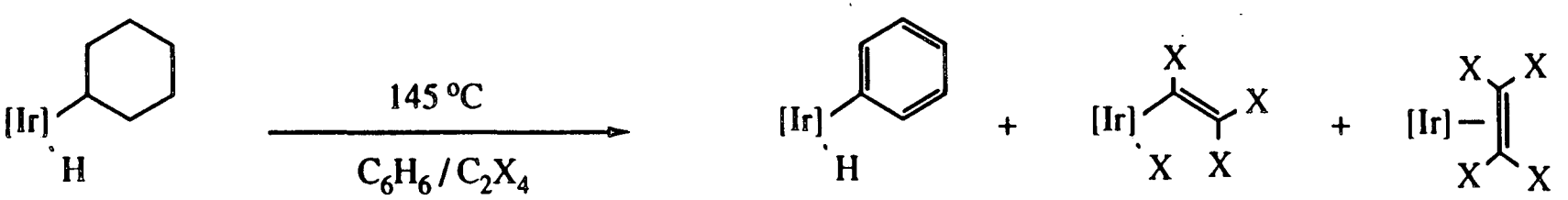

[Ir] = $Cp^*(PMe_3)Ir$

$H_2C{=}CH_2$	(1.00)	0.79	0.39
$D_2C{=}CD_2$	(1.00)	0.54	0.49

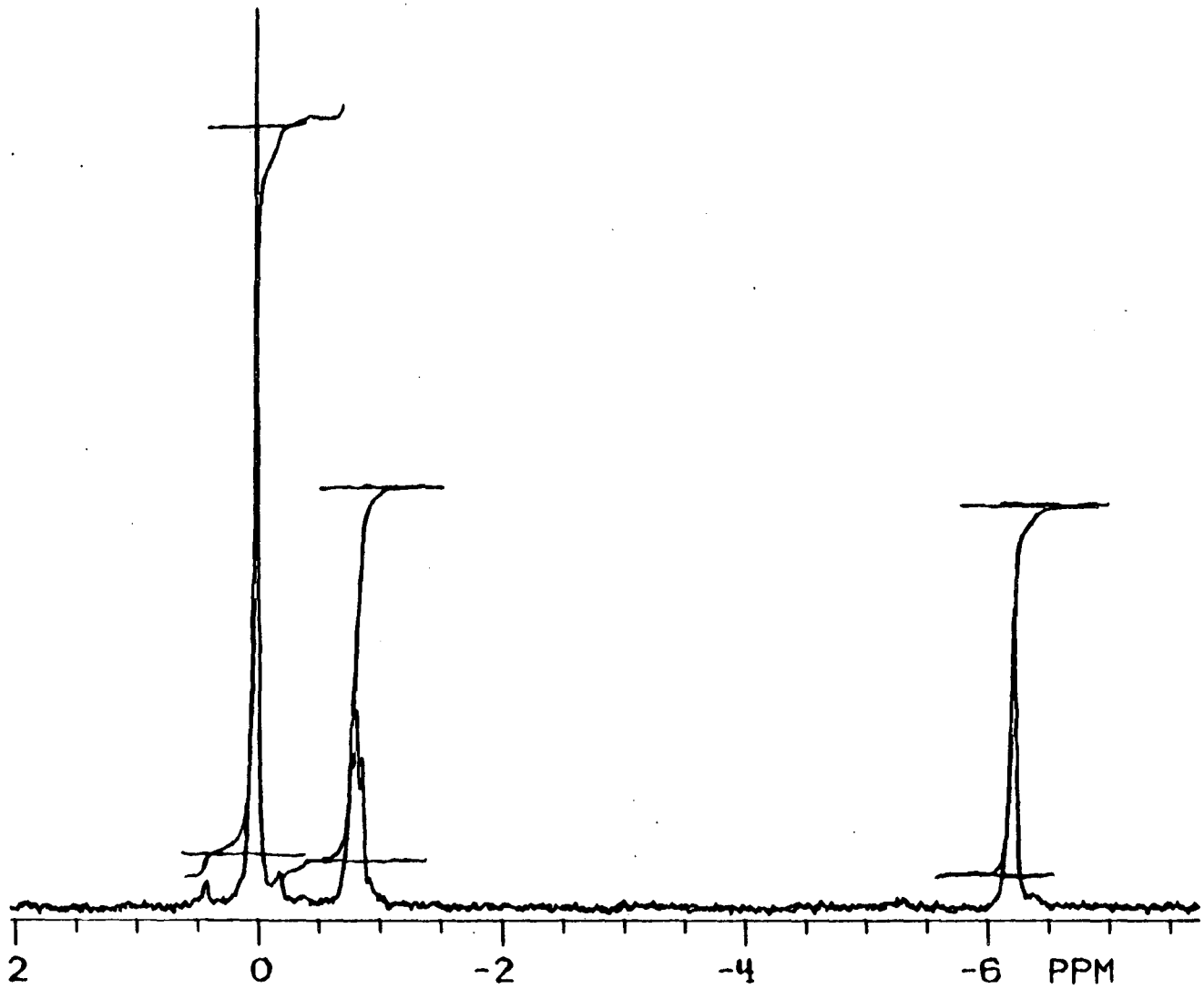

Figure 2.6. ^{31}P NMR of the reaction mixture resulting from thermolysis of $(\eta^5\text{-}Me_5C_5)(PMe_3)Ir(C_6H_{11})(H)$ in the presence of $D_2C{=}CD_2$ and C_6H_6, from left to right is $(\eta^5\text{-}Me_5C_5)(PMe_3)Ir(C_6H_5)(H)$, $(\eta^5\text{-}Me_5C_5)(PMe_3)Ir(DC{=}CD_2)(D)$, and $(\eta^5\text{-}Me_5C_5)(PMe_3)Ir(D_2C{=}CD_2)$.

Scheme 2.8

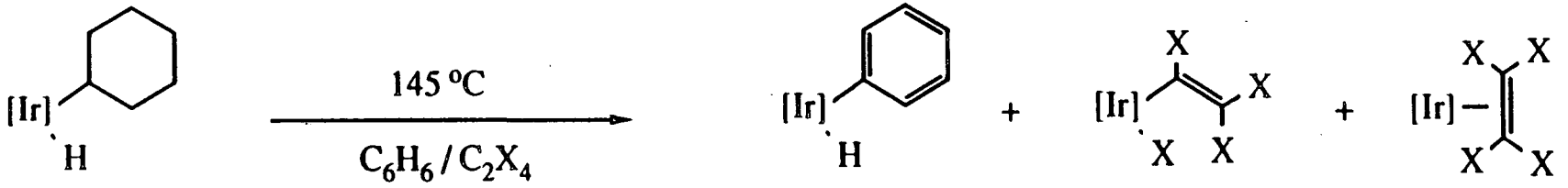

[Ir] = $Cp^*(PMe_3)Ir$

$H_2C{=}CH_2$	(1.00)	0.79	0.39
$D_2C{=}CD_2$	(1.00)	0.54	0.49

d_2-ethylenes is compared to ethylene, however, complications arise. We define the rate of insertion into one C-H bond of $H_2C{=}CH_2$ to be k_H. The total rate of insertion into $H_2C{=}CH_2$ is then $4k_H$, and the total rate of insertion into the C-H(D) bonds of ethylene-d_2 is $2k_H + 2k_D$. Knowing the relative rates of insertion into ethylene and ethylene-d_2 one can thus solve for k_H/k_D. Propagation of errors in solving for k_H/k_D, however, makes the uncertainty in k_H/k_D large (0.2 - 0.3). The values we found were consistent with this. While they were centered on the value found using ethylene and ethylene-d_4 (where the comparison is simple, $4k_H$ vs $4k_D$), they varied considerably and therefore are not included in our final value for the intermolecular isotope for insertion in a C-H bond. Comparing rates of reaction of $H_2C{=}CH_2$ with those for $D_2C{=}CD_2$ gave intermolecular isotope effects of 1.45, 1.46, and 1.55 ± 0.15 (error based on 5% error in NMR integration). Averaging these values resulted in a final value of $k_H/k_D = 1.49 \pm 0.08$.

Similarly, the intermolecular isotope effect on formation of **2** can be determined. If we assume the transition state for formation of the π-complex involves a symmetrical interaction of iridium with the π-electrons, the isotope effect will consist entirely of a secondary effect where $k_D = \delta^n k_H$, with n = number of deuterium atoms on the ethylene, and δ being the effect that each deuterium has on the rate. For the three experiments the relative ratios of **2** to **2-d$_4$** were found to be 0.81, 0.80, and 0.84 ± 0.08. Averaging these values results in $k_H/k_D = 0.82 \pm 0.05$. The effect of one deuterium, δ, is thus $(k_H/k_D)^{1/4} = 0.95 \pm 0.02$.

The accuracy of the intermolecular isotope effects also depends on there being equal ratios of benzene and of ethylene or ethylene-d_4 in each tube. We are confident that the amounts of benzene in each tube are the same as the tubes were filled from a standard solution. The amount of ethylene in each tube, however, depended on $H_2C{=}CH_2$ and $D_2C{=}CD_2$ having the same solubility in cyclohexane. While we did not initially expect there to be any significant difference, earlier measurements have indicated that liquid

ethylene-d_4 has a slightly higher vapor pressure (3 %) than ethylene.[33] We thus elected to measure the relative solubilities.

We measured the relative solubilities using the apparatus shown in Figure 2.7. Briefly, it consists of stainless steel bomb fitted to a stainless steel pipe with a valve. At the other end of the pipe is another valve with a fitting for attachment to a vacuum line. The bomb was filled with cyclohexane and thoroughly degassed (freeze-pump-thawed 5 to 10 times). A known amount of ethylene was then condensed into the apparatus, the top valve closed, and the apparatus allowed to warm to room temperature over 2 to 3 h. Closure of the lower valve resulted in nearly all of the ethylene below it being dissolved in the cyclohexane (9.4 mL of cyclohexane in the 11.2 mL lower section). Using a vacuum line and a Toepler pump, we then measured the gas above the lower valve, which is inversely related to the amount in solution. These results show an insignificant difference ($D_2C{=}CD_2$ is 2 ± 4 % more soluble) in the solubility of ethylene and ethylene-d_4 in cyclohexane under these conditions. We did not correct the isotope effects for this slight difference. Details of the experimental procedure and the actual solubilities are given in the Experimental section.

Intramolecular Isotope effects

Thermolysis of $(\eta^5\text{-}Me_5C_5)(PMe_3)Ir(C_6H_{11})(H)$ at 145 °C in cyclohexane-d_{12} in the presence of ethylene-d_2 allowed observation of the competition between insertion into a C-H or into a C-D bond in the same molecule (an intramolecular isotope effect). For example, reaction with ethylene-1,1-d_2 results in a mixture of $(\eta^5\text{-}Me_5C_5)(PMe_3)Ir(DC{=}CH_2)(D)$ (**A**) and $(\eta^5\text{-}Me_5C_5)(PMe_3)Ir(HC{=}CD_2)(H)$ (**B**). The use of ^2H NMR allowed us to determine the relative amounts of deuterium in each position, thus allowing us to determine the relative amounts of **A** and **B** formed (Scheme 2.9). In Figure 2.8 is shown a representative ^2H NMR spectrum of the vinyl region.

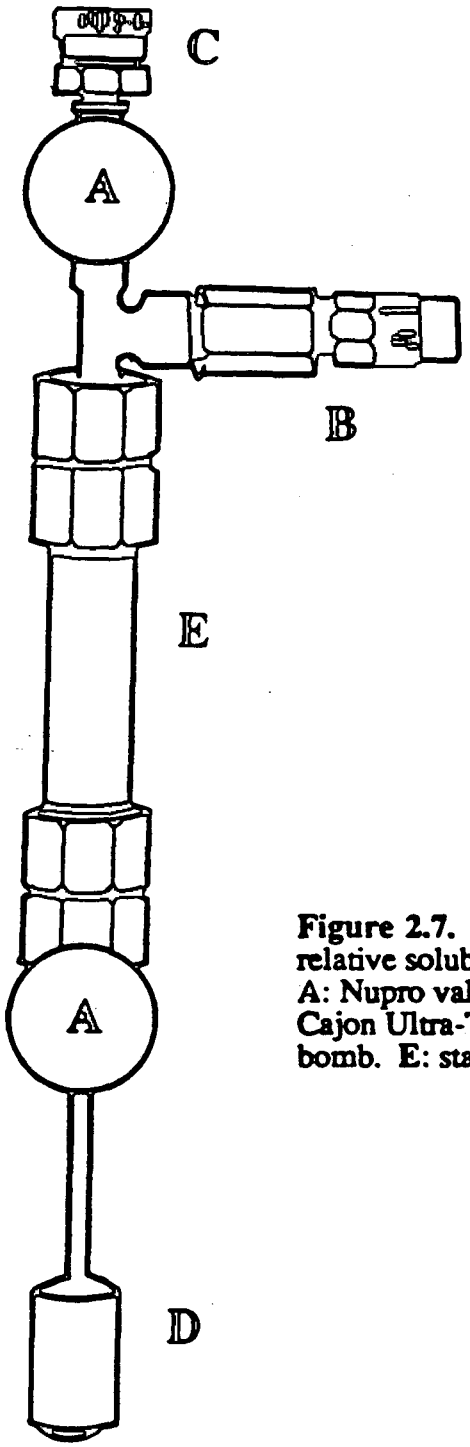

Figure 2.7. Appartus used to measure the relative solubilities of $H_2C{=}CH_2$ and $D_2C{=}CD_2$. A: Nupro valves. B: pressure release valve. C: Cajon Ultra-Torr fitting. D: stainless steel bomb. E: stainless steel tubing.

Scheme 2.9

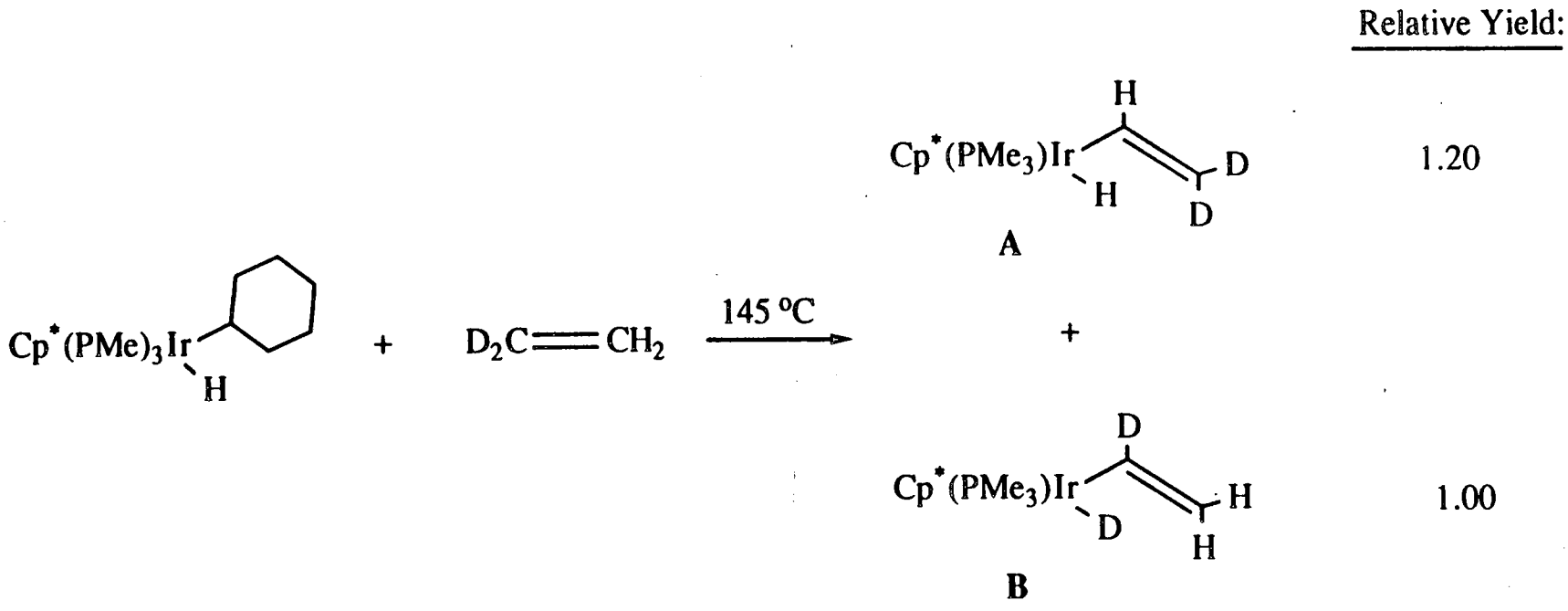
Relative Yield:
Cp*(PMe)3Ir
H
+
D2C=CH2
145 °C
Cp*(PMe3)Ir
H
H
D
D
A
1.20
+
Cp*(PMe3)Ir
D
D
H
H
B
1.00

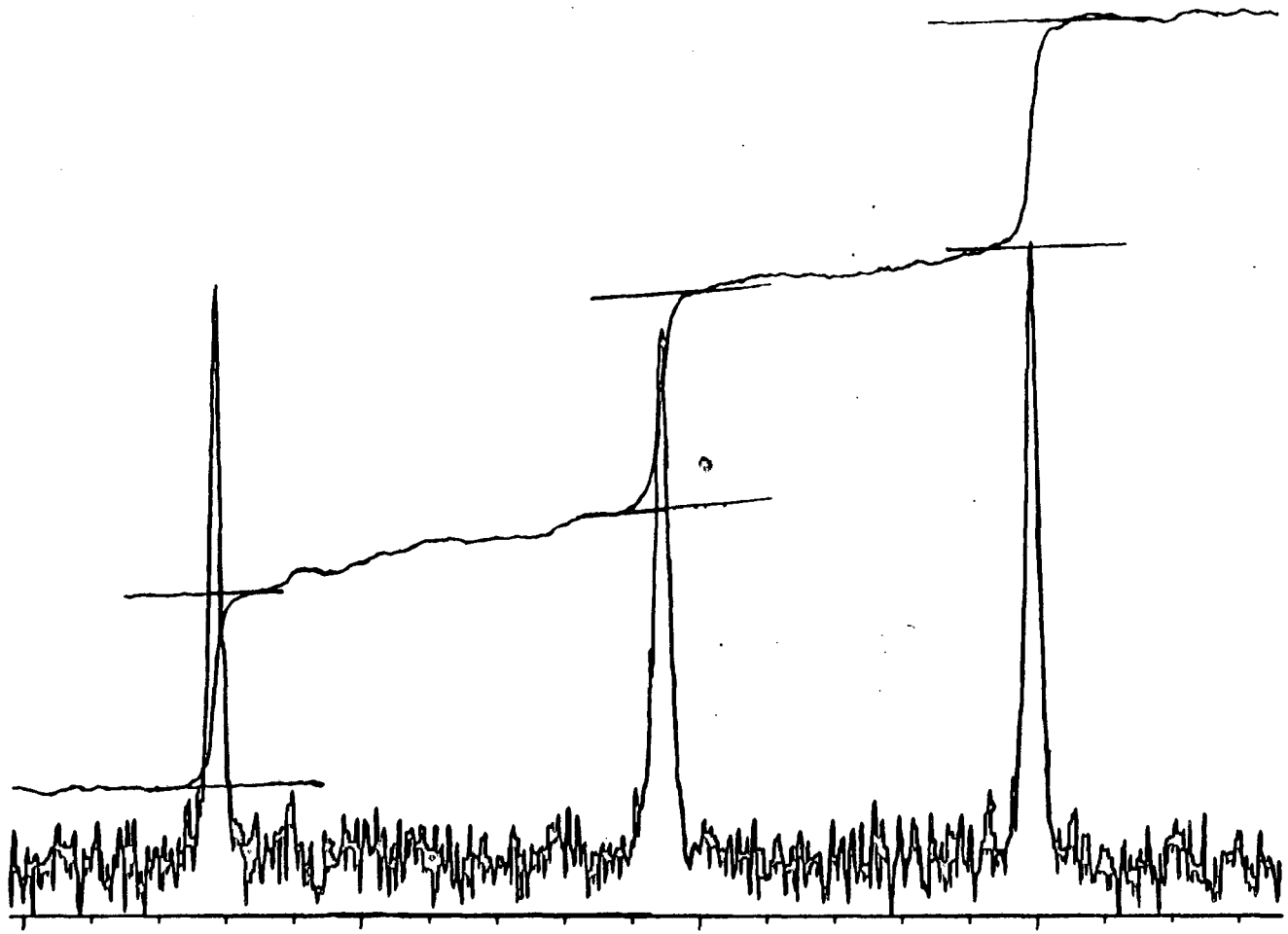

Figure 2.8. The vinyl region of the ^2H NMR of a reaction mixture resulting from the thermolysis of $(\eta^5\text{-}Me_5C_5)(PMe_3)Ir(C_6H_{11})(H)$ in the presence of ethylene-1,1-d_2.

In three separate reactions with ethylene-1,1-d_2 we observed that the ratio of **A** to **B** was independent of the length of the thermolysis (between 10 and 24 h), suggesting that the ratio observed was under kinetic control. This did not preclude, however, a fast process (compared to the overall reaction rate) in which hydrogen and deuterium atoms were exchanged between the vinyl group and the metal.[34] In this case the ratio of **A** to **B** would reflect a thermodynamic isotope effect. In order to examine this possibility, we synthesized (η^5-Me_5C_5)(PMe_3)Ir(HC=CH_2)(D), to look for exchange of the deuterium label into the vinyl group. Thermolysis at temperatures up to those at which conversion to **2** took place revealed no scrambling of the deuterium into the β-position of the vinyl group, as determined by ^{2}H NMR. A small amount of scrambling (< 10 %) was occasionally observed into the α-position. This was not uniformly repeatable, and we therefore conclude it is a process catalyzed by adventitious impurities.[35] This result indicates that the position of the deuterium in (η^5-Me_5C_5)(PMe_3)Ir(HC=CH_2)(D) is not under thermodynamic control; the intramolecular isotope distribution is kinetically controlled.

Because the products are formed under kinetic control, the final relative concentrations of **A** and **B** can be used to calculate the relative rates of insertion into the C-H and C-D bonds. In Table 2.4 the intramolecular isotope effects are compiler for reaction with ethylene-d_2.

We found that if care was taken, each integration of the ^{2}H NMR was accurate to ± 5 %. This leads to an error in k_H/k_D for each experiment of ± 0.08. We gained further confidence in our numbers by making sure that each experiment was internally consistent. To do this we integrated the different vinyl resonances against each other, and against the hydride resonance Within experimental error, the isotope effects were independent of the resonances chosen for comparison.[36] Comparisons between the vinyl resonances typically showed less scatter, and thus were used for the k_H/k_D values shown in Table 2.4. Averaging the values shown reduces our random error, resulting in a final value of 1.18 ± 0.03.

Table 2.4. Intramolecular isotope effects for formation of **1**.

Ethylene-d_2	k_H/k_D
ethylene-1,1-d_2	1.13 1.20 1.20
cis-ethylene-1,2-d_2	1.17
trans-ethylene-1,2-d_2	1.21

Discussion of Isotope Effects

The intermolecular isotope effects we observed are kinetic isotope effects, as the products are completely stable to the reaction conditions. The effects are much smaller than the maximum values for kinetic isotope effects, but are consistent with other observations. The isotope effect observed upon oxidative addition of cyclohexane to "(η^5-Me_5C_5)(PMe_3)Ir" was found to be 1.38.[37] The intermolecular isotope effect for insertion into a C-H bond of benzene by "(η^5-Me_5C_5)(PMe_3)Rh" was found to be 1.05.[38] In this case, it was discovered that the intramolecular isotope effect (found by using 1,2,3-d_3-benzene) was significantly larger (1.4). Small isotope effects such as these have typically been considered to be associated with either a very early transition state, in which little C-H bond breakage has occurred, or with a non-linear transition state. It is difficult to predict the geometry of the transition state, but the high exothermicity of the C-H insertion reaction between "(η^5-Me_5C_5)(PMe_3)Ir" and $H_2C{=}CH_2$ (ca. 40 kcal/mol) does predict an early transition state.

As no C-H bonds are broken in the formation of (η^5-Me_5C_5)(PMe_3)Ir($H_2C{=}CH_2$), the isotope effect observed is a secondary effect. Secondary effects are typically caused by rehybridization of C-H bonds, which when changing from sp^2 to sp^3 results in a loosening of the C-H bending modes.[39] This change in the bending frequency is different for C-H and C-D bonds, giving rise to an isotope effect. The carbons in the ethylene ligand of

(η^5-Me_5C_5)(PMe_3)Ir($H_2C{=}CH_2$) are not sp^3 hybridized, but are probably significantly perturbed from free ethylene. The X-ray structure of a related compound, (η^5-Me_5C_5)($P(C_6H_5)_3$)Rh($H_2C{=}CH_2$),[40] shows a lengthening of the C-C bond, and a bending back of the C-H bonds, consistent with a significant contribution from a metallacyclopropane resonance form. Our spectroscopic data are consistent with this formulation.

The size of the isotope effect observed when sp^2 carbons are changing to sp^3 carbons depends on the nature of the transition state, and on the number of hydrogen atoms attached to the carbon undergoing rehybridization. Reasonable estimates can often be made for simple systems by considering the changes in the bending force constants.[39] Some literature precedent for organometallic systems is available, but the values known are thermodynamic (K_H/K_D as opposed to k_H/k_D) isotope effects. For example, the thermodynamic isotope effect for the addition/elimination of ethylene/ethylene-d_4 from Ag^+ was found to be 0.89.[41] Since interactions of alkenes with Ag^+ consist almost entirely of donation of electron density from the alkene to the metal center, it is likely that the ethylene ligand is perturbed only slightly from that found in the free ligand. If it were possible to measure the thermodynamic isotope effect for binding of ethylene/ethylene-d_4 to "(η^5-Me_5C_5)(PMe_3)Ir", it would undoubtedly be larger.

Comparison of Inter- and Intramolecular Isotope Effects

The values found for the isotope effect for insertion into a C-H bond are similar to those found earlier for alkanes; the distinguishing factor, however, is that the inter- and intramolecular kinetic isotope effects are not equivalent. The only way to reconcile such a difference is to propose that there is an intermediate on the reaction pathway from which partitioning can occur. In the present case, this means that there is an intermediate of the stoichiometry [(η^5-Me_5C_5)(PMe_3)Ir · ($H_2C{=}CH_2$)] which is formed upon reaction with

ethylene (an intermolecular reaction) and can then go on to insert into any of the four C-H bonds (a unimolecular, intramolecular reaction).

This accommodates having different intra- and intermolecular isotope effects in the following way. In the first step "(η^5-Me_5C_5)(PMe_3)Ir" can compete for any of the ethylenes present. The relative rate of formation of insertion products formed with $H_2C{=}CH_2$ and $D_2C{=}CD_2$ will be affected by the rate of reaction with ethylene/ethylene-d_4 (the intermolecular step), and/or the rate of the actual insertion (the intramolecular step), depending on the relative rates. An intermolecular competition experiment thus potentially provides information on both steps of the reaction. When a partially labeled ethylene such as ethylene-d_2 is used, only one intermediate [(η^5-Me_5C_5)(PMe_3)Ir · ($C_2H_2D_2$)] can result. This, however, can lead to both C-H and C-D insertion products. The isotope effect observed with a partially deuterated ethylenes thus reflects the isotope effect of the second step. Our system is more complex than this however, as isotopic substitution also affects another pathway, formation of (η^5-Me_5C_5)(PMe_3)Ir($H_2C{=}CH_2$).

As mentioned above, different inter- and intramolecular isotope effects were also observed in the reaction of benzene with "(η^5-Me_5C_5)(PMe_3)Rh". In this case the intermolecular isotope effect was very small (1.05), indicating that little C-H bond breakage was occurring in the first step. Use of 1,3,5-d_3-benzene allowed determination of the isotope effect for the second step, insertion into the C-H bond. This isotope effect was found to be larger, $k_H/k_D = 1.4$. It was proposed that the first step resulted in production of an η^2-arene complex. Such a complex would have C-H bonds very similar to those found in benzene, and this could account for the small isotope effect observed. The second step would then involve insertion into one of the C-H bonds, which would be expected to have a larger isotope effect as a C-H bond was being broken (Scheme 2.10). In our system, the ethylene π-complex cannot be an intermediate--it is stable to the reaction conditions. Later we will return to the nature of the intermediate in our system.

Scheme 2.10

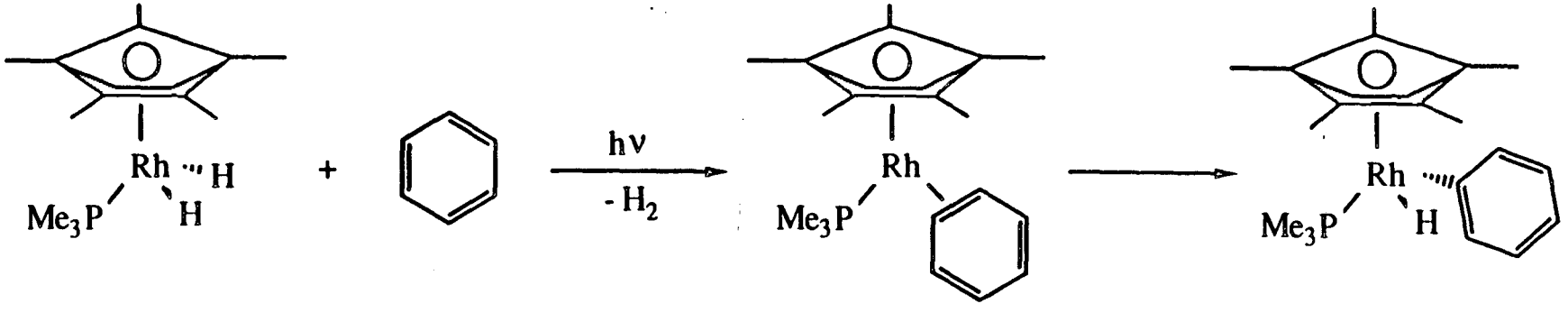

Since two products are formed in the activation of ethylene by iridium, the analysis of the isotope effects is more complex, but potentially more informative. The significance of the intermolecular isotope effect is not clear because we do not know (referring to Scheme 2.11) if it reflects (a) just the selectivity of the first step (k_1 rate determining), (b) the selectivity of the first step and the insertion step (k_1 and k_2 competitive), or (c) the thermodynamic selectivity of the first step followed by the insertion step (a preequilibrium k_1/k_{-1}, followed by a rate determining step k_2). By combining the information from the intermolecular competition experiment with the isotope effect for π-complex formation and the intramolecular isotope effect, we can determine the effect of isotopic substitution on each step of potential reaction mechanisms. Any reaction mechanism we might consider must at least satisfy the requirement that an intermediate lie on the reaction pathway leading to $(\eta^5\text{-}Me_5C_5)(PMe_3)Ir(HC{=}CH_2)(H)$.

Two of the possible mechanisms are shown in Scheme 2.12. Let us first consider Mechanism A. Here the intermediate formed upon reaction of ethylene with "$(\eta^5\text{-}Me_5C_5)(PMe_3)Ir$" can go on to insert into any of the C-H bonds or can form the π-complex. Summarized in Scheme 2.13 are the rate constants involved in this mechanism, and the relative amounts of products formed in the intermolecular competition experiment. Comparing the relative amounts of products derived from reaction with $H_2C{=}CH_2$ with those from reaction with $D_2C{=}CD_2$ allows us to determine the isotope effect ($[k_H/k_D]_1$) for the first step in the reaction (Equation 2.1).

$$[k_H/k_D]_1 = (18 + 35) / (22 + 25) = 1.16 \qquad (2.1)$$

From the intramolecular competition experiment we know that the isotope effect associated with insertion into a C-H(D) bond (k_V^H/k_V^D) is 1.18. This allows us to determine the isotope effect associated with formation of the π-complex from the

Scheme 2.11

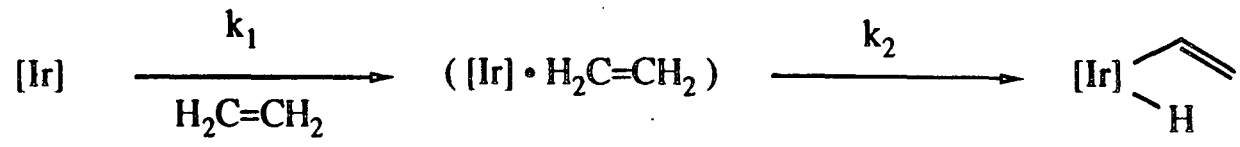

[Ir] = $Cp^*(PMe_3)Ir$

Scheme 2.12

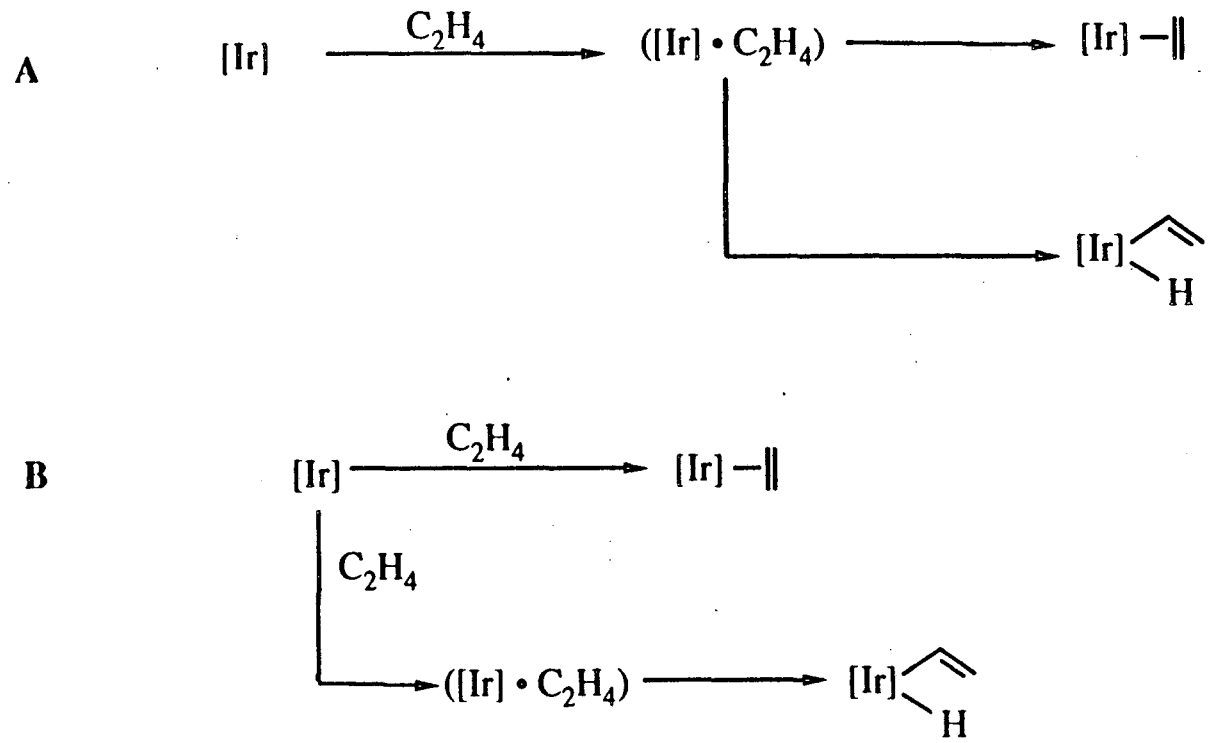

[Ir] = $Cp^*(PMe_3)Ir$

Scheme 2.13 (Mechanism A)

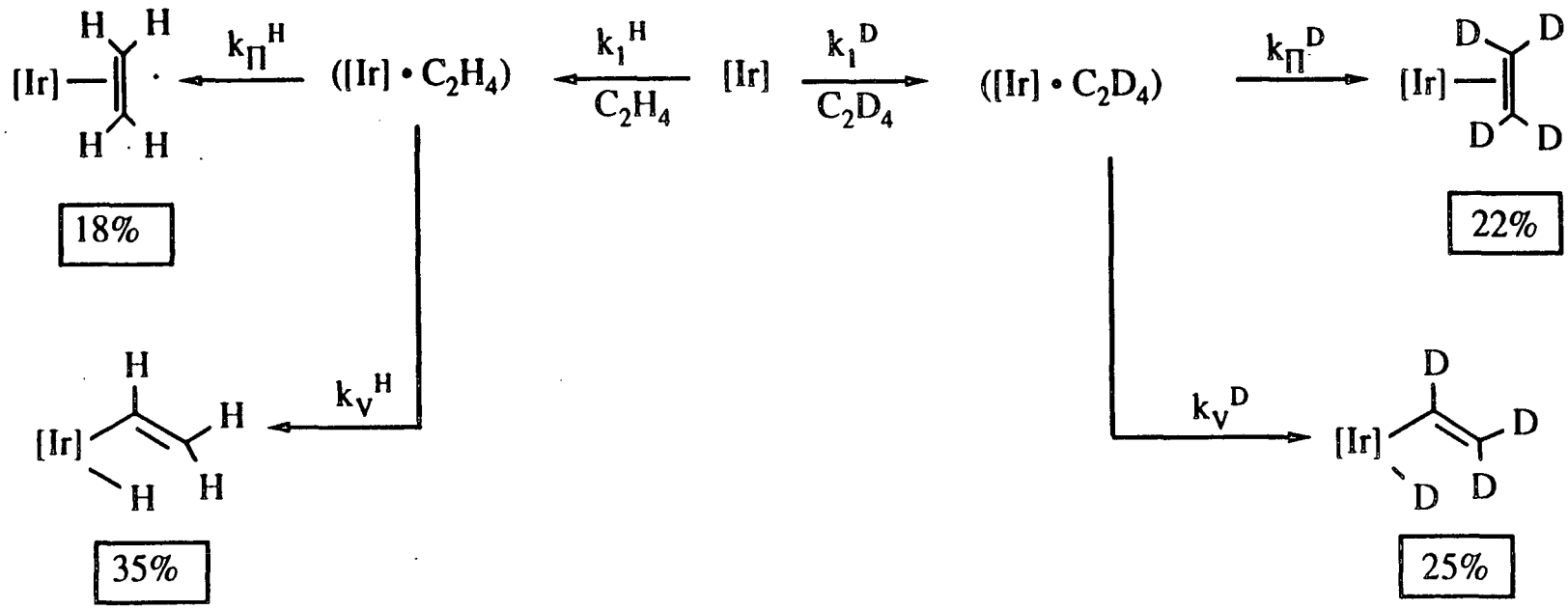

intermediate (k_π^H/k_π^D). Because we know how the intermediate partitions between (η^5-Me_5C_5)(PMe_3)Ir(HC=CH_2)(H) and (η^5-Me_5C_5)(PMe_3)Ir(H_2C=CH_2) (k_V/k_π), we can solve for $[k_H/k_D]_\pi$ in the following way (Equations 2.2 - 2.5).

$$([k_H]_V / [k_H]_\pi) \cdot ([k_D]_\pi / [k_D]_V) = (35/18) \cdot (22/25) = 1.84 \quad (2.2)$$

$$(k_V^H/k_V^D) \cdot (k_\pi^D/k_\pi^H) = 1.84 \quad (2.3)$$

$$(1.18) \cdot (k_\pi^D/k_\pi^H) = 1.84 \quad (2.4)$$

$$(k_\pi^H/k_\pi^D) = 0.64 \quad (2.5)$$

Mechanism **B** is distinct from Mechanism **A** in that (η^5-Me_5C_5)(PMe_3)Ir(H_2C=CH_2) is formed directly from "(η^5-Me_5C_5)(PMe_3)Ir" and H_2C=CH_2 in Mechanism **B**. In Scheme 2.14 are again summarized the appropriate rate constants and relative amounts of products found in the intermolecular competition experiment. Here, as in Mechanism **A**, the intramolecular isotope effect $k_V^H/k_V^D = 1.18$. In this case, however, the isotope effect on formation of (η^5-Me_5C_5)(PMe_3)Ir(H_2C=CH_2) is simply the amount of (η^5-Me_5C_5)(PMe_3)Ir(H_2C=CH_2) (18 %) divided by the amount of (η^5-Me_5C_5)(PMe_3)Ir(D_2C=CD_2) (22 %): $k_\pi^H/k_\pi^D = 0.80$. Similarly, the isotope effect on formation of the intermediate (k_1^H/k_1^D), is simply the ratio of (η^5-Me_5C_5)(PMe_3)Ir(HC=CH_2)(H) to (η^5-Me_5C_5)(PMe_3)Ir(DC=CD_2)(D): $k_1^H/k_1^D = 35/25 = 1.49$. A summary of the isotope effects derived for Mechanism **A** and **B** are give in Table 2.5. It is possible in either mechanism, that the k_1 step is reversible. If k_{-1} were sufficiently fast, the isotope effect found for the first step would not be a kinetic isotope effect, but a thermodynamic effect.

Scheme 2.14 (Mechanism B)

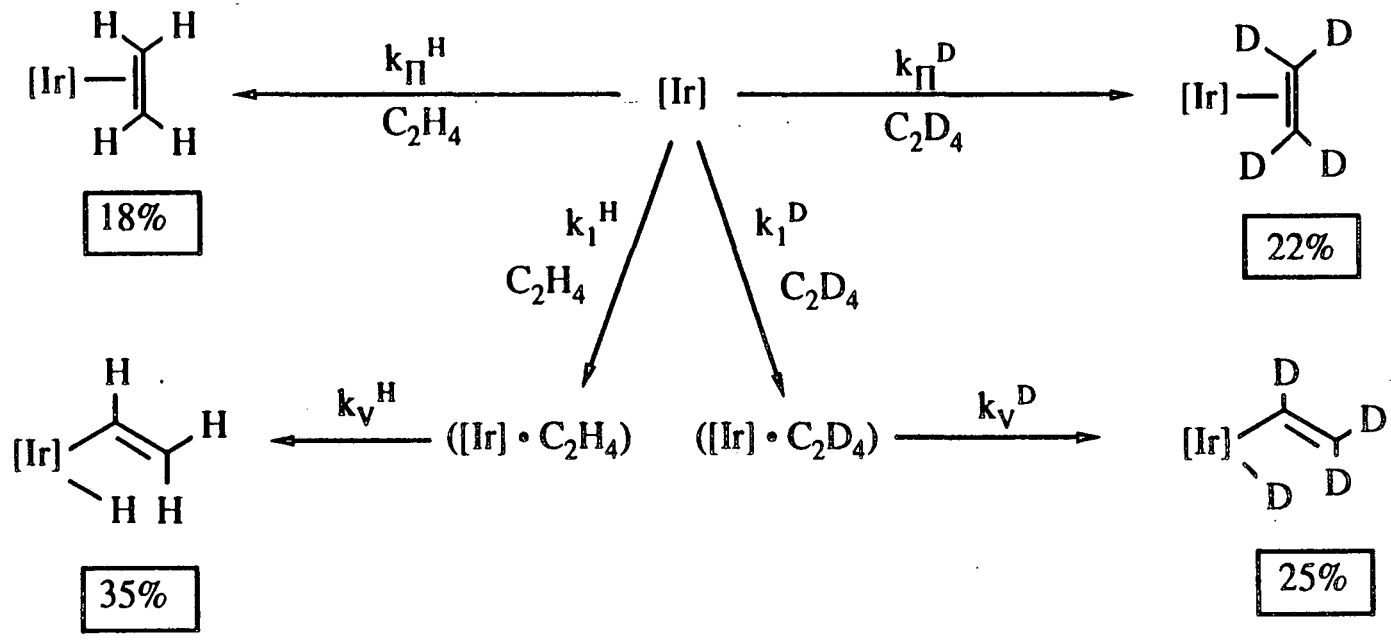

Table 2.5. A summary of the individual isotope effect for Mechanisms **A** and **B**.

Step	k_H/k_D (Mech. A)	k_H/k_D (Mech. B)
k_1	1.16	1.49
k_V	1.18	1.18
k_π	0.64	0.80

The Nature of the Intermediate

From thermochemical and kinetic experiments discussed earlier, we can make good estimates for the energy of this intermediate relative to the starting materials and products. Our calorimetric studies (vide supra) suggest that $(\eta^5\text{-}Me_5C_5)(PMe_3)Ir(HC{=}CH_2)(H)$ lies 46 kcal/mol lower in energy (ΔH) than "$(\eta^5\text{-}Me_5C_5)(PMe_3)Ir$" and free ethylene. The small kinetic selectivities we observe for the intermediate suggests to us that the barrier for oxidative addition is 2 - 5 kcal/mol. Our activation energy experiments require that the transition state leading from **1** to **2** lie 35 kcal/mol above **1**. Furthermore, upon thermolysis of $(\eta^5\text{-}Me_5C_5)(PMe_3)Ir(HC{=}CH_2)(D)$, no scrambling of the deuterium into the vinyl group is seen up to temperatures at which conversion to **2** is seen. This indicates that the intermediate responsible for the different inter- and intramolecular isotope effects must lie <u>higher</u> than 35 kcal/mol above **1** (Figure 2.9).

The potential energy surface describing this reaction is much different from that found by Jones for the reaction of "$(\eta^5\text{-}Me_5C_5)(PMe_3)Rh$" with benzene. In the reaction of "$(\eta^5\text{-}Me_5C_5)(PMe_3)Rh$" with benzene, it has been demonstrated that the η^2-arene complex is an intermediate on the pathway leading to C-H bond activation. Indeed, this intermediate was shown to be ca. 20 kcal/mol less stable that $(\eta^5\text{-}Me_5C_5)(PMe_3)Rh(C_6H_5)(H)$. In our case, however, the η^2-olefin complex is <u>more</u> stable than the C-H insertion product. This change in the relative stability of the η^2-complex could be caused either by the products being of much different stabilities, or by different relative stabilities of the η^2-complexes. Thermodynamic studies conducted on the

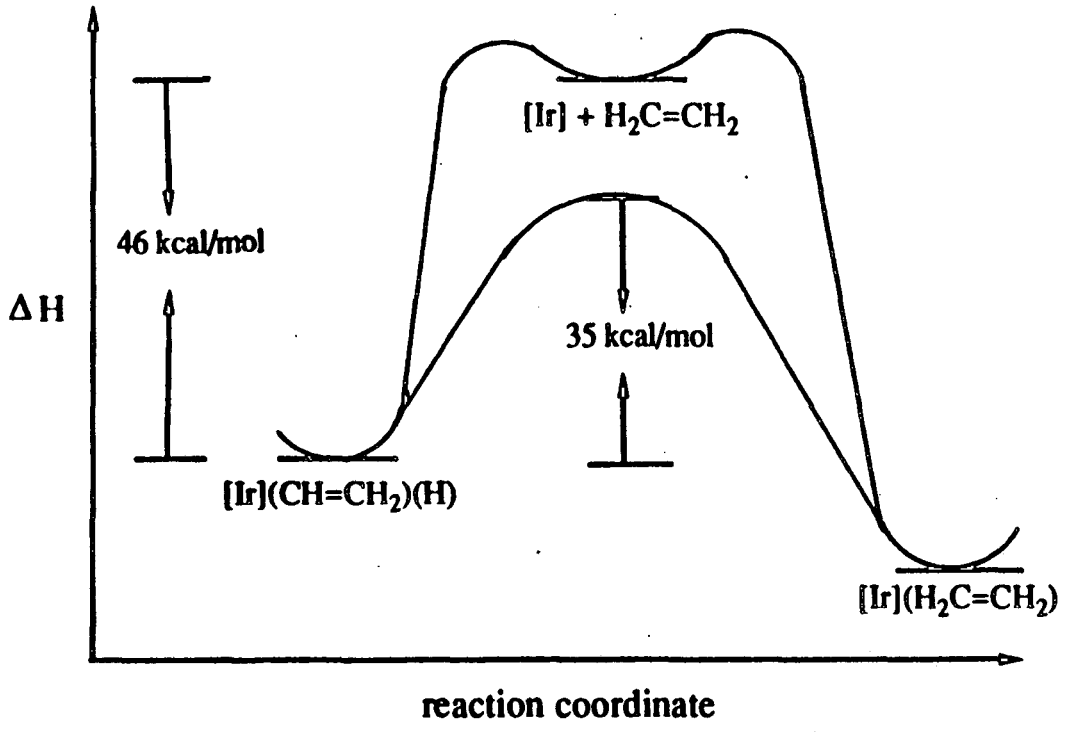

Figure 2.9. Proposed approximate reaction coordinate diagram for the reaction of "(η^5-Me_5C_5)(PMe_3)Ir" with ethylene, and the conversion of **1** to **2**.

iridium system predict that the phenyl hydride and the vinyl hydride for a given system should be of comparable stability, indicating that the η^2-complex is responsible for the different ordering of stabilities. This is indeed reasonable, as one would predict that the loss of resonance energy during formation of an η^2-arene complex, as well as a larger steric demand, would tend to destabilize it relative to an η^2-olefin complex.

Because the ethylene π-complex is stable to the reaction conditions, we propose that the intermediate required by our isotope studies is a metastable species formed by weak coordination of one or more ethylene C-H bonds to the iridium center. For reasons of brevity, we refer to this species as a σ-complex (interacting through the σ-bonds of ethylene as opposed to the π-bond); analogous intramolecular species have been referred to as having "agostic" interactions.[9] There are a variety of possibilities for the structure of the σ-complex intermediate (Figure 2.10). We had hoped that experiments using the different d_2-ethylenes would exhibit different intramolecular isotope effects which might have led us to favor one of these intermediates. For example, if an intermediate of type A (Figure 2.10), formed by reaction with 1,1-d_2-ethylene, could only insert into the two C-H bonds near the metal center, we would anticipate an isotope effect different from that found for 1,2-cis-d_2-ethylene. Furthermore, if in this intermediate the iridium center were not able to insert into the distant C-H bonds , the isotope effect observed would be the same as that seen for <u>intermolecular</u> competition experiment (no competition is present in the second step). A similar situation exists for intermediates of type B when the ethylene used is 1,2-cis-d_2-ethylene. Our equivalent intramolecular isotope effects, which are different from the intermolecular effect, indicate that if only <u>one</u> intermediate is present, it must be able to choose between all four C-H bonds.

Other possibilities that we cannot rule out are mechanisms in which more than one intermediate is formed. One of the simplest of these is a mechanism in which two intermediates are formed, and that each of them can insert into either of two C-H bonds (Scheme 2.15). Because of the equivalent isotope effects observed with ethylene-1,1-d_2,

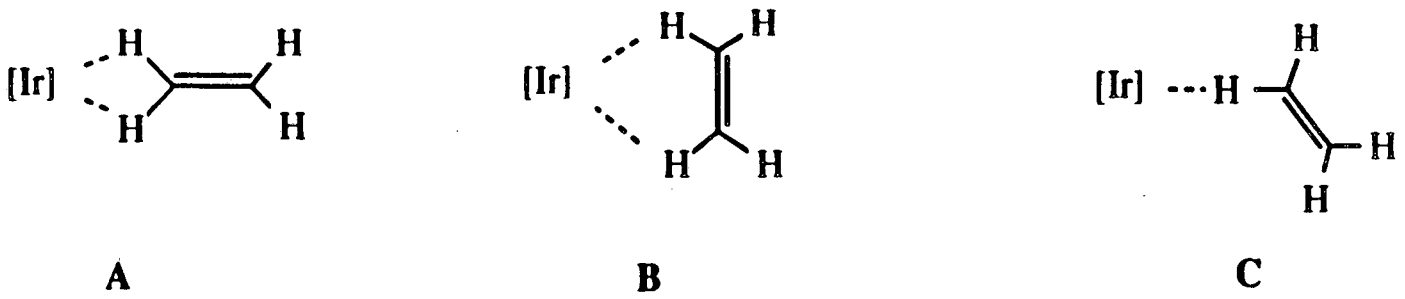

Figure 2.10. Possible structures for the intermediate on the pathway leading to C-H bond insertion.

cis-ethylene-1,2-d_2, and *trans*-ethylene-1,2-d_2 however, **A** and **B** must be formed in approximately equal amounts. For example, if only intermediate **B** was formed upon reaction with *cis*-ethylene-1,2-d_2, no partitioning would be possible in the second step (k_{2b}). Thus the intramolecular isotope should be of the same magnitude as the intermolecular effect--it is not. Unfortunately, due to the complexity of mechanisms with two or more intermediates, it is difficult to consider the effect of isotope substitution on each step. Despite the increase complexity of the mechanism shown in Scheme 2.15, we feel it provides a reasonable alternative to mechanisms with one intermediate (Schemes 2.13 and 2.14). Intermediates similar to **A** and **B** have recently been proposed in rearrangements involving alkyl hydrides between hydrogens bound to the metal with those on an α-carbon (Scheme 2.16).[42]

σ-Complex intermediates such as those discussed here have been proposed earlier. Upon co-condensation of iron atoms and ethylene in a matrix, ethylene-iron adducts are formed which upon irradiation isomerize to $(H)Fe(HC{=}CH_2)$.[43] Based on infrared evidence which indicated a weakening of a C-H stretching vibration, the structures shown in Scheme 2.17 were proposed. In addition, ab inito calculations in which the energy surface for $M(CH_3)(H)$ ----> $M + CH_4$ (M = Pd, Pt), was explored, have shown an energy minimum corresponding to methane σ-complexes in which more than one C-H bond simultaneously interacts with the metal.[44]

Conclusions

These results constitute one of the first direct observations of insertion into the C-H bonds of unactivated olefins. Along with more recent studies of similar systems, our experiments show that at least in cases where the vinyl hydride is stable, it is the predominant, if not the exclusive, kinetic product. Furthermore, in all of the studies the olefin π-complex was found to be the thermodynamically preferred product. This suggests that vinyl hydrides may not be as predominant in the chemical literature for thermodynamic

Scheme 2.15

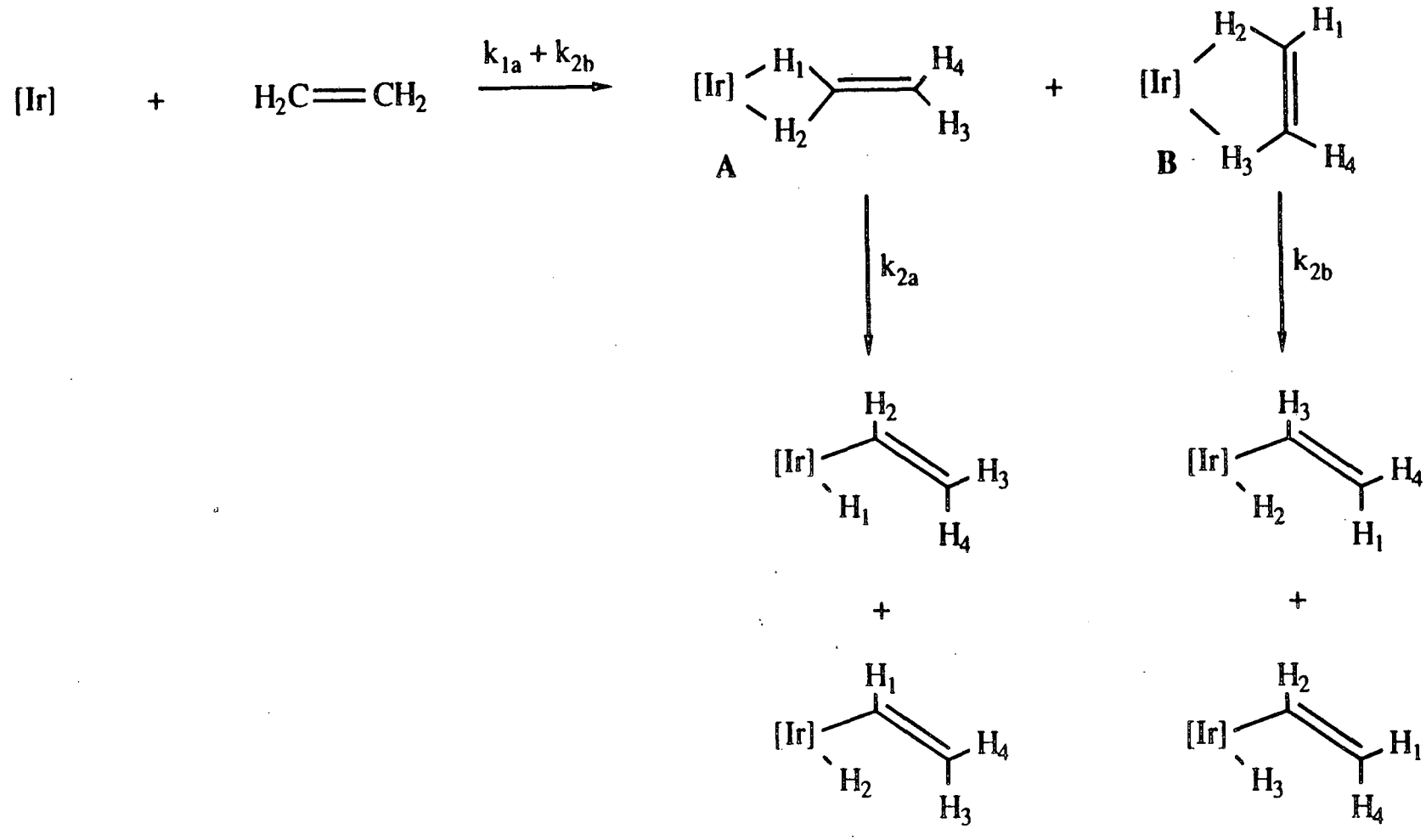
[Ir]
+
H2C=CH2
k1a + k2b
[Ir]
H1
H2
H4
H3
A
+
[Ir]
H2
H1
H3
H4
B
k2a
k2b
[Ir]
H2
H1
H3
H4
+
[Ir]
H1
H2
H4
H3
[Ir]
H3
H2
H4
H1
+
[Ir]
H2
H3
H1
H4

Scheme 2.16

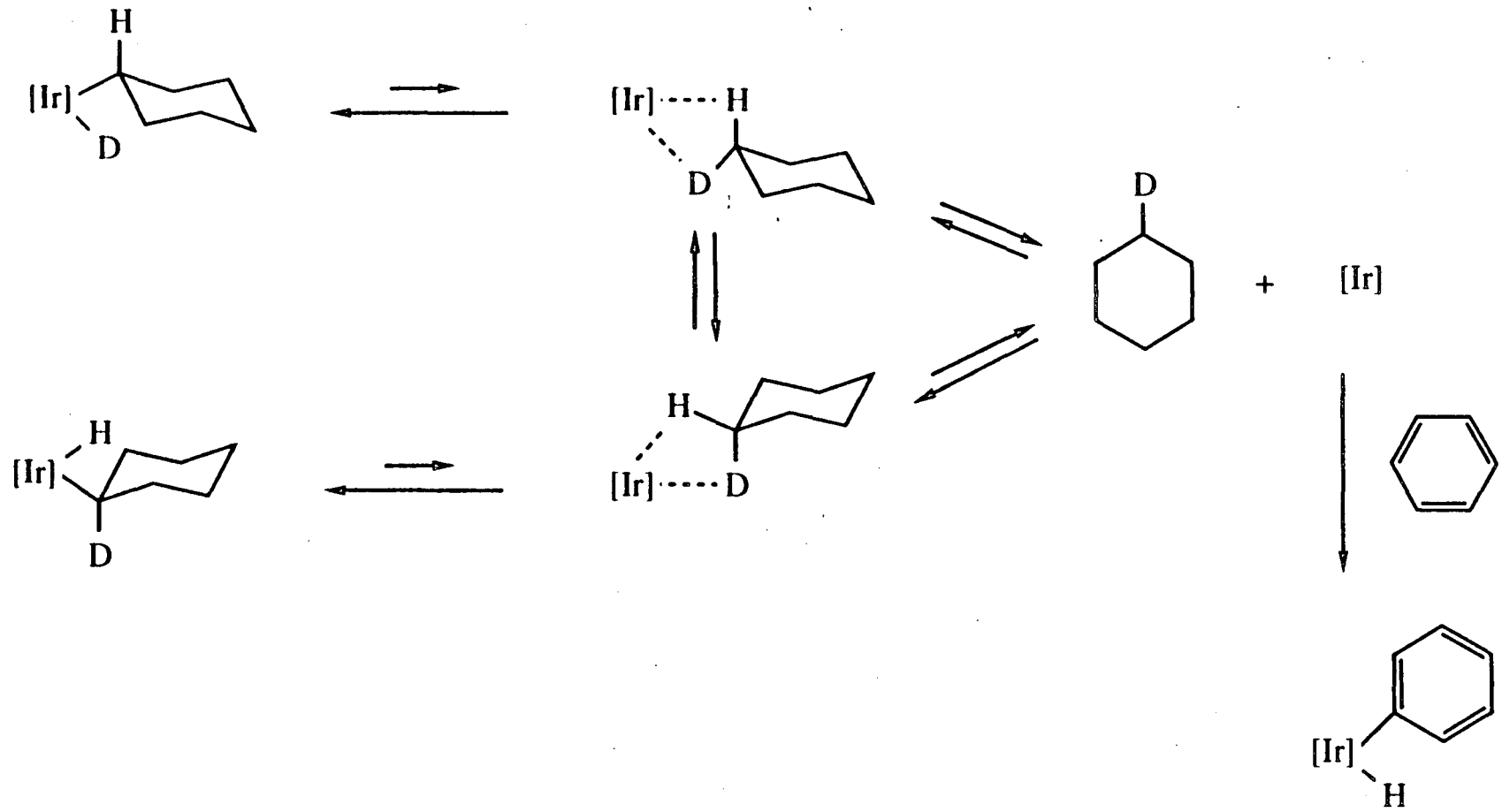

Scheme 2.17

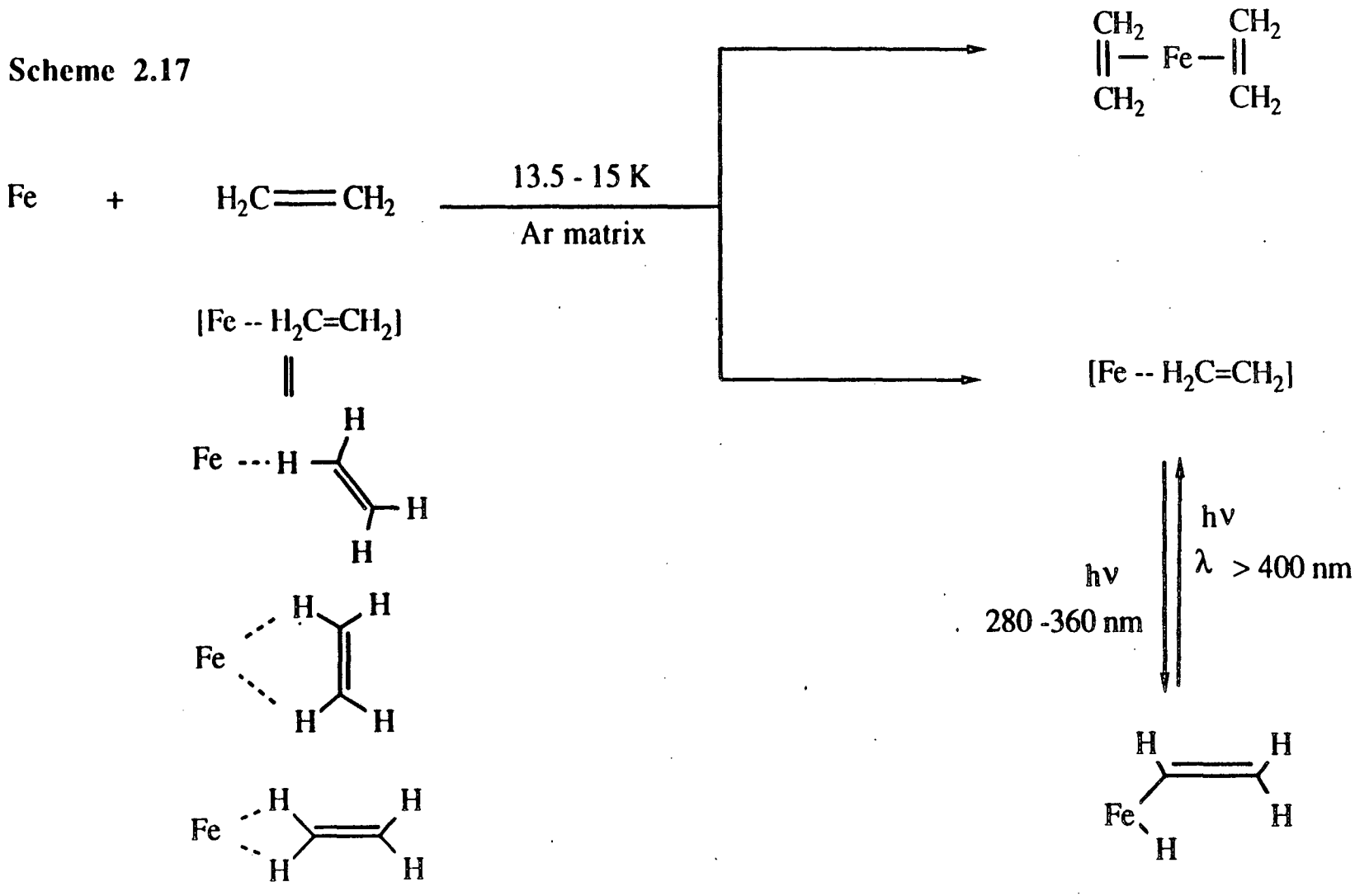
Fe
+
$H_2C{=}CH_2$
13.5 - 15 K
Ar matrix
CH_2
Fe
CH_2
$[Fe -- H_2C{=}CH_2]$
$[Fe -- H_2C{=}CH_2]$
Fe
H
hν
λ > 400 nm
hν
280 -360 nm
Fe
H

reasons, and that there may be examples where vinyl hydrides are kinetically important intermediates on the pathway leading to formation of olefin complexes. This may be especially important for the later transition elements which are known to be capable of oxidative addition.

It is also important to consider the relative barriers to C-H activation and π-complex formation. In all of the cases where intermolecular insertion into the C-H bonds of unactivated alkenes has been observed, the metal containing species is a highly unstable, unsaturated metal fragment. In our system, for example, "(η^5-Me_5C_5)(PMe_3)Ir", formed by reductive elimination of cyclohexane from (η^5-Me_5C_5)(PMe_3)Ir(C_6H_{11})(H), cannot exist in the square planar geometry normally preferred by Ir(I) due to restrictions imposed by the cyclopentadienyl ligand. The high energy of intermediates such as these results in a lowering of the barrier to C-H insertion, and is also one of the reasons they form very strong M-C and M-H bonds. It is not clear, however, that more stable organometallic fragments, many of which form π-complexes, are capable of overcoming the barrier to C-H insertion. Thus, while it is tempting to speculate that many reactions between olefins and transition metal complexes go via metal-vinyl species which rearrange to the more stable η^2-olefin complexes, olefin complex formation may be kinetically favored relative to C-H insertion for less reactive metal complexes.

The thermodynamic stability of olefin complexes has been shown to be particularly sensitive to steric effects.[5] The kinetic barriers for formation of these complexes are also sensitive to steric effects. Considering the three systems known to be capable of both C-H insertion and π-complex formation,[21] is the least sterically demanding of the three, the iridium complex, that gives rise to the largest amount of olefin complex formation. Extended Huckel calculations of the reaction of "(η^5-Me_5C_5)(PMe_3)Ir" with ethylene, predict that while the enthalpic barrier to formation of (η^5-Me_5C_5)(PMe_3)Ir($H_2C{=}CH_2$) may be very small, its rate of formation is likely to be strongly influenced by the sterically demanding pentamethylcyclopentadienyl ligand.[45] This suggests that metal-vinyl species

may be especially important intermediates when the metal is in a sterically demanding environment.

While there is good evidence that many catalytic processes go via metal-olefin π-complexes, evidence for metal-vinyl intermediates in some processes is beginning to accumulate. Faller and Felkin[46] have recently provided evidence for the intermediacy of metal-vinyl intermediates in H/D exchange reactions between benzene-d_6 and 3,3-dimethyl-butene catalyzed by $[(i\text{-}Pr_3P)_2IrH_5]$. In these experiments deuterium exchanged into the the position trans to the *tert*-butyl group ten times faster than exchange into the geminal position. This is not consistent with the traditional mechanism involving addition/elimination of the olefin, where there would be expected to be deuterium in both terminal positions and in the geminal position. The selectivity observed suggests a different mechanism, perhaps vinylic C-H activation, similar to the mechanisms proposed for arene H/D exchange (Scheme 2.18).

Kinetic evidence supports the intermediacy of metal-vinyl species in the formation of molybdenum metathesis catalysts.[47] The initial rates of propene metathesis were shown to be particularly sensitive to deuterium in the terminal position of the olefin. No isotope effect was observed for the rate of propene metathesis when propene was admitted onto a surface on which the carbene catalyst had earlier been formed. This was judged to be most consistent with a rate-determining formation of a metal vinyl hydride which then undergoes a hydrogen shift to give the species believed to be responsible for metathesis (Scheme 2.19). Similarly, there are other catalytic reactions in which one may wish to consider metal-vinyl complexes as viable intermediates.[48] Recently, studies of the interaction of olefins with single metal crystals have shown that metal-vinyl species may be formed here as well.[49]

Scheme 2.18

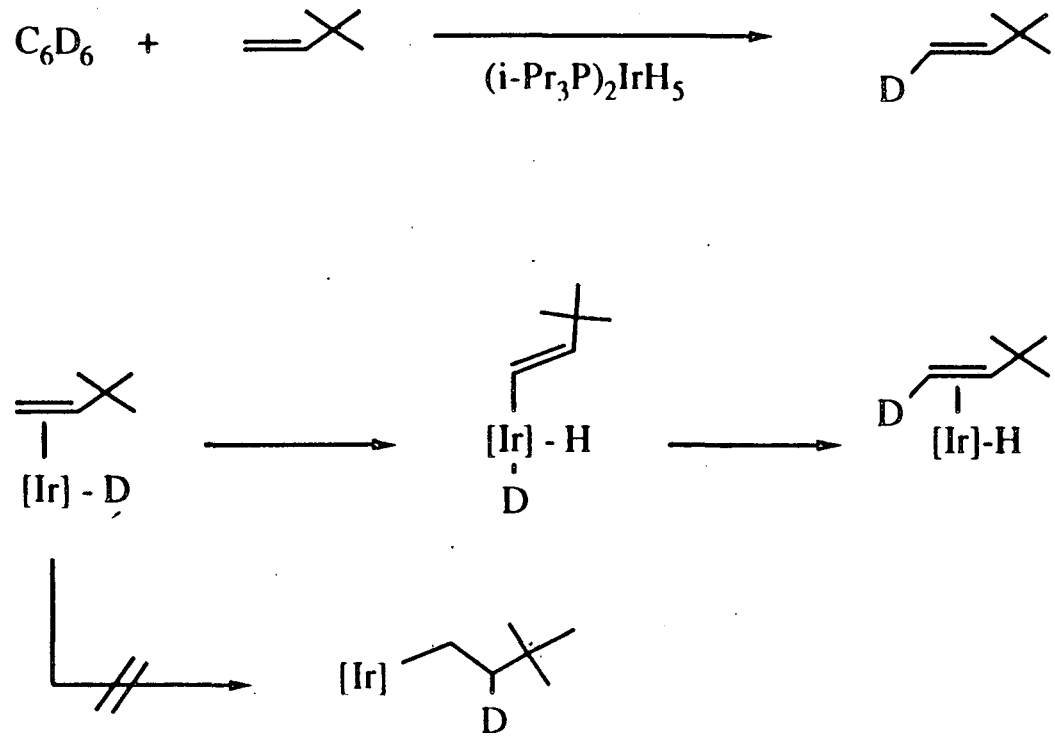

Scheme 2.19

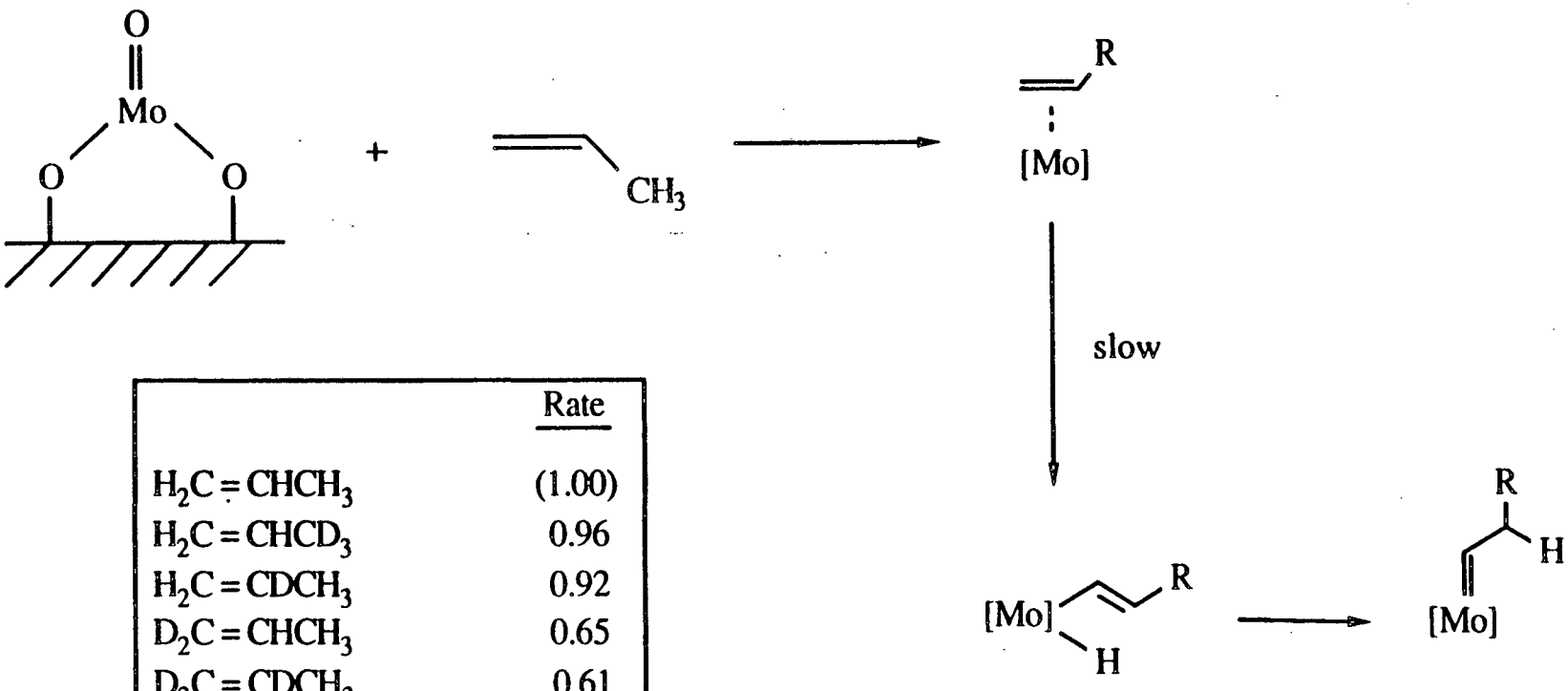

	Rate
$H_2C=CHCH_3$	(1.00)
$H_2C=CHCD_3$	0.96
$H_2C=CDCH_3$	0.92
$D_2C=CHCH_3$	0.65
$D_2C=CDCH_3$	0.61

Experimental

General. All manipulations were carried out under argon or nitrogen using standard Schlenk or vacuum line techniques, or under a nitrogen atmosphere in a Vacuum Atmospheres 553-2 Dri-lab equipped with an MO-40-1(2)Dri-train, unless otherwise stated. ^{1}H NMR spectra were obtained on a 300 MHz spectrophotometer constructed using a Cryomagnet Systems 300/50 7.05 T magnet and a Nicolet 1280 computer by Mr. Rudi Nunlist of the UCB NMR Facility. ^{13}C NMR and ^{31}P NMR spectra were obtained on the same instrument operating at 74.4 and 121.5 MHz, respectively. ^{2}H NMR spectra were obtained using a Bruker AM-500 spectrophotometer operating at 76.77 MHz. ^{1}H, ^{2}H, and ^{13}C chemical shifts were referenced to the chemical shift of the solvent used as found in Tables distributed by MSD Isotopes, and are reported in parts per million downfield from tetramethylsilane. ^{31}P NMR shifts were referenced to an external standard of 85% H_3PO_4 and are reported in parts per million downfield from H_3PO_4. All coupling constants are reported in Hertz. Infrared spectra were recorded on a Perkin-Elmer model 283 grating spectrophotometer, or on a Perkin-Elmer model 1550 Fourier transform spectrophotometer. Melting points were determined in sealed capillaries using a Thomas-Hoover melting point apparatus and are uncorrected. Elemental analyses were performed in the UCB elemental analysis facility. Mass spectroscopic analyses were obtained on an AEI MS-1 spectrophotometer interfaced with a Finnigan 2300 data system.

Pentane, hexane, and cyclohexane were spectral-grade and were distilled from $LiAlH_4$. THF, toluene, and benzene were spectral-grade and were distilled from Na/benzophenone. Ether was distilled from Na/benzophenone. Sodium borohydride and sodium borodeuteride (98% D) were purchased from Alpha and Aldrich Chemical Companies, respectively. Vinylmagnesiumbromide was purchased as a 1.0 M solution in THF from the Aldrich Chemical Co. $(\eta^5\text{-}Me_5C_5)(PMe_3)Ir(H)_2$,[50] $(\eta^5\text{-}Me_5C_5)(PMe_3)Ir(Cl)_2$,[51] and $(\eta^5\text{-}Me_5C_5)(PMe_3)Ir(C_6H_{11})(H)$[52] were prepared according to published procedures; the latter complex was purified by low-temperature

chromatography (vide post). PMe_3 was purchased from Strem Chemicals and was dried over a sodium mirror and then vacuum transferred.

Ethylene used was CP grade and was transferred to a glass vessel fitted with a teflon vacuum stopcock (#K-826500) where it was subjected to several freeze-pump-thaw cycles to remove any non condensible gases. Deuterated ethylenes were purchased in glass vessels from MSD Isotopes or from CIL, fitted with teflon vacuum stopcocks and thoroughly degassed. The identity of ethylene-h_4 and ethylene-d_4 were confirmed by mass spectroscopy. The identities of ethylene-1,1-d_2, *cis*-ethylene-1,2-d_2, and *trans*-ethylene-1,2-d_2 were confirmed by infrared spectroscopy, and were all > 98 % pure.[33] Gas quantities were measured using known-volume bulbs, and an MKS Baratron gauge to measure the pressure. The ideal gas law was used to determine the number of moles of gas present.

Benzene-d_6 was dried over Na/benzophenone. Cyclohexane-d_{12} was washed with a 2:1 mixture of HNO_3/H_2SO_4 to remove traces of benzene-d_6, and then washed with 25% NaOH and water. It was predried over $MgSO_4$, stirred over sodium/potassium alloy, and vacuum transferred into a glass vessel fitted with a teflon vacuum stopcock.

All kinetics and reactions performed over 130 °C were done in a factory calibrated Neslab EX-250HT high temperature bath accurate to 0.03 °C, and filled with Dow Corning 210H fluid. Photolyses were performed using a 450 W Conrad-Hanovia mercury immersion lamp in an Ace 7874B-38 immersion well. The immersion well was placed into a dewar filled with water cooled to 5 - 10 °C by a recirculating bath. The sample was typically irradiated in an NMR tube 2 inches from the light source.

The columns used in our laboratory for low temperature chromatography consist of a vacuum jacketed middle jacket which has a solvent reservoir at the top. Between the inner tube and the vacuum jacket is a space with an inlet at the top and at the bottom. The top of the column has a 24/40 female joint leading into the column, as well as an inlet for gas which is fitted with a Kontes 4 mm teflon stopcock (#K-826500). The bottom of the

column is also equipped with a vacuum stopcock which leads to a luer tip for connection to a syringe needle. The column is cooled by bubbling gaseous N_2 through a dewar of liquid N_2 and then through the middle jacket of the column. The temperature may be regulated by changing the rate of N_2 flow through the column. We have measured the temperature by inserting a thermocouple into the column, and have found that temperatures of -80 to -100 °C are easily attainable. The chromatography is performed under air-free conditions using Schlenk techniques, with detection by an MPLC UV detector (Altex model 153 fitted with a preparatory cell).

Silica gel (SiO_2) was purchased from EM Reagents, and was dried under vacuum at ca. 200 °C overnight. Alumina (Al_2O_3) was purchased from MCB Reagents and was deactivated to the appropriate grade by the addition of water as stated in The Chemists Companion.

Thermolysis of $(\eta^5\text{-}Me_5C_5)(PMe_3)Ir(HC{=}CH_2)(H)$. In a typical experiment 11.5 mg (0.0266 mmol) of $(\eta^5\text{-}Me_5C_5)(PMe_3)Ir(C_6H_{11})(H)$, and 2.7 μl of hexamethyldisiloxane (0.013 mmol) as an internal standard were dissolved in 0.433 g (0.485 mL) of C_6D_{12} in the dry box. This was put into a Wilmad 504PP NMR tube and sealed in vacuo. The tube was heated at 200.0 °C. The extent of reaction was monitored by comparison of the signals from the cyclopentadienyl ligand or from the PMe_3 ligand with those of the internal standard. During the reaction, it was clear that some (<5%) of the iridium containing material was decomposing to NMR-silent material. To minimize the effect of this on the kinetics, we estimated the concentration of the product at $t = \infty$. This was done by an iterative procedure on an IBM-PC whereby C_∞ was varied until the best correlation coefficient was found for a plot of $-\ln(C_\infty - C_t)$ vs time. The rates reported are those determined from the slope of the line resulting from a plot of $-\ln(C_\infty - C_t)$ vs. time. The slope of the line found in this manner lead to a rate constant of $3.49 \times 10^{-3}\ s^{-1}$ for this particular experiment ($r = 0.998$). A similar procedure was used for the other temperatures.

We have found it difficult to isolate analytically pure **2**. In contrast to the iridium alkyl hydride complexes, it moves only slowly on chromatography supports and elutes impure. In cases where the conversion of **1** to **2** is particularly clean, we have been able to isolate analytically pure (η^5-Me_5C_5)(PMe_3)Ir($H_2C{=}CH_2$) by high vacuum sublimation at slightly above ambient temperature, with the product being isolated as an amorphous solid. ^1H NMR (C_6D_6) δ 1.86 (d, η^5-Me_5C_5, $J_{P\text{-}H}$ = 1.5 Hz), 1.01 (d, PMe_3, $J_{P\text{-}H}$ = 9.0 Hz), 1.13, 1.27 (m, $H_2C{=}CH_2$); ^{13}C NMR (C_6D_6) δ 10.29 (q, η^5-$\underline{Me}_5C_5$, $J_{C\text{-}H}$ = 126.1 Hz), 90.19 (s, η^5-$Me_5\underline{C}_5$), 10.55 (dd, $H_2C{=}CH_2$, $J_{C\text{-}H1} = J_{C\text{-}H2}$ = 150.6 Hz), 16.93 (q, PMe_3, $J_{P\text{-}C}$ = 33.9 Hz), $J_{C\text{-}H}$ = 128.3 Hz); IR (C_6D_6) 2960 (s), 2900 (s), 1360 (s), 940 (s); MS (70 eV) 432 (M^+), 404 (M^+ - C_2H_4). Anal. Calcd: C, 41.75; H, 6.54. Found: C, 41.77; H, 6.55.

Photolysis of (η^5-Me_5C_5)(PMe_3)Ir($H_2C{=}CH_2$). In the drybox an NMR tube was charged with 5.3 mg (0.0123 mmol) of (η^5-Me_5C_5)(PMe_3)Ir($H_2C{=}CH_2$) in 1.0 mL of C_6D_{12}. This was irradiated, and monitored by ^1H NMR. After 1 h the reaction mixture was > 95 % (η^5-Me_5C_5)(PMe_3)Ir($HC{=}CH_2$)(H).

Intermolecular Isotope Effects. A typical experiment was done in the following way. In the drybox a solution of 34.4 mg (0.0706 mmol) of (η^5-Me_5C_5)(PMe_3)Ir(C_6H_{11})(H) and 60 μl (0.671 mmol) of C_6H_6 (as measured by syringe) was dissolved in 1.2980 g (1.4535 mL) of cyclohexane-d_{12}. This was split equally among three Wilmad 504PP NMR tubes, two of which were used for this experiment. The NMR tubes were subsequently attached to a vacuum line using Cajon Ultra-Torr adapters. PMe_3 (17.2 torr in 5.72 mL) and $H_2C{=}CH_2$ (150.0 torr in 141.2 mL; 1.14 mmol) were vacuum transferred into one tube. PM_3 (16.8 torr in 5.72 mL; 0.005 mmol) and $D_2C{=}CD_2$ (149.8 torr in 141.2 mL; 1.14 mmol) were transferred into the other tube. Both tubes were then sealed at a length of ca. 25 ± 0.3 cm. These were then heated, side-by-side, at 145.5 °C for 15.5 h. ^1H NMR analysis revealed the reaction to be complete. The relative amounts of (η^5-Me_5C_5)(PMe_3)Ir(C_6H_5)(H),

(η^5-Me_5C_5)(PMe_3)Ir(HC=CH_2)(H), and (η^5-Me_5C_5)(PMe_3)Ir(H_2C=CH_2), determined using ^{31}P NMR with pulse delays of at least $10T_1$, were determined to be 1.00 : 0.79 : 0.39. In the second tube, the relative amounts of (η^5-Me_5C_5)(PMe_3)Ir(C_6H_5)(H), (η^5-Me_5C_5)(PMe_3)Ir(DC=CD_2)(D), and (η^5-Me_5C_5)(PMe_3)Ir(D_2C=CD_2) were found to be 1.00 : 0.54 : 0.49. By comparing the amount of (η^5-Me_5C_5)(PMe_3)Ir(HC=CH_2)(H) to (η^5-Me_5C_5)(PMe_3)Ir(DC=CD_2)(D) (both normalized to the amount of (η^5-Me_5C_5)(PMe_3)Ir(C_6H_5)(H) formed), one can determine the intermolecular isotope effect: k_H/k_D = 1.46. Similarly for the π-complex formation: k_H/k_D = 0.80. This experiment was repeated 3 times, reducing the uncertainty in each of these isotope effects. The final values are: k_H/k_D (insertion) = 1.49 +- 0.08, k_H/k_D (π-complex formation) = 0.82 +- 0.05. In Table 2.6 are summarized the data from three experiments.

Table 2.6. Intermolecular isotope effect data. Amounts of products are relative to [Ir](C_6H_5)(H).

Exp. #	Gas	[Ir](C_6H_5)(H)	1	2	k_H/k_D(1)	k_H/k_D(2)
1	H_2C=CH_2	(1.00)	0.79	0.43	1.55	0.84
	D_2C=CD_2	(1.00)	0.51	0.51		
2	H_2C=CH_2	(1.00)	0.79	0.39	1.46	0.80
	D_2C=CD_2	(1.00)	0.54	0.49		
3	H_2C=CH_2	(1.00)	0.77	0.41	1.45	0.81
	D_2C=CD_2	(1.00)	0.53	0.50		

Intramolecular Isotope Effects. In a typical experiment, 10.0 mg (0.0205 mmol) of (η^5-Me_5C_5)(PMe_3)Ir(C_6H_{11})(H) was dissolved in 0.4349 g (0.4870 mL) of C_6H_{12} in a Wilmad 504PP NMR tube. The NMR tube was attached to a Kontes teflon vacuum stopcock with a Cajon Ultra-Torr fitting (SS-6-UT-6-4) and evacuated on a vacuum line. Cis-1,2-d_2-ethylene (148.5 torr in 141.2 mL) was vacuum transferred into the NMR tube, and the tube flame sealed. The tube was heated for 20 h at 145.0 °C.

Using an apparatus which allows an NMR tube to be broken open under vacuum, we froze the solution at -196 °C and broke open the tube. It was allowed to warm to -78 °C and the ethylene remaining was collected at - 196 °C in another vessel. The NMR tube was then resealed in vacuo at -196 °C. Mass spectral analysis of the ethylene removed showed that it was > 96% d_2-ethylene. The ^2H NMR of the organometallic products, using sufficiently long relaxation times for accurate integrations (5 sec), showed that insertion into a C-H bond in ethylene was favored over insertion into a C-D bond by a factor of 1.20. This was determined by comparing the amount of deuterium in the hydride position versus that in the β-position on the vinyl group trans to the metal, which was equal to the ratio found by comparing the amount of deuterium in the α-positions on the vinyl group to that in the β-position cis to the metal. Experiments with all of the d_2-ethylenes showed no significant difference in the values found. The values from 5 experiments were averaged, reducing the error from a single measurement, k_H/k_D (intramolecular insertion effect) = 1.18 +- 0.03. A table showing the isotope effects found for each experiment is given in the text.

Relative Solubilities of Ethylene and Ethylene-d_4. The relative solubilities were measured using the apparatus shown in Figure 2.8. It consists of a stainless steel bomb (fitted with a long neck so as to prevent the Nupro valve from freezing during the freeze-pump-thaw cycles) attached to a stainless steel pipe with a Nupro bellows valve (# SS-2H2). The top of the stainless steel tube is fitted with another Nupro valve which has a fitting to allow connection to a vacuum line. The volume of the lower bomb was 11.2 mL, and the volume between the two valves was approximately 30 mL.

A typical measurement was performed as follows. The stainless steel bomb was removed from the apparatus and filled with 7.300 g (9.37 mL) of cyclohexane. This was then re-attached to the apparatus. On a vacuum line, this was subjected to seven freeze-pump-thaw cycles. Completely degassed ethylene was expanded into a 508.5 mL bulb at a pressure of 136 torr (3.734 mmol), and was then condensed into the apparatus. The pressure in the vacuum line decreased steadily until it was less than 0.1 torr, at which time

the upper valve of the apparatus was closed. After 2.5 h at room temperature the apparatus had equilibrated, and the lower valve was closed. The gases is the upper section of the apparatus were passed through two -78 °C traps to freeze out any cyclohexane, and then measured using a Toepler pump. The amount of gas collected increased sharply for the first 15 min, and then remained constant for 2 h, at which time the experiment was stopped. The amount of gas measured was converted in moles using the ideal gas law; in this case 2.893 mmol (31.26 mm in 169 mL) was collected. Subtraction of the amount above the solution from the total amount of ethylene used resulted in determination of the amount in solution (3.734 - 2.893 = 0.841 mmol).

The solubilities of ethylene and ethylene-d_4 were each measured twice. The two experiments using ethylene showed 2.893 and 2.833 mmol of ethylene above the solution, respectively. Whereas, the two experiments using ethylene-d_4 showed 2.814 and 2.740 mmol above the solution, respectively.

(η^5-Me_5C_5)(PMe_3)Ir(HC=CH_2)(Br). In the dry box, 1.0438 g (2.200 mmol) of (η^5-Me_5C_5)(PMe_3)Ir$(Cl)_2$ was dissolved in 65 mL of THF. With stirring, 2.6 mL of a 1.0 M solution (2.6 mmol) of H_2C=CHMgBr in THF was added. This stirred at the drybox temperature (15 - 20 °C) for 12 h during which time the solution changed from orange to yellow. This was then passed through a short pad of SiO_2. Further purification was effected on the benchtop (in air). Chromatography using a 3.5 x 20 cm column of SiO_2 with 30 % ether/hexane as the eluent allowed us to isolate the product which eluted as a broad yellow band, occasionally contaminated with what is thought to be (η^5-Me_5C_5)(PMe_3)Ir(HC=CH_2)(Cl) in an insufficient amount of H_2C=CHMgBr was used: yield 757 mg (67.4 %). ^{1}H NMR (C_6D_6) δ 1.26 (d, PMe_3, J_{P-H} = 10.5 Hz), 1.51 (d, η^5-Me_5C_5, J_{P-H} = 1.9 Hz), 5.39, 6.68 (m, -CHC$\underline{H}_2$), 9.40 (ddd, -C$\underline{H}$CH_2, J_{P-H} = 1.2 Hz, $J_{H-H(cis)}$ = 10.2 Hz, $J_{H-H(trans)}$ = 17.3 Hz); ^{13}C NMR (C_6D_6) δ 9.18 (q, η^5-$\underline{Me}_5C_5$, J_{C-H} = 128.2 Hz), 14.58 (dq, PMe_3, J_{P-C} = 40.1 Hz, J_{C-H} = 129.4 Hz), 92.44 (s, η^5-$Me_5\underline{C}_5$), 118.71 (dt, -CH$\underline{C}H_2$, J_{P-C} = 4.8 Hz, J_{C-H} = 151.1 Hz), 142.52

(dd, -$\underline{C}$HCH$_2$, J_{P-C} = 17.5 Hz, J_{C-H} = 144.6 Hz); IR (KBr) 1550 (m), 1415 (s), 1280 (s), 945 (s); MS (70 eV) 510 (M^+), 483 (M^+ - C_2H_3); mp dec. 192 - 204 °C. Anal. Calcd: C, 35.29; H, 5.33. Found: C, 35.43; H, 5.27.

(η^5-Me$_5$C$_5$)(PMe$_3$)Ir(HC=CH$_2$)(H). In a Schlenk flask, 214.2 mg (0.420 mmol) of (η^5-Me$_5$C$_5$)(PMe$_3$)Ir(HC=CH$_2$)(Br), and 40.5 mg (1.071 mmol) of $NaBH_4$ were dissolved in isopropanol. The solution was then degassed and put under argon. This was stirred for 6 h at 50 °C during which time the solution became nearly colorless. The solvent was removed in vacuo leaving a white solid. Chromatography at - 80 °C under Ar using Al_2O_3 (III) and 5 % ether/pentane was used to purify the product, which eluted near the solvent front. Yield: 150.0 mg (82.8 %). Positive argon pressure was used to elute the product, as it isomerizes to (η^5-Me$_5$C$_5$)(PMe$_3$)Ir(H$_2$C=CH$_2$) if left on the column for longer than ca. 5 min. Alternatively, the product may be taken up in pentane and filtered through celite, and then recrystallized from highly concentrated solutions of pentane or hexamethyldisiloxane. ^{1}H NMR (C_6D_6) δ 1.86 (dd, η^5-Me$_5$C$_5$, J_{P-H} = 1.8 Hz, J_{H-H} = 0.8 Hz), 1.24 (d, PMe$_3$, J_{P-H} = 10.1 Hz), 5.75, 6.95 (m, -CHC$\underline{H}_2$), 8.12 (ddd, -C$\underline{H}$CH$_2$, J_{P-H} = 3.3 Hz, $J_{H-H(cis)}$ = 10.2 Hz, $J_{H-H(trans)}$ = 17.5 Hz), -16.88 (d, -H, J_{P-H} = 36.0 Hz); ^{13}C (C_6D_6) δ 10.27 (s, η^5-$\underline{Me}_5$C$_5$), 18.82 (d, PMe$_3$, J_{P-C} = 38.6 Hz), 92.50 (d, η^5-Me$_5\underline{C}_5$, J_{P-C} = 2.6 Hz), 123.78 (d, -CH$\underline{C}$H$_2$, J_{P-C} = 3.0 Hz), 129.18 (d, -$\underline{C}$HCH$_2$, J_{P-C} = 13.4 Hz); IR (KBr) 2903 (s), 2105 (s), 1553 (s), 953 (s), 940 (s); MS (70 eV) 432 (M^+), 404 (M^+ - C_2H_4); mp 65 - 68 °C. Anal. Calcd: C, 41.75; H, 6.54. Found: C, 41.65; H, 6.63.

X-ray Data Collection, Structure Determination, and Refinement for (η^5-Me$_5$C$_5$)(PMe$_3$)Ir(HC=CH$_2$)(H). Clear, yellow needle-like crystals were obtained by slow crystallization from hexamethyldisiloxane. Fragments cleaved from some of these crystals were mounted in capillaries in the air, flushed with dry nitrogen, and then flame sealed. Precession photographs indicated monoclinic Laue symmetry and yielded

preliminary cell dimensions. Systematic absences were consistent only with space group $P2_1/n$.

The crystal used for data collection was transferred to our Enraf-Nonius CAD-4 diffractometer and centered in the beam. It was cooled to -118 °C by a gaseous nitrogen flow apparatus, and the temperature monitored by an in-stream thermocouple which had been previously calibrated against a second thermocouple in the sample position. Automatic peak search and indexing procedures yielded the monoclinic reduced primitive cell. The final cell parameters and specific collection parameters are given in Table 2.7.

The 4143 raw intensity data were converted to structure factor amplitudes and their esd's by correction for scan speed, background and Lorentz and polarization effects. No correction for crystal decomposition was necessary. Inspection of the azimuthal scan data showed a variation $I_{min}/I_{max} = 0.75$ for the average curve. An empirical correction for absorption, based on the azimuthal scan data, was applied to the intensities since it was not possible to accurately measure the sample crystal. Removal of systematically absent and redundant data left 3775 unique data.

The structure was solved by Patterson methods and refined via standard least-squares and Fourier techniques. In a difference Fourier map calculated following refinement of all non-hydrogen atoms with anisotropic thermal parameters, peaks corresponding to the expected positions of most of the hydrogen atoms were found. A difference Fourier map calculated after inclusion of all other hydrogen atoms clearly showed the position of the hydride ligand attached to the metal. All hydrogen atoms were then allowed to refine with isotropic thermal parameters. A secondary extinction parameter was refined in the final cycles of least-squares. The final residuals for 267 variables refined against the 3100 data for which $F^2 > 3\ |F^2|$ were R = 2.04%, wR = 2.53%, and GOF = 1.356. The R value for all 3775 data was 3.49%.

The quantity minimized by the least squares program was $w(|F_0| - |F_c|)^2$ where w is the weight of a given observation. The p-factor, used to reduce the weight of intense

reflections, was set to 0.025 in the last cycles of the refinement. The analytical forms of the scattering factor tables fo the neutral atoms were used, and all non-hydrogen scattering factors were corrected for both the real and imaginary components of anomalous dispersion.

Inspection of the residuals ordered in ranges of $\sin(\theta)/\lambda$, $|F_0|$, and parity and value of the individual indices showed no unusual features or trends. The largest peak in the final difference Fourier map had an electron density of 2.14 e^-/A^3 and was located only 0.74 A from the iridium atom. All other peaks in the final difference Fourier map had densities of less than 1 e^-/A^3. The positional parameters of the atoms and their estimated standard deviations are given in Table 2.8.

Table 2.7. Crystal and Data Collection Parameters for **1**.

Compound: $(\eta^5\text{-}Me_5C_5)(PMe_3)Ir(HC{=}CH_2)(H)$

(A) Crystal Parameters at -118±4 °C[a,b]

a = 10.5245(12) A	Space Group: $P2_1/n$
b = 12.7267(16) A	Formula Weight = 431.6 amu
c = 12.3606(18) A	Z = 4
β = 94.052(11) °	d_c = 1.74 g/cm^3
V = 1651.5(7) A^3	
μ (calc) = 81.3 cm^{-1}	

Size of crystal: 0.18 x 0.20 x 0.40 mm

(B) Data Measurement Parameters

radiation: Mo Kα (λ = 0.71073 A)
monochrometer: highly-oriented graphite (2θ = 12.2°)
detector: crystal scintillation counter, with PHA.
reflections measured: +h, +k, ±l
2θ range: 3° --> 55° Scan Type: θ - 2θ
scan width: Δθ = 0.55 + 0.347 tan(θ)
scan speed: 0.66 --> 6.7 (θ, °/min)
background: measured over 0.25(Δθ) added to each end of the scan.
aperture --> crystal = 173 mm vertical aperture = 3.0 mm
horizontal aperture = 2.0 + 1.0 tan(θ) mm (variable).
no. of reflections collected: 4143
no. of unique reflections: 3268
intensity standards: (474), (447), (635); measured every hour of x-ray exposure time. Over the data collection period no decrease in intensity was observed.
orientation: 3 reflections were checked after every 250 measurements. crystal orientation was redetermined if any of the reflections were offset from their predicted positions by more than 0.1°. Reorientation was performed one during data collection.

[a] Unit cell parameters and their esd's were derived by a least-squares fit to the setting angles of the unresolved Mo Kα components of 24 reflections with 2θ between 29° and 31°.
[b] The esd's of all parameters are given in parentheses, right-justified to the least significant digit(s) given.

Table 2.8. Positional Parameters and Their Estimated Standard Deviations.

atom	x	y	z	B(A)^2
IR	0.00156(1)	0.18211(1)	0.30935(1)	1.568(2)
P	0.0241(1)	0.00962(8)	0.28788(8)	2.01(2)
C1	-0.1724(3)	0.2269(3)	0.1988(3)	2.02(7)
C2	-0.2084(3)	0.2218(3)	0.3093(3)	1.97(6)
C3	-0.1364(4)	0.2996(3)	0.3702(3)	2.06(7)
C4	-0.0533(4)	0.3509(3)	0.3007(3)	2.03(7)
C5	-0.0790(4)	0.3066(3)	0.1931(3)	2.07(7)
C6	-0.2340(4)	0.1663(4)	0.1057(4)	3.21(9)
C7	-0.3160(4)	0.1592(4)	0.3489(4)	3.01(8)
C8	-0.1512(5)	0.3288(3)	0.4861(4)	3.16(9)
C9	0.0344(4)	0.4404(3)	0.3286(4)	3.09(9)
C10	-0.0211(5)	0.3432(4)	0.0933(3)	3.26(9)
C11	0.1817(4)	0.1940(3)	0.2566(4)	2.96(8)
C12	0.2943(5)	0.1868(4)	0.3057(5)	3.8(1)
C13	0.1484(5)	-0.0541(3)	0.3734(4)	3.18(9)
C14	0.0620(5)	-0.0305(4)	0.1527(3)	3.9(1)
C15	-0.1120(5)	-0.0725(3)	0.3119(4)	3.53(9)
H1	0.071(5)	0.158(4)	0.427(4)	5(1)*
H11	0.183(5)	0.200(4)	0.171(4)	5(1)*
H12A	0.366(5)	0.197(3)	0.263(4)	4(1)*
H12B	0.305(4)	0.168(3)	0.378(3)	2.4(9)*
H6A	-0.310(6)	0.194(4)	0.077(5)	6(2)*
H6B	-0.177(5)	0.139(4)	0.064(4)	5(1)*
H6C	-0.251(5)	0.090(4)	0.125(4)	4(1)*
H7A	-0.395(5)	0.197(4)	0.335(4)	4(1)*
H7B	-0.328(4)	0.106(3)	0.312(3)	3(1)*
H7C	-0.308(6)	0.135(5)	0.424(4)	6(1)*
H8A	-0.215(5)	0.387(4)	0.485(4)	4(1)*
H8B	-0.189(5)	0.275(4)	0.528(4)	5(1)*
H8C	-0.073(6)	0.353(5)	0.519(5)	6(1)*
H9A	-0.009(4)	0.491(4)	0.314(3)	5(1)*
H9B	0.075(4)	0.439(3)	0.400(3)	3(1)*
H9C	0.103(4)	0.444(3)	0.281(3)	2.4(9)*
H10A	-0.061(5)	0.407(4)	0.061(4)	4(1)*
H10B	0.068(5)	0.372(4)	0.110(4)	4(1)*
H10C	-0.034(5)	0.298(4)	0.035(4)	4(1)*
H13A	0.160(4)	-0.117(3)	0.353(3)	2.3(9)*
H13B	0.231(5)	-0.009(4)	0.368(4)	5(1)*
H13C	0.118(6)	-0.048(4)	0.439(4)	6(1)*
H14A	0.073(7)	-0.088(6)	0.150(5)	9(2)*
H14B	-0.007(5)	-0.008(4)	0.109(4)	5(1)*
H14C	0.147(5)	0.021(4)	0.129(4)	5(1)*
H15A	-0.090(5)	-0.135(4)	0.306(4)	4(1)*
H15B	-0.139(4)	-0.057(3)	0.381(3)	4(1)*
H15C	-0.183(5)	-0.050(4)	0.261(4)	4(1)*

* Atoms refined with isotropic thermal parameters.

References.

[1] See for example: Collman, J.P.; Hegedus, L.S.; Norton, J.R.; Finke, R.G. *Principles and Applications of Organotransition Metal Chemistry*; University Science Books: Mill Valley, CA, 1987.

[2] Some of the difficulties have been pointed out by Halpern. (a) Dawans, R.; Morel, D. *J. Mol. Catal.* **1977-78**, *3*, 403. (b) Halpern, J.; Okamoto, T.; Zakhariev, A. *J. Mol. Catal.* **1976**, *2*, 65. (c) Chan, A.S.C.; Halpern, J. *J. Am. Chem. Soc.* **1980**, *102*, 838. (d) Halpern, J. *Inorg. Chim. Acta.* **1981**, *50*, 11. (e) Halpern, J.; Riley, D.P.; Chan, A.S.C.; Pluth, J.J. *J. Am. Chem. Soc.* **1977**, *99*, 8055. (f) Halpern, J. *Science* **1982**, *217*, 401.

[3] Parshall, G.W. *Homogeneous Catalysis*; Wiley: New York, 1980 and references therein.

[4] Ziese, W.C. *Ann. Phys. Chem.* **1827**, *9*, 632.

[5] (a) Herberhold, M. *Metal π-Complexes*; Elsevier: New York, Vol. 2, *Complexes with Monoolefinic Ligands*, 1974. (b) Collman, J.P.; Hegedus, L.S.; Norton, J.R.; Finke, R.G. *Principles and Applications of Organotransition Metal Chemistry*; University Science Books: Mill Valley, CA, 1987, Chapter 3.

[6] (a) Jones, W.D.; Feher, F.J. *J. Am. Chem. Soc.* **1984**, *106*, 1650. (b) Sweet, J.R.; Graham, W.A.G. *J. Am. Chem. Soc.* **1983**, *105*, 305. (c) Sweet, J.R.; Graham, W.A.G. *Organometallics* **1983**, *2*, 135. (d) Silverthorne, W.E. *Adv. Organomet. Chem.* **1975**, *13*, 47. (e) Brauer, D.J.; Kruger, C. *Inorg. Chem.* **1977**, *16*, 884.

[7] Parshall, G.W. *Homogeneous Catalysis*, Wiley: New York, 1980

[8] Bonneau, R.; Kelly, J.M. *J. Am. Chem. Soc.* **1980**, *102*, 1220. Similar results have been observed for $(\eta^5\text{-}C_5H_5)Mn(CO)_3$: Wasserman, E.P; Stoutland, P.O.; Moore, C.B.; Bergman, R.G. unpublished results.

[9] (a) Cracknell, R.B.; Orpen, G.A.; Spencer, J.L. *J. Chem. Soc., Chem. Comm.* **1984**, 326. (b) Brookhart, M.; Green, M.L.H. *J. Organomet. Chem.* **1983**, *250*, 395. (c) Schmidt, G.F.; Brookhart, M. *J. Am. Chem. Soc.* **1985**, *107*, 1443 and references therein.

[10] (a) Somorjai, G.A. *Philos. Trans. R. Soc. London, A.* **1986**, *318*, 81. (b) Woodruff, D.P.; Delchar, T.A. *Modern Techniques of Surface Science*, Cambridge University Press: Cambridge, UK, 1986.

[11] For recent reviews of C-H activation see: (a) Halpern, J. *Inorg. Chim. Acta.* **1985**, *100*, 41. (b) Aktogu, N.; Baudry, D.; Cox, D.; Ephritikhine, M.; Felkin, H.; Holmes-Smith, R.; Zakrzewski, J. *Bull. Soc. Chim. France* **1985**, 381. (c) Green, M.L.H.; O'Hare, D. *Pure & Appl. Chem.* **1985**, *57*, 1897. (d) Crabtree, R.H. *Chem. Rev.* **1985**, *85*, 245.

[12] See for example: (a) Connor, J.A. *Top. Curr. Chem.* **1977**, *71*, 71. (b) Halpern, J. *Acc. Chem. Res.* **1982**, *15*, 238. (c) Halpern, J. *Inorg. Chem.* Acta. **1985**, *100*, 41.

[13] Stoutland, P.O.; Bergman, R.G. *J. Am. Chem. Soc.* **1985**, *107*, 4581.

[14] As the reaction proceeds cyclohexane-d_{12} is incorporated into the iridium complex. On thermolysis in mixed benzene/alkane solvents, (η^5-Me_5C_5)(PMe_3)Ir(C_6H_{11})(H) is converted cleanly and quantitatively to cyclohexane and the benzene C-H activation product (η^5-Me_5C_5)(PMe_3)Ir(C_6H_5)(H). In studies parallel to those reported here (Buchanan, J.M.; Stryker, J.M.; Bergman, R.G. *J. Am. Chem. Soc.* **1986**, *108*, 1537) we have demonstrated that this reaction proceeds by kinetics that are first order in (η^5-Me_5C_5)(PMe_3)Ir(C_6H_{11})(H) and zero order in benzene. The rates are inhibited at high concentration of added cyclohexane. These data are consistent with a mechanism involving reversible, rate-determining reductive elimination of cyclohexane to give "(η^5-Me_5C_5)(PMe_3)Ir", followed by trapping of this intermediate by benzene in a subsequent fast step. We assume the same type of mechanism operates with ethylene in place of benzene as the trap.

[15] Reaction of (η^5-Me_5C_5)(PMe_3)Ir$(H)_2$ with 2-methylpropene under photochemical conditions resulted in vinylic C-H insertion products, the reaction was not particularly clean, however. McGhee, W.D. personal communication.

[16] We feel the scrambling is most likely caused by small amounts (< 1 %) of iridium byproducts formed during the reaction, as there is a slight darkening of the solution.

[17] (a) Komiya, S.; Ito, T.; Cowie, M.; Yamamoto, A.; Ibers, J.A. *J. Am. Chem. Soc.* **1976**, *98*, 3874. (b) Van Baar, J.F.; Vrieze, K.; Stufkens, D.J. *J. Organomet. Chem.* **1975**, *85*, 249. (c) Foot, R.J.; Heaton, B.T. *J. Chem. Soc., Chem. Comm.* **1973**, 838. (d) Aumann, R.; Henkel, G.; Krebs, B. *Angew. Chem. Int. Ed. Engl.* **1982**, *21*, 204.

[18] Tolman, C.A.; Ittel, S.D.; English, A.D.; Jesson, J.P. *J. Am. Chem. Soc.* **1979**, *101*, 1742.

[19] (a) Nubel, P.O.; Brown, T.L. *J. Am. Chem. Soc.* **1984**, *106*, 644. (b) Fryzuk, M.D.; Jones, T.; Einstein, F.W.B. *Organometallics* **1984**, *3*, 185. (c) Keister, J.B.; Shapley, J.R. *J. Organomet. Chem.* **1975**, *85*, C29.

[20] (a) Baker, M.V.; Field, L.D. *J. Am. Chem. Soc.* **1986**, *108*, 7433. (b) Baker, M.V.; Field, L.D. *J. Am. Chem. Soc.* **1986**, *108*, 7436.

[21] Wenzel, T.T.; Bergman, R.G. *J. Am. Chem. Soc.* **1986**, *108*, 4856.

[22] In competition experiments between benzene and ethylene (vide post), we have determined the relative selectivity between benzene and ethylene to be ca. 1.0.

[23] This was not a controlled oxidation. During an attempted recrystallization of **1** in a Schlenk tube at -40 °C oxygen apparently got into the solution as O=PMe_3 was observed. The major organometallic product was **2**.

[24] (a) Nolan, S.P.; Hoff, C.D.; Stoutland, P.O.; Newman, L.J.; Buchanan, J.M.; Bergman, R.G.; Yang, G.K.; Peters, K.S. *J. Am. Chem. Soc.* **1987**, *109*, 3143. (b)

Stoutland, P.O.; Bergman, R.G.; Nolan, S.P.; Hoff, C.D. *Polyhedron: Symposium in Print* submitted for publication.

[25] The same value can be calculated using $\Delta H^{\neq}$ for reductive elimination of cyclohexane from $(\eta^5\text{-}Me_5C_5)(PMe_3)Ir(C_6H_{11})(H)$, the relevant hydrocarbon C-H BDE's, and the bond dissociation enthalpy of the iridium-cyclohexyl bond (52 kcal/mol).

[26] Chang, J.; Bergman, R.G. *J. Am. Chem. Soc.* **1987**, *109*, 4298 and references therein.

[27] Vollhardt, K.P.C.; Weidman, T.W. *J. Am. Chem. Soc.* **1983**, *105*, 1676.

[28] Haddleton, D.M.; Perutz, R.N. *J. Chem. Soc., Chem. Comm.* submitted for publication.

[29] Moseley, K.; Kang, J.W.; Maitlis, P.M. *J. Chem. Soc. A* **1970**, 2875.

[30] Lichtenberger, D.L.; Blevins, C.H.,II.; Ortega, R.B. *Organometallics* **1984**, *3*, 1614.

[31] Byers, L.R.; Dahl, L.F. *Inorg. Chem.* **1980**, *19*, 277.

[32] It is possible that the scrambling is caused by adventitious impurities which PMe_3 is able to inactivate.

[33] Bigeleisen, J.; Ribnikar, S.V.; Van Hook, W.A. *J. Chem. Phys.* **1963**, *38*, 489.

[34] Similar rearrangements have been observed in this and other systems. (a) Buchanan, J.M.; Stryker, J.M.; Bergman, R.G. *J. Am. Chem. Soc.* **1986**, *108*, 1537. (b) Erker, G. *Acc. Chem. Res.* **1984**, *17*, 103.

[35] α-Scrambling has been observed in other systems, and often has erratic rates: (a) Buchanan, J.M.; Stryker, J.M.; Bergman, R.G. *J. Am. Chem. Soc.* **1986**, *108*, 1537. (b) Norton, J.R. personal communication.

[36] For experiments using ethylene-1,1-d_2, the ratio of **A** to **B** (Scheme 2.8) can be determined by comparing the α-deuterium to either β-deuterium, or by comparing the deuteride to either β-deuterium.

[37] Janowicz, A.H.; Bergman, R.G. *J. Am. Chem. Soc.* **1983**, *105*, 3929.

[38] Jones, W.D.; Feher, F.J.; *J. Am. Chem. Soc.* **1986**, *108*, 4814.

[39] (a) Lowry, T.H.; Richardson, K.S. *Mechanism and Theory in Organic Chemistry*, Harper and Row: New York, 1981, chap. 2. (b) Streitweiser, Jr., A.; Jagow, R.H.; Fahey, R.C.; Suzuki, S. *J. Am. Chem. Soc.* **1958**, *80*, 2326.

[40] Porzio, W.; Zocchi, M. *J. Am. Chem. Soc.* **1978**, *100*, 2048.

[41] Cvetanovic, R.J.; Duncan, F.J.; Falconer, W.E.; Irwin, R.S. *J. Am. Chem. Soc.* **1965**, *87*, 1827. See also: Schurig, V.V. *Chem. Zeit.* **1977**, *101*, 173 and references therein.

[42] Buchanan, J.M.; Stryker, J.M.; Bergman, R.G. *J. Am. Chem. Soc.* **1986**, *108*, 1537.

[43] Kafafi, Z.H.; Hauge, R.H.; Margrave, J.L. *J. Am. Chem. Soc.* **1985**, *107*, 7550.

[44] Low, J.J.; Goddard, W.A. *J. Am. Chem. Soc.* **1984**, *106*, 8321.

[45] Silvestre, J.; Calhorda, M.J.; Hoffman, R.; Stoutland, P.O.; Bergman, R.G. *Organometallics* **1986**, *5*, 1841.

[46] Faller, J.W.; Felkin, H. *Organometallics* **1985**, *4*, 1488.

[47] Iwasawa, Y. Hamamura, H. *J. Chem. Soc., Chem. Comm.* **1983**, 130.

[48] (a) Pez, G.P. *J. Chem. Soc., Chem. Comm.* **1977**, 560. (b) Baudry, D.; Cormier, J.-M. Ephritikhine, M.; Felkin, H. *J. Organomet. Chem.* **1984**, *277*, 99. (c) Green, M.L.H.; Knight, J. *J. Chem. Soc., Dalton Trans.* **1974**, 311. (d) Hudson, B.; Webster, D.E.; Wells, P.B. *J. Chem. Soc., Dalton Trans.* **1972**, 1204.

[49] Lehwald, S.; Ibach, H. *Surface Sci.* **1979**, *89*, 425.

[50] Janowicz, A.H.; Bergman, R.G. *J. Am. Chem. Soc.* **1983**, *105*, 3929.

[51] Kang, J.W.; Moseley, K.; Maitlis, P.M. *J. Am. Chem. Soc.* **1969**, *91*, 5970.

[52] Buchanan, J.M.; Stryker, J.M.; Bergman, R.G. *J. Am. Chem. Soc.* **1986**, *108*, 1537.

Chapter 3

Stoichiometric Functionalization of Benzene and Ethylene: Attempts to Understand Potential Alkane Functionalization Processes

Introduction.

One of the long standing goals of both industrial and academic chemists has been to discover efficient and selective hydrocarbon functionalization processes. Despite the attention given to this problem, stimulated by the rise in oil prices, a solution is still in the early stages. This difficult and complex problem has encouraged researchers in several different areas to vigorously pursue solutions. Industrial chemists have been most interested in heterogeneous processes for the conversion of methane to other fuels, such as methanol and ethane, which are less difficult to handle. With many of the discoveries in only the patent literature, it is clear that many advances have been made in this area.[1] For example, catalytic processes have been reported in which methane is converted to methanol in yields above 90%.[2] These processes are a significant improvement over older methane functionalization processes which first required conversion of methane into synthesis gas.[3] These new processes are not used to any great extent commercially at present, but the expected increase in the price of oil is likely to make them more economically feasible.

The oxidation of hydrocarbons by metal porphyrin systems has recently been shown to provide another route to hydrocarbon functionalization. In this area, many reports have appeared.[4] These reactions are particularly significant because saturated hydrocarbons can be oxidized, and the reactions are often performed under mild conditions. Free radicals have been implicated in many of these reactions, suggesting that selectivity may be limited to those typical of free radicals. Other systems have also been shown to be capable of oxidizing alkanes, usually in a nonselective manner.[5]

The use of homogeneous organometallic catalysts seems to be ideally suited to this problem of selective hydrocarbon functionalization as many of the steps in potential functionalization schemes are well precedented. The major problem has been that C-H bonds, especially those of alkanes, are notoriously unreactive toward transition metal complexes. Until the last ten years, their reactivity was, for the most part, limited to H/D exchange reactions. In the last five years however, we have witnessed many advances in

this area, and there are now several systems known which will insert into the C-H bonds of alkanes, resulting in formation of stable alkyl hydrides.[6]

While these results are encouraging, the hope for efficient functionalization processes starting from the alkyl hydrides has not been realized. A few examples of hydrocarbon functionalization have appeared, but these processes have not been shown to be general. For example, there have been several observations of complexes capable of dehydrogenation reactions; such processes will, of course, not be suitable for methane.[7] Other examples where functionalization of aromatic hydrocarbons has been achieved with organometallic compounds have been described.[8]

In our group, we have extensively investigated the chemistry of the alkyl hydrides, $(\eta^5\text{-}Me_5C_5)(PMe_3)M(R)(H)$ (M = Rh, Ir), formed by insertion into the C-H bonds of hydrocarbons.[9] The chemistry of these complexes is dominated by reductive elimination of R-H, with the iridium complexes being considerably more stable than the rhodium complexes. This is particularly frustrating, as it has been generally assumed that the latter steps in a possible functionalization scheme, insertion and reductive elimination, would present fewer difficulties than the insertion step itself. For example, thermolysis of $(\eta^5\text{-}Me_5C_5)(PMe_3)Ir(R)(H)$ in the presence of added ligand such as CO or $H_2C{=}CH_2$ results in reductive elimination of R-H and addition of L to the metal center.[10] A survey of the complexes which are capable of intermolecular C-H insertion indicates that such problems may be commonplace, as the complexes are typically coordinatively saturated.

We have had some success in functionalizing alkanes from $(\eta^5\text{-}Me_5C_5)(PMe_3)Ir(R)(H)$, but these processes are stoichiometric and will clearly not be amenable to large scale or catalytic processes. For example, treatment of $(\eta^5\text{-}Me_5C_5)(PMe_3)Ir(R)(H)$ with $HCBr_3$ resulted in formation of $(\eta^5\text{-}Me_5C_5)(PMe_3)Ir(R)(Br)$. Subsequent treatment of the bromide with $HgCl_2$ results in production of $(\eta^5\text{-}Me_5C_5)(PMe_3)Ir(Br)(Cl)$ and R-Hg-Cl. Treatment of the alkyl mercury compound with Br_2 results in production of R-Br (Scheme 3.1).[11]

We have recently been investigating the interaction of (η^5-Me_5C_5)(PMe_3)Ir(R)(H) with unsaturated organic molecules, under conditions where reversible reductive elimination of R-H takes place. In the course of these studies, we found that thermolysis of (η^5-Me_5C_5)(PMe_3)Ir(R)(H) is the presence of acetylene resulted in formation of (η^5-Me_5C_5)(PMe_3)Ir(R)(HC=CH_2). Further investigations have revealed that in the cases where R = $CHCH_2$ or C_6H_5, reductive elimination of RHC=CH_2 can be induced, thus resulting in functionalization of R-H (Scheme 3.2). Because of the importance of stoichiometric hydrocarbon functionalization processes as model systems for potentially catalytic processes, we have investigated the details of these reactions. Described in this Chapter are the results of this study, some of which are still preliminary.

Insertion reactions.

Thermolysis of (η^5-Me_5C_5)(PMe_3)Ir(R)(H) in C_6H_6 in the presence of acetylene results in insertion of acetylene into the M-H bond yielding (η^5-Me_5C_5)(PMe_3)Ir(R)(HC=CH_2). This is the only product seen when R = C_6H_5, $CHCH_2$, or CH_3. With other alkyl groups, other products are also observed (vide post). When R = H, a double insertion is observed, leading to the production of (η^5-Me_5C_5)(PMe_3)Ir(HC=CH_2)$_2$.

The rates of these insertion reactions were found to be very erratic. The insertion was occasionally observed to proceed at temperatures as low as room temperature; at other times, the reaction proceeded to partial conversion and then stopped, even at temperatures above 100 °C . Ultraviolet irradiation of the reaction mixture through a uranium filter was found to give more predictable results; 2 - 4 hours of irradiation with a 450 W lamp was typically sufficient to induce the insertion reaction. All subsequent insertion reactions were therefore performed using the photochemical method.

The products formed when R = $CHCH_2$ or C_6H_5 have been fully characterized. When R = CH_3, only one product is observed which spectroscopic evidence indicates is

Scheme 3.1

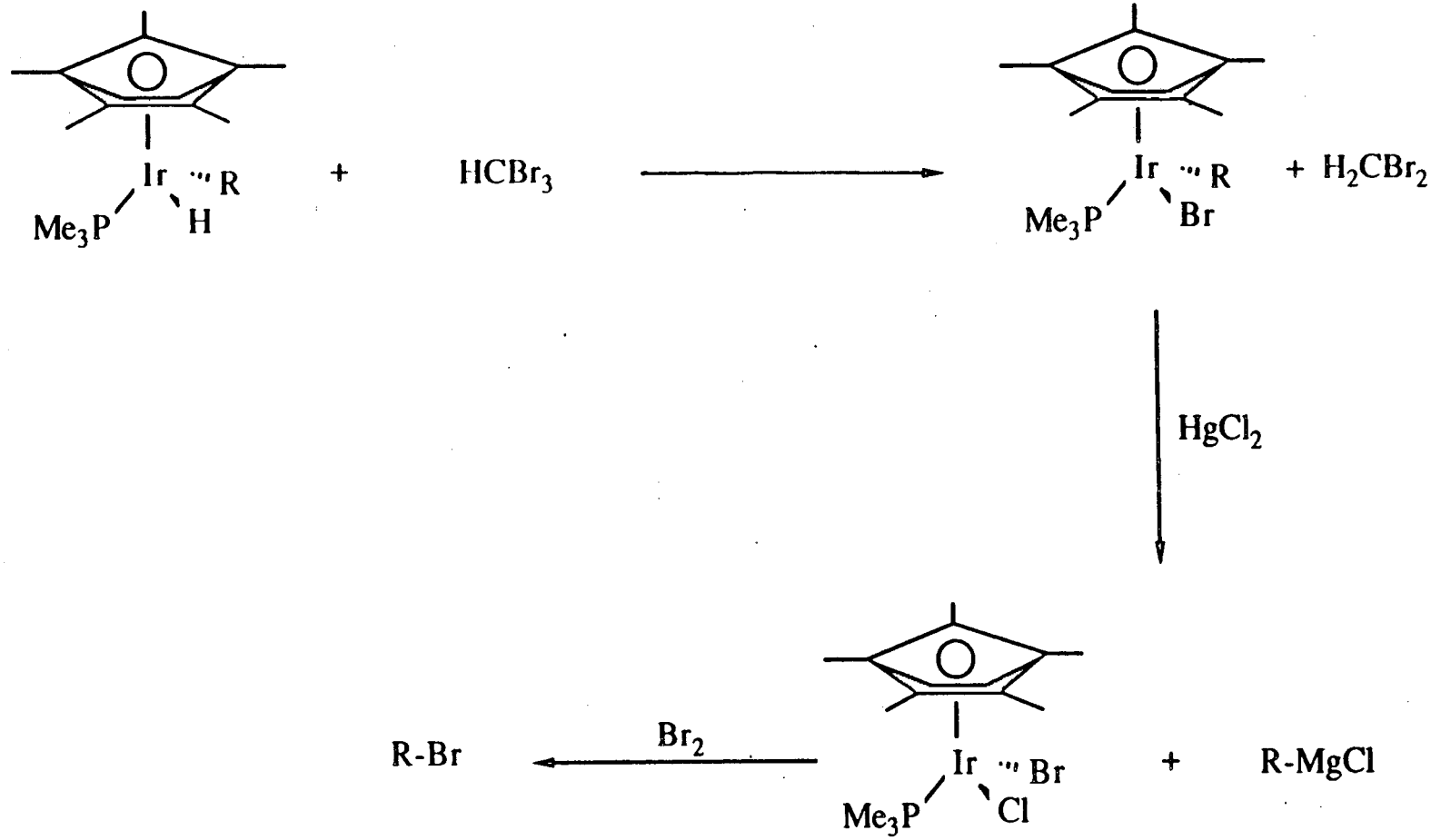
Ir
R
Me3P
H
+
HCBr3
Ir
R
Me3P
Br
+ H2CBr2
HgCl2
Ir
Br
Me3P
Cl
+
R-MgCl
Br2
R-Br

Scheme 3.2

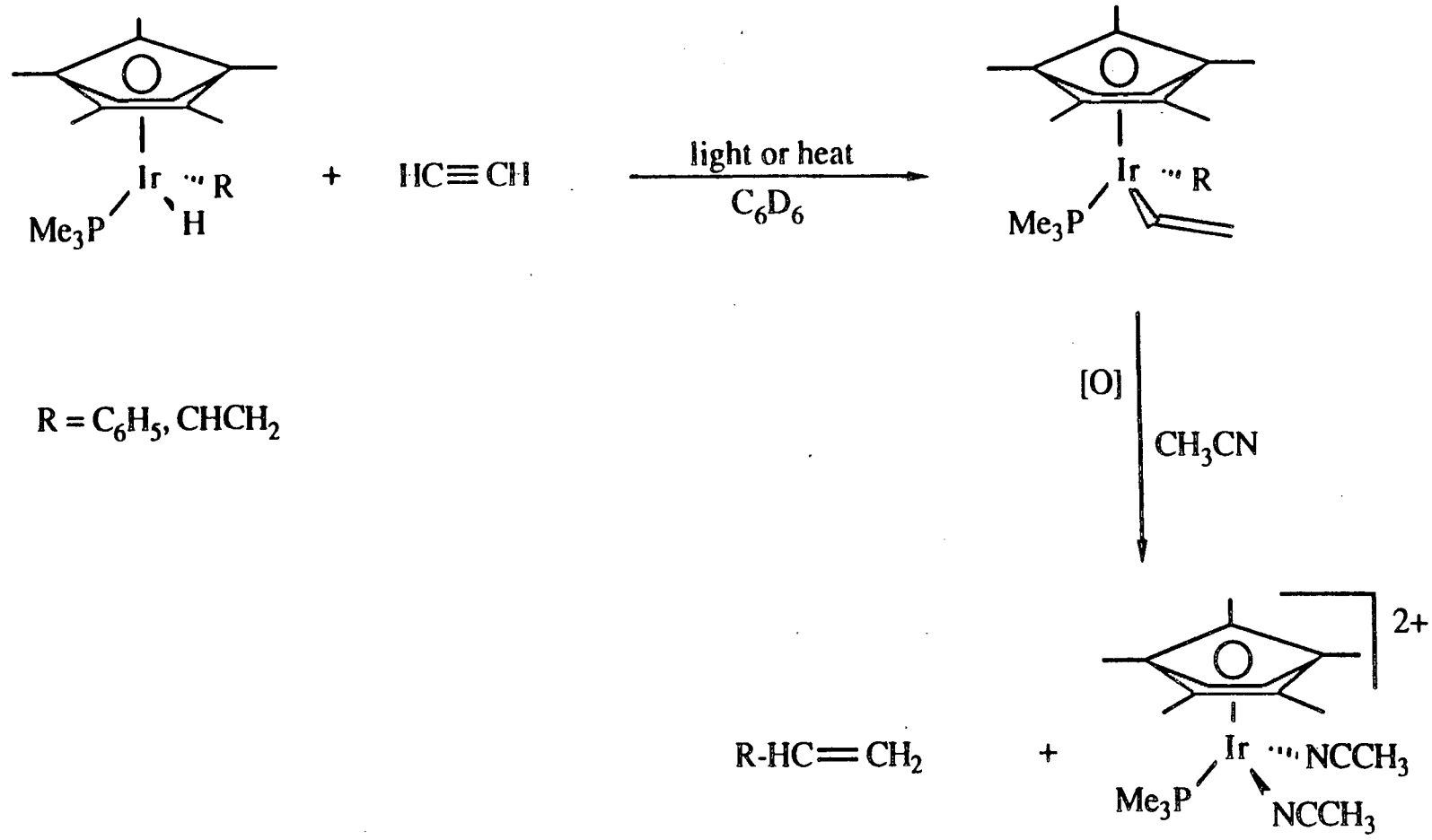

$R = C_6H_5, CHCH_2$

(η^5-Me_5C_5)(PMe_3)Ir(HC=CH_2)(CH_3). However, attempts to purify and fully characterize this product have been frustrated by its propensity to equilibrate to a mixture of (η^5-Me_5C_5)(PMe_3)Ir(HC=CH_2)$_2$, (η^5-Me_5C_5)(PMe_3)Ir(CH_3)$_2$, and (η^5-Me_5C_5)(PMe_3)Ir(HC=CH_2)(CH_3) on column supports. Exactly how this occurs is not presently understood. Only preliminary evidence is available for the reactions with R = C_6H_{11} and C_5H_{11}. In these cases two products are formed in similar amounts. Both have vinyl resonances, assignable to a vinyl group on the metal, and cyclopentadienyl and PMe_3 resonances which are very similar to each other. The alkyl resonances are unresolved multiplets. Comparison of the spectroscopic data with those from the reactions described above suggests that one of the products is the product of acetylene insertion into the metal-hydrogen bond. The identity of the other product is unknown, but it appears to slowly decompose thermally to a product with similar cyclopentadienyl and trimethylphosphine resonances, but <u>without</u> vinyl resonances. The two insertion products derived from (η^5-Me_5C_5)(PMe_3)Ir(C_6H_{11})(H) do not interconvert up to 160 °C.

The yields of the insertion reactions are sensitive to the ancillary ligands attached to the metal. Use of an internal standard revealed a yield of 70% and 81% for R = C_6H_5 and $CHCH_2$, respectively. For R = -CH_3, the yield was 70%, and for R = C_6H_{11} and C_5H_{11} 47% and 50%, respectively. Attempts to observed insertion reactions with (η^5-Me_5C_5)(PMe_3)Ir($CH_2C(CH_3)_3$)(H) were unsuccessful, probably due to the steric bulk of the neopentyl group.

Independent syntheses. In order to confirm the identity of the insertion products, we have independently synthesized some of them. Reaction of (η^5-Me_5C_5)(PMe_3)Ir(Cl)$_2$ with two equivalents of LiHC=CH_2 in THF resulted in a 71% isolated yield of (η^5-Me_5C_5)(PMe_3)Ir(HC=CH_2)$_2$ which was purified by column chromatography or by recrystallization from pentane (Scheme 3.3). Reaction of (η^5-Me_5C_5)(PMe_3)Ir(HC=CH_2)(Br) with C_6H_5Li in THF resulted in a 12.5% isolated

Scheme 3.3

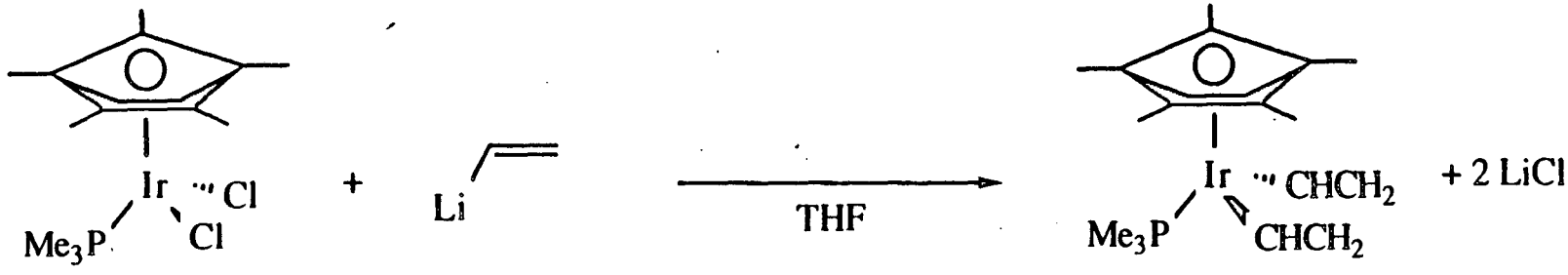

Scheme 3.4

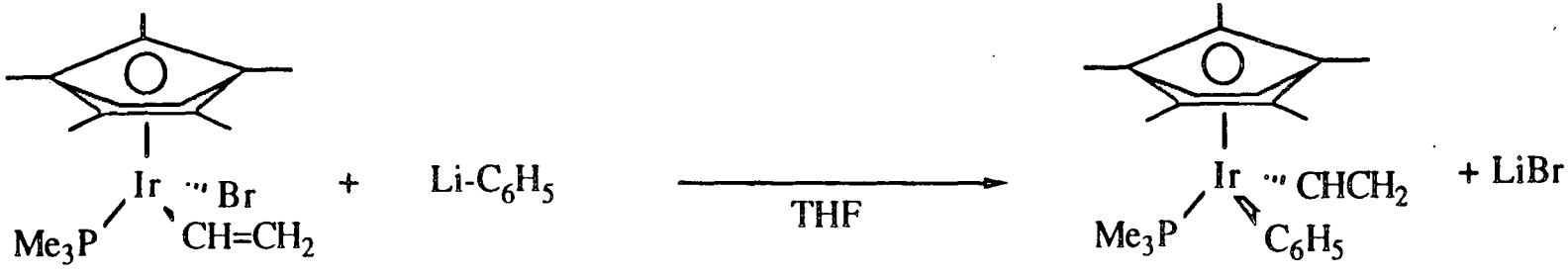

yield of (η^5-Me_5C_5)(PMe_3)Ir(C_6H_5)(HC=CH_2), which was also be purified by column chromatography or recrystallization (Scheme 3.4).

Reaction of (η^5-Me_5C_5)(PMe_3)Ir(HC=CH_2)(Br) with MeMgCl in diethyl ether results in a product which is spectroscopically consistent with (η^5-Me_5C_5)(PMe_3)Ir(HC=CH_2)(CH_3), and is the same as that formed in the reaction of HCCH with (η^5-Me_5C_5)(PMe_3)Ir(CH_3)(H) (Scheme 3.5). We have been unable to completely purify this compound as noted above. Similarly reaction of $BrMgC_5H_{11}$ with (η^5-Me_5C_5)(PMe_3)Ir(HC=CH_2)(Br) results in formation of the same mixture of products as formed in the reaction of (η^5-Me_5C_5)(PMe_3)Ir(C_5H_{11})(H) with HCCH. We have succeeded in getting small amounts of the insertion product pure by column chromatography, but have yet to fully characterize it.

Other acetylenes and metal complexes. Reaction with many other acetylenes was investigated under both thermal and photochemical conditions, including: $HCCC_6H_5$, CH_3CCCH_3, $HCCCH_2CH_3$, $HCCC(CH_3)_3$, and $CH_3OC(O)CCC(O)OCH_3$. In all cases except the last, no reaction was observed. In the case of CH_3O_2C-CC-CO_2CH_3, a reaction occurs which is believed to involve insertion into the M-H bond; this was not pursued.[12] Reactions analogous to those seen for (η^5-Me_5C_5)(PMe_3)Ir(R)(H) with acetylene were tried for other alkyl hydride complexes formed by C-H insertion reactions. Under both photochemical and thermal conditions (up to temperatures at which reductive elimination took place), no insertion reactions were observed for (η^5-Me_5C_5)(PMe_3)Rh(C_6H_5)(H) or for (η^5-C_5H_5)$(PMe_3)_2$Re(C_6H_5)(H).

Discussion of insertion reactions. Insertion of acetylenes into M-H and M-C bonds is believed to be one of the key steps in alkyne hydrogenation and polymerization processes.[13] Because of the importance of such processes, many researchers have studied homogeneous model systems in an attempt to better understand the insertion process. There are now many examples of unsaturated metal complexes which, when reacted with acetylenes, lead to M-H insertion products. In most cases it is believed that the alkyne first

Scheme 3.5

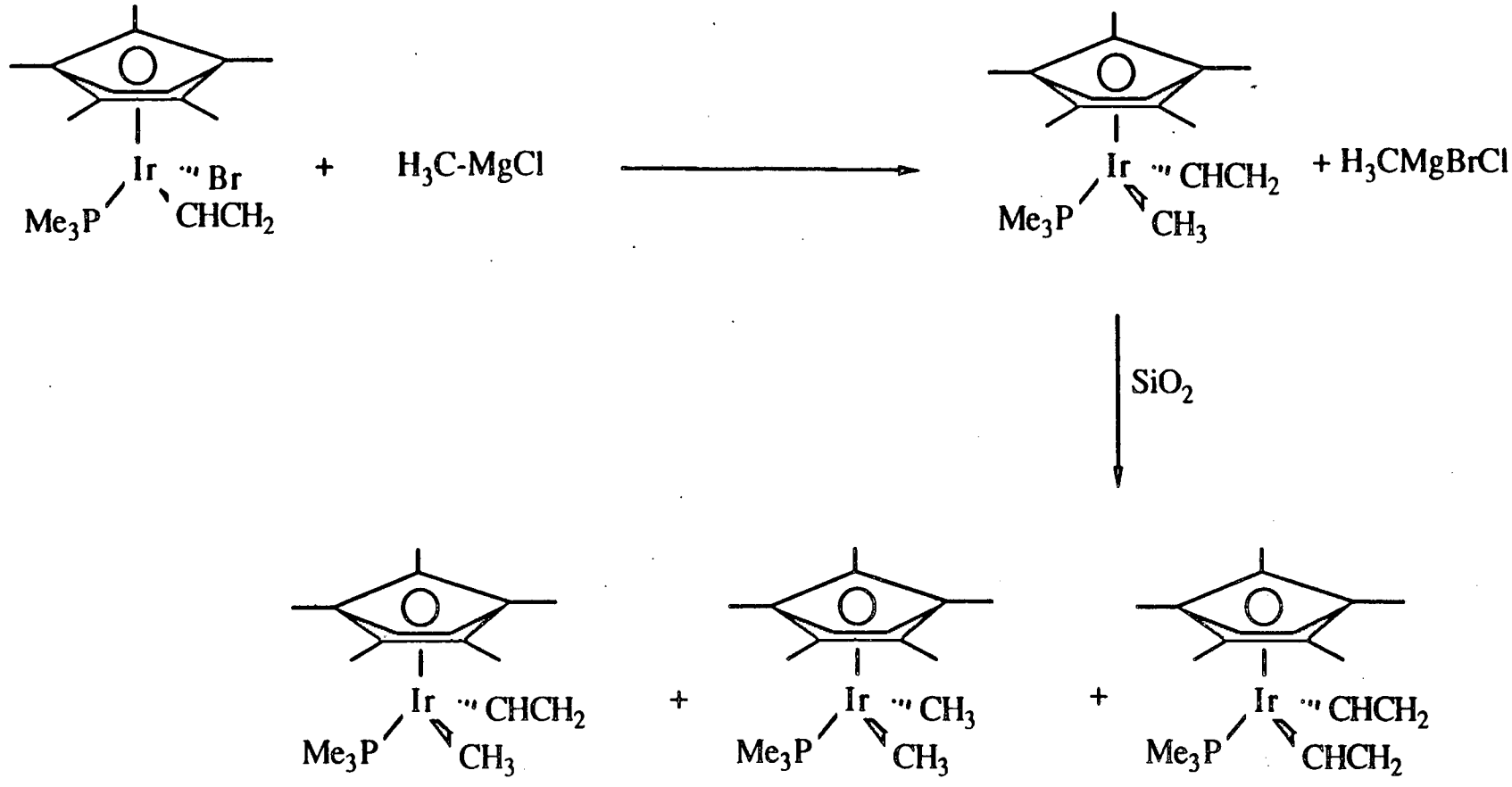
Ir
Br
Me_3P
$CHCH_2$
+
H_3C-MgCl
Ir
$CHCH_2$
Me_3P
CH_3
+ $H_3CMgBrCl$
SiO_2
Ir
$CHCH_2$
Me_3P
CH_3
+
Ir
CH_3
Me_3P
CH_3
+
Ir
$CHCH_2$
Me_3P
$CHCH_2$

coordinates to a vacant coordination site on the metal and then inserts into the M-H(R) bond forming a metal-alkenyl species.

Coordinatively saturated organometallic species, such as (η^5-Me_5C_5)(PMe_3)Ir(R)(H), are typically much less reactive than those with a vacant coordination site. In these cases usually the only acetylenes observed to react are those highly electrophilic in nature. For example, cyanoacetylene will insert into the W-H bond of Cp_2(CO)M-H (M = Ta, Nb) (Scheme 3.6),[14] and F_3C-CC-CF_3 will insert into the Re-H bond of Cp_2Re-H (Scheme 3.7).[15] These reactions are believed to be proceed by an electrophilic attack on these relatively electron-rich, late transition metal systems.

There are very few examples however, of insertion reactions involving simple acetylenes with coordinatively saturated transition metal complexes. We were thus surprised when we observed insertion of acetylene into the Ir-H bond of (η^5-Me_5C_5)(PMe_3)Ir(R)(H). One would expect that activated (electrophilic) acetylenes might insert into the Ir-H bond, and preliminary results are consistent with this. The seemingly anomalous reaction of HCCH with (η^5-Me_5C_5)(PMe_3)Ir(R)(H) thus raised the question of the mechanism of the insertion. Clearly, the reaction was not proceeding by complexation of the acetylene to a vacant coordination site as the thermal insertions were performed at temperatures well below those at which reductive elimination or phosphine dissociation occurs. Furthermore, the alkyl hydrides are known to be photochemically stable.

There are typically three mechanisms proposed for acetylene insertion reactions: (1) ionic,[16] (2) radical (chain or nonchain),[17] and (3) concerted.[18] Many studies have been performed in an attempt to sort out the mechanisms for various systems.[19] Many stereospecific insertions have been shown to be concerted. Stereospecificity has not been shown, however, to be a clear indication of a concerted mechanism, as some ionic processes, and even radical processes, can be fairly stereoselective.

Scheme 3.6

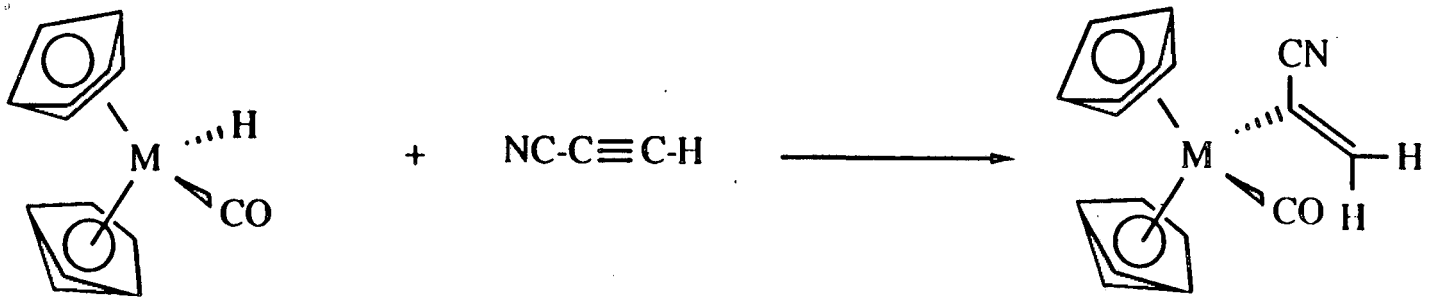

M = Nb, Ta

Scheme 3.7

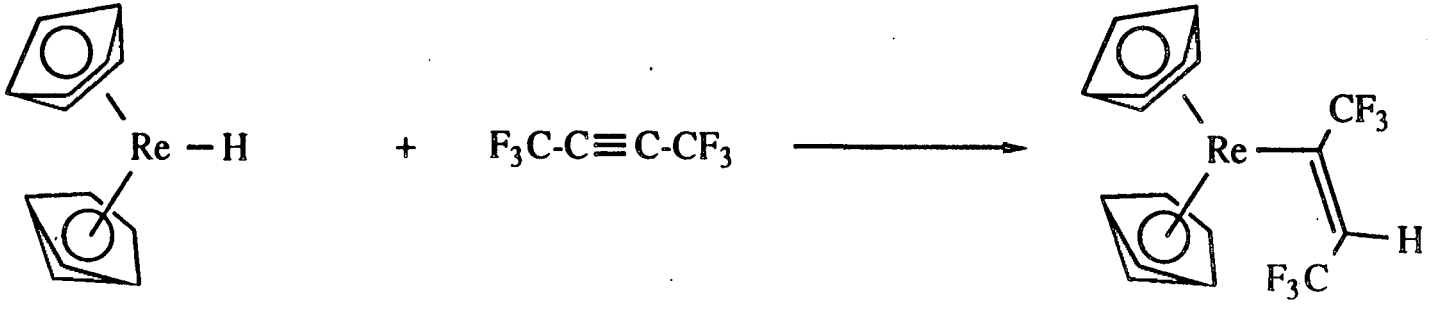

In order to determine the stereochemistry of the insertion reaction, the insertion of DCCD into the Ir-H bond of (η^5-Me_5C_5)(PMe_3)Ir(C_6H_5)(H) was examined. Analysis of the insertion product revealed complete deuteration of the α-position of the vinyl group and approximately equal amounts of deuterium in the two β-positions (Scheme 3.8). Thus insertion is not stereoselective, as a 1:1 mixture of cis and trans insertion products are observed.[20] The lack of stereoselectivity, and the erratic rates suggested to us that a radical process might be responsible for the insertion reaction. If a radical mechanism is operating, however, it is not a chain process (or has very short chains) as the reaction stops upon removal of the light source.

In order to further test this hypothesis, we irradiated a mixture of (η^5-Me_5C_5)(PMe_3)Ir(C_6H_5)(H) and (η^5-Me_5C_5)(PMe_3)Ir(C_6D_5)(D) in C_6D_6 in the presence of HCCH. Subsequent mass spectral analysis revealed products with no deuterium, one deuterium, five deuterium, and six deuterium atoms in a ratio of 32:21:29:18 (Scheme 3.9). A control experiment in which (η^5-Me_5C_5)(PMe_3)Ir(C_6H_5)(H) and (η^5-Me_5C_5)(PMe_3)Ir(C_6D_5)(D) were irradiated in separate tubes with HCCH, and then combined and submitted for mass spectral analysis revealed a mixture of d_0, d_1, d_5, and d_6 in a ratio of 62:0:24:14 (Scheme 3.10).

The observation that irradiation of (η^5-Me_5C_5)(PMe_3)Ir(C_6D_5)(D) in the presence of acetylene results in some d_5 product indicates that a hydrogen atom can be scavenged from another iridium complex, the acetylene, or adventitious hydrogen sources present.[21] But since irradiation of (η^5-Me_5C_5)(PMe_3)Ir(C_6H_5)(H) results in formation of some d_1 product <u>only</u> in the presence of (η^5-Me_5C_5)(PMe_3)Ir(C_6D_5)(D), some of the hydrogen(deuterium) atoms are coming from either the phenyl group or from the hydride of another molecule. With the iridium-hydrogen bond being 35 kcal/mol weaker than a C-H bond in benzene,[22] we are led to believe that the hydrogen atoms come from the hydride position. The observation of some d_5 product in the control experiment, however,

Scheme 3.8

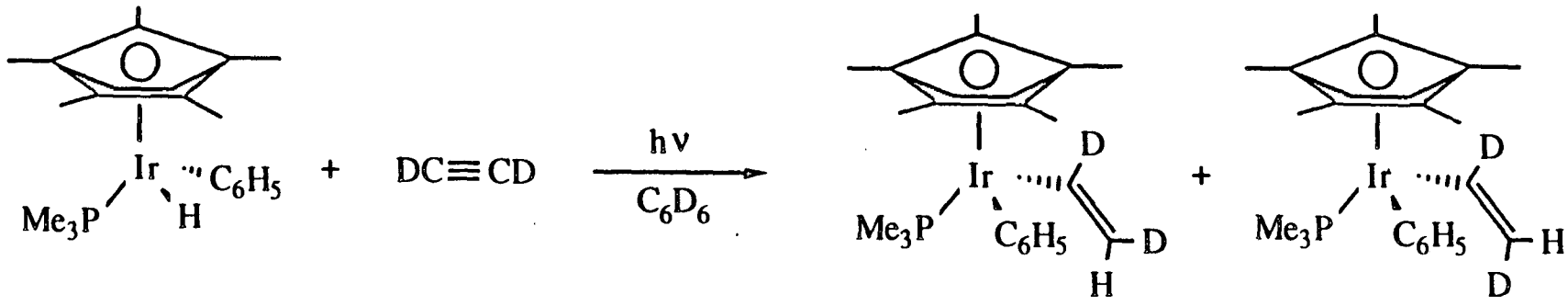

Scheme 3.9

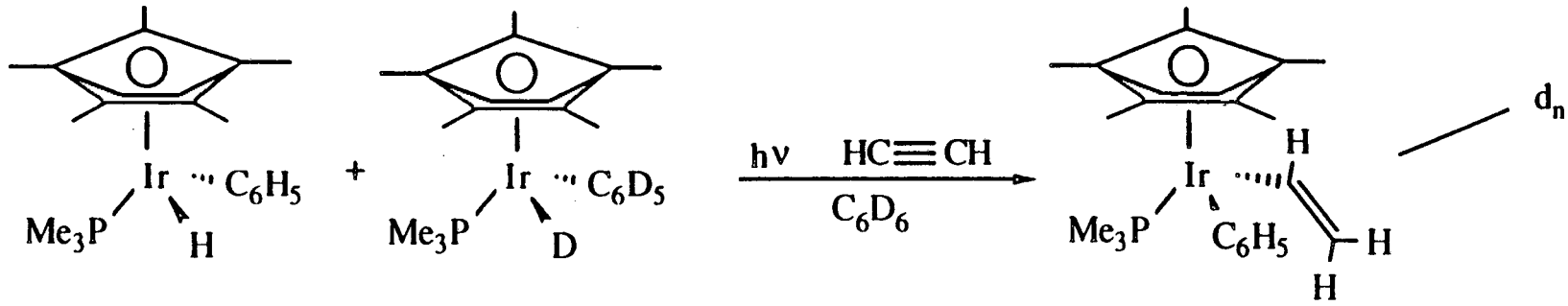

Number of D	Relative Amount
1	32
2	21
5	29
6	18

Scheme 3.10

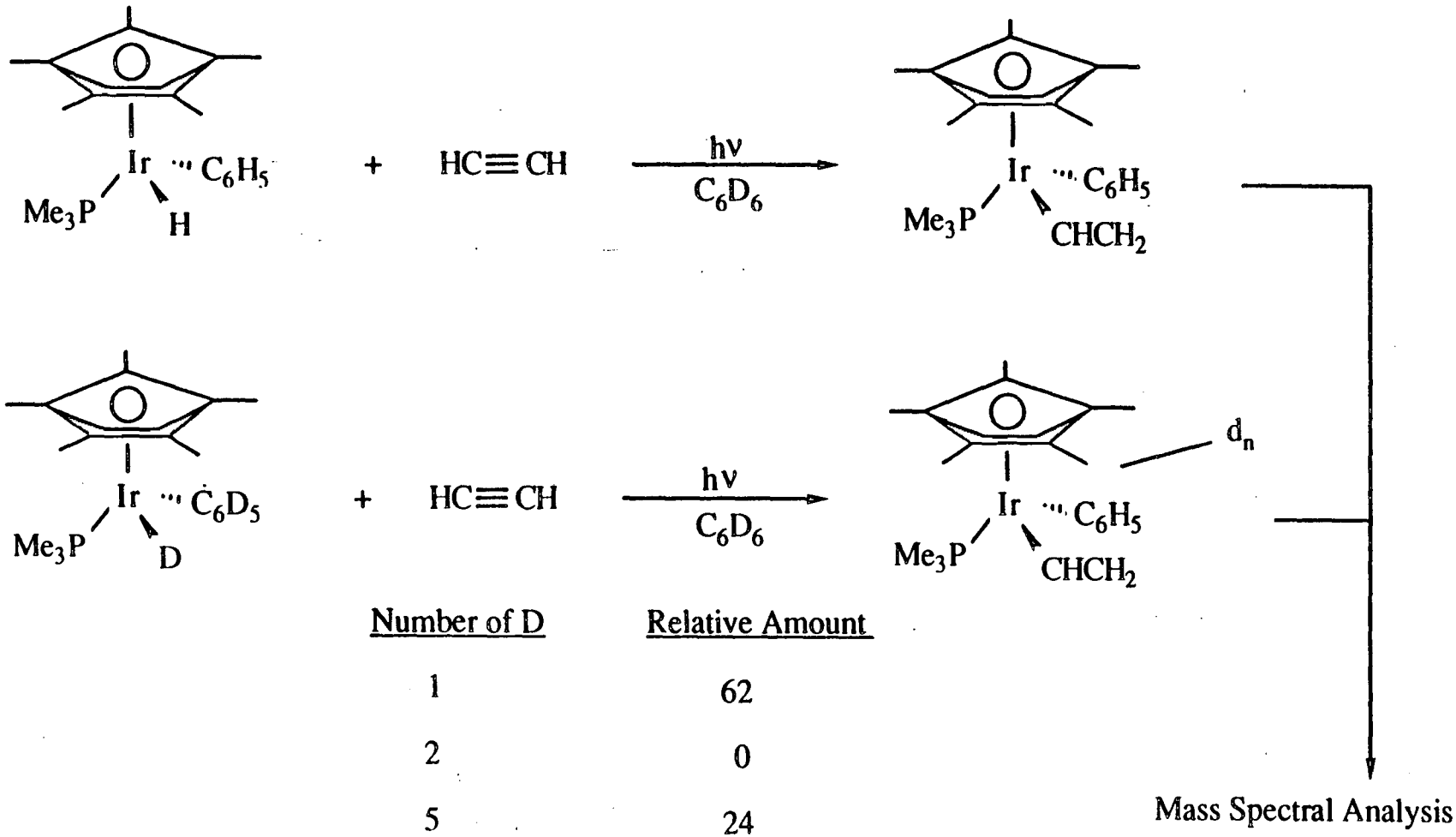

Number of D	Relative Amount
1	62
2	0
5	24
6	14

indicates that there is also another hydrogen source, perhaps small amounts of water absorbed onto the walls of the reaction vessel.

In this regard it is particularly frustrating that no other acetylenes were observed to undergo these insertion reactions. We would have expected phenyl acetylene to insert particularly rapidly if a radical pathway was operative, due to the influence of the phenyl group on radical stability. Because no other acetylenes were observed to undergo this insertion, we took great care to purify our acetylene to avoid the possibility of trace impurities which might catalyze the reaction. Details are given in the experimental section. Another control experiment was used to further test the possibility of the reaction being catalyzed by impurities present in acetylene. Reaction of $(\eta^5\text{-}Me_5C_5)(PMe_3)Ir(C_6H_5)(H)$ with a mixture of HCCH and HCCPh resulted only in insertion of HCCH, leading us to conclude that even if impurities are responsible for the insertion, the rate of insertion of HCCH still must be much faster than that of HCCPh, perhaps because of steric reasons.

Since the erratic rates as well as the crossover experiments suggest a radical mechanism, we have tried to inhibit the reaction. Use of reagents which are known to initiate radical reactions were not tried, as the reaction occasionally proceeded at room temperature even in the absence of added initiator. Furthermore, many potential initiators are light initiated which would not have been compatible with our reaction, as the insertions proceeded upon irradiation in the absence of initiators. All attempts to inhibit the reaction were similarly unsuccessful. Many good radical traps such as CCl_4 and $BrCCl_3$ react with the starting alkyl hydrides. Less good radical traps such as dihydroanthracene were not observed to inhibit the reaction. Spin traps such as TEMPO and galvinoxyl initially appeared to inhibit the reaction under photochemical conditions, but closer analysis revealed that this inhibition could be attributed to the spin trap simply absorbing some of the light. Similarly, PMe_3 was not observed to inhibit the reaction.

While we have not been able to confirm our hypothesis concerning the mechanism of the insertion reaction, the erratic rates and the crossover products still lead us to believe

that these insertion reactions may proceed by a radical type mechanism. One such mechanism is shown in Scheme 3.11.

Reductive elimination of $H_2C{=}CHR$.

Since the starting alkyl hydrides, (η^5-Me_5C_5)(PMe_3)Ir(R)(H), were initially formed by C-H bond activation of R-H, the reductive elimination of $H_2C{=}CHR$ would formally constitute functionalization of the alkane. Because of the importance of this system as a model for systems which might catalytically activate and functionalize hydrocarbons, we have sought to understand the properties of (η^5-Me_5C_5)(PMe_3)Ir(R)($HCCH_2$). We first attempted to induce reductive elimination of $H_2C{=}CHR$ by simple thermolysis. Since reductive elimination of R-R is usually a higher energy process than reductive elimination of R-H, it was anticipated that if reductive eliminations were to occur thermally, they would require high temperatures as the alkyl hydrides are stable to well above 100 °C. We were encouraged somewhat however, by the report that reductive elimination of R-R appears to be faster for sp^2 hybridized R groups.[23]

Thermolysis. Thermolysis of (η^5-Me_5C_5)(PMe_3)Ir(R)($CHCH_2$) (R = C_6H_5, $CHCH_2$, CH_3, C_5H_{11}) in benzene does not result in reductive elimination of $H_2C{=}CHR$. In all cases reaction did not occur until ca. 190 °C. In the case of R = $CHCH_2$ and C_5H_{11}, a single (thought to be the same) product was apparently produced, but was difficult to characterize (see Experimental section). For R = C_6H_5 the reaction is fairly clean, resulting in formation of a single product, which by comparison of the ^1H NMR to a similar compound, is believed to be (η^5-Me_5C_5)(PMe_3)Ir(C_8H_8) (Scheme 3.12).[24] When R = CH_3 products derived from Ir-C bond homolysis (CH_4 and $H_2C{=}CH_2$) are produced (Scheme 3.13).

As (η^5-Me_5C_5)(PMe_3)Ir($HC{=}CH_2$)(H) and (η^5-Me_5C_5)(PMe_3)Ir(C_6H_5)(H) are stable to above 180 °C,[25] the temperatures at which (η^5-Me_5C_5)(PMe_3)Ir(R)($HCCH_2$) decomposed seem somewhat low. This may be one of the few systems were an aryl

Scheme 3.11

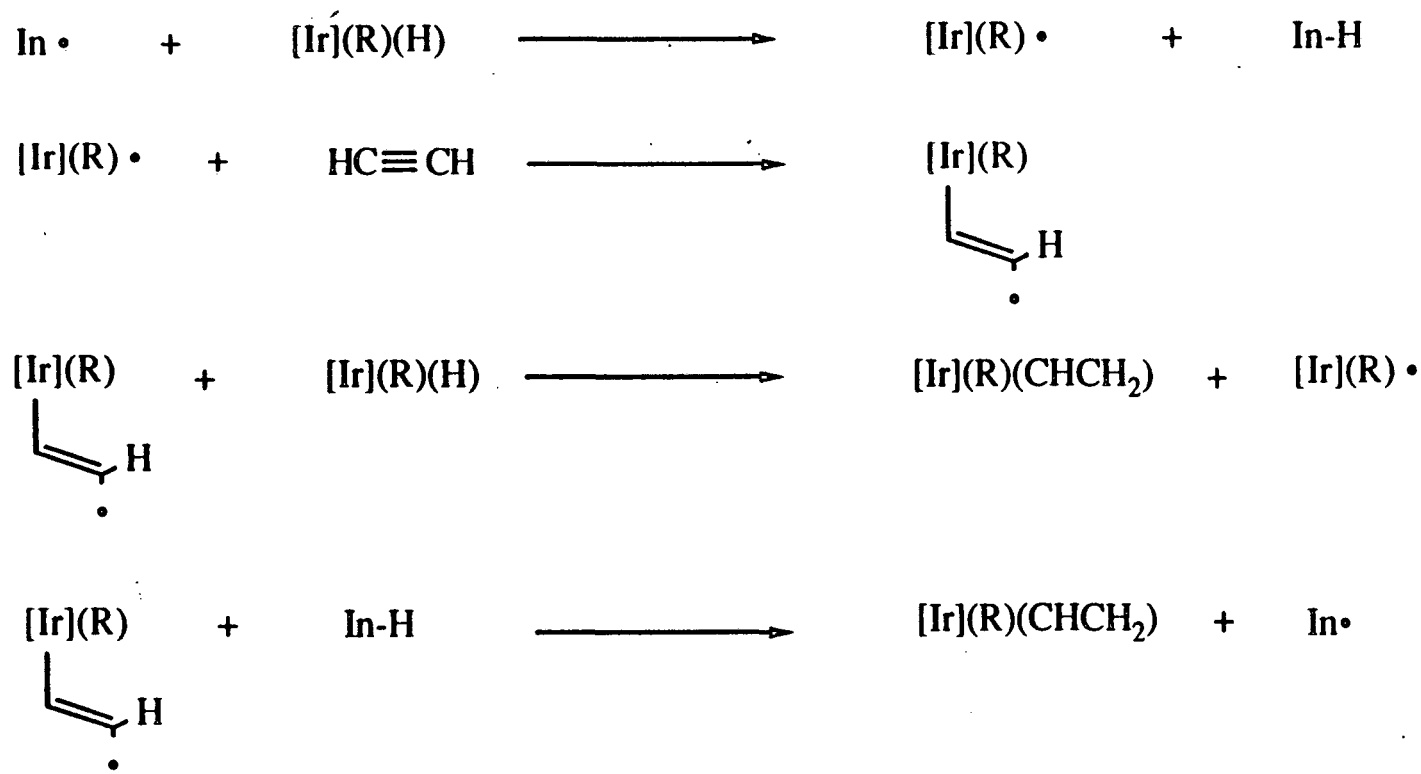

[Ir] = $(Cp^*)(PMe_3)Ir$

Scheme 3.12

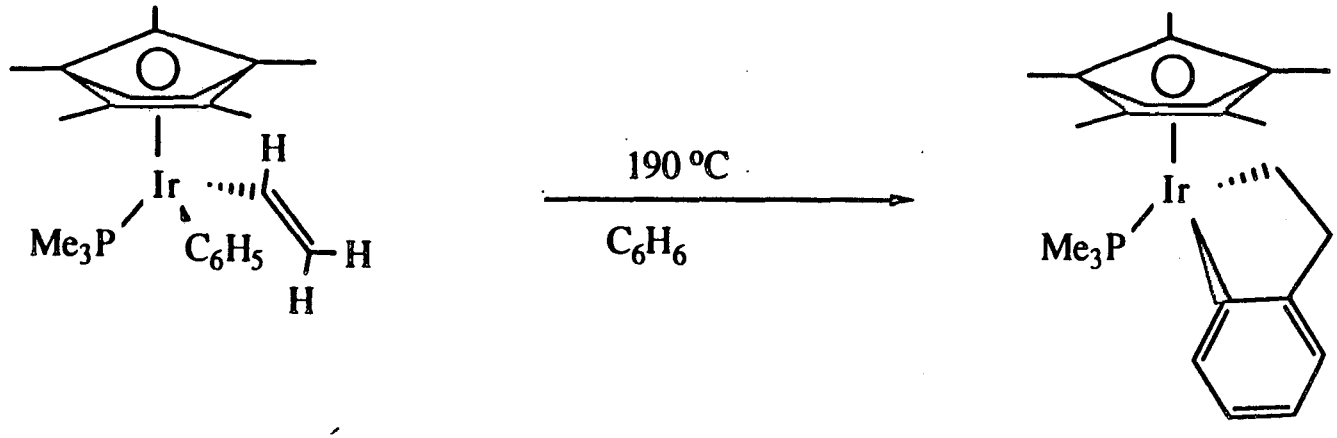

Scheme 3.13

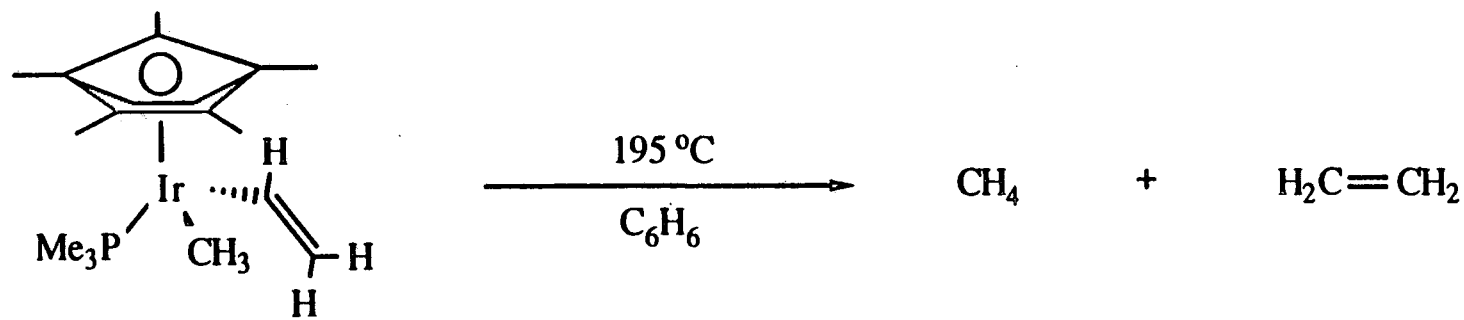

hydride is more stable than an aryl alkenyl complex. Presumably this is caused by the strong iridium-phenyl bond (82 kcal/mol) in (η^5-Me_5C_5)(PMe_3)Ir(C_6H_5)(H) (which may be weakened in (η^5-Me_5C_5)(PMe_3)Ir(C_6H_5)($HCCH_2$) by steric effects),[26] and the presence of a second reaction pathway for (η^5-Me_5C_5)(PMe_3)Ir(C_6H_5)($HCCH_2$). The lack of reductive elimination was somewhat discouraging as is suggested that this might be a common problem with similar stoichiometric functionalization schemes: when alkyl hydrides were stable enough to isolate, the dialkyls may be too stable to allow reductive elimination to occur.

In Chapter 1 of this Thesis, we considered the iridium-carbon and iridium-hydrogen bond strengths in this system. Assigning the iridium-vinyl, iridium-phenyl, iridium-alkyl, and iridium-hydrogen BDE's values of 71, 82, 56, and 76 kcal/mol respectively, and using accepted C-C and C-H BDE's,[27] it is possible to estimate the enthalpy of Equation 3.1.

$$(\eta^5\text{-}Me_5C_5)(PMe_3)Ir(R)(HCCH_2) + C_6H_6 \text{ ------> } (\eta^5\text{-}Me_5C_5)(PMe_3)Ir(C_6H_5)(H) + RHC{=}CH_2 \quad (3.1)$$

In Table 3.1 are compiled the approximate enthalpies of these reactions.

Table 3.1. Enthalpies for [Ir](R)($CHCH_2$) + C_6H_6 ----> [Ir](Ph)(H) + RHC=CH_2

R	ΔH (kcal/mol)
C_6H_5	-8
$CHCH_2$	-18
C_5H_{11}	-8
CH_3	-11

Since the iridium-carbon BDE's roughly parallel the C-H BDE's, replacement of benzene with pentane would increase the enthalpy of the reaction by only ca. 10 - 15 kcal/mol. There should also be little entropic component to the free energy of the reaction (ΔG). While these estimates are rough at best, they do seem to indicate that these reactions

are at least thermodynamically feasible. Our failure to observe reductive elimination under thermal conditions is therefore due to a kinetic barrier.

Chemical oxidation. Another way to induce reductive elimination in thermally stable systems is by oxidation of the metal center. For example, Kochi and coworkers[28] observed that thermolysis of cis-$[R_2Fe(bipy)_2]$ at 50 °C resulted in products derived from β-elimination pathways. Oxidation by one electron followed by thermolysis at 30 °C led to Fe-C bond homolysis products. Oxidation of the metal center by two electrons, however, led exclusively to coupled products at room temperature (Scheme 3.14). The observation that an oxidized metal complex is more prone to reductive elimination is consistent with the notion that the metal is being reduced during reductive elimination. Hoping to use this strategy to our advantage, we examined the oxidation of $(\eta^5\text{-}Me_5C_5)(PMe_3)Ir(R)(HCCH_2)$ ($R = C_6H_5$, $CHCH_2$, C_5H_{11}) using several different reagents.

All of the complexes examined were very easy to oxidize, as expected for such electron rich molecules. The products observed, however, were dependent on the oxidizing agent used. Reaction of $(\eta^5\text{-}Me_5C_5)(PMe_3)Ir(HC{=}CH_2)_2$ with $AgPF_6$ or $(BrC_6H_4)_3NBF_4$ in acetonitrile resulted in reductive elimination of butadiene, and production of $[(\eta^5\text{-}Me_5C_5)(PMe_3)Ir(NCCH_3)_2][X]_2$ (Scheme 3.15). Its identity was confirmed by independent synthesis starting from $(\eta^5\text{-}Me_5C_5)(PMe_3)Ir(Cl)_2$ and $AgPF_6$ (Scheme 3.16).[29] The best yields of butadiene were obtained when the $AgPF_6$ was used as the oxidant (69%). Reaction of $(\eta^5\text{-}Me_5C_5)(PMe_3)Ir(C_6H_5)(HCCH_2)$ with $(BrC_6H_4)_3NBF_4$ or with $AgPF_6$ results in reductive elimination of styrene and production of $[(\eta^5\text{-}Me_5C_5)(PMe_3)Ir(NCCH_3)_2][X]_2$ (Scheme 3.17). When $AgPF_6$ was used as the oxidant, $[(\eta^5\text{-}Me_5C_5)(PMe_3)Ir(NCCH_3)_2][X]_2$ was produced in 88% yield, and the yield of styrene was determined to be 50% by gas chromatography (this may have been lowered by reaction of styrene with Ag^0. While oxidation resulted in reductive elimination in both cases, the rates of the reactions were very different. Reaction of

Scheme 3.14

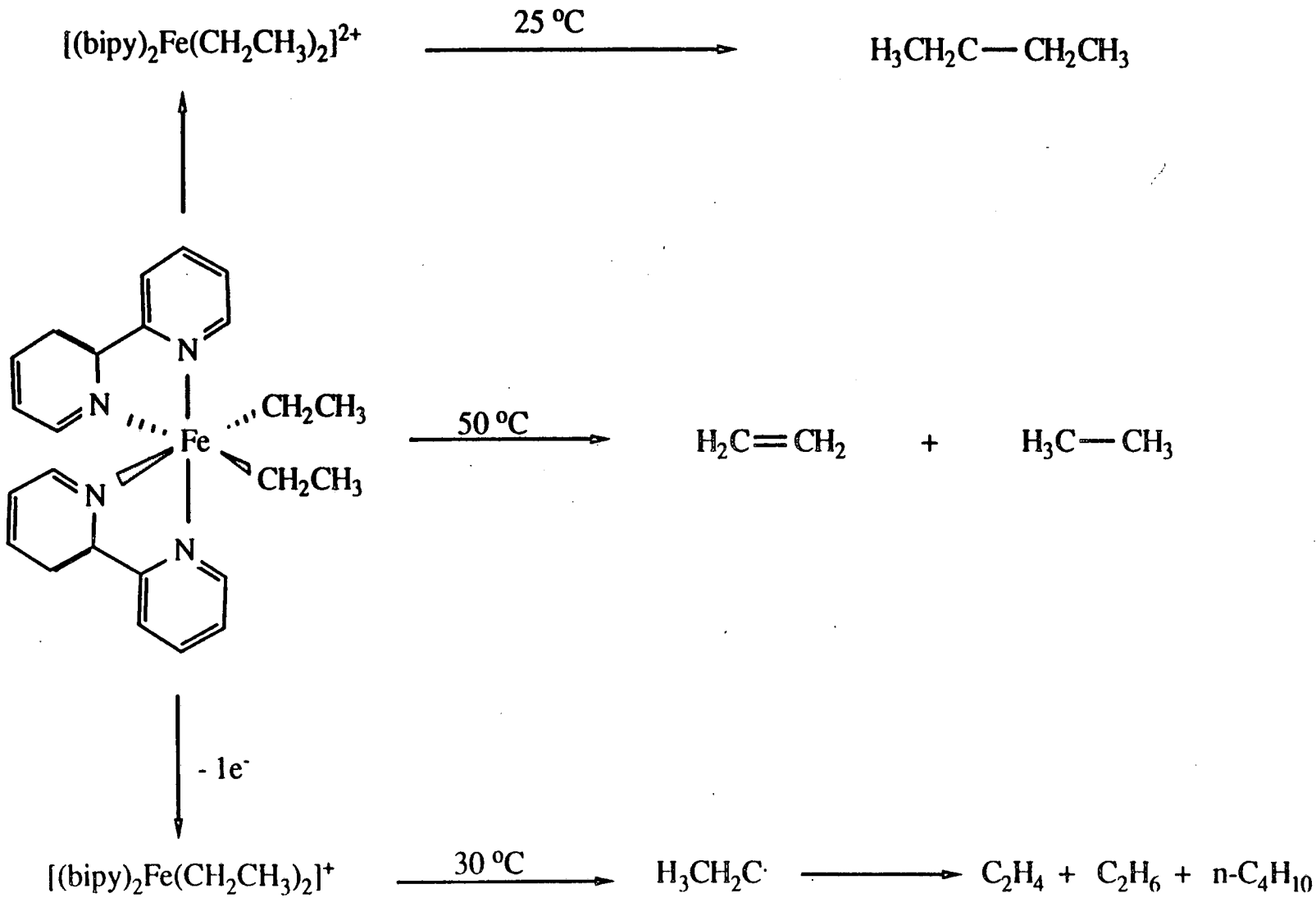
[(bipy)2Fe(CH2CH3)2]2+
25 °C
H3CH2C—CH2CH3
N
N
N
N
Fe
CH2CH3
CH2CH3
50 °C
H2C=CH2
+
H3C—CH3
- 1e-
[(bipy)2Fe(CH2CH3)2]+
30 °C
H3CH2C·
C2H4 + C2H6 + n-C4H10

Scheme 3.15

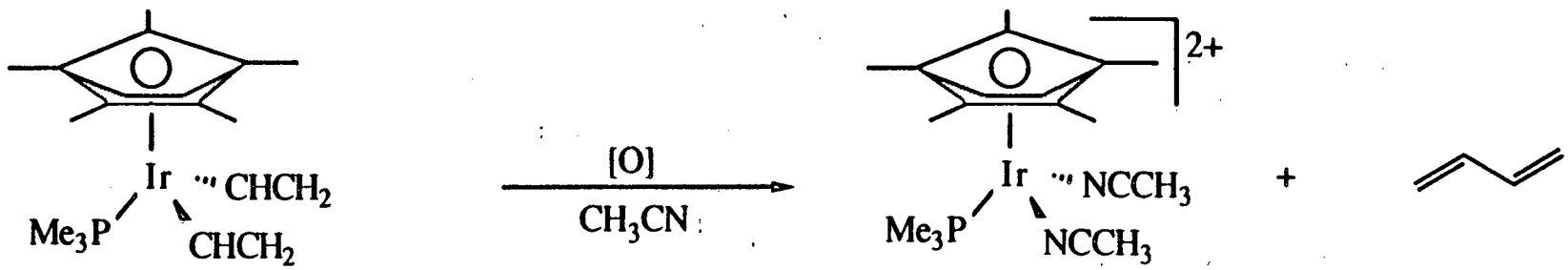

[O] = $AgPF_6$ or $(BrC_6H_4)_3NBF_4$

Scheme 3.16

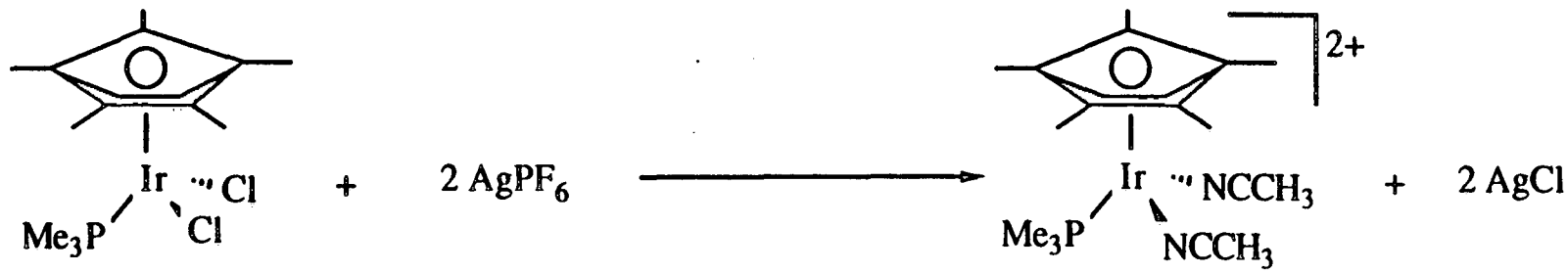

Scheme 3.17

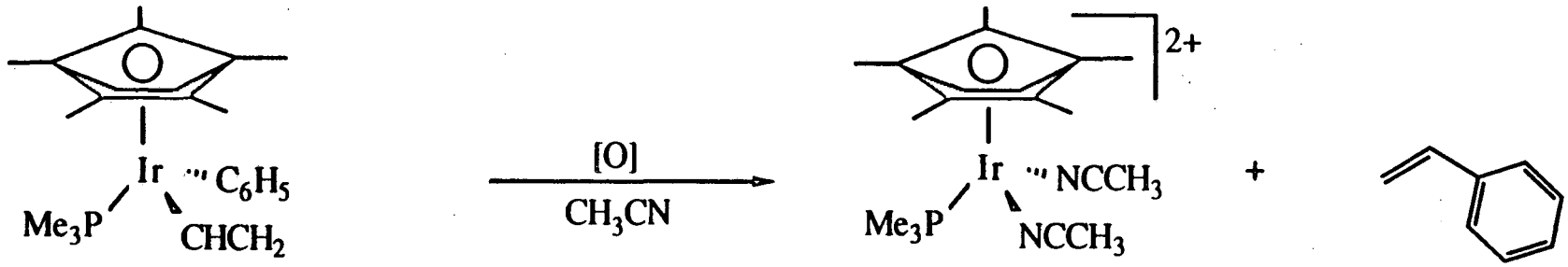

[O] = $AgPF_6$ or $(BrC_6H_4)_3NBF_4$

(η^5-Me_5C_5)(PMe_3)Ir(C_6H_5)($HCCH_2$) with $AgPF_6$ required 2-3 days, while reaction with (η^5-Me_5C_5)(PMe_3)Ir($HCCH_2$)$_2$ occurred much more quickly, and required stirring to give clean reductive elimination. In both cases oxidation with I_2, Cp_2FeBF_4, Na_2IrCl_6, or Ce(IV) did not lead to reductive elimination. When [Cp_2Fe][BF_4] was used, however, production of [(η^5-Me_5C_5)(PMe_3)Ir($NCCH_3$)$_2$][X]$_2$ was observed. During the course of optimizing the reaction conditions with [(BrC_6H_4)$_3$N][BF_4], it was discovered that yields were improved if (η^5-Me_5C_5)(PMe_3)Ir(R)($HCCH_2$) were added dropwise to a solution of [(BrC_6H_4)$_3$N][BF_4]. By monitoring the disappearance of the deep blue color of the oxidizing agent, we were able to determine that approximately two equivalents of the oxidizing agent were necessary for complete reaction.

Reaction of the compounds where R = alkyl (-CH_3 or -C_5H_{11}) with any of the oxidants described above, under a variety of conditions, did not lead to reductive elimination of R-$CHCH_2$, but formation of [(η^5-Me_5C_5)(PMe_3)Ir($NCCH_3$)$_2$][X]$_2$ was observed with some oxidizing agents. In an attempt to understand the differences between the reactions with saturated R groups and those with unsaturated R groups, we carried out electrochemical experiments.

Electrochemical oxidation. The single sweep cyclic voltammograms (CV) of (η^5-Me_5C_5)(PMe_3)Ir($HC{=}CH_2$)$_2$, (η^5-Me_5C_5)(PMe_3)Ir($HC{=}CH_2$)(C_6H_5), and (η^5-Me_5C_5)(PMe_3)Ir(C_5H_{11})($HCCH_2$) were very similar. A positive potential scan revealed a single oxidation wave between 50 and 200 mV vs ferrocene. This wave was found to be irreversible up to scan rates of 50,000 mV/s, and no further oxidation waves were observed out to the limit of the solvent. While we have not carried out controlled potential coulometry experiments, the chemical oxidation experiments indicate that two electrons are being transferred during this oxidation. Upon reversing the scan direction after the oxidation, a reduction wave was visible between -1500 and -1600 mV. No further reduction waves were visible before reduction of the solvent. When the oxidation was not carried out, no reduction waves were seem before the limit of the solvent. The reduction

wave at -1500 - -1600 mV has been identified as reduction of $[(\eta^5\text{-}Me_5C_5)(PMe_3)Ir(NCCH_3)_2][X]_2$.

The appearance of the reduction wave is sensitive to scan rate; it is not being seen with either very fast or very slow scan rates. At slow scan rates the reduction wave is not expected to be visible as the oxidized species will diffuse away from the electrode. Since what we are presumably observing is an electrochemical reaction followed by a chemical reaction (reductive elimination), in theory fast scan rates can set a limit on the rate of the chemical reaction. If the scan rate is competitive with the rate of the chemical reaction, the reducible species will not be present and no reduction wave will be visible. It was also observed, however, that the oxidation/reduction waves flattened out with increasing scan rate.[30] We do not know whether the absence of a reduction wave is due to the scan rate being competitive with the rate of reductive elimination, or a simple flattening of the wave due to increased scan rate.

That we can oxidatively induce reductive elimination in some $(\eta^5\text{-}Me_5C_5)(PMe_3)Ir(R)(HCCH_2)$ is encouraging, but would be especially significant if we could recycle the organometallic product $[(\eta^5\text{-}Me_5C_5)(PMe_3)Ir(NCCH_3)_2][X]_2$. With this in mind we have carried out several attempts at reduction of this species. Reduction by two electrons would regenerate iridium(I). In acetonitrile solvent, it is expected that this would result either in $(\eta^5\text{-}Me_5C_5)(PMe_3)Ir(NCCH_3)$[31] or in insertion into the C-H bond of acetonitrile yielding $(\eta^5\text{-}Me_5C_5)(PMe_3)Ir(CH_2CN)(H)$. However, reaction with reducing agents such as MeLi, Mn (powder), NaNap, $LiEt_3BH$, or with $NaBH_4$ failed to produce any pentane soluble products.[32]

A summary of the electrochemical data is given in Table 3.2. It should be noted that the potentials are likely to have considerable errors associated with them, as the waves are irreversible and the positions are somewhat dependent on the scan rate. The potentials listed are those at i_p(max).

Table 3.2. Electrochemical Potentials of [Ir](R)($CHCH_2$).

Complex	Oxidation (vs Cp_2Fe)	Reduction (vs Cp_2Fe)
[Ir](C_6H_5)($CHCH_2$)	200 mV	-1520 mV
[Ir]($CHCH_2$)$_2$	100 mV	-1500 mV
[Ir](C_5H_{11})($CHCH_2$)	30 mV	-1580 mV
[[Ir]($NCCH_3$)$_2$][PF_6]	--	-1600 mV

[Ir] = $Cp^*(PMe_3)Ir$

One of the problems to overcome if such processes are ever to become practical arises from the fact that electrochemistry is typically performed in polar solvents; we, however, wish to regenerate the reactive iridium(I) intermediate in the presence of hydrocarbons. In this way one would be able to regenerate an alkyl hydride, perform the insertion reaction, and then induce reductive elimination, completing the cycle. This necessitates having a polar solvent which has no C-H bonds, and will not react with the iridium(I) species. We have not investigated this, but it is possible that liquid NH_3 would suitable. It could stabilize the dication as acetonitrile does and one could perform reductions in it. If the reductions were performed in vigorously stirred alkane/NH_3 mixtures, and the reaction with NH_3 was sufficiently slow, we might observe reaction with the alkane. These experiments remain to be investigated.

Discussion.

The experiments described above, aimed at understanding possible C-H activation and functionalization processes for "(η^5-Me_5C_5)(PMe_3)Ir", lead one to consider in a general way similar hydrocarbon functionalization processes. As the complexes studied here have many features in common with other systems capable of C-H activation, much of what we have learned should be applicable to similar systems. While processes common in organometallic chemistry, such as olefin/acetylene insertion and reductive elimination, are

fairly well understood; we are still struggling to utilize these reactions with alkyl hydrides formed from C-H activation reactions.

The problem partly lies in the nature of the alkyl hydrides formed by C-H insertion; they are all coordinatively saturated, electron rich species. Typically the lowest energy process for these complexes is reductive elimination of R-H. Because there are no vacant coordination sites available, insertion reactions involving neutral ligands such as CO and $H_2C{=}CH_2$ are high energy processes. Frequently, reaction with such ligands simply results in replacement of R-H with the neutral ligand. Direct insertions of very electrophilic ligands, which probably occur by direct attack on the metal or the M-H bond, have been observed in these systems. But if one ever hopes to do such reactions on a large scale, easily handled ligands such as CO, $H_2C{=}CH_2$, or acetylene must be used. As we noted in Chapter 1 of this Thesis, many insertions reactions are, however, thermodynamically favored. Thus if the activation barriers can be lowered, such insertions will be observed. A case in point is the acetylene insertion into $(\eta^5\text{-}Me_5C_5)(PMe_3)Ir(R)(H)$, a reaction which *a priori* might have been expected to have a high activation barrier. Undoubtedly, methods can be developed for the insertion of other ligands under mild conditions into M-R and M-H bonds.

The second hurdle to overcome is the reductive elimination of R-R from the insertion product. Furthermore, since one will generate the unsaturated fragment believed to be responsible for C-H insertion, it is highly desirable to perform the reductive elimination under conditions which allow another alkyl hydride to be formed. This means that for any given system the rates of reductive elimination of R-R must be comparable to that found for R-H. Unfortunately, there are no such examples. Our system is typical in that the alkyl hydrides are much less stable than the dialkyls, consistent with the general belief that dialkyls are much more stable than alkyl hydrides, despite having a larger (more negative) enthalpy of reductive elimination. Theorticians have expressed the view that this is due to the directionality of sp^3 orbitals on carbon which make the necessary overlap with

the other carbon atom difficult.[33] One way around this problem is to utilize the strategy we adopted, and to oxidize the metal center. This, however, results in production of a cationic metal product which then needs to be reduced if it is going to be recycled. Such a process would only be feasible if an electrocatalytic process could be discovered. Furthermore, oxidation/reduction reactions need to be carried out in polar solvents. Only if the organometallic species were found to be unreactive toward certain polar solvents (such as NH_3 and H_2O), would these reactions be useful (in this cases the use of solvent mixtures such as H_2O/RH might be possible, vide supra).

The problems evident in functionalizing hydrocarbons from the alkyl hydrides suggest that we should consider other possibilities. Some examples of alkane dehydrogenation reactions have observed, but will not be suitable for hydrocarbons such as methane.[7] Particularly promising results have recently been obtained with electrophilic activation of C-H bonds by early transition metals and lanthanides. For example, Watson[34] has observed that $Cp^*_2Lu\text{-}CH_3$ will react with $^{13}CH_4$ to give $Cp^*_2Lu\text{-}^{13}CH_3$ + CH_4. Subsequent reaction with one equivalent of propene results in production of $Cp^*_2Lu\text{-}CH_2CH(CH_3)(^{13}CH_3)$. While the reaction was not reported, reaction with CH_4 would presumably yield $Cp^*_2Lu\text{-}CH_3$ and $CH_3CH(CH_3)(^{13}CH_3)$ (Scheme 3.18). Practical problems such as multiple insertions preclude this from being a useful process, but modification of ligands and conditions may provide the necessary selectivity. Similar chemistry has recently been observed for $(\eta^5\text{-}Me_5C_5)_2Sc\text{-}R$.[35] These or similar systems appear to be have more promising prospects as practical hydrocarbon functionalization catalysts, than those systems in which alkyl hydrides are formed.

Scheme 3.18

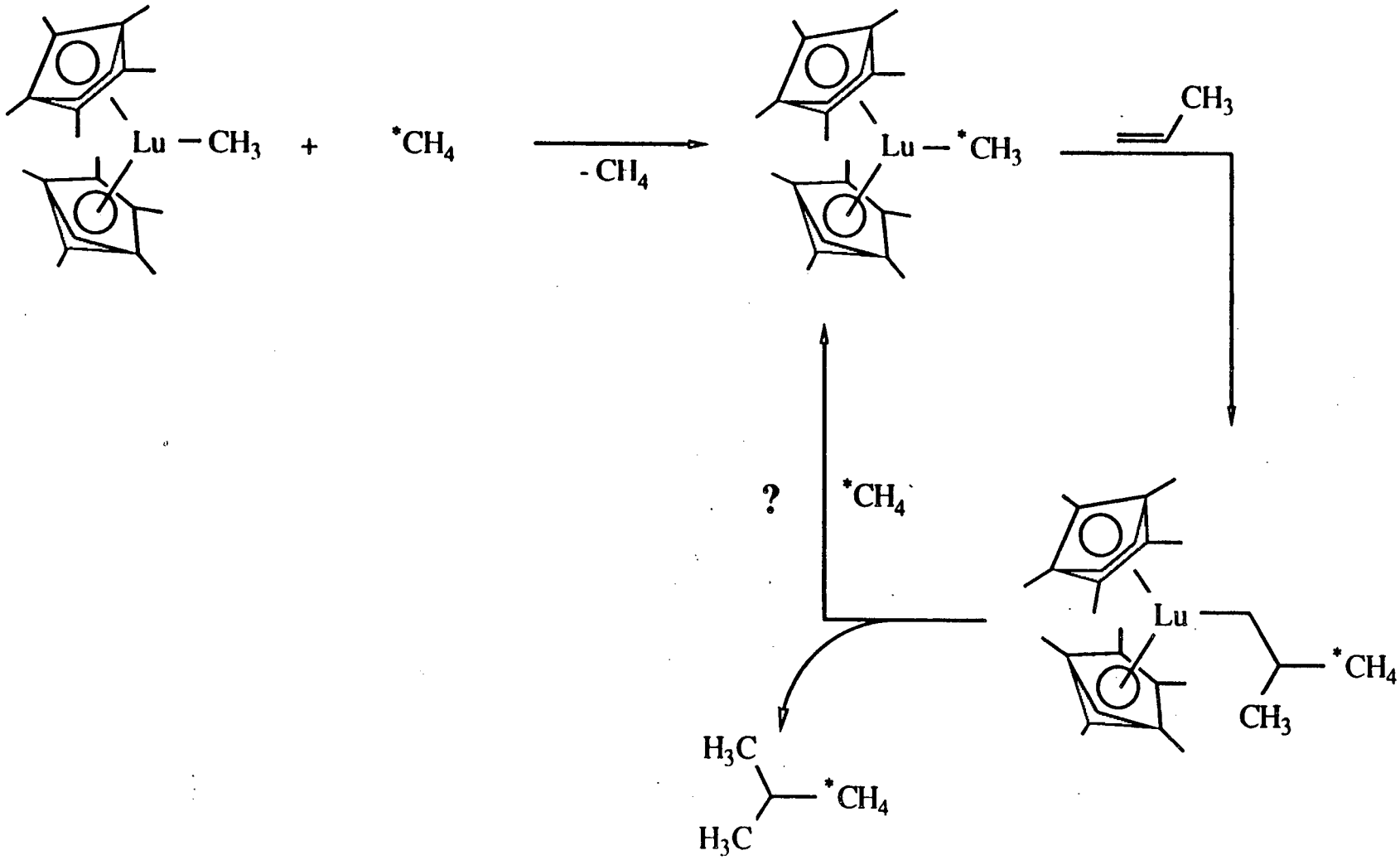

Experimental.

General. General procedures are given in the experimental section of Chapter 2 of this Thesis.

$(\eta^5\text{-}Me_5C_5)(PMe_3)Ir(Cl)_2$,[36] $(\eta^5\text{-}Me_5C_5)(PMe_3)Ir(HC{=}CH_2)(Br)$,[37] $(\eta^5\text{-}Me_5C_5)(PMe_3)Ir(HC{=}CH_2)(H)$,[37] and $(\eta^5\text{-}Me_5C_5)(PMe_3)Ir(R)(H)$[38] were synthesized according to published procedures. $LiHCCH_2$ was purchased from Organometallics as a 2.2 M solution in THF. MeMgCl and PhLi were purchased from Aldrich Chemical Co. as 3.0 M and 2.0 M solutions in ether and THF, respectively. $BrMgC_5H_{11}$ was purchased from Aldrich Chemical Co. as a 2.0 M solution in ether. *Tert*-butylammonium perchlorate was dried under high vacuum prior to use.

Gas chromatography was carried out on a Perkin-Elmer Sigma 300 gas chromatograph fitted with a capillary column (10 M methyl silicone). Response factors were determined by using standard solutions containing the compound of interest (styrene) and an internal standard (toluene).

Acetylene was washed by bubbling it through $NaHSO_3$, H_2SO_4, and finally passing it through a -78 °C trap prior to use. Addition of acetylene to the reaction mixture was accomplish by the use of a specially constructed adapter (Figure 3.1) which allows needles to be inserted into NMR tubes attached to a vacuum line. Initially, acetylene was simply bubbled through the solution using a cannula needle. After the solution was saturated, the cannula was removed and the stopcock was closed. The solution was then frozen at -196 °C, and the tube evacuated and sealed. More consistent results (due to the higher reproducibility of the amount of acetylene added) were obtained by adding the acetylene via syringe. Here the solution was frozen and the tube evacuated. The valve to the vacuum line was then closed. Gaseous acetylene was then added and immediately condensed on top of the solvent. The stopcock under the septum was then closed, and the valve to the vacuum opened to allow for the tube to be sealed under dynamic high vacuum.

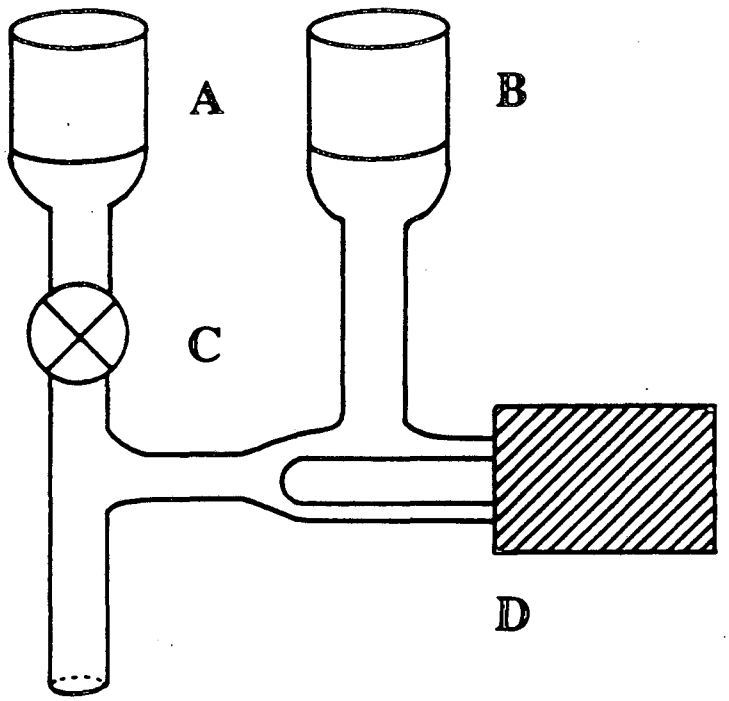

Figure 3.1. Apparatus used to add acetylene to NMR tubes. **A**: glass joint, fitted with a septum. **B**: glass joint attached to vacuum line. **C**: glass stopcock. **D**: teflon stopcock. Attached to NMR tube with a Cajon Ultra-Torr adapter.

Results were found to be independent of the way in which the acetylene was added. Furthermore, the results do not change if the acetylene is not washed prior to usage.

Insertion reactions. All insertion reactions were carried out in NMR tubes. A typical experiment was performed as follows. In the dry box an NMR tube was charged with 10.5 mg (0.0218 mmol) of (η^5-Me_5C_5)(PMe_3)Ir(C_6H_5)(H), 2.5 µl of $(CH_3)_3SiOSi(CH_3)_3$, and 0.65 mL of C_6D_6. Outside of the box, 15 mL of acetylene (1 atm) was added via syringe, as described in the General Experimental. The tube was then sealed under dynamic vacuum and irradiated at ca. 10 °C for 2.5 h. Comparison to the internal standard revealed a 70% yield of (η^5-Me_5C_5)(PMe_3)Ir(C_6H_5)($HCCH_2$), with 8% of (η^5-Me_5C_5)(PMe_3)Ir(C_6H_5)(H) remaining. Further photolysis did not change the relative amounts of the products.

Crossover experiment. In the dry box 9.6 mg (0.0200 mmol) of (η^5-Me_5C_5)(PMe_3)Ir(C_6D_5)(D) and 9.2 mg (0.0193 mmol) of (η^5-Me_5C_5)(PMe_3)Ir(C_6H_5)(H) were dissolved in 0.6 mL of C_6D_6. Outside of the drybox, acetylene was bubbled through the solution and it was then freeze-pump-thawed twice as described in the General Experimental. The tube was irradiated for 3 h, opened, and the solution passed through a short Al_2O_3 column with C_6H_6. Mass spectral analysis showed a mixture of d_0, d_1, d_5, and d_6 products in a ratio of 32:21:29:18. Control experiments were also performed in which (η^5-Me_5C_5)(PMe_3)Ir(C_6H_5)(H) (24.4 mg in 0.6 mL of C_6D_6) and (η^5-Me_5C_5)(PMe_3)Ir(C_6D_5)(D) (19.8 mg in 0.6 mL of C_6D_6) were separately reacted with acetylene and purified as above. Mass spectral analysis of a sample containing ca. 2 mg of each insertion product revealed a mixture of d_0, d_1, d_5, and d_6 in a ratio of 62:0:25:14. Control experiments have shown that reaction of (η^5-Me_5C_5)(PMe_3)Ir(C_6H_5)(H) with acetylene in C_6D_6 results in only d_0 products.

Thermolysis of (η^5-Me_5C_5)(PMe_3)Ir(R)($HCCH_2$).

Thermolysis of (η^5-Me_5C_5)(PMe_3)Ir(C_6H_5)($HCCH_2$). In the dry box 45 mg (0.089 mmol) of (η^5-Me_5C_5)(PMe_3)Ir(C_6H_5)($HCCH_2$) was dissolved in 0.6 mL of

C_6H_6. This was heated for 3 days at 190 °C (earlier experiments revealed that no reaction took place at lower temperatures). ^1H NMR revealed clean conversion to another product with some (η^5-Me_5C_5)(PMe_3)Ir(C_6H_5)(H) being the major impurity. Column chromatography of Al_2O_3 (III) with 3% ether/hexane as the eluent isolated the product. ^1H NMR (C_6D_6) δ 1.66 (d, η^5-Me_5C_5, J_{P-H} = 1.8 Hz), 0.85 (d, PMe_3, J_{P-H} = 9.6 Hz), 1.2, 2.0, 3.2, 3.3 (m, $C\underline{H_2}C\underline{H_2}C_6H_4$), 7.0, 7.1, 7.3 (m, $CH_2CH_2C_6\underline{H_4}$); MS (70 eV) 508, 506 ($C_{20}H_{32}P_1Ir_1$).

Thermolysis of other (η^5-Me_5C_5)(PMe_3)Ir(R)($HCCH_2$) compounds. Thermolysis of (η^5-Me_5C_5)(PMe_3)Ir($HC{=}CH_2$)$_2$, (η^5-Me_5C_5)(PMe_3)Ir(CH_3)($HCCH_2$), and (η^5-Me_5C_5)(PMe_3)Ir(C_5H_{11})($HCCH_2$) were carried out under similar conditions. In the case of (η^5-Me_5C_5)(PMe_3)Ir(CH_3)($HCCH_2$) significant amounts of CH_4 and $H_2C{=}CH_2$ were observed. The thermolyses of (η^5-Me_5C_5)(PMe_3)Ir($HC{=}CH_2$)$_2$ and (η^5-Me_5C_5)(PMe_3)Ir(C_5H_{11})($HCCH_2$) were not clean, but the same product seems to predominate in both cases. ^1H NMR revealed one set of resonances belonging to a coordinated PMe_3 (δ 1.01, J_{P-H} = 9.0 Hz), and several peaks which could belong to the methyl groups of the cyclpentadienyl ligand: 2.10 (s), 2.06 (s), 2.00 (d, J_{P-H} = 2.0 Hz), 1.92 (s). The product could not be purified by recrystallization, sublimation, or by chromatography even at -100 °C.

Oxidation reactions.

Oxidation of (η^5-Me_5C_5)(PMe_3)Ir(C_6H_5)($HCCH_2$). In the dry box, 7.0 mg (0.0138 mmol) of (η^5-Me_5C_5)(PMe_3)Ir(C_6H_5)($HCCH_2$) and 2.5 μl of hexamethyldisiloxane were dissolved in 0.6 mL of CD_3CN. This was then added to 10.7 mg (0.0423 mmol) of $AgPF_6$. After 18 h at 15 - 20 °C, ^1H NMR analysis revealed 65% conversion to [(η^5-Me_5C_5)(PMe_3)Ir($NCCH_3$)$_2$][PF_6]$_2$. After 3 days the reaction was complete, and comparison to the internal standard revealed an 88% yield of [(η^5-Me_5C_5)(PMe_3)Ir($NCCH_3$)$_2$][PF_6]$_2$. Gas chromatographic analysis of the solution

revealed a yield of greater than 47% styrene. Repeating the experiment resulted in a 50% yield of styrene. The yields of styrene may be low due some reaction with Ag^0.

In the dry box, 19.5 mg (0.0341 mmol) of $[(BrC_6H_4)_3N][BF_4]$ was dissolved in 0.2 mL of CD_3CN. With stirring, a solution of 10 mg (0.0197 mmol) of $(\eta^5\text{-}Me_5C_5)(PMe_3)Ir(C_6H_5)(HCCH_2)$ in CD_3CN (0.4 mL) was added until the solution changed from blue to colorless (approximately 2 equivalents). As $(\eta^5\text{-}Me_5C_5)(PMe_3)Ir(C_6H_5)(HCCH_2)$ was added $(BrC_6H_4)_3N$ precipitated from solution. ^1H NMR analysis revealed styrene and $[(\eta^5\text{-}Me_5C_5)(PMe_3)Ir(NCCH_3)_2][BF_4]_2$ as the major organometallic product. The yields were not determined. Oxidation with $[Cp_2Fe][BF_4]$ led to a complicated mixture of products.

Oxidation of $(\eta^5\text{-}Me_5C_5)(PMe_3)Ir(HC{=}CH_2)_2$. In the dry box, 10.3 mg (0.025 mmol) of $(\eta^5\text{-}Me_5C_5)(PMe_3)Ir(HC{=}CH_2)_2$ was dissolved in 0.5 mL of CH_3CN and added to a rapidly stirred suspension of 16.9 mg (0.0669 mmol) of $AgPF_6$. After ca. 1 day the reaction was judged complete (previous experiments indicate ca. 1 day is necessary: note this is faster than the oxidation of $(\eta^5\text{-}Me_5C_5)(PMe_3)Ir(C_6H_5)(HCCH_2)$). When the reaction was performed in CD_3CN, butadiene was evident in the ^1H NMR. In this case, measurement of the butadiene with a Toepler pump revealed a 69% yield. Mass spectral analysis of the gases collected revealed that > 95% of the gases collected were butadiene. ^1H NMR analysis of the nonvolatile products showed only $[(\eta^5\text{-}Me_5C_5)(PMe_3)Ir(NCCH_3)_2][PF_6]_2$. Oxidation with I_2, Na_2IrCl_6, cerium tetrafluoroacetate, or $[Cp_2Fe][BF_4]$ did not result in production of butadiene, although in the case of $[Cp_2Fe][BF_4]$, $[(\eta^5\text{-}Me_5C_5)(PMe_3)Ir(NCCH_3)_2][BF_4]_2$ was seen. Oxidation with $[(BrC_6H_4)_3N][SbCl_6]$ resulted in production of some butadiene, but several organometallic products.

Oxidation of $(\eta^5\text{-}Me_5C_5)(PMe_3)Ir(n\text{-}C_5H_{11})(CHCH_2)$. Reaction of $(\eta^5\text{-}Me_5C_5)(PMe_3)Ir(C_5H_{11})(HCCH_2)$ with $AgPF_6$, $[(BrC_6H_4)_3N][BF_4]$, or I_2, using the procedures described above, led to no measurable amounts of 1-heptene. In the first two

cases however, reasonable amounts of $[(\eta^5\text{-}Me_5C_5)(PMe_3)Ir(NCCH_3)_2][X]_2$ were seen. Similarly reduction with Na/K did not result in production of any 1-heptene. In all cases the fate of the alkyl and alkenyl ligands in unknown. Small vinyl resonances belonging to several products were seen in the ^1H NMR spectrum, but results varied from one experiment to the next.

Electrochemistry. Electrochemistry was performed in the dry box using a BAS-100 electrochemical analyzer. The working and counter electrodes were platinum, and reference electrode was silver. Potentials were recorded vs the silver electrode which was then calibrated to ferrocene by addition of a small amount of ferrocene to each solution. The scan rates were typically between 50 and 200 mV/s. In all cases the solvent used was acetonitrile freshly distilled from CaH_2, with *tert*-butylammonium perchlorate (TBAP) (0.1 M) as the supporting electrolyte. The concentration of the iridium complexes were 1 mmolar.

Independent synthesis and characterization.

$(\eta^5\text{-}Me_5C_5)(PMe_3)Ir(HC{=}CH_2)_2$. In the dry box, 1.3574 g (0.0029 mol) of $(\eta^5\text{-}Me_5C_5)(PMe_3)Ir(Cl)_2$ was slurried in 100 mL of THF and cooled to -40 °C. Over a 1 min period, 2.2 equivalents (2.9 mL of a 2.2 M solution in THF) of $LiHCCH_2$ was added. The resulting solution solution was stirred for ca. 20 h. The solvent was removed in vacuo and the residue taken up in ether and filtered through celite. The product was further purified by chromatography on Al_2O_3 using benzene as the eluent. Yield: 950 mg (0.0021 mol, 71%). Analytically pure material was obtained by recrystallization from pentane. ^1H NMR (C_6D_6) δ 1.64 (d, $\eta^5\text{-}Me_5C_5$, $J_{P\text{-}H}$ = 1.7 Hz), 1.08 (d, PMe_3, $J_{P\text{-}H}$ = 10.3 Hz), 5.45 (dd, -CHC$\underline{H}_2$, $J_{H\text{-}H(trans)}$ = 17.7 Hz, $J_{H\text{-}H(gem)}$ = 3.2 Hz), 6.68 (dd, -CHC$\underline{H}_2$, $J_{H\text{-}H(cis)}$ = 10.2 Hz, $J_{H\text{-}H(gem)}$ = 3.0 Hz), 7.97 (dd, -C$\underline{H}$CH$_2$, $J_{H\text{-}H(cis)}$ = 10.3 Hz, $J_{H\text{-}H(trans)}$ = 17.9 Hz); ^{13}C NMR (C_6D_6) δ 9.43 (s, $\eta^5\text{-}\underline{Me}_5C_5$), 13.61 (d, PMe_3, $J_{P\text{-}C}$ = 39.6 Hz), 93.41 (d, $\eta^5\text{-}Me_5C_5$, $J_{P\text{-}C}$ = 2.7 Hz), 118.85 (d, -CHC$\underline{H}_2$, $J_{P\text{-}C}$ = 4.8 Hz), 143.71 (d, -C$\underline{H}$CH$_2$, $J_{P\text{-}C}$ = 15.4 Hz); IR (C_6D_6) 1654 (m), 1551 (m), 953 (s), 937 (s).

MS (70 eV) 458,456 (M^+), 402, 400 (M^+ - C_4H_8); mp >180°C (decomp). Anal. Calcd: C, 44.63; H, 6.66. Found: C, 45.05; H, 6.62.

(η^5-Me_5C_5)(PMe_3)Ir(C_6H_5)($HCCH_2$). In the dry box 647.5 mg (1.27 mmol) of (η^5-Me_5C_5)(PMe_3)Ir($HC{=}CH_2$)(Br) was dissolved in 40 mL of THF and cooled to -40 °C. With stirring, 1.4 mmol (0.7 mL of a 2.0 M solution in THF) of PhLi was added. After 20 h the solvent was removed in vacuo, and the residue extracted with pentane. ^1H NMR revealed approximately 40% of the desired product and 40% of the starting material. Chromatography on Al_2O_3 with 5% ether/pentane as the eluent was used to isolate the product as white crystals. Yield (based on starting material): 80.7 mg (12.5%). ^1H NMR (C_6D_6) δ 1.51 (d, η^5-Me_5C_5, J_{P-H} = 1.8 Hz), 1.04 (d, PMe_3, J_{P-H} = 10.0 Hz), 5.44 (dd, -CHC$\underline{H}_2$, $J_{H-H(trans)}$ = 17.9 Hz, $J_{H-H(gem)}$ = 2.9 Hz), 6.72 (dd, -CHC$\underline{H}_2$, $J_{H-H(cis)}$ = 10.5 Hz, $J_{H-H(gem)}$ = 3.2 Hz), 7.10 (m, -C_6H_5), 7.56 (m, -C_6H_5), 8.13 (dd, -C$\underline{H}$CH$_2$, $J_{H-H(cis)}$ = 10.5 Hz, $J_{H-H(trans)}$ = 17.9 Hz); ^{13}C NMR (C_6D_{12}) δ 9.48 (s, η^5-$\underline{Me}_5C_5$), 14.72, (d, PMe_3, J_{P-C} = 38.6 Hz), 94.24 (d, η^5-$Me_5\underline{C}_5$, J_{P-C} = 3.5 Hz), 119.60 (d, -CH$\underline{C}$H$_2$, J_{P-C} = 5.0 Hz), 121.90 (s, -C_6H_5), 127.81 (s, -C_6H_5), 138.74 (d, -C_6H_5, J_{P-C} = 12.2 Hz), 141.13 (d, -C_6H_5, J_{P-C} = 3.4 Hz), 141.48 (d, -$\underline{C}$HCH$_2$, J_{P-C} = 17.0 Hz); IR (KBr) 1568 (s), 1552 (s), 947 (s), 738 (s), 705 (s); MS (70 eV) 508, 506 (M^+), 404, 402 (M^+ - C_8H_8), 104 (C_8H_8); mp > 125°C (decomp). Anal. Calcd: C, 49.68; H, 6.35. Found: C, 49.07; H, 6.49.

[(η^5-Me_5C_5)(PMe_3)Ir($NCCH_3$)$_2$][PF_6]$_2$. In the dry box, $AgPF_6$ was slurried in 10 mL of CH_3CN and 471.0 mg (0.993 mmol) of (η^5-Me_5C_5)(PMe_3)Ir(Cl)$_2$ in 5 mL of CH_3CN was added with stirring. A white precipitate formed immediately. The mixture was stirred for 2.5 h and then filtered through celite. The solvent was removed in vacuo leaving a yellow/brown gum. This was redissolved in 2 mL of CH_3CN, layered with 2 mL of ether, and put into a -40 °C freezer for 3 days. The crystals were collected and washed with ether. Yield: 290 mg (38%). ^1H NMR (CD_3CN) δ 1.79 (d, η^5-Me_5C_5, J_{P-H} = 2.4 Hz), 1.74 (d, PMe_3, J_{P-H} = 11.8 Hz); ^1H NMR (D_2O) δ 2.56 (d, $NCCH_3$,

J_{P-H} = 2.4 Hz), 1.70 (d, η^5-Me_5C_5, J_{P-C} = 2.4 Hz), 1.65 (d, PMe_3, J_{P-C} = 11.7 Hz); ^{13}C NMR (CD_3CN) δ 4.42 (sept., $NC\underline{C}D_3$ J_{C-D} = 20.3 Hz (coordinated)), 9.13 (s, η^5-$\underline{Me}_5C_5$), 13.77 (d, PMe_3, J_{P-C} = 39.2 Hz), 97.80 (s, η^5-$Me_5\underline{C}_5$), 124.81 (s, $N\underline{C}CD_3$ (coordinated)); IR (KBr) 1332 (s), 1156 (s), 850 (s), 499 (s); MS (FAB) 505 ($[Ir]^{2+}$ + F^-), 429 ($[Ir]^{2+}$ + F^- - PMe_3); Anal. Calcd: C, 26.33; N, 3.61;H, 3.90. Found: C, 26.56; N, 3.88; H, 4.25.

(η^5-Me_5C_5)(PMe_3)Ir(CH_3)($HCCH_2$). In the dry box 127.7 mg (0.2544 mmol) of (η^5-Me_5C_5)(PMe_3)Ir($HC{=}CH_2$)(Br) was dissolved in 10 mL of ether and cooled to -40 °C. To this slightly greater than 1 equivalent (95 μl of a 2.8 M solution) of CH_3MgCl was added. The solution stirred for 24 h and the solvent was removed in vacuo. The residue was extracted with pentane and filtered through celite. ^1H NMR analysis showed 90% (η^5-Me_5C_5)(PMe_3)Ir(CH_3)($HCCH_2$), 5% (η^5-Me_5C_5)(PMe_3)Ir($HC{=}CH_2$)(Br), and 5% (η^5-Me_5C_5)(PMe_3)Ir(CH_3)$_2$. Attempts to further purify the product by chromatography on Al_2O_3 (III) resulted in a mixture of (η^5-Me_5C_5)(PMe_3)Ir(CH_3)($HCCH_2$), (η^5-Me_5C_5)(PMe_3)Ir(CH_3)$_2$, and (η^5-Me_5C_5)(PMe_3)Ir($CHCH_2$)$_2$. The following NMR resonances were attributed to the methyl vinyl compound: ^1H NMR (C_6D_6) δ 1.63 (d, η^5-Me_5C_5, J_{P-H} = 1.7 Hz), 1.06 (d, PMe_3, J_{P-H} = 9.9 Hz), 0.58 (d, -CH_3, J_{P-H} = 5.9 Hz), 5.45 (dd, -$CHC\underline{H}_2$, $J_{H-H(trans)}$ = 17.7 Hz, $J_{H-H(gem)}$ = 3.5 Hz), 6.67 (dd, -$CHC\underline{H}_2$, $J_{H-H(cis)}$ = 10.3 Hz, $J_{H-H(gem)}$ = 3.5 Hz), 7.95 (ddd, -$C\underline{H}CH_2$, $J_{H-H(cis)}$ = 10.3 Hz, $J_{H-H(trans)}$ = 17.7 Hz, J_{P-H} = 1.8 Hz); ^{13}C NMR (C_6D_6) δ -21.54 (d, -CH_3, J_{P-C} = 8.8 Hz), 9.14 (s, η^5-$\underline{Me}_5C_5$), 13.93 (d, PMe_3, J_{P-C} = 37.3 Hz), 92.14 (d, η^5-$Me_5\underline{C}_5$, J_{P-C} = 3.5 Hz), 118.35 (d, -$CH\underline{C}H_2$, J_{P-C} = 4.6 Hz), 141.14 (d, -$\underline{C}HCH_2$, J_{P-C} = 15.3).

(η^5-Me_5C_5)(PMe_3)Ir(n-C_5H_{11})($HCCH_2$). In the dry box, 400 mg (0.78 mmol) of (η^5-Me_5C_5)(PMe_3)Ir($HC{=}CH_2$)(Br) was dissolved in 50 mL of ether. To this 0.80 mmol of $BrMgC_6H_{11}$ (2.0 M solution in 0.40) was added with a syringe. This was stirred for several hours, and the solvent removed in vacuo. ^1H NMR analysis revealed a

mixture of two products. Using chromatography (Al_2O_3 5% ether/pentane) these were partially separated. The first fraction contained a ca. 1:1 mixture of these two products, the second and the third were >90% one product, believed to be (η^5-Me_5C_5)(PMe_3)Ir(n-C_5H_{11})($HCCH_2$) (vide post). Leaving the first two fractions in C_6D_6 in the dry box for ca. 1 week resulted in the appearance of a new product having no vinyl resonances associated with it (δ 1.65 (d, η^5-Me_5C_5, J_{P-H} = 1.8 Hz), 1.14 (d, PMe_3, J_{P-H} = 9.4 Hz)). The following spectral data have been attributed to (η^5-Me_5C_5)(PMe_3)Ir(n-C_5H_{11})($HC{=}CH_2$): ^1H NMR (C_6D_6) δ 1.65 (d, η^5-Me_5C_5, J_{P-H} = 1.7 Hz), 1.08 (d, PMe_3, J_{P-H} = 10.3 Hz), 5.46 (dd, -CHC$\underline{H}_2$, $J_{H-H(trans)}$ = 17.8 Hz, $J_{H-H(gem)}$ = 3 Hz), 6.67 (dd, -CHC$\underline{H}_2$ (dd, $J_{H-H(cis)}$ = 10.2 Hz, $J_{H-H(gem)}$ = 3 Hz), 7.97 (dd, -C$\underline{H}$CH$_2$, $J_{H-H(cis)}$ = 10.2 Hz, $J_{H-H(trans)}$ = 17.8 Hz); ^{13}C NMR (C_6D_6) δ 143.48 (d, -$\underline{C}$HCH$_2$, J_{P-C} = 15.1 Hz), 118.52 (d, -CH$\underline{C}$H$_2$, J_{P-C} = 5.0 Hz), 93.08 (d, η^5-Me_5C_5, J_{P-C} = 3.5 Hz), 13.30 (d, PMe_3, J_{P-C} = 39.2 Hz), 9.17 (s, η^5-Me_5C_5), 8.69, 8.56, 8.50 (s, -C_5H_{11}, (other peaks attributed to the pentyl ligand were not observed)); MS (70 eV) 502,500 (M^+), 404, 402 (M^+ - C_7H_{14}). The following spectral data are believed to belong to the other compound produced in this reaction: ^1H NMR (C_6D_6) δ 1.65 (d, η^5-Me_5C_5, J_{P-H} = 1.8 Hz), 1.14 (d, PMe_3, J_{P-H} = 11.8 Hz), 7.70, 6.60, 5.40 (m, CH=CH$_2$).

References.

[1] (a) Gesser, H.D.; Hunter, H.R.; Prakash, C.B. *Chem. Rev.* **1985**, *85*, 235. (b) Labinger, J.A.; Ott, K.C. *J. Phys. Chem.* **1987**, *91*, 2682 and references therein.

[2] Koenig, G. *Appl. Catal.* **1983**, *6*, 263.

[3] Well established methane to synthesis gas technology exists; these processes are very energy intensive. (a) Witcoff, H.A.; Reuben, B.G. *Industrial Organic Chemicals in Perspective*; Wiley: New York, 1980; Part 1, pp 108-119. (b) Dybkjaer, I. *CEER Chem. Econ. Eng. Rev.* **1981**, *13*, 17-25. (c) Weissermel, K.; Arpe, H.-J. *Industrial Organic Chemistry*; Verlag Chemie: Weinheim, 1978. (d) Haggin, J. *Chem. & Eng. News* **1987**, June 1, pp 22-28. There have also been recent reports describing other routes leading to higher hydrocarbons: (a) Labinger, J.A.; Ott, K.C. *J. Phys. Chem.* **1987**, *91*, 2682 and references therein. (b) Gesser, H.D.; Hunter, N.R.; Prakash, C.B. *Chem. Rev.* **1985**, *85*, 235.

[4] (a) Smegal, J.A.; Hill, C.L. *J. Am. Chem. Soc.* **1983**, *105*, 3515. (b) Hill, C.J.; Smegal, J.A.; Henley, T.J. *J. Org. Chem.* **1983**, *48*, 3277. (c) Groves, J.T.; Nemo, T.E. *J. Am. Chem. Soc.* **1983**, *105*, 6243. (d) Tabushi, I.; Yazaki, A. *J. Am. Chem. Soc.* **1981**, *103*, 7371. (e) Mansuy, D.; Fontecave, M.; Bartoli, J.F. *J.C.S. Chem. Comm.* **1983**, 253.

[5] (a) Hanotier, J.; Camerman, P.; Hanotier-Bridoux, M.; De Radzitzky, P. *J. C. S. Perkin II* **1972**, 2247. (b) Barton, D.H.R.; Hay-Motherwell, R.S.; Motherwell, W.B. *Tett. Lett.* **1983**, *24*, 1979. (c) Barton, D.H.R.; Gustiger, M.J.; Motherwell, W.B. *J.C.S. Chem. Comm.* **1983**, 41.

[6] For recent reviews of C-H bond activation see: (a) Halpern, J. *Inorg. Chim. Acta.* **1985**, *100*, 41. (b) Aktogu, N.; Baudry, D.; Cox, D.; Ephritikhine, M.; Felkin, H.; Holmes-Smith, R.; Zakrzewski, J. *Bull. Soc. Chim. France* **1985**, 381. (c) Green, M.L.H.; O'Hare, D. *Pure & Appl. Chem.* **1985**, *57*, 1897. (d) Crabtree, R.H. *Chem. Rev.* **1985**, *85*, 245.

[7] (a) Crabtree, R.H.; Mihelcic, J.M.; Quirk, J.M. *J. Am. Chem. Soc.* **1979**, *101*, 7738. (b) Crabtree, R.H.; Mellea, M.F.; Mihelcic, J.M.; Quirk, J.M. *J. Am. Chem. Soc.* **1982**, *104*, 107. (c) Crabtree, R.H.; Parnell, C.P. *Organometallics* **1984**, *3*, 1727. (d) Crabtree, R.H.; Demou, P.C.; Eden, D.; Mihelcic, J.M.; Parnell, C.P.; Quirk, J.M.; Morris, G.E. *J. Am. Chem. Soc.* **1982**, *104*, 6994. (e) Baudry, D.; Ephritikine, M.; Felkin, H. *J. Chem. Soc., Chem. Comm.* **1980**, 1243. (f) Baudry, D.; Ephritikine, M.; Felkin, H.; Holmes-Smith, R. *J. Chem. Soc., Chem. Comm.* **1983**, 788. (g) Baudry, D.; Ephritikine, M.; Felkin, H.; Zakrzewski J. *J. Chem. Soc., Chem. Comm.* **1982**, 1235. (h) Baudry, D.; Ephritikine, M.; Felkin, H.; Zakrzewski, J. *Tetrahedron Lett.* **1984**, 1283. (i) Burchard, T.; Felkin, H. *Nouv. J. Chim.* **1986**, *10*, 673. (j) Aktogu, N.; Baudryt, D.; Cox, D.; Ephritikhine, M.; Felkin, H.; Holmes-Smith, R.; Zakrzewski, J. *Bull. Soc. Chim. Fr.* **1985**, 381. (k) Felkin, H.; Fillebeen-Khan, T.; Holmes-Smith, R.; Lin, Y. *Tett. Lett.* **1985**, 1999. (l) Baudry, D.; Ephritikhine, M.; Felkin, H.; Zakrzewski, J. *Tett. Lett.* **1984**, 1283. (m) Felkin, H.; Fillebeen-Khan, T.; Gault, Y.; Holmes-Smith, R.; Zakrzewski, J. *Tett. Lett.* **1984**, 1279.

[8] (a) Fisher, B.J.; Eisenberg, R. *Organometallics* **1983**, *2*, 764. (b) Jones, W.D.; Kosar, W.P. *J. Am. Chem. Soc.* **1986**, *108*, 5640. There are, of course, many examples of electrophilic oxidation and metalation of aromatic hydrocarbons, see: Shilov, A.E. *Activation of Saturated Hydrocarbons by Transition Metal Complexes*, D. Reidel: Boston, 1984.

[9] (a) Janowicz, A.H.; Bergman, R.G. *J. Am. Chem. Soc.* **1983**, *105*, 3929. (b) Buchanan, J.M.; Stryker, J.M.; Bergman, R.G. *J. Am. Chem. Soc.* **1986**, *108*, 1537. See also: Jones, W.D.; Feher, F.J. *J. Am. Chem. Soc.* **1984**, *106*, 1650.

[10] In the case of ethylene, C-H insertion also results, see: Chapter 2 of this Thesis.

[11] Janowicz, A.H.; Bergman, R.G. *J. Am. Chem. Soc.* **1983**, *105*, 3929.

[12] A similar insertion has been observed in the related rhodium system. Jones, W.D. personal communication. Other electrophiles such as *tert*-butylisonitrile behave similarly.

[13] Collman, J.P.; Hegedus, L.S.; Norton, J.R.; Finke, R.G. *Principles and Applications of Organotransition Metal Chemistry* ; University Science Books: Mill Valley, CA, 1987.

[14] Amaudrut, J.; Leblanc, J-C.; Moise, C.; Sala-Pala, J. *J. Organomet. Chem.* **1985**, *295*, 167.

[15] Nakamura, A.; Otsuka, S. *J. Mol. Cat.* **1975-76**, *1*, 285.

[16] (a) Amaudrut, J.; Leblanc, J-C.; Moise, C.; Sala-Pala, J. *J. Organomet. Chem.* **1985**, *295*, 167. (b) Baddley, W.H.; Tupper, G.B. *J. Organomet. Chem.* **1972**, *36*, 377. (c) Cullen, W.R.; Dowson, D.S.; Styan, G.E. *Can. J. Chem.* **1965**, *43*, 3365.

[17] Clark, H.C.; Wong, C.S. *J. Am. Chem. Soc.* **1977**, *99*, 7073.

[18] Nakamura, A.; Otsuka, S. *J. Mol. Catal.* **1975-76**, *1*, 285.

[19] For a general review of acetylene insertions, see: Otsuka, S.; Nakamura, A. *Adv. Organomet. Chem.* **1976**, *14*, 245.

[20] We have not been able to conduct the control experiment to see if a cis product would equilibrate under the reaction conditions, but we feel this to be unlikely.

[21] We have not yet ruled out that this scrambling could be taking place in the mass spectrometer, but we feel this to be unlikely.

[22] Stoutland, P.O. Chapter 1 of this Thesis.

[23] Chang, J.; Bergman, R.G. *J. Am. Chem. Soc.* **1987**, *109*, 4298 and references therein.

[24] McGhee, W.D. personal communication.

[25] At 180 °C, (η^5-Me_5C_5)(PMe_3)Ir(HC=CH_2)(H) starts to undergo an isomerization to (η^5-Me_5C_5)(PMe_3)Ir(H_2C=CH_2). See Chapter 2 of this Thesis.

[26] Nolan, S.P., Hoff, C.D., Stoutland, P.O., Newman, L.J., Buchanan, J.M., Bergman, R.G., Yang, G.K., Peters, K.S. *J. Am. Chem. Soc.* **1987**, *109*, 3143.

[27] We estimate the C-C bond dissociation enthalpies in biphenyl, butadiene, 1-heptene, and propene to be 114, 115, 89, and 92 kcal/mol, respectively. These were calculated from the heats of formation of the appropriate compounds and radicals: (a) Cox, J.D.; Pilcher, G. *Thermochemistry of Organic and Organometallic Compounds;* Academic: London, 1970. (b) McMillen, D.F.; Golden, D.M. *Annu. Rev. Phys. Chem.* **1982**, *33*, 493-532.

[28] (a) Tsou, T.T.; Kochi, J.K. *J. Am. Chem. Soc.* **1978**, *100*, 1634. (b) Kochi, J.K.; Lau, W.; Huffman, J.C. *Organometallics* **1982**, *1*, 155.

[29] Maitlis has made several similar iridium salts: (a) Thompson, S.J; White, C.; Maitlis, P.M. *J. Organomet. Chem.* **1977**, *136*, 87. (b) White, C.; Thompson, S.J.; Maitlis, P.M. *J.Chem. Soc. Dalton Trans.* **1977**, 1654. (c) White, C.; Thompson, S.J.; Maitlis, P.M. *J.Chem. Soc. Dalton Trans.* **1978**, 1305.

[30] We do not know the origin of theis phenomenon.

[31] Chetcuti, P.A.; Knobler, C.B.; Hawthorne, M.F. *Organometallics* **1986**, *5*, 1913.

[32] Complexes of the type (η^5-Me_5C_5)(PMe_3)Ir$(R)_2$, where R = alkyl, aryl, or hydride ligands are very pentane soluble.

[33] (a) Low, J.J.; Goddard, W.A., III. *J. Am. Chem. Soc.* **1984**, *106*, 6928. (b) Low, J.J.; Goddard, W.A., III. *J. Am. Chem. Soc.* **1984**, *106*, 8321.

[34]Watson, P.L.; Roe, D.C.; *J. Am. Chem. Soc.* **1982**, *104*, 6471.

[35] Thompson, M.E.; Baxter, S.M.; Bulls, A.R.; Burger, B.J.; Nolan, M.C.; Santarsiero, B.D.; Schaefer, W.P.; Bercaw, J.P. *J. Am. Chem. Soc.* **1987**, *109*, 203.

[36] Kang, J.W.; Moseley, K.; Maitlis, P.M. *J. Am. Chem. Soc.* **1969**, *91*, 5970.

[37] Stoutland, P.O. Chapter 2 of this Thesis.

[38] Buchanan, J.M.; Stryker, J.M.; Bergman, R.G. *J. Am. Chem. Soc.* **1986**, *108*, 1537.

Chapter 4

Study of Organometallic Transients by Time-Resolved Infrared Spectroscopy: An Exploratory Study

Introduction

Coordinatively unsaturated species are prevalent in organometallic chemistry. Such species participate in a multitude of reactions, many of which proceed by coordination of a ligand to the vacant coordination site. Many stable 16 electron complexes are known, including the square planar complexes of cobalt, rhodium, and iridium.[1] In most cases, however, the unsaturated species are not directly observed. For example, kinetic evidence has shown that substitution reactions of coordinatively saturated (18 electron complexes), often go through a dissociative process involving ligand loss to form a 16 electron complex which is then trapped by the added ligand.[2] Indeed, this cycle of 18 ---> 16 ---> 18 electron complexes forms the basis for the mechanisms of many catalytic processes.[3] The C-H activation reactions discussed in Chapters 1-3 are similarly thought to proceed by production of the highly reactive 16 electron fragment, "(η^5-Me_5C_5)(PMe_3)Ir", which then inserts into the C-H bonds of hydrocarbons.

In most cases very little is known about the transient fragments formed in these reactions. Many interesting questions, however, present themselves. For example, in what geometries are these fragments formed, and which geometry is the most stable? Also, how are the rates of reaction of these fragments with added ligands affected by the solvent and the ligand used? All of these questions are fundamental to the development of an understanding of organometallic reaction mechanisms. Despite the pervasiveness of transient, unsaturated species in both homogeneous and heterogeneous reactions in organometallic chemistry, however, only recently have some of these questions been addressed.

Matrix techniques. The technique of isolating reactive intermediates in low temperature matrices has recently been applied to the study of organometallic fragments.[4] In these experiments the precursor to the unstable intermediate is isolated in the matrix material at low temperature. Typically, the matrix material is a noble gas or methane, although hydrocarbon glasses at 77 K, or polymer films at room temperature have been

used.[5] The matrix is then irradiated with a UV lamp to generate the reactive species. The combination of the low temperatures, and the rigidity and "diluteness" of the matrix allows normally unstable fragments to be observed with a variety of spectroscopic tools.

The majority of the organometallic compounds studied have been metal carbonyl compounds. This is due to the photolability of such compounds, as well as the strong absorptions of the C-O stretching vibrations which allow structurally sensitive vibrational (Raman and infrared) spectroscopy to be used. These studies have shown that unsaturated metal carbonyl compounds are very reactive and appear to form weak complexes even with the matrix itself. Furthermore, the structures of many metal carbonyl fragments have been determined by the use of infrared spectroscopy. Unfortunately, it is difficult to investigate bimolecular reactions due to the limited diffusion possible in matrices. Since irradiation in a matrix is usually accomplished with continuous UV irradiation, characterization of photosensitive fragments is also difficult.

Some of these problems have recently been circumvented by performing irradiations in inert gas solutions.[6] This allows the study of bimolecular reactions, and since inert gases have no infrared absorption, analysis is easily accomplished by standard FT IR techniques. These experiments are not without problems, however. Liquid xenon and krypton are difficult to handle, expensive, and have poor solubility properties. Furthermore, in some cases the reactions, even in inert gases, will be too fast for FT IR techniques.

Flash photolysis in solution. The technique of flash photolysis has also been applied to the study of organometallic reactions in solution.[7] In these experiments the transient species is generated by a short light pulse (typically less than 1 μs); a second, less intense, light pulse is then used to observe the transient. For the most part, these studies have been limited to simple metal carbonyl complexes. Of these, $Cr(CO)_6$ has been the most extensively investigated. From these studies several general principles have emerged.

First, irradiation of $Cr(CO)_6$ in cyclohexane results in extrusion of only one CO ligand, presumably due to rapid quenching of excess vibrational energy present in $Cr(CO)_5$ by the solvent. The resulting organometallic fragment, $Cr(CO)_5$, reacts with the solvent in less than 0.8 ps forming a metal-cyclohexane complex. Upon saturation of the solution with CO, $Cr(CO)_6$ is regenerated in ca. 25 μs.[8] Moreover, the stability of the solvate is quite sensitive to the solvent used. Irradiation of $Cr(CO)_6$ in perfluoromethylcyclohexane results in formation of a solvate that reacts with CO approximately 1000 times faster![9]

The metal-solvent interaction was further investigated by Adamson.[10] Flash photolysis of $W(CO)_6$ in methylcyclohexane resulted in formation of S-$W(CO)_6$. In the presence of the ligand 4-acetylpyridine, this reacted to form L-$W(CO)_5$. At high concentrations of L the rate approached a limiting value (i.e. saturation kinetics). This is consistent with a mechanism involving reversible, rate-determining loss of S and formation of $W(CO)_5$ which may be trapped by L (Scheme 4.1). Monitoring the reaction over a 30 °C temperature range showed that the activation energy for the loss of S was 3.9 kcal/mol. Furthermore, it was shown that the reaction of S with $W(CO)_5$ had an activation barrier ca. 3 kcal/mol higher in energy than reaction with L. Since reaction of $W(CO)_5$ with L must have an activation barrier greater than 0 kcal/mol, the activation barrier for formation of $W(CO)_5(S)$ from $W(CO)_5$ and S must be at least 3 kcal/mol. Therefore the strength of the tungsten-solvent bond must be less than 0.9 kcal/mol.

While flash photolysis, followed by UV-VIS detection, is capable of providing good kinetic information on a picosecond to millisecond timescale, the structural information is poor due to the broad, featureless UV-VIS spectra of many organometallic compounds. In the case of simple systems, such as $Cr(CO)_6$, a combination of matrix isolation/IR spectroscopy and flash photolysis with UV-VIS detection has provided a reasonable picture of the reaction mechanism.

Fast infrared and Raman techniques. If one wishes to investigate more complex reactions, however, it is highly desirable to have a technique whereby both kinetic

Scheme 4.1

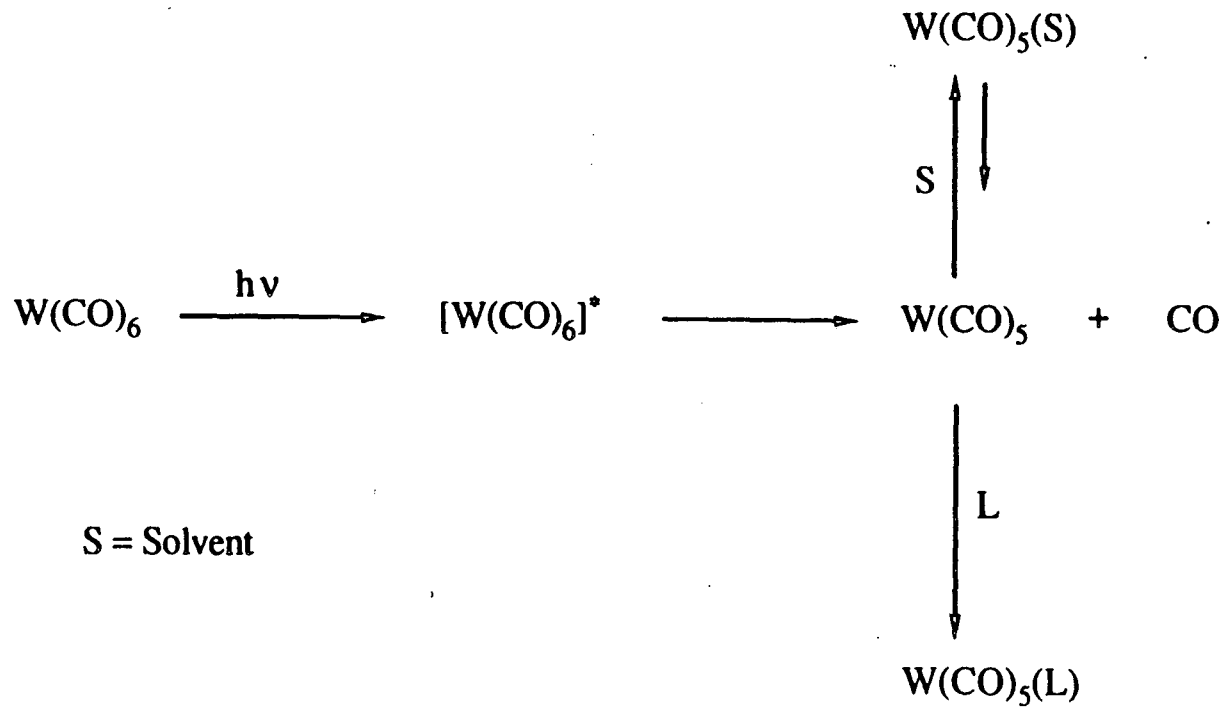

and structural information can be obtained in the same experiment. Time-resolved vibrational spectroscopy could, in theory, provide the necessary structural information, as well as the desired kinetic information.[11] Raman spectroscopy with its power to obtain structural information, and the existence of spectrometers which can resolve absorbance changes in the picosecond time regime, seems to be ideally suited for the investigation of reactive organometallic fragments. Unfortunately, Raman spectroscopy suffers from sensitivity problems unless the probe laser is tuned to an electronic transition of the species of interest (resonance Raman). In these cases strong signals can be observed, but in the case of organometallic fragments the probe laser would in many cases induce further fragmentation. This would result in a complex mixture of photoproducts, which would be dependent on the power and frequency of the probe pulse.

Time-resolved infrared spectroscopy can also provide the necessary kinetic and structural information. Historically, however, infrared detectors have been thought to be insensitive and slow. To some extent this is still true, and time-resolved IR experiments are less sensitive than UV-VIS experiments partly because the strong absorbances of solvents in the IR necessitate having a cell thickness of only 0.5 - 1.0 mm; this compares to cell lengths of several centimeters in flash UV-VIS experiments. Fortunately, the carbonyl stretching vibration of organometallic carbonyl compounds is one of the strongest known; organometallic compounds containing CO ligands are thus ideally suited for this technique. Infrared detectors are also slower than UV-VIS detectors, but this will not be a significant problem for the study of <u>bimolecular</u> reactions, as the rate of reaction may be controlled by lowering the concentrations. The range of concentrations usable will also, of course, be dependent on the sensitivity of the apparatus.

In the last five years several groups have begun to investigate organometallic reactions with time-resolved infrared spectroscopy (TRIR).[12] With the exception of one group, all of these investigations have focused on the study of transients in the gas phase. Studies in the gas phase are important because they allow investigation of the intrinsic

reactivity of unsaturated species, in the absence of coordinating solvents. Irradiation of organometallic carbonyl compounds in the gas phase frequently results in loss of more than one CO, leading to compounds not seen in solution due to collisional relaxation.

Turner's group has pioneered the use of TRIR in solution, and has now looked at several simple systems. For example, irradiation of $[Cp(CO)_2Fe]_2$ results in decomposition via two pathways: metal-metal bond homolysis and CO loss.[13] In this case, CO loss has been shown to lead to formation of a triply bridging dimer. Very recent results have demonstrated that irradiation of $L\text{-}W(CO)_5$ results in formation of two isomers of $L\text{-}W(CO)_4$ which do not interconvert, and exhibit considerably different stabilities towards substitution reactions.[14]

Our interest in the properties of unsaturated fragments was initiated by the recent discoveries of metal fragments capable of insertion into the C-H bonds of alkanes.[15] With the hope of deepening our understanding of unsaturated intermediates we have started an investigation of photochemically generated metal carbonyl fragments in solution using infrared spectroscopy. Our approach was to investigate a wide variety of species, so as to understand the properties in a general way before investigating any system extensively. We were especially interested in systems similar to those known to participate in C-H activation reactions. Described below are some of the preliminary exploratory studies we have carried out. From these experiments we have gained an understanding of the types of systems which will be amenable to further study.

Experimental Setup

In transient absorption experiments there must be a light source capable of generating the species of interest, a light source for probing the transients, and a detector capable of monitoring the changes in the intensity of the probe light due to absorbance of the transients produced. In addition, there must be a transient digitizer capable of digitizing the signal from the detector so that the data can be further analyzed. Our experimental

apparatus is shown in Figure 4.1. It consists of a UV excimer laser which generates unsaturated metal carbonyl species within 20 ns. Colinear with the UV beam is a frequency tunable infrared beam from a CO laser. Upon firing of the UV laser, the transient digitizer is triggered and records changes in the number of IR photons falling on the detector. Changes in the number of photons striking the detector are due to the appearance or disappearance of organometallic products. Thus the disappearance of C-O stretching bands leads to an increase in the number of photons striking the surface. Below we consider in more detail each element in the TRIR apparatus currently in use in our laboratories.

UV light source. We have elected to use a laser to produce the unsaturated organometallic fragments.[16] Flash lamps are less expensive, but lasers have significant advantages for these types of experiments. First, flash lamps typically have pulse widths of ca. 1 μs.[17] Lasers, on the other hand, commonly have pulse widths of less than 30 ns. In the case of IR detection, this results in the response time of the detector usually being the limiting factor. Lasers have the additional benefit of providing nearly monochromatic light. Flash lamps may be restricted to a narrow frequency range by filters, but only at the expense of power.

Commercial excimer lasers are currently the lasers of choice for these experiments as they provide sufficiently short pulses (ca. 20 ns), ample power (50 - 100 mJ/pulse), and are easy to operate. Excimer lasers are well suited for the study of a variety of organometallic molecules as the laser may be run on several gas mixtures, the most common being KrF(248 nm), XeCl(308 nm), and XeF(351). This is especially important because of the considerable diversity organometallic compounds exhibit in their UV-VIS spectra. For example, some absorb far into the visible region of the spectrum (e.g., $Mn(NO)(CO)_4$), while others show no significant absorbance above 300 nm (e.g. $CpRe(CO)_3$). For solution phase investigations the capability of using more than one wavelength is especially important, as many common ligands and solvents absorb in the

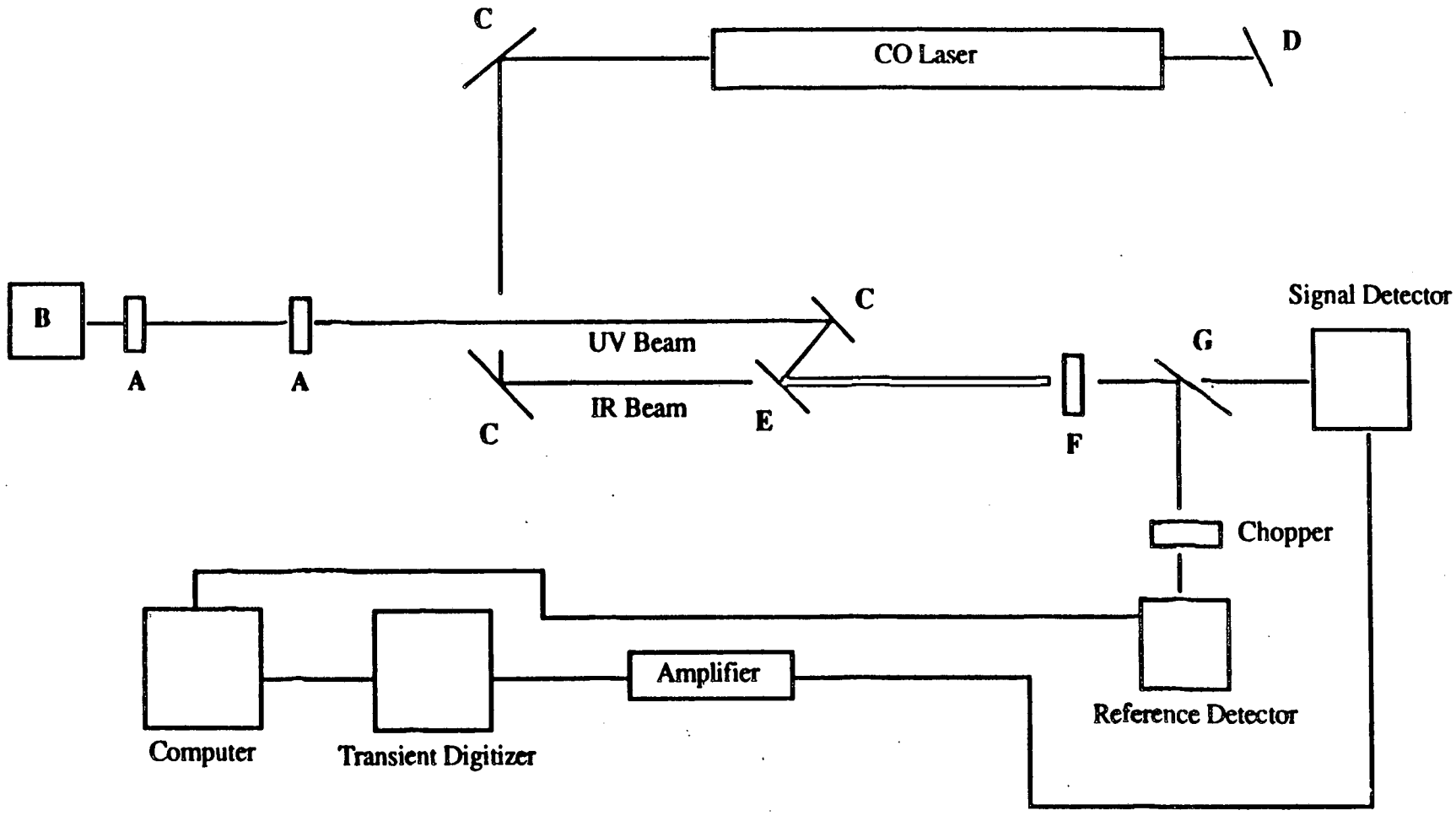

Figure 4.1. Schematic of experimental setup. A: lenses. B: Excimer UV laser. C: mirrors. D: grating. E: UV reflective/IR transmitting optic. F: sample cell. G: infrared beam splitter.

near UV.[18] Most of our experiments have been conducted using a Lambda-Physik EMG 103 excimer laser operating on XeCl which produces 20 ns wide pulses of 50 - 100 mJ at 308 nm. After exiting the laser, the beam is collimated by two lenses to a rectangle which is approximately 1 x 1 cm square when it strikes the solution cell.

Infrared sources. Two different sources of infrared light have been used as the probe: globars and CO lasers.[12] Globars are capable of emitting continuous infrared irradiation throughout the infrared spectrum, and in principle could provide infrared spectra of very high resolution. Despite this, most groups (including ourselves) are using CO lasers which are capable of providing infrared irradiation from 2150 to less than 1600 cm^{-1} roughly every 4 cm^{-1}. The most important reason for selecting a CO laser is the up to 1000-fold increase in signal to noise ratios possible due to the much higher photon fluxes compared to globars[19] Furthermore, since lasers provide a monochromatic light source, a monochrometer (which would further reduce the light intensity) is not needed.

Principles of operation. Carbon monoxide lasers operate, as do all lasers, on the principle of population inversion.[20] In the case of CO lasers, this is achieved by applying an electrical potential (ca. 12 kV) to a gas mixture which consists of 66% He, 33% N_2, and 0.17% CO. In addition a small amount of Xe is added to stabilize the laser, and a small amount of O_2 (0.03%) is added to prevent carbon deposits. In this medium the helium is ionized, causing the N_2 to become vibrationally excited. Since N_2 is isoelectronic with CO, it easily transfers its vibrational energy to CO by collision, driving CO up the vibrational energy ladder. Vibrationally excited CO can lose its energy in several ways. One is radiationless decay, which serves only to repopulate the ground state and generate heat. The other way is through radiative decay, either stimulated or spontaneous (Equation 4.1).

$$CO(V, J) \text{ -----> } CO(V\text{-}1, J + 1) + h\nu(IR) \qquad (4.2)$$

Photons which are spontaneously emitted are then trapped in the laser cavity which consists of a mirror at one end and a partially reflecting mirror at the other. The resonant electric field of these photons then interacts with the remaining molecules of vibrationally excited CO, producing stimulated emission of infrared irradiation. Continuous wave (CW) lasers such as our CO laser maintain the necessary population inversion by allowing only a fraction of the emitted photons to exit the laser cavity through the partially reflecting mirror.

Lasing occurs exclusively from the P rotational branch of vibrational transitions 1 ---> 0 to above 36 ---> 35. This results in a series of lines from approximately 2100 cm^{-1} to 1200 cm^{-1}. It is, however, desirable to have a monochromatic light source so a grating is used as the mirror.[21] This allows only a single frequency to be resonant in the cavity at a time, and is the only frequency possible for laser emission. The grating we use is scored for 5 μm light, which effectively limits our wavelength range from ca. 2100 to 1750 cm^{-1}. By changing the angle of the grating lasing may be observed approximately every 4 cm^{-1} as the rotational B value for CO is 1.93. The actual lines observed for a CO laser are dependent on the voltage, the pressure, the gas composition, and the temperature of the plasma.

While commercial sealed CO lasers are available, we use a flowing system, and cool the laser with liquid nitrogen which is necessary to obtain lasing from vibrational states lower than 5 ---> 4. Under normal operating conditions our laser shows lasing from vibrational energy levels 3 ---> 2 through 16 ---> 15. Our CO laser has previously been described in detail.[22]

Detectors. There are two main classes of detectors used for high speed infrared detection: photovoltaic and photoconductive.[23] Photovoltaic detector elements are made of semiconductors with energy gaps of the wavelength to be measured. When photons hit the detector element (InSb for example), a current is produced which is directly proportional to the number of photons striking the surface. Photoconductive detectors, on the other hand, change their resistance when irradiated with photons of the proper wavelength. Intrinsic

photoconducting detectors have elements made of semiconductors such as InSb or HgCdTe with appropriate band gaps. Extrinsic photoconducting detector elements are made of a semiconductor material doped with an impurity having an ionization energy corresponding to the wavelength to be detected; Cu doped Ge and Hg doped Ge are examples. When a constant current is provided across a photoconductive detector, any change in the resistance caused by a change in the number of photons striking the sample will manifest itself as a change in voltage in the detector.

A key feature of all the detectors is that they are capacitively coupled, which means that only changes in voltage will be registered; this results in a much more sensitive detector. Currently the most commonly used IR detector has an InSb element and operates at 77 K. We are currently using a Cu:Ge detector which operates at 4 K. While the necessity for liquid helium cooling is inconvenient, the Cu:Ge detector has proven to have significant advantages over the InSb detector we used earlier. First, the detector element itself is much larger (3 x 10 mm) which allows a less precise alignment of the IR beam. Second, Cu:Ge detectors are among the fastest IR detectors. Our detector presently has a response time of ca. 200 ns and a long time constant of 1-2 ms.[24] Previously, however, this detector was operated with slightly different electronics which exhibited an intrinsic response time of 15 ns.[25] Finally, InSb detectors have a low frequency limit of 1750 cm^{-1} which precludes observation of many bridging carbonyl and nitrosyl stretching vibrations. Copper doped germanium detectors are sensitive to over 15 μm.

Experimental procedure. The signal from the detector is amplified and sent to a transient digitizer (Tektronix 7912AD) which records the trace. The transient digitizer (after being triggered by the excimer pulse) generates 512 data points (voltages) from the detector signal during a time window which can be changed from 2 μs up to 1 ms in length (this is detector, not digitizer, limited). Signals from many excimer shots can be averaged in order to increase the signal to noise ratio: typically 8 to 32 traces are averaged, limited only by the amount of solution one has (8 shots used ca. 1 mL of solution(vide post)).

After adding the desired number of traces, the light from the excimer laser is blocked with a shutter and an equal number of traces is acquired. This is then subtracted from the data acquired with the excimer on, reducing spurious electronic signals. A sample kinetic trace of the product resulting from irradiation of $W(CO)_6$ is shown in Figure 4.2 of a transient produced "immediately"[26] following the excimer pulse which then disappears due to a chemical reaction.

By changing the CO laser grating from one line to another, one generates a series of kinetic traces. By taking data points acquired at the same time after the excimer pulse from each of these kinetic traces, one can construct a transient spectrum which resembles a normal infrared spectrum. In order to do this, however, it is first necessary to correct the voltages of each kinetic trace for the power of the signal falling on the detector (before the excimer pulse). This is necessary because a change of 10 mV in a signal of 10 mV is a much larger percentage change than a change of 10 mV in a 1 V signal. The power of the IR beam after it passes through the solution cell is determined by sending a chopped signal to a reference detector (measuring the power after the cell automatically corrects for solution absorbances and laser power fluctuations). The voltage is normalized by dividing the voltage changes measured by the transient digitizer by the power of the respective laser lines.

The transient spectra thus constructed differ from normal IR spectra in that products which have grown in since the excimer pulse result in positive bands, and compounds which have disappeared are seen as negative bands. In Figure 4.3 a transient spectrum taken 8 μs after the irradiation of $CpMn(CO)_3$ is shown.

Solution handling. As most of the organometallic compounds used are air sensitive, it is necessary to use cannula techniques to handle the solution. Furthermore, since many transition metal fragments will bind to N_2, all the solutions were purged with argon for several minutes prior to use. To flow the solution though the cell, positive argon pressure was used to force the solution into a needle connected to 1/8 inch Teflon tubing

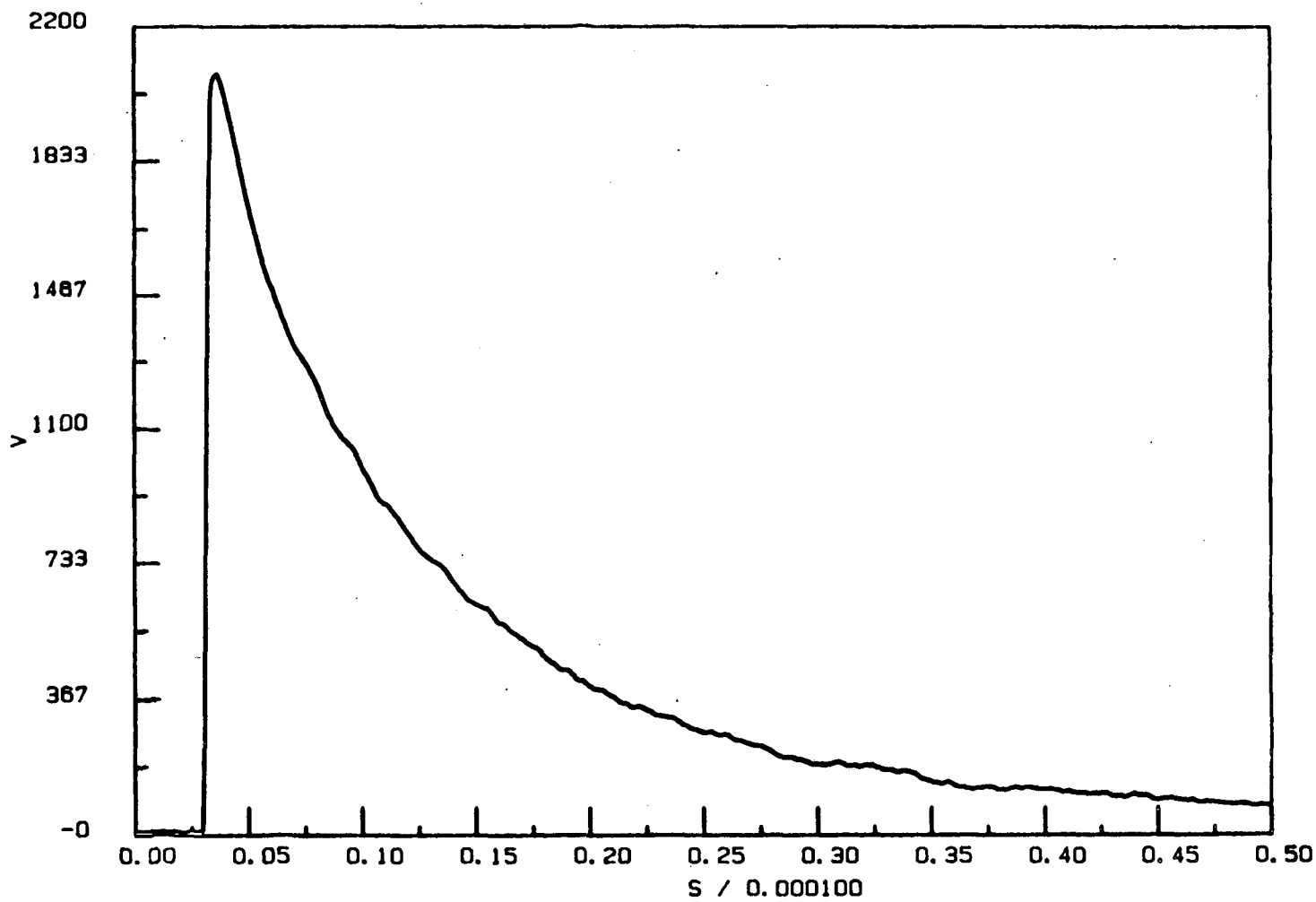

Figure 4.2. A selected kinetic trace showing the temporal behavior of a signal due to $W(CO)_5(S)$ produced by the laser pulse to 50μs.

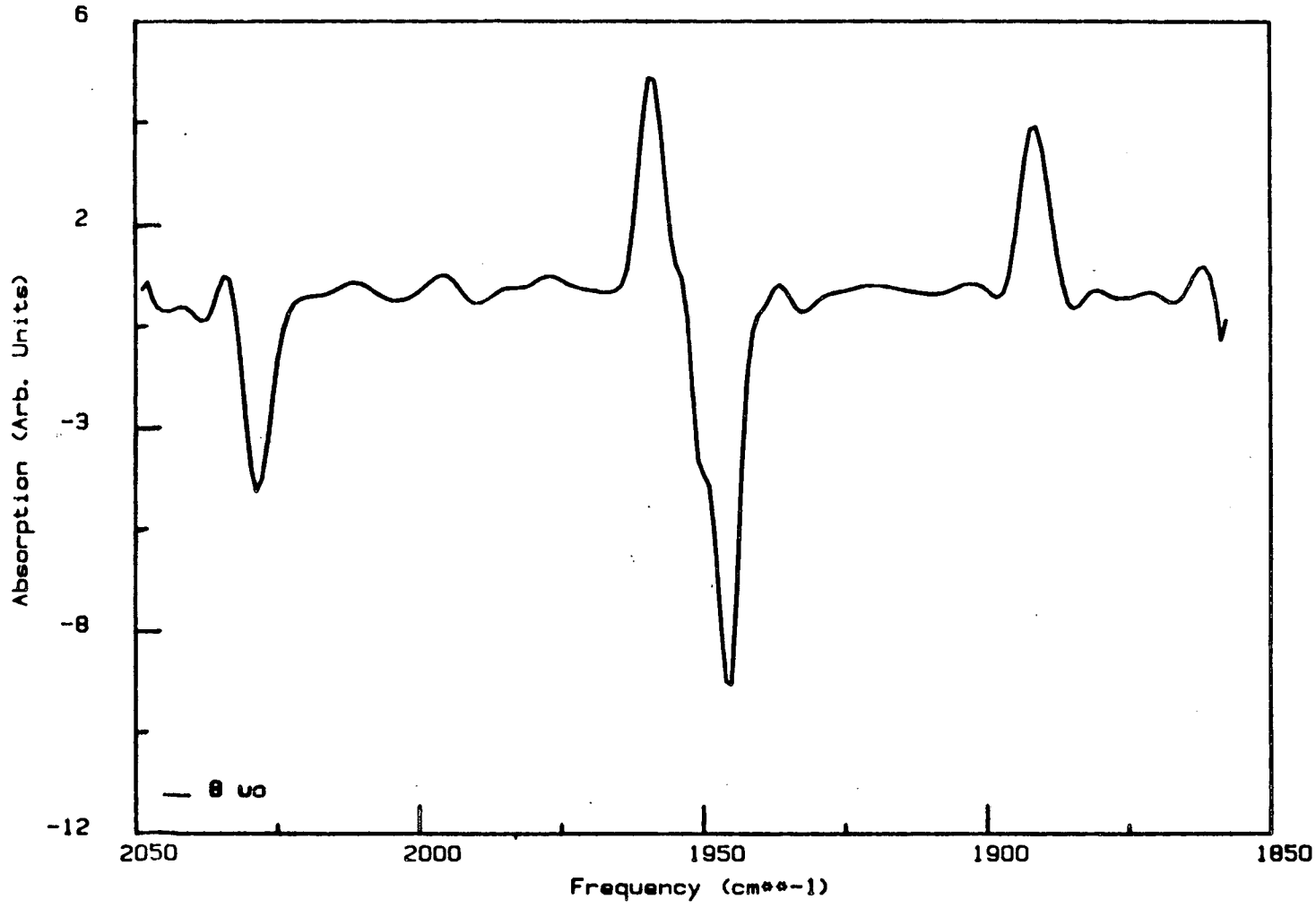

Figure 4.3. A selected transient spectrum taken at 8 μs after the flash photolysis of $CpMn(CO)_3$ in cyclohexane. The bands of negative intensity (1947 and 2029 cm^{-1}) are due to the disappearance of $CpMn(CO)_3$ upon photolysis. The bands of positive intensity (1959 and 1892 cm^{-1}) are due to a new product, thought to be $CpMn(CO)_2(S)$. The 50 data points have been smoothed by the use of a cubic-spine function.

which was fitted with a luer tip and connected to the cell. The IR cell used was a standard IR cell fitted with CaF_2 windows and a 0.50 to 1.0 mm Teflon spacer.

The amount of compound in the solution cell which decomposes with each laser pulse is dependent on the quantum yield and the absorption cross section of the compound of interest. Typically, for compounds with high quantum yields, 10% - 30% of the compound in the cell decomposed with each laser pulse. To eliminate secondary photoprocesses, we flowed the solution so that the solution was changed between each laser shot. The rate of flow through the cell was controlled by the amount of argon pressure. Between experiments the flow was stopped completely with a small valve controlled by a solenoid. Using these procedures we found than a survey of the region from 2040 to 1840 cm^{-1} required ca. 100 mL of solution (10 - 20 mg of the compound).

The data collection was made considerably easier and faster by interfacing most of the equipment to a micro computer. In order to acquire a kinetic trace, the computer signals a solenoid to open which allows the solution to flow through the cell. Immediately after this, a solenoid is opened which allows the excimer beam to reach the cell. The data is then collected by the transient digitizer and stored on the computer, along with the power of the laser line. The grating is then moved to the next line by a stepping motor interfaced to our computer and the procedure is repeated. This allows acquisition of a complete spectrum (2040 - 1840 cm^{-1}) in approximately 15 - 30 min.

Results

Background: Relative stabilities of S-M(CO)$_n$. As noted above, there are now many indications from matrix and solution phase studies that the unsaturated fragments generated by photolysis of metal carbonyl compounds form weak complexes with the solvent (or the matrix) very rapidly. For example, when $Cr(CO)_6$ is irradiated in cyclohexane, the solvate S-$Cr(CO)_5$ has been found to form within 0.8 ps.[8] Recent results from Turner's laboratory have provided further support for this belief.[14] Upon flash

photolysis of L-$W(CO)_5$ (L = $P(O\text{-}i\text{-}Pr)_3$) or *cis*-(pip)$LW(CO)_4$ (L = $P(OEt)_3$, $P(O\text{-}i\text{-}Pr)_3$, and $P(C_6H_5)_3$; pip = piperidine), both cis and trans-$LW(CO)_4(S)$ (S = heptane) are produced and do not interconvert under the reaction conditions. In each case, the cis isomer reacts with added CO more rapidly, leading to regeneration of the starting material. This is the opposite of what one would expect for a molecule having a bulky ligand cis to a vacant coordination site. In related systems, however, bulky ligands have been observed to labilize cis-ligands, presumably because of steric destabilization.[27] This suggests that in this case heptane is acting as the sixth ligand, its interaction with the metal being weakened in the presence of cis, sterically-demanding ligands.

Similar species, where there is an interaction between the σ-bonds of a hydrocarbon and the metal have been proposed as intermediates in C-H activation reactions.[28] Furthermore, there are now several structure determinations of complexes where a C-H bond of an alkyl group attached to the metal is coordinated to the metal center so as to make the metal center coordinatively saturated (commonly called "agostic" interactions).[29] As the stability of the alkyl hydrides resulting from C-H insertion reactions has been shown to depend on the alkane activated,[30] it was of interest to determine how the stability of metal solvates were also dependent on the alkane used.

We were particularly excited by the report of Lees and Adamson in which the substitution reaction of $W(CO)_5(S)$ with 4-acetylpyridine was examined (vide supra). They observed that the rate of reaction of $W(CO)_5(S)$ with added ligand approached a limiting value ($1.5 \times 10^6\ s^{-1}$) as the concentration of L was increased to 0.1 M (i.e. saturation kinetics). By measuring the rates over a 30°C temperature range it was possible to set at upper limit on the strength of the M-S bond.

We decided to initially study systems which were similar to those which are known to insert into C-H bonds of alkanes under photochemical conditions. $CpMn(CO)_3$ and $CpRe(CO)_3$ seemed to be ideal, as the photochemistry of both species has been studied in solution and in matrices, so that the quantum yields of substitution are known and the IR

bands of $CpM(CO)_2$ have been identified.[31] Furthermore, these compounds are similar to $Cp^*Ir(CO)_2$ and $CpRe(PMe_3)_3$ which are both known to activate alkanes under photochemical conditions.[32]

$CpMn(CO)_3$. $CpMn(CO)_3$ is a yellow compound which has an extinction coefficient of 600 at 308 nm, the frequency of our excimer laser when operating on XeCl. Its photochemistry in the presence of ligands is dominated by simple ligand substitution which has been shown to have a quantum yield of 0.65.[33] Upon photolysis of $CpMn(CO)_3$ in cyclohexane with the 20 ns excimer laser pulse, disappearance of the starting material was observed, and two new bands were immediately visible at 1959 cm^{-1} and at 1892 cm^{-1} (Figure 4.3). These bands are very similar to those assigned to $CpMn(CO)_2$ generated in a matrix (1955 and 1886 cm^{-1}).[34] After 2 ms these new bands had decreased in intensity only slightly. An exponential fit to the stronger of the two bands (1959 cm^{-1}) revealed a decay rate of 1.8×10^3 s^{-1} ($\tau = 0.6$ ms). No new bands could be seen growing in upon decay of these bands.

While tentatively assigning the new IR bands seen to $CpMn(CO)_2(S)$, we examined the irradiation of $CpMn(CO)_3$ in the presence of added ligand. Tri-*n*-butylphosphine was chosen as it does not absorb at 308 nm, is inexpensive, and is an easily handled liquid. Irradiation of $CpMn(CO)_3$ in the presence of 3.01×10^{-3} M P-*n*-Bu_3 again resulted in the appearance of two new bands (1959 and 1892 cm^{-1}). Here, however, the bands were observed to decay more quickly (rate = 6.4×10^3 s^{-1}, Figure 4.4) and the growth of new bands was observed at 1874 and 1933 cm^{-1} (Figure 4.5). Transient IR spectra assembled by taking points from the kinetic traces at 8, 72, and 152 μs after the laser pulse are shown in Figure 4.6. These new IR bands are close to those expected for $CpMn(CO)_2(P\text{-}n\text{-}Bu_3)$ (lit:[35] 1929 and 1848 cm^{-1} in CS_2). It thus appears that the reaction is proceeding as expected, with initial loss of CO resulting in formation of $CpMn(CO)_2(S)$. Subsequent reaction with P-*n*-Bu_3 results in production of $CpMn(CO)_2(P\text{-}n\text{-}Bu_3)$ (Scheme 4.2).

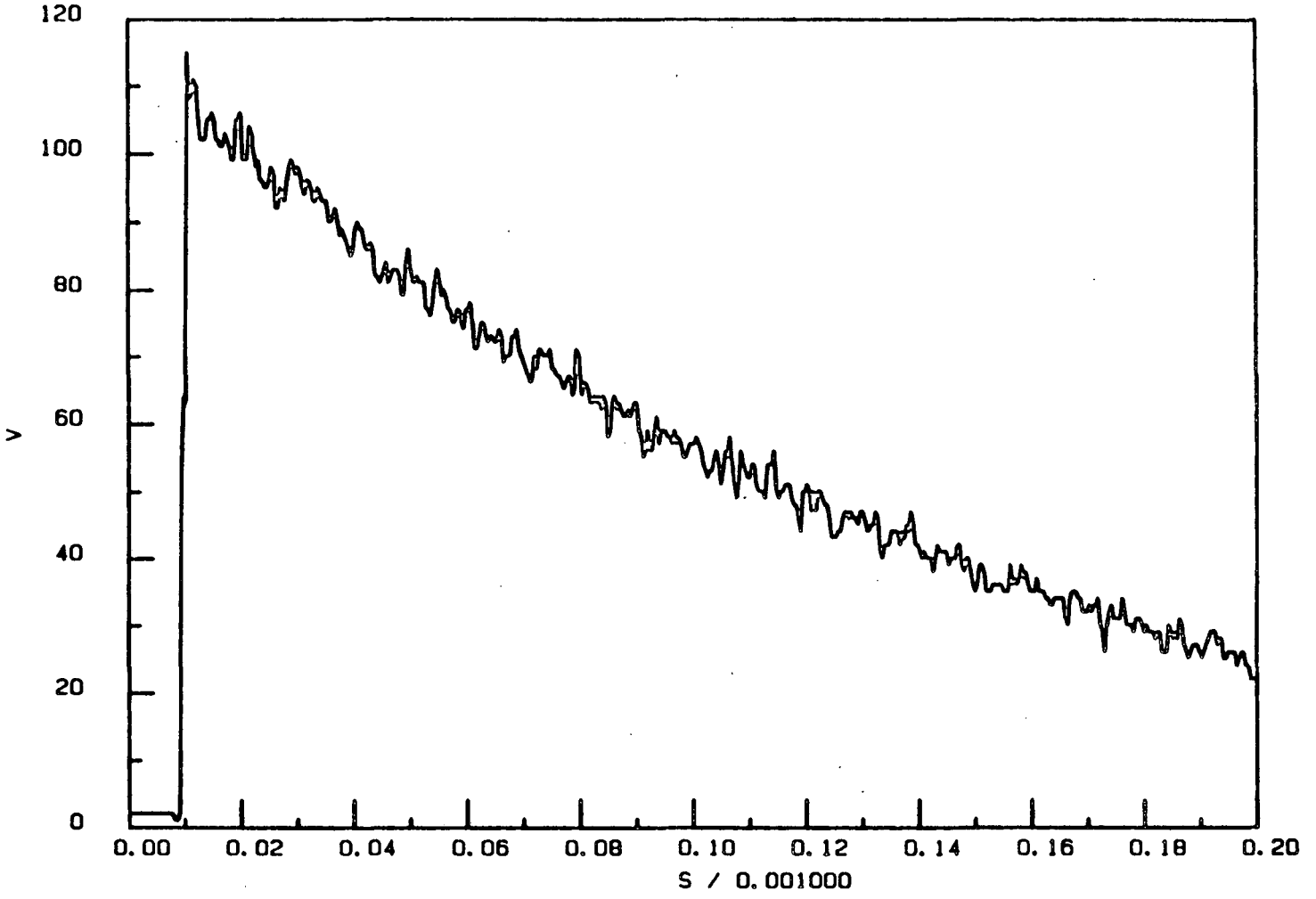

Figure 4.4. Kinetic trace taken at 1959 cm^{-1} showing the temporal behavior to 200 μs of $CpMn(CO)_2(S)$ in a 3 x 10^{-3} M solution of P-*n*Bu_3 in cyclohexane. The calculated rate is 6.4 x 10^3 s^{-1}.

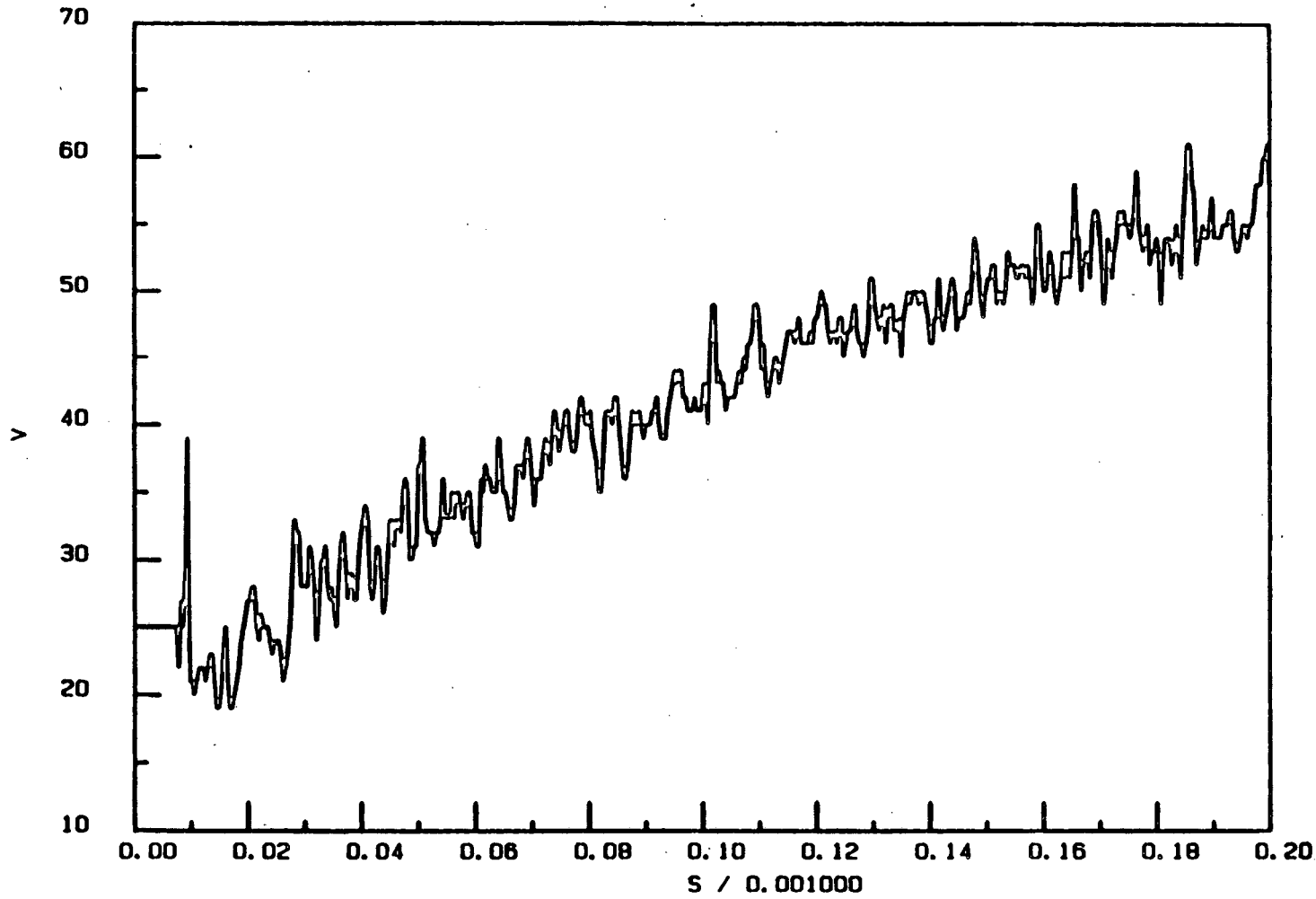

Figure 4.5. Kinetic trace at 1907 cm^{-1} showing the appearance of a new product (rate = $6.1 \times 10^3\ s^{-1}$) over 200 µs. This is thought to be $CpMn(CO)_2(P\text{-}nBu_3)$ formed upon reaction of $CpMn(CO)_2(S)$ with $P\text{-}nBu_3$.

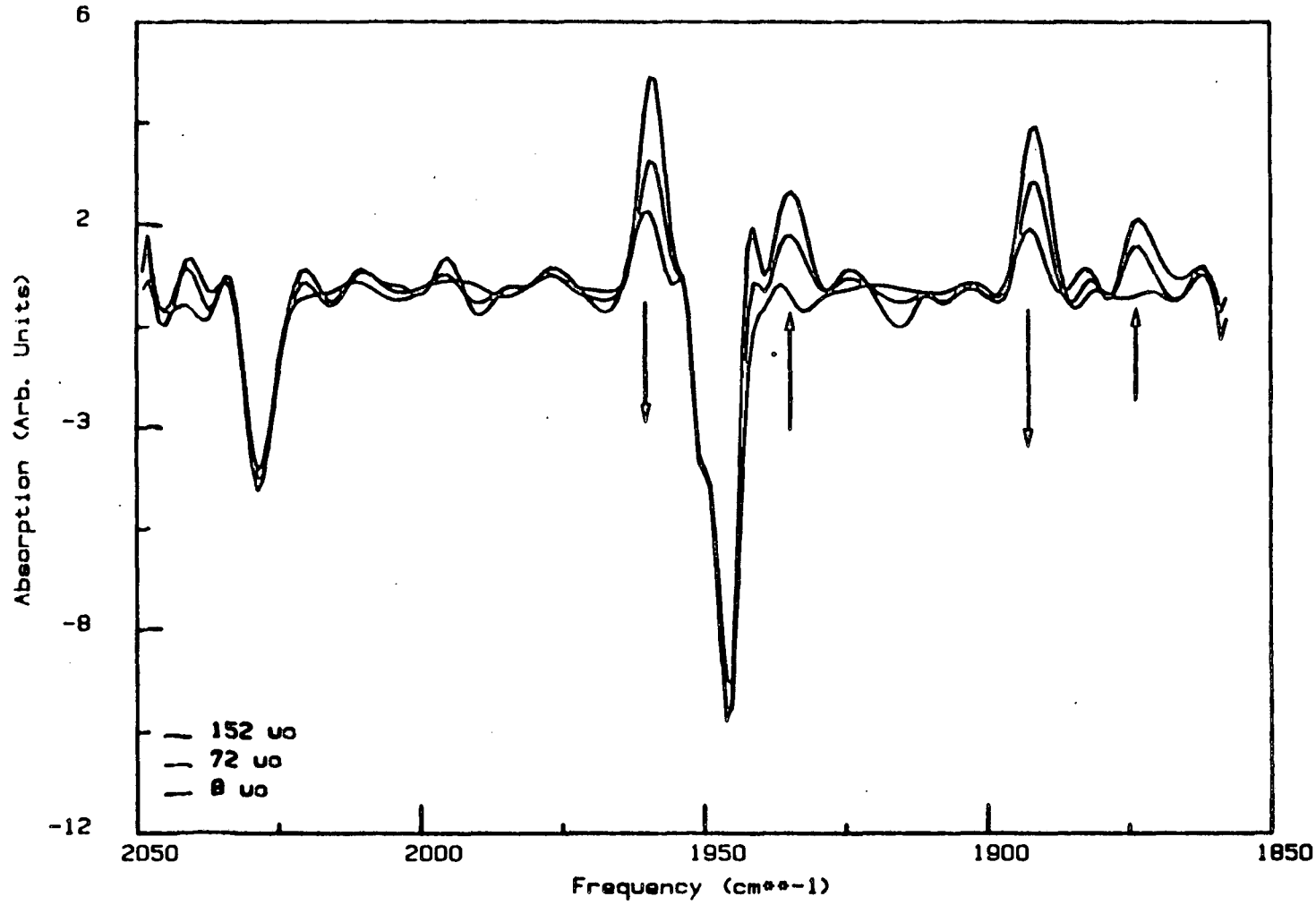

Figure 4.6. Spectra assembled at 8, 72, and 152 μs after the laser pulse showing the reaction of $CpMn(CO)_2(S)$ with P-nBu$_3$. Spectra have been smoothed. Arrows indicate bands increasing and decreasing in intensity.

Scheme 4.2

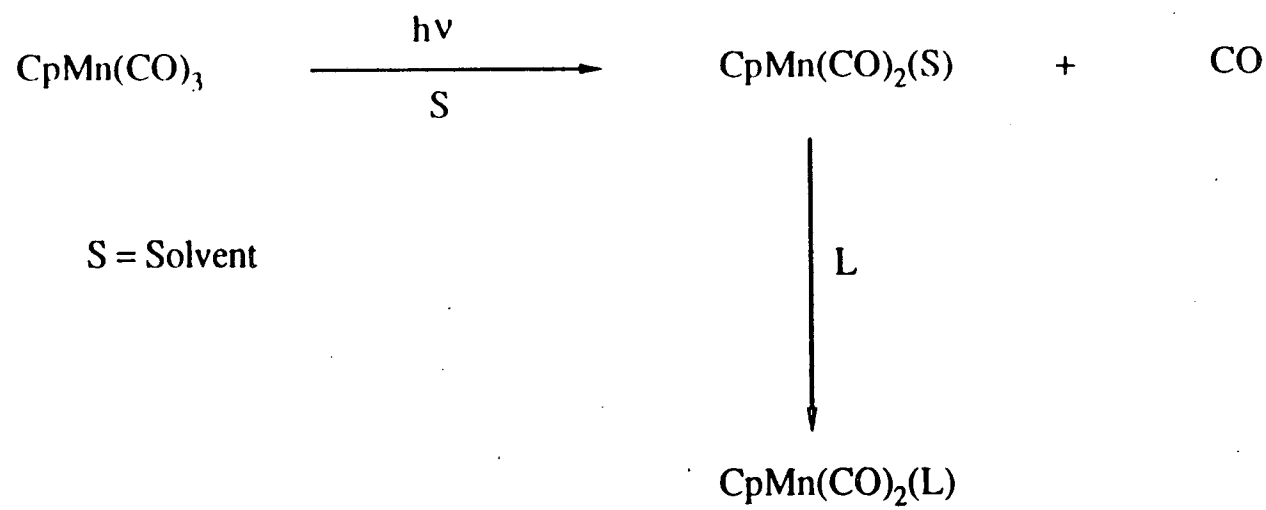

In order to examine the dependence of the rate of the substitution reaction on the phosphine concentration, we varied it from 3.01 x 10^{-3} M to 4.01 x 10^{-1} M. Even at the highest phosphine concentration[36] the rates appeared to be first order in phosphine, in contrast to the results seen for $W(CO)_5(S)$. Therefore, in this case the substitution could simply be a displacement reaction as shown in Scheme 4.2. Alternatively, the reaction could involve a rapid dissociative pre-equilibrium as proposed for the reaction of $W(CO)_5(S)$ with L, but is not in the region where $k_2[L]$ is competitive with k_{-1} (Scheme 4.3). In the absence of saturation kinetics little information can be gained concerning the strength of the metal-solvent interaction.

Nevertheless, we decided to change the solvent to hexane in order to examine, in a qualitative sense, the effect of changing the solvent. In Table 4.1 are compiled the phosphine concentrations and the associated rates of reaction in n-hexane and in cyclohexane. The rates of reaction are approximately twice that seen for similar concentration of phosphine with cyclohexane as the solvent. In Figure 4.7, the cyclohexane and the hexane data are presented graphically. Contrary to what we might have expected based on the relative stabilities of the analogous alkyl hydride formed from cyclohexane and hexane,[37] the transient species is observed to decay approximately twice as fast in hexane. It does appear, however, that the relative rates of reaction correlate quite well with the relative viscosities of the solvents.[38] This would be expected for a reaction having a diffusion controlled rate, where the viscosity of the solvent controls the rate of diffusion.

We also performed the flash photolysis of $CpMn(CO)_3$ in perfluorohexane. Consistent with early studies involving $Cr(CO)_6$ in perfluorinated solvents, the transient ($CpMn(CO)_2(S)$) was much less stable and decayed with a rate constant of 5.1 x 10^5 s^{-1} in the presence of 4.82 x 10^{-3} M P-*n*-Bu_3.

Scheme 4.3

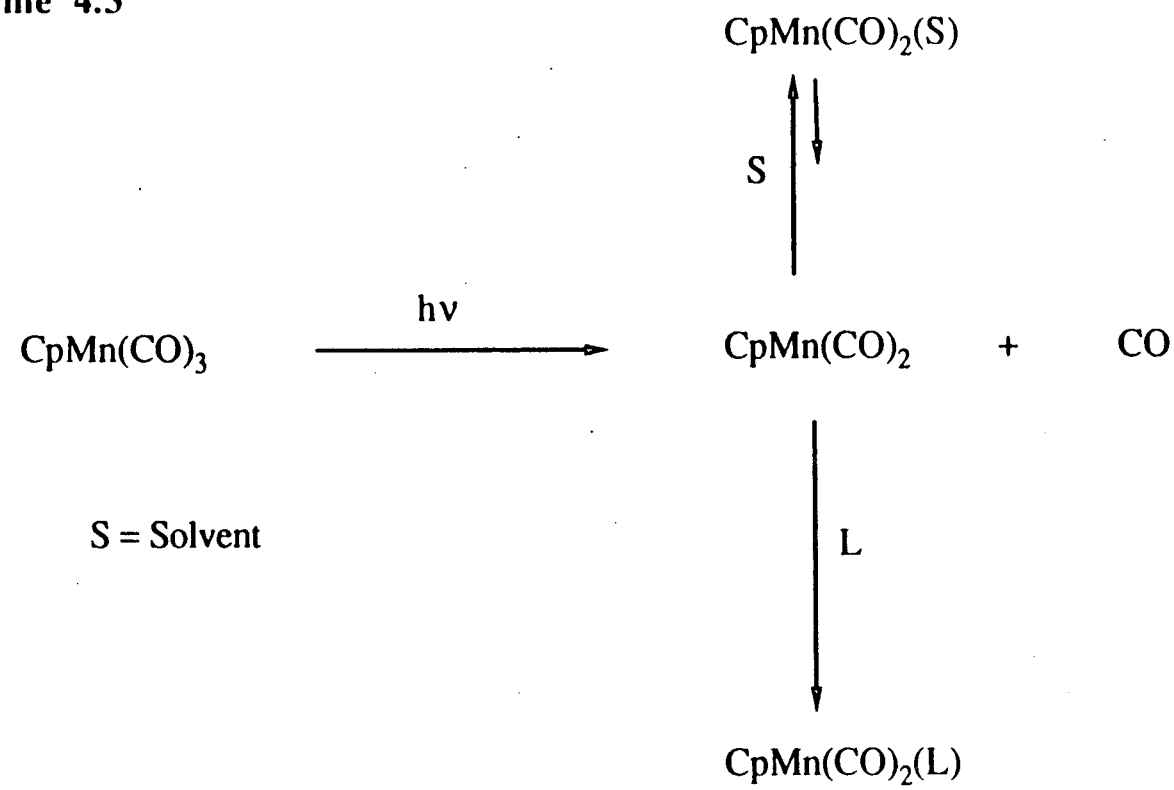

Table 4.1. Rates of reaction of $CpMn(CO)_2(S)$ with P-nBu$_3$ in selected solvents.

Solvent	[P-nBu$_3$] (x 10^3)	Rate (x 10^{-3} s^{-1})
C_6H_{12}	3.01	6.43
	20.1	41.2
	40.1	69.8
	161	343
	401	709
C_6H_{14}	1.93	14.2
	4.82	57.9
	9.64	68.7
	48.2	248
	96.3	666
C_6F_{14}	4.82	510

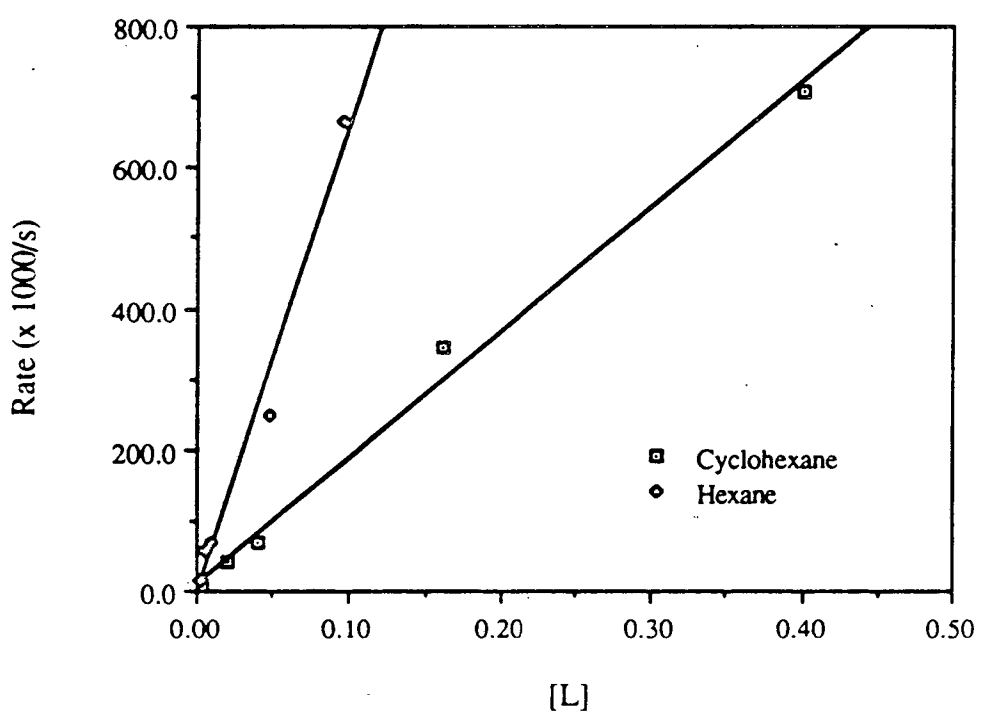

Figure 4.7. Comparison of the rates of reaction of $Cp(CO)_2Mn(S)$ with P-nBu$_3$ in cyclohexane and in hexane.

$CpRe(CO)_3$. We also investigated the flash photolysis of $CpRe(CO)_3$. However, due to a very low extinction coefficient at 308 nm ($\varepsilon = 280$) and a lower quantum yield ($\phi = 0.30$), the signals observed were much weaker. Nevertheless, weak positive transients were observed at 1948 and 1885 cm^{-1} similar to those seen for $CpRe(CO)_2$ in a matrix (1961 and 1895 cm^{-1}).[39] In the absence of added ligand these bands did not decay over 2 ms. Even in the presence of 0.4 M P-*n*-Bu_3, the transient decayed with a rate constant of only 1.3×10^4 s^{-1}.

$W(CO)_6$. The observation that reactions of $CpMn(CO)_2(S)$ with phosphine were first order in phosphine even at high ligand concentration was perplexing because the reaction between $W(CO)_5(S)$ and 4-acetylpyridine did not exhibit this behavior. We thus decided to explore some reactions of $W(CO)_6$ to see if this system was special in some way. Upon flash photolysis at 308 nm in cyclohexane, a transient is produced with bands at 1955 and 1929 cm^{-1} which has been previously assigned to $W(CO)_5(S)$.[40] In the presence of phosphine, this transient decays resulting in production of $W(CO)_5(PR_3)$, with bands at 1925 and 1943-47 cm^{-1} (lit:[41] 2068, 1943, 1936 cm^{-1} in hexane for $(CO)_5W(P\text{-}nBu_3)$). In Figures 4.8 and 4.9 are shown representative kinetic traces at 1955 and 1925 cm^{-1}, respectively. We have measured the rate of the reaction of $W(CO)_5(S)$ with P-*n*Bu_3 and with $P(C_6H_{11})_3$ at concentrations from 5×10^{-3} M to 0.1 M. The results are presented graphically in Figure 4.10. It is interesting to compare the rates found here with those found for the reaction of $CpMn(CO)_2(S)$ with P-*n*Bu_3 (Figure 4.7)--$CpMn(CO)_2(S)$ is much more stable than $W(CO)_5(S)$.

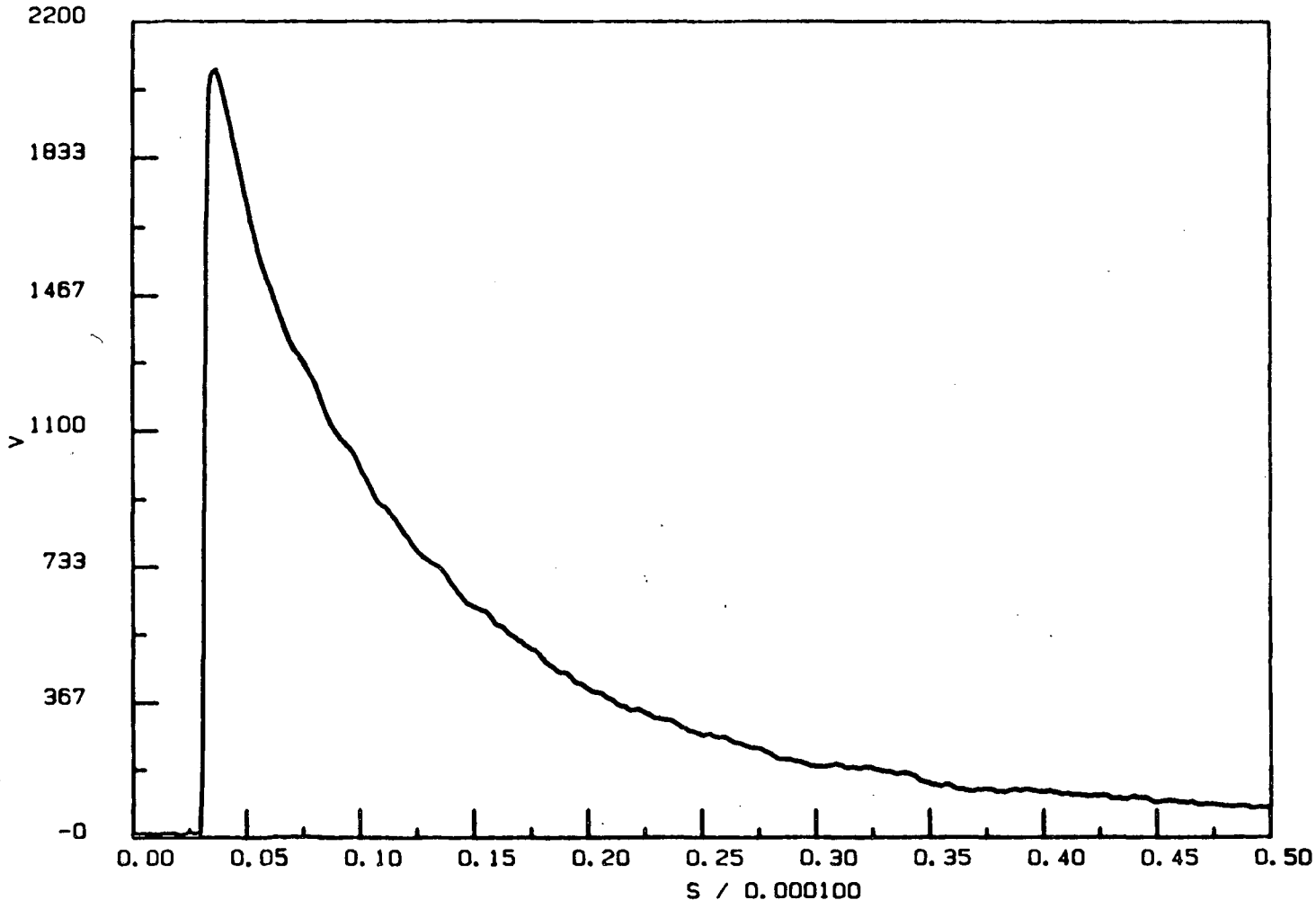

Figure 4.8. A kinetic trace taken at 1955 cm^{-1} showing the temporal behavior of a transient produced upon flash photolysis of $W(CO)_6$ in the presence of 0.005 M P-*n*Bu_3. The rate, as determined by an exponential fit to the trace, is 9 x 10^4 s^{-1}.

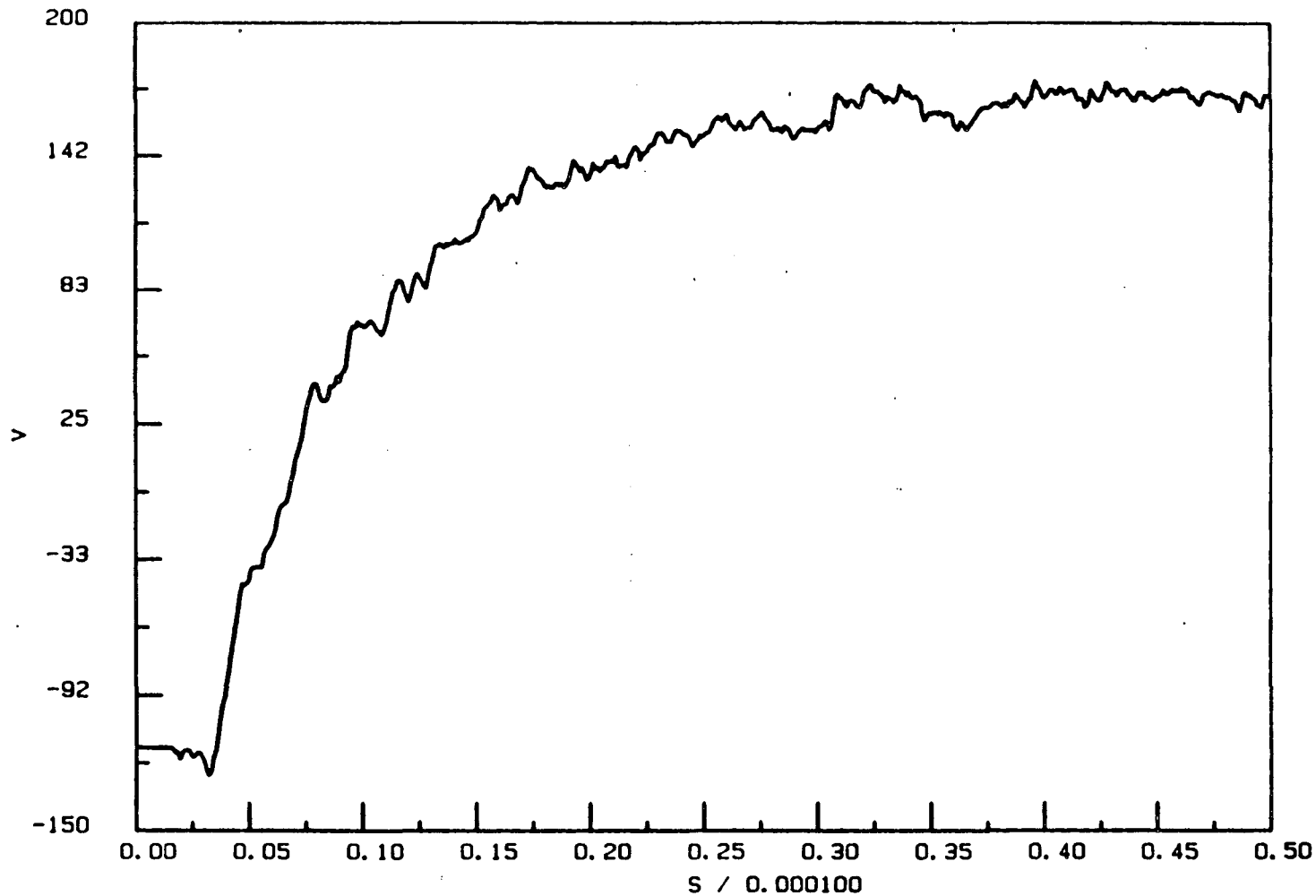

Figure 4.9. A kinetic trace taken at 1921 cm^{-1} showing the appearance of a new band over 50 μs in the flash photolysis of $W(CO)_6$ in the presence of 0.005 M P-*n*Bu_3. The rate, as determined by an exponential fit to the trace, is $1.4 \times 10^5\ s^{-1}$.

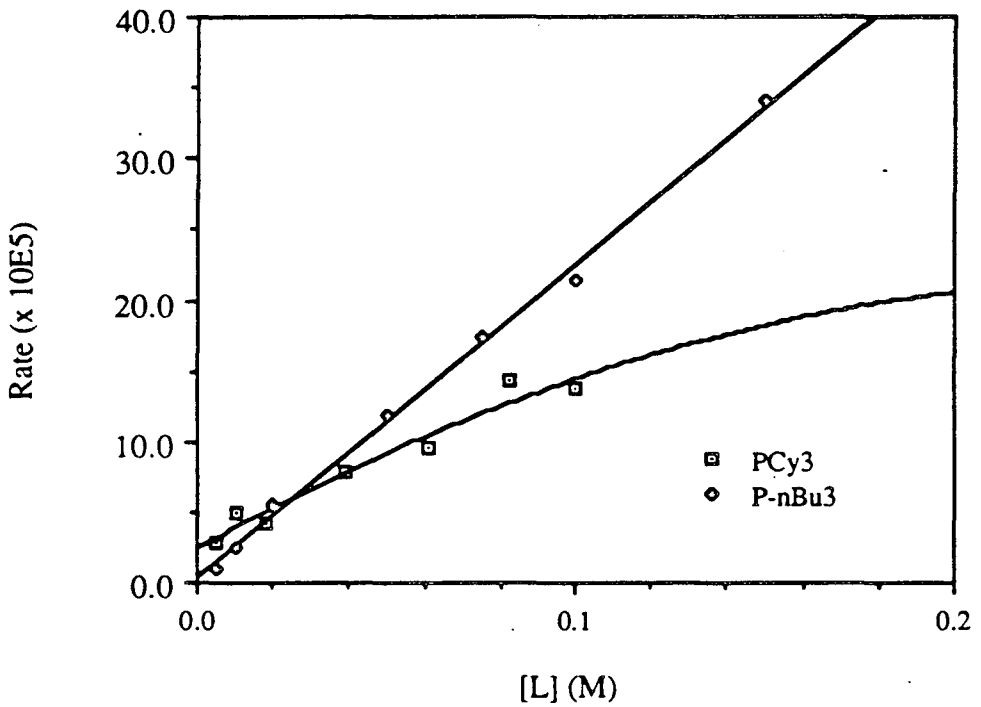

Figure 4.10. Comparison of the rates of reaction of $W(CO)_5(S)$ with P-*n*Bu_3 and with $P(C_6H_{11})_3$ in cyclohexane.

The reaction with P-*n*Bu_3 is clearly first order in phosphine even at 0.15 M phosphine as seen for the reaction with $CpMn(CO)_2(S)$. The data from reaction with $P(C_6H_{11})_3$ show more scatter, but it appears that there may be a slight curvature to a line drawn through the points. If so, this would be consistent with the reaction of $W(CO)_5(S)$ with 4-acetylpyridine, where a limiting rate constant of ca. $1.5 \times 10^6\ s^{-1}$ was reached at a ligand concentration of 0.1 M. In our experiments, with a $P(C_6H_{11})_3$ concentration of 0.10 M the transient was observed to decay with a rate of $1.37 \times 10^6\ s^{-1}$, suggesting that $P(C_6H_{11})_3$ and 4-acetylpyridine may be behaving similarly.

While these data are preliminary, they seem to indicate that in the case of P-*n*Bu_3, the ligand is not only acting as a trap for $W(CO)_5$, but is actually displacing the solvent

from $W(CO)_5(S)$ in a bimolecular reaction. If this is true, we will not observe saturation kinetics with P-*n*Bu_3, and if one hopes to study the dissociation of S from $(S)M(CO)_n$ one should be using $P(C_6H_{11})_3$ or other similar, less-nucleophilic ligands. This suggests that a investigation of the photochemistry of $CpMn(CO)_3$ using $P(C_6H_{11})_3$ as the ligand might be fruitful.

Study of $Cp(CO)_2Re(CH_3)_2$

Our investigation of the flash photolysis of $Cp(CO)_2Re(CH_3)_2$ was inspired by the recent work of Goldberg and Bergman.[42] While the main thrust of their study was studying the photochemistry of the acyl methyl complex, $Cp(CO)_2Re(CH_3)(COCH_3)$, they also examined the photochemistry of $Cp(CO)_2Re(CH_3)_2$. In both cases, competitive Re-CH_3 and Re-CO bond homolysis were observed, with Re-CH_3 bond homolysis being the favored pathway. In the presence of 20 atm of CO and $BrCCl_3$, $BrCH_3$, $Br(CO)CH_3$, $Cp(CO)_2Re(COCH_3)(CH_3)$, and $Cp(CO)_2Re(R)(Br)$ were formed (in the presence of ^{13}CO, labeled CO is exchanged into the starting material slowly due to the CO loss pathway). This is shown is Scheme 4.4.

We were particularly intrigued by these results as they presented an opportunity to study the substitution chemistry of a 17 electron radical **1** <u>and</u> the substitution chemistry of a 16 electron species **2** in the same system. It has long been thought that 17 electron species were particularly prone to substitution reactions, but there has been some controversy concerning whether these reactions proceed through 19 electron intermediates.[43] As we had earlier attributed the stability of other 16 electron fragments to an interaction with the solvent, it was also of interest to see if the 17 electron radical was particularly unstable, perhaps due to poorer stabilization by the solvent.

Upon flash photolysis of $Cp(CO)_2Re(CH_3)_2$ at 308 nm the disappearance of the starting material and the appearance of new products were observed. The signal was so weak, however, that no meaningful kinetic information could be gained. As

Scheme 4.4

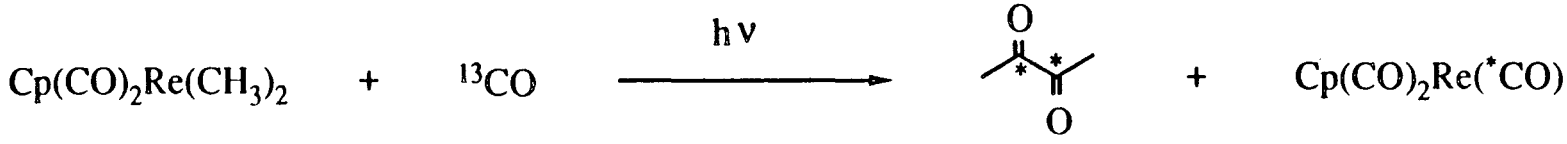
Cp(CO)2Re(CH3)2
+
13CO
hν
O
O
+
Cp(CO)2Re(*CO)

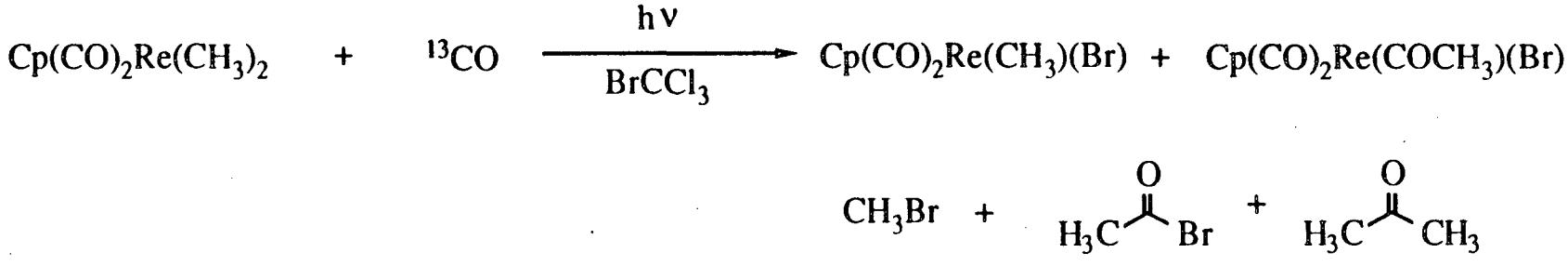
Cp(CO)2Re(CH3)2
+
13CO
hν
BrCCl3
Cp(CO)2Re(CH3)(Br)
+
Cp(CO)2Re(COCH3)(Br)
CH3Br
+
O
H3C
Br
+
O
H3C
CH3

$Cp(CO)_2Re(CH_3)_2$ has only a small UV absorbance at 308 nm, we elected to use KrF (248 nm) as the lasing medium. In this case, after averaging 8 - 64 laser shots a good kinetic trace could be obtained. Upon disappearance of the starting material, three new bands appear at 1888, 1903, and 1981 cm^{-1}. In the absence of any added ligand the bands at 1888 and 1981 cm^{-1} decrease in intensity quickly (rate = 9.4×10^4 and 6.9×10^4 s^{-1}, respectively). These are shown in Figures 4.11 and 4.12, respectively. With about the same rate, a broad new band centered at 1866 cm^{-1} grows in. In contrast, the band at 1903 cm^{-1} disappears slowly with a rate constant of 9.6×10^3 s^{-1} (Figure 4.13). From our earlier work (vide supra) with $CpRe(CO)_3$, it is clear that no $CpRe(CO)_2(S)$ is being produced. In Figure 4.14 spectra at 4, 12, and 36 μs after the laser pulse are shown. Based on the observation that two bands disappear quickly and the third relatively slowly, we are tentatively assigning the quickly disappearing bands to a short lived species with two CO ligands, and the third band to a complex with one CO ligand. In analogy to the preparative photochemistry, we are assigning the band at 1903 to $Cp(CO)Re(CH_3)_2$ and the bands at 1888 and 1981 cm^{-1} to $Cp(CO)_2Re(CH_3)$.

In order to verify these assignments we have attempted to trap the radical with CCl_4 and $BrCCl_3$. Unfortunately, both of these compounds (and many other radical traps) absorb strongly in the UV. This not only lessens the amount of unsaturated rhenium products produced, but causes strong shock waves in the solution which make it impossible to interpret the kinetic traces.

We next irradiated $Cp(CO)_2Re(CH_3)_2$ in the presence of 9.3×10^{-3} M $P(C_6H_{11})_3$. Upon flash photolysis, the same bands as previously observed were seen. In this case, however, a very rapid appearance (in less than 10 μs) of new bands was seen at 1999 , 1920, and 1892 cm^{-1}. None of these new bands was seen in the photolysis of $CpRe(CO)_3$ in the presence of $P(C_6H_{11})_3$. Due to overlapping peaks, it is difficult to measure rates accurately, but the band at 1903 cm^{-1} does not seem to decay much faster than in the absence of phosphine. The band at 1981, on the other hand, decayed much more quickly

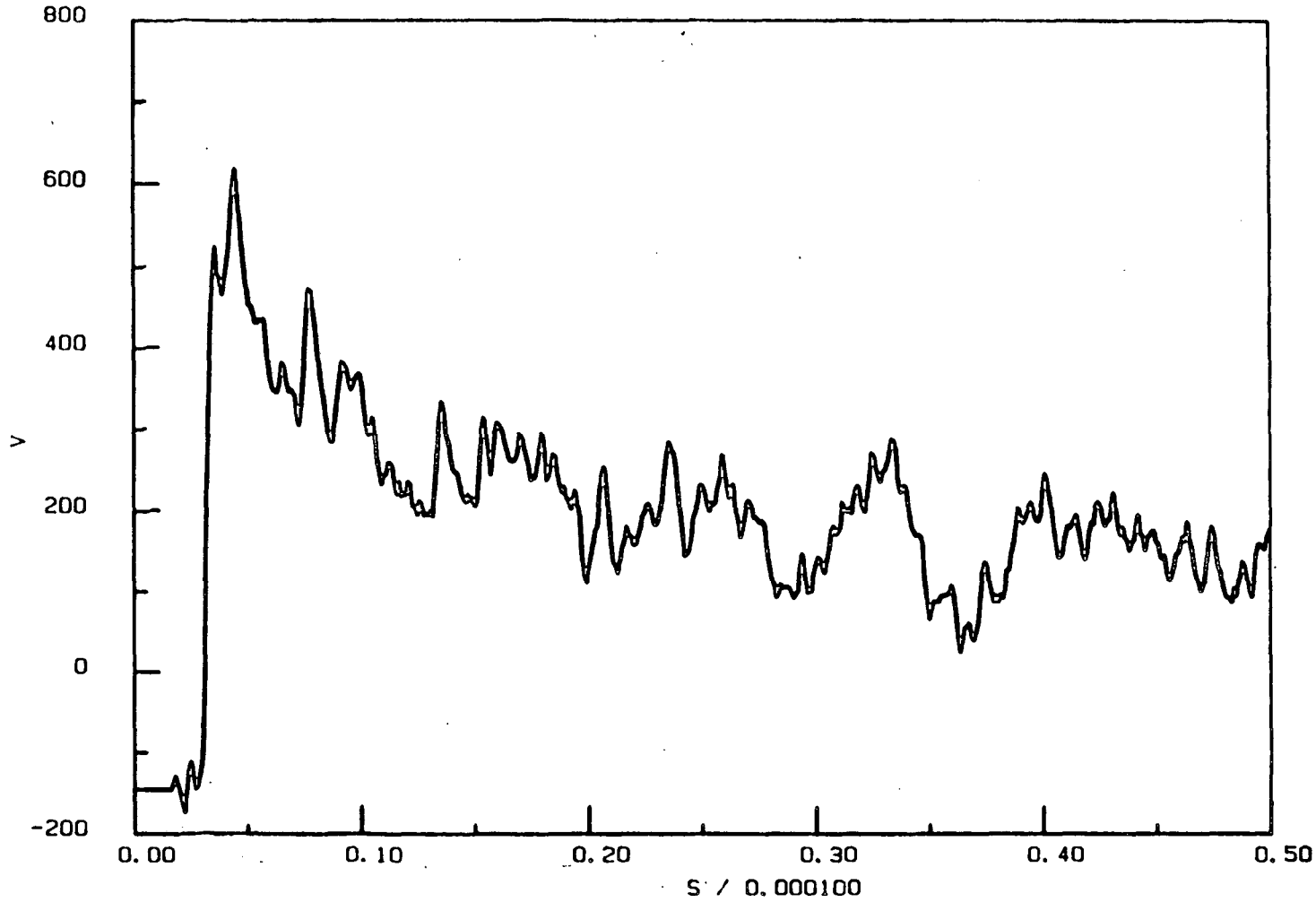

Figure 4.11. A kinetic trace taken at 1888 cm^{-1} showing the temporal behavior to 50 μs after the photolysis of $CpRe(CO)_2(CH_3)_2$ in cyclohexane. This signal disappears with a rate of $9.4 \times 10^4\ s^{-1}$.

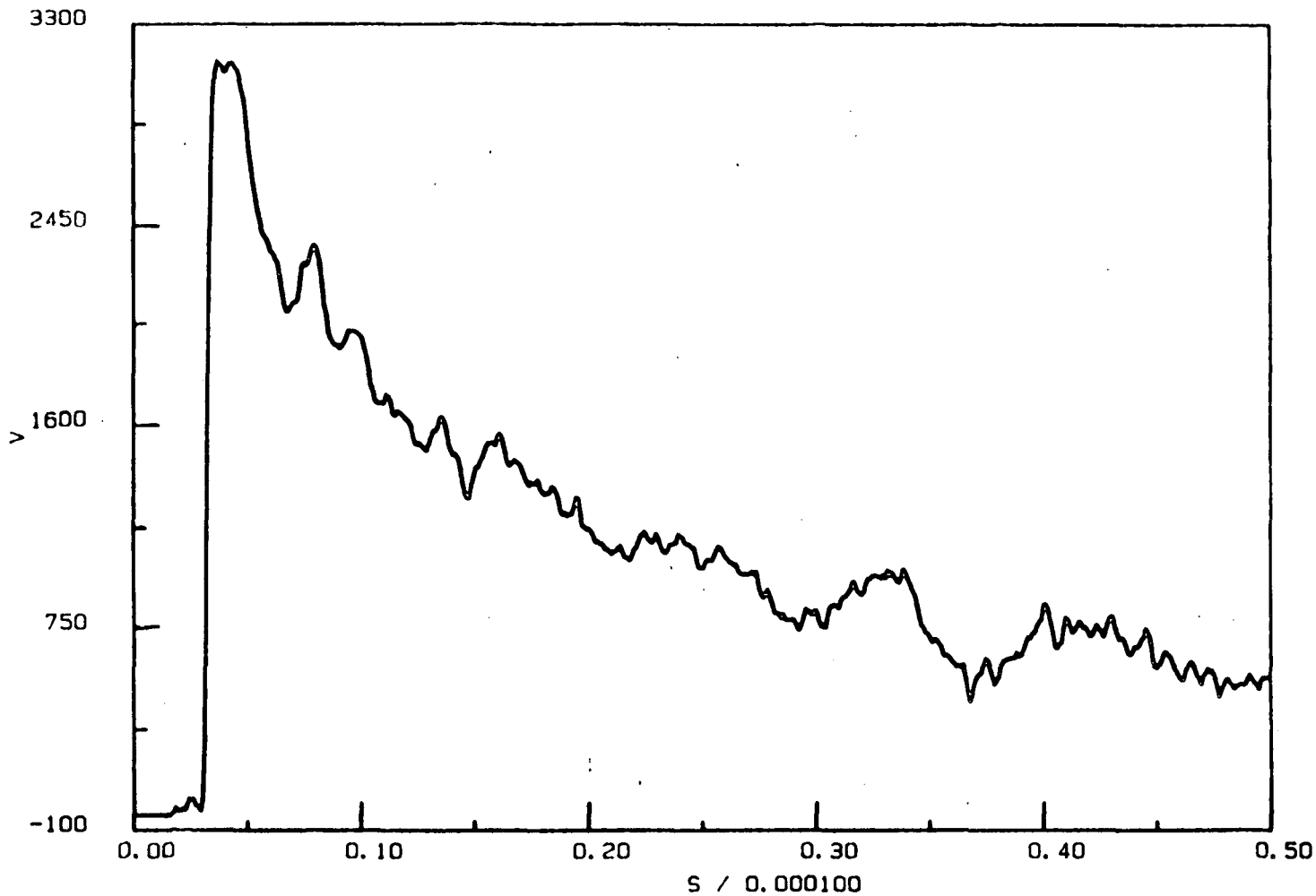

Figure 4.12. A kinetic trace taken at 1981 cm^{-1} showing the temporal behavior to 50 μs after the photolysis of $CpRe(CO)_2(CH_3)_2$ in cyclohexane. This signal disappears with a rate of $6.9 \times 10^4\ s^{-1}$.

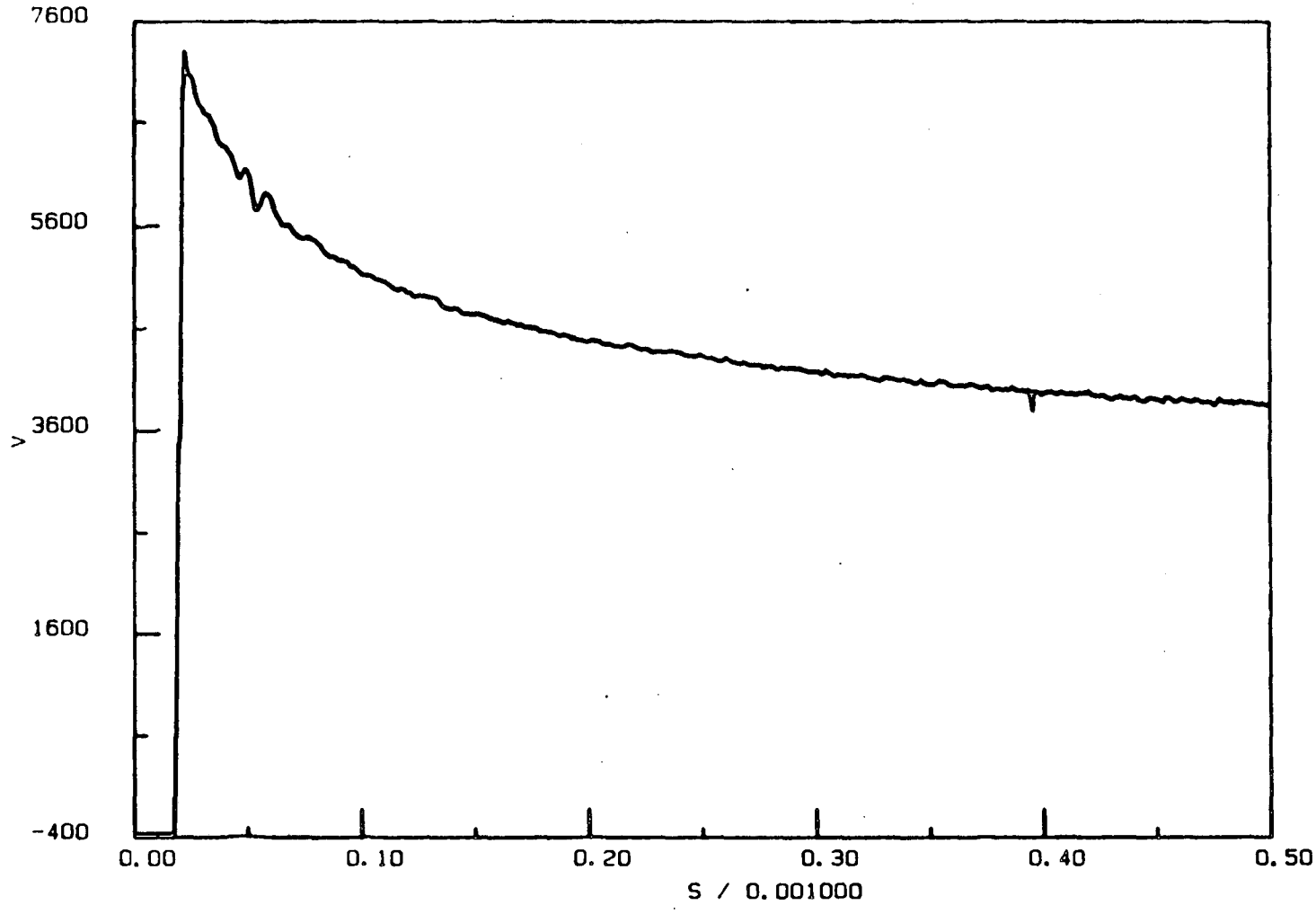

Figure 4.13. A kinetic trace taken at 1903 cm^{-1} showing the temporal behavior to 50 μs after the photolysis of $CpRe(CO)_2(CH_3)_2$ in cyclohexane. This signal disappears with a rate of $9.6 \times 10^3\ s^{-1}$, but does not appear to be a simple exponential decay.

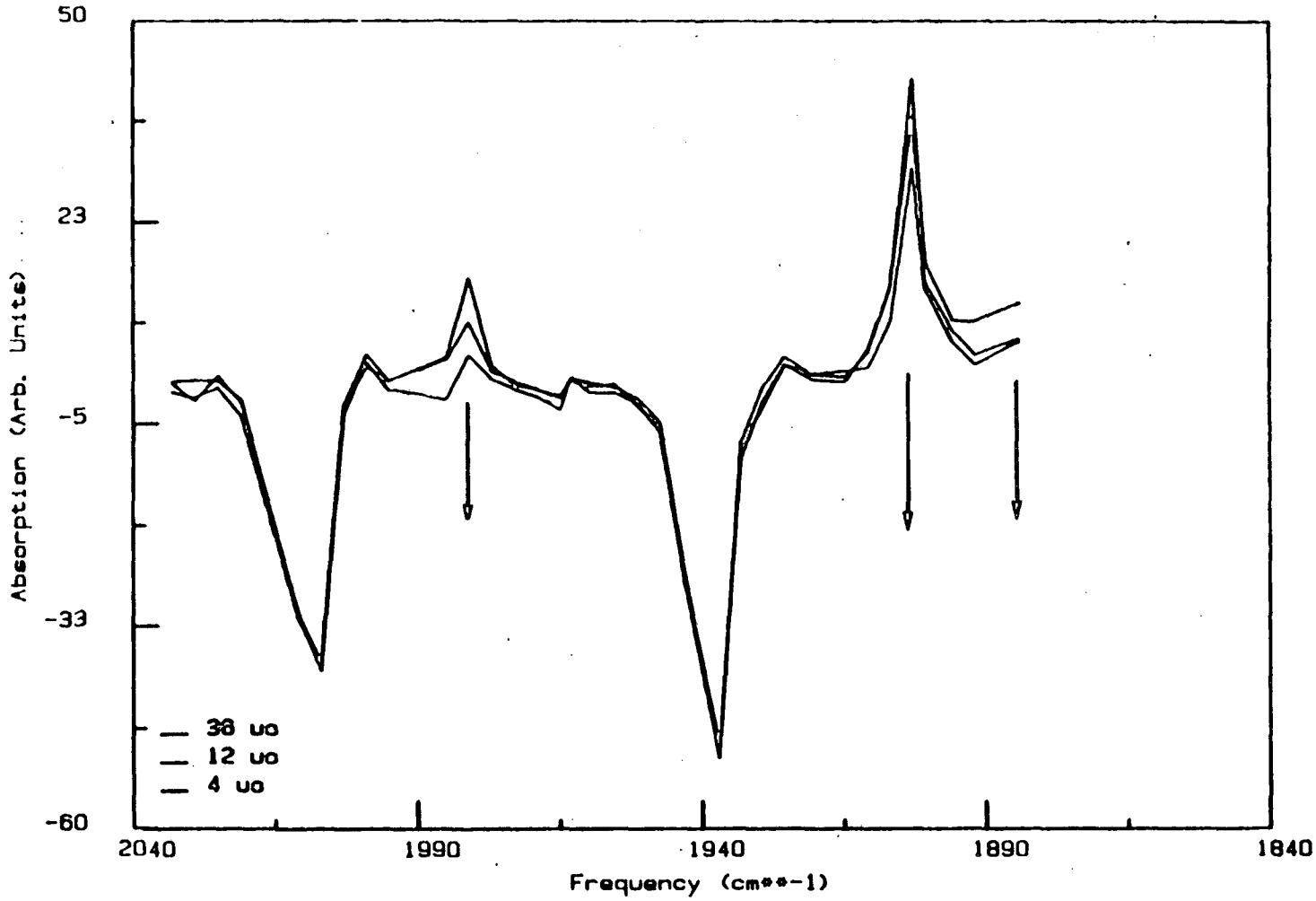

Figure 4.14. Spectra assembled at 4, 12, and 36 μs after the laser pulse of $CpRe(CO)_2(CH_3)_2$ in cyclohexane. Arrows indicate bands increasing and decreasing in intensity. Spectra have not been smoothed.

(within 10 μs). In Figure 4.15 are shown spectra taken at 5, 10, and 20 μs after the laser pulse.

We also investigated the flash photolysis in the presence of P-*n*Bu$_3$. While the reaction is qualitatively similar to the reaction with $P(C_6H_{11})_3$, in this case we observed a strong positive transient centered at 1865 cm^{-1} along with the band at 1904 cm^{-1}. The band at 1981 cm^{-1} observed initially upon photolysis, decayed within 5 μs. Spectra taken at 1 and 2 μs are shown in Figure 4.16. While it is difficult, due to overlapping peaks in the region 1915 - 1890 cm^{-1}, to draw conclusions from these few experiments, it seems that the transient which we have assigned to the radical, $Cp(CO)_2Re(CH_3)$ (1981 and 1888 cm^{-1}), is considerably more reactive towards phosphine than is the transient believed to be $Cp(CO)Re(CH_3)_2$ (1903 cm^{-1}).

Study of $Mn(NO)(CO)_4$

We elected to study $Mn(NO)(CO)_4$ in order to test the potential of TRIR for observing compounds containing nitrosyl ligands, and because earlier work has suggested the presence of a photochemically induced change in the nitrosyl bonding mode from a 3 electron to a 1 electron donor. The photochemically induced substitution chemistry of $Mn(NO)(CO)_4$ has been postulated to proceed by two pathways (Scheme 4.5).[44] In the pathway labeled **A**, absorption of a photon by $Mn(NO)(CO)_4$ results in loss of CO leading to $Mn(NO)(CO)_3(S)$. In the presence of added ligand, this is trapped forming $Mn(\dot{N}O)(CO)_3(L)$. A second pathway **B** was shown to be important for nucleophilic ligands. In this case, absorption of a photon leads to another intermediate, which hasn't lost a CO ligand. This coordinatively unsaturated species can then be attacked by added ligand, which upon loss of CO leads to $Mn(NO)(CO)_3(L)$. It was proposed that this intermediate was one in which electron transfer had taken place from the metal to the NO ligand, resulting in a bending of the M-NO linkage. The photochemistry of this system has also been studied in a matrix, and is consistent with this mechanism.[45] Unfortunately, the

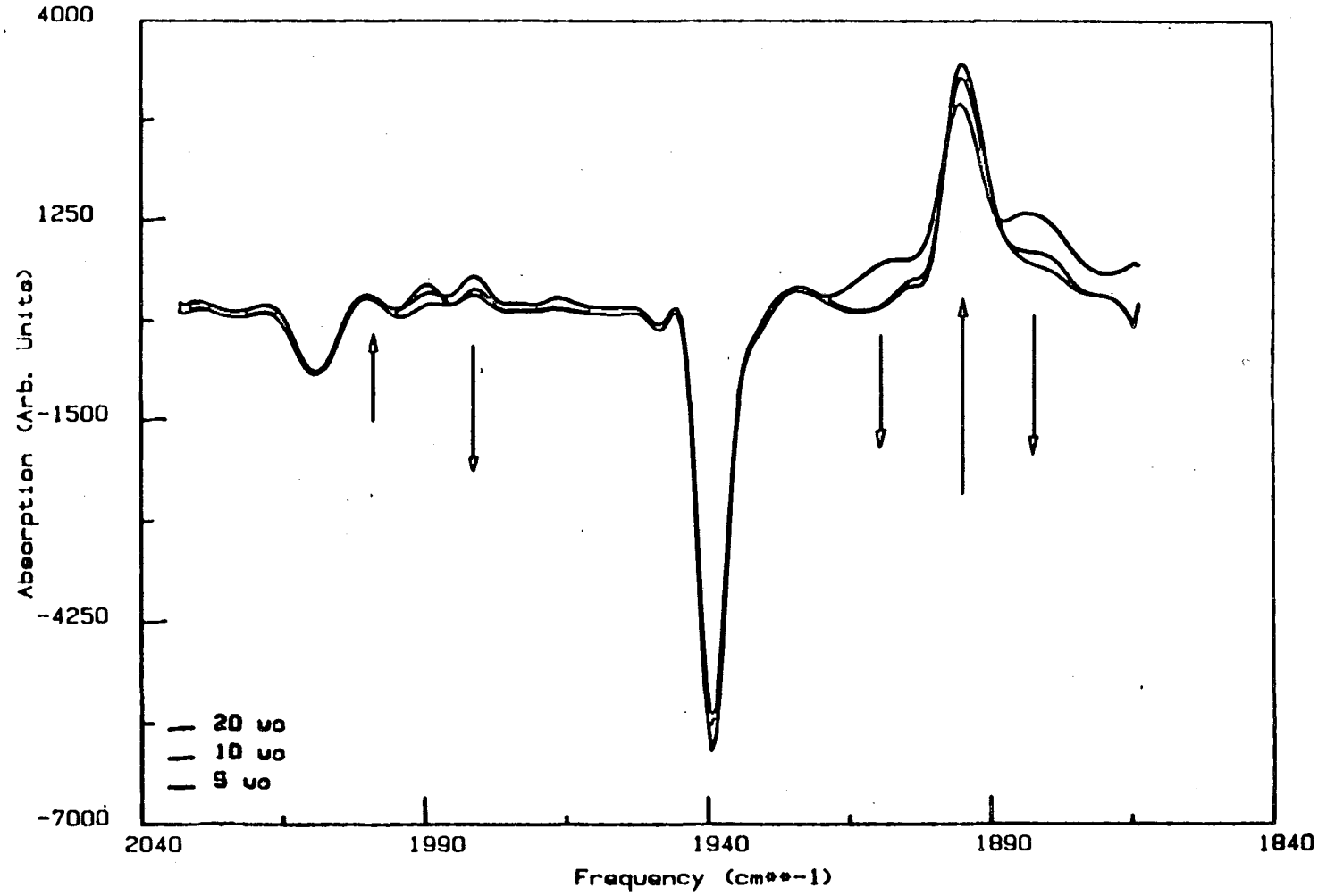

Figure 4.15. Spectra assembled at 5, 10, and 20 μs after the laser pulse of $CpRe(CO)_2(CH_3)_2$ in a cyclohexane solution 9.3 x 10^{-3} M in $P(C_6H_{11})_3$. Arrows indicate bands increasing and decreasing in intensity. Spectra have been smoothed.

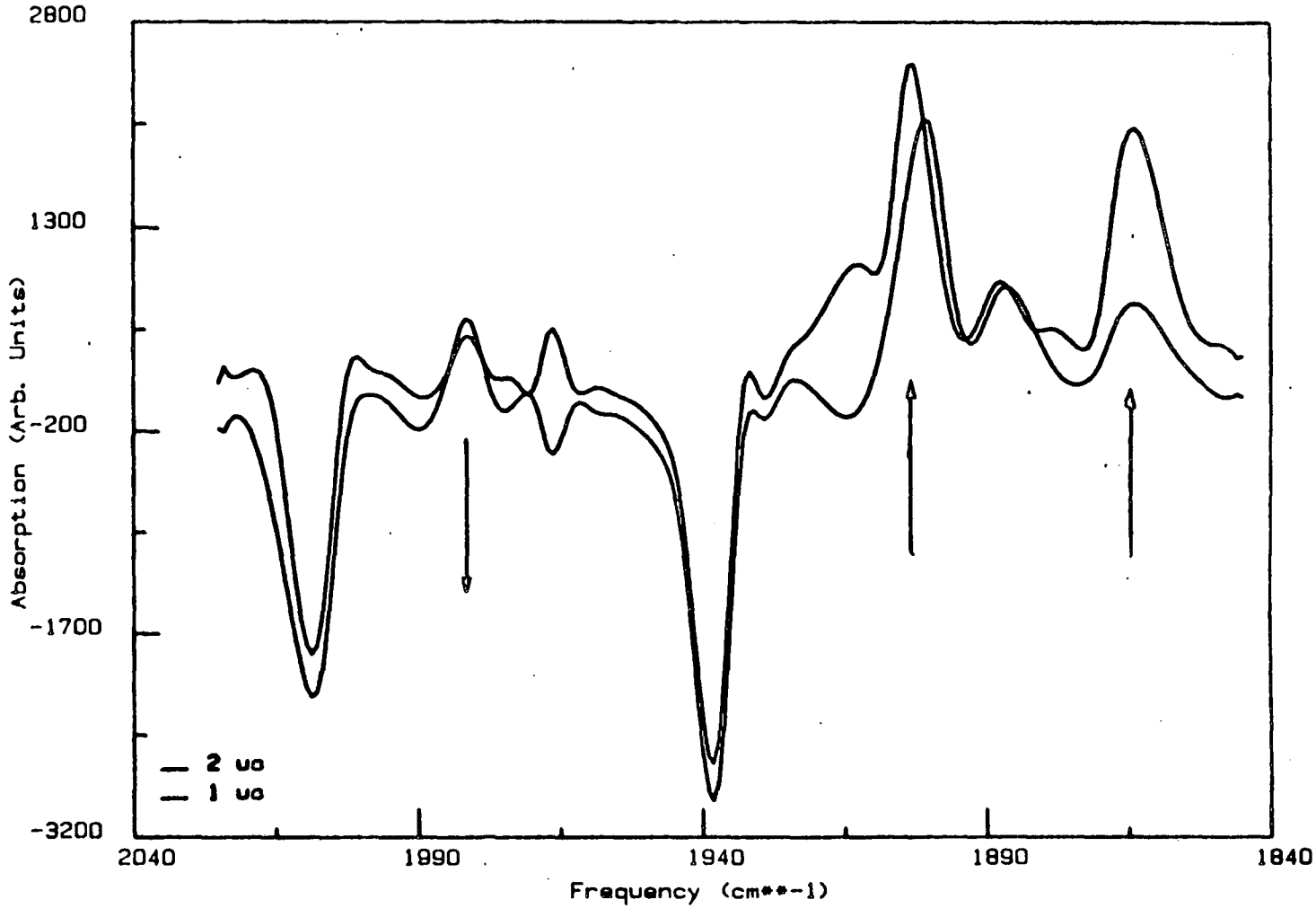

Figure 4.16. Spectra assembled at 1 and 2 μs after the laser pulse of $CpRe(CO)_2(CH_3)_2$ in a cyclohexane solution 8.0 x 10^{-3} M in P-*n*Bu_3. Arrows indicate bands increasing and decreasing in intensity. Spectra have been smoothed.

Scheme 4.5

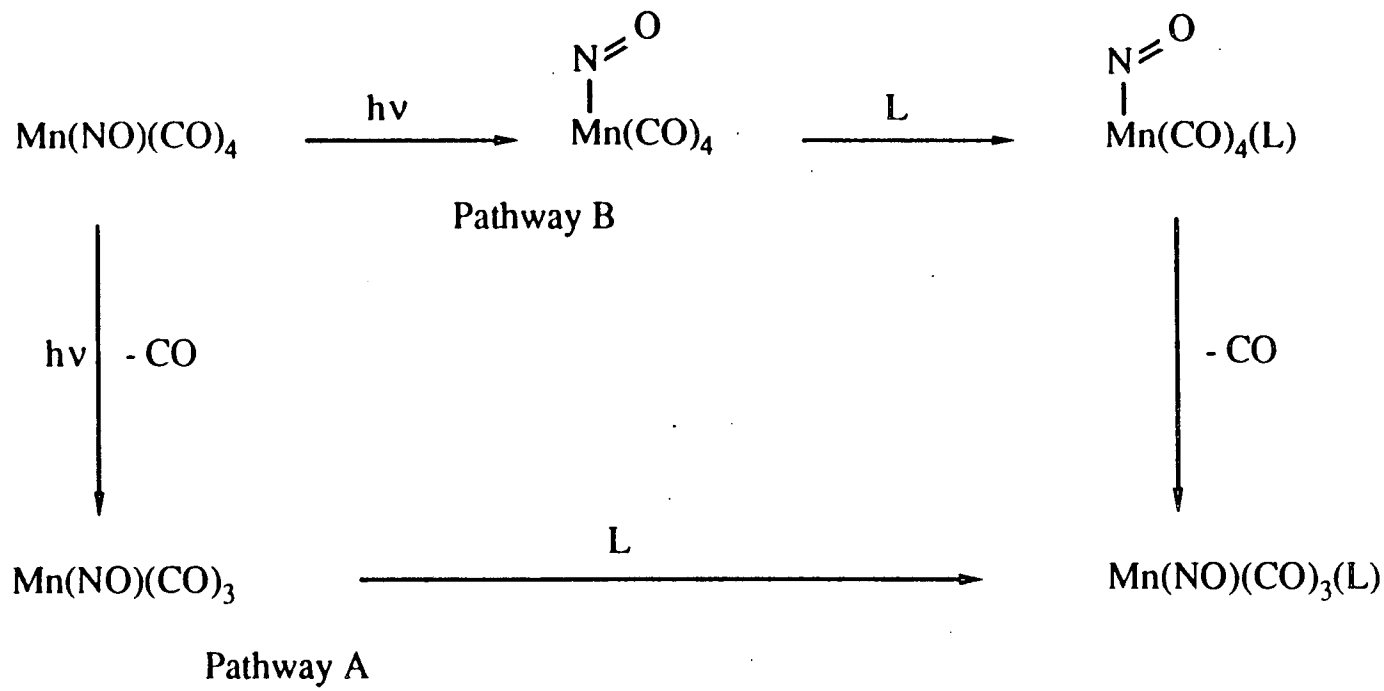
Mn(NO)(CO)4
hν
N=O
Mn(CO)4
L
N=O
Mn(CO)4(L)
Pathway B
hν
- CO
- CO
Mn(NO)(CO)3
L
Mn(NO)(CO)3(L)
Pathway A

primary photoproducts are not photostable, making their identification in a matrix more difficult.

This system thus seemed ideally suited for a TRIR study--the quantum yield of $Mn(NO)(CO)_4$ has been shown to be near 1, and all the CO bands and the NO band are within the range of the laser. In the exploratory studies described below we were not able to see all of the bands. The band at 2097 cm^{-1} is at the high frequency limit of a CO laser, and the NO band (1764 cm^{-1}), while well within the CO laser and detector limits, would have required a laser modification in order to be visible. For these preliminary studies we thus did not attempt to observe the NO bands, but rather tried to get a qualitative idea of the stability and geometry of the transients formed upon flash photolysis.

Upon flash photolysis of $Mn(NO)(CO)_4$ with 308 nm light, three positive transients immediately appear between 2033 and 1845 cm^{-1}. The band seen at 1925 cm^{-1} decayed within ca. 10 μs, while the band at 1947 - 1955 cm^{-1} decayed more slowly with a rate constant of 2.5×10^4 s^{-1} (Figure 4.17). It was difficult to measure the decay rate of the band at 1985 cm^{-1} due to overlapping bands. Upon disappearance of the initial transients, two new bands were observed. One at 2011 to 2021 cm^{-1} (rate = 2×10^4 s^{-1}) was partially obscured by the negative peak resulting from disappearance of starting material. The other band, centered at 1939 cm^{-1}, grew in much more rapidly (rate = 1.2×10^5 s^{-1}). Spectra taken at 5, 20, and 45 μs after the laser pulse are shown in Figure 4.18.

From matrix studies it was proposed that bands seen at 2072, 1994, 1932, and 1733 cm^{-1} (NO stretch) were due to $Mn(NO)(CO)_3$. If these assignments are correct and the proposed mechanism is correct, our bands seem to be shifted to lower frequency by approximately 5 - 10 cm^{-1}. Although the assignment was somewhat more tenuous, bands were seen in a CH_4 matrix at 2010, 1966, and 1460 cm^{-1} (NO stretch) which were assigned to $Mn(NO^*)(CO)_4$. The band seen in our experiments at 1947 - 1955 cm^{-1} is again approximately 10 cm^{-1} lower than that expected from the matrix work.

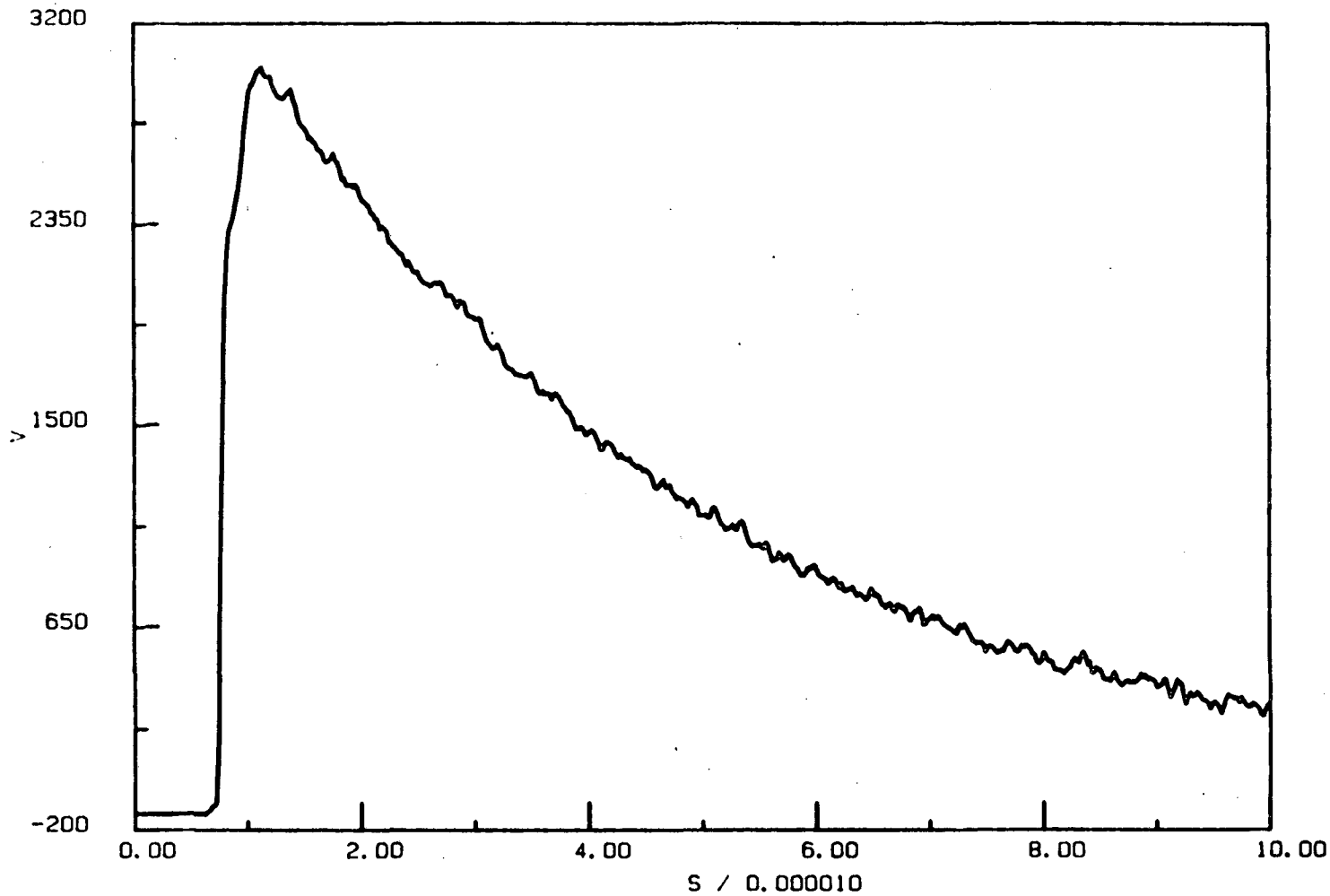

Figure 4.17. Kinetic trace at 1951 cm^{-1} over 100 μs of a transient resulting from flash photolysis of $Mn(NO)(CO)_4$. The observed rate of decay is $2.5 \times 10^4\ s^{-1}$.

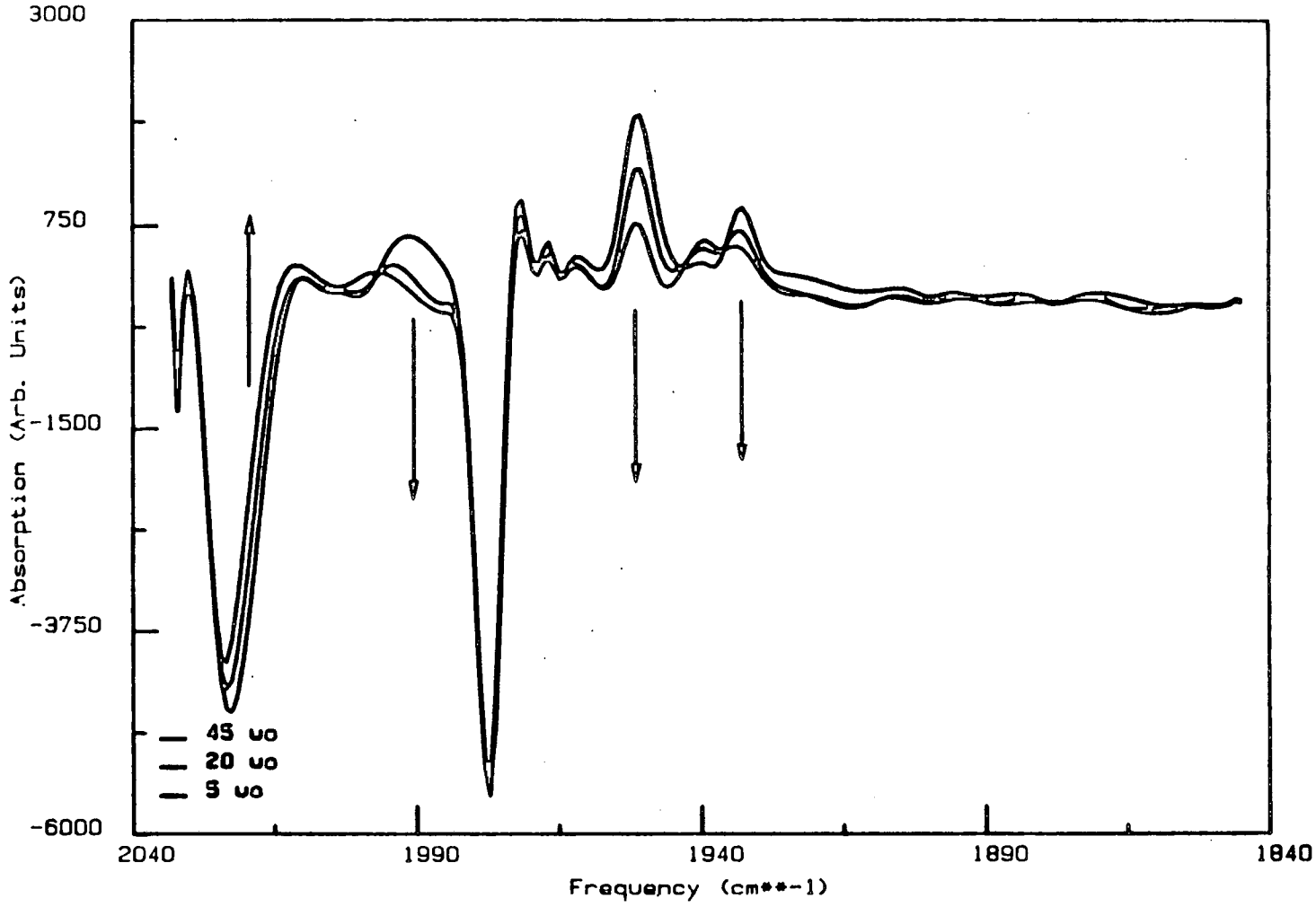

Figure 4.18. Spectra assembled at 5, 20, and 45 μs after the laser pulse of $Mn(NO)(CO)_4$ in cyclohexane. Arrows indicate bands increasing and decreasing in intensity. Spectra have been smoothed.

Flash photolysis of $Mn(NO)(CO)_4$ in the presence of 3×10^{-3} M $P(C_6H_{11})_3$ results in appearance of new transients which are visible essentially immediately and do not decay over 100 μs. A strong band is seen at 1903 - 1920 cm^{-1}, as well as a very broad band from 1960 to 1920 cm^{-1} and a narrow band at 2029 - 2033 cm^{-1} (Figure 4.19). Irradiating in the presence of less phosphine (1.4×10^{-3} M), and observing over a shorter timescale allowed us to see the bands of phosphine substitution products grow in as those seen in the photolysis without phosphine disappeared. In Table 4.2 are shown the rate constants for the disappearance of the the initially formed transient bands and the appearance of a phosphine substitution band. In the presence of phosphine, the band at 1925 cm^{-1} is not seen.

Table 4.2. Selected rate constants for the flash photolysis of $Mn(NO)(CO)_4$ with $P(C_6H_{11})_3$.

ν (cm^{-1})	1.4×10^{-3} M PR_3	3.2×10^{-3} M PR_3	no PR_3
1951	4.2×10^5 s^{-1}	8.4×10^5 s^{-1}	2.5×10^4 s^{-1}
1907	5.4×10^5 s^{-1}	9.6×10^5 s^{-1}	-------
1995	2.8×10^5 s^{-1}	(poor S/N)	4.6×10^4 s^{-1}

Poor S/N precluded the determination of accurate rate constants for other bands. Upon decay of the bands visible immediately upon photolysis, bands weaker than those listed in Table 4.2 were observed to grow in at 2029, 1959, 1939, and 1921 - 1929 cm^{-1}. In Figures 4.20 and 4.21 are shown kinetic traces at 1951 and 1907 cm^{-1} in the presence of 1.4×10^{-3} M $P(C_6H_{11})_3$. In Figure 4.22 spectra of the flash photolysis of $Mn(NO)(CO)_4$ in the presence of 1.4×10^{-3} M $P(C_6H_{11})_3$ are shown at 0.4, 2.8, and 7.6 μs after the laser pulse.

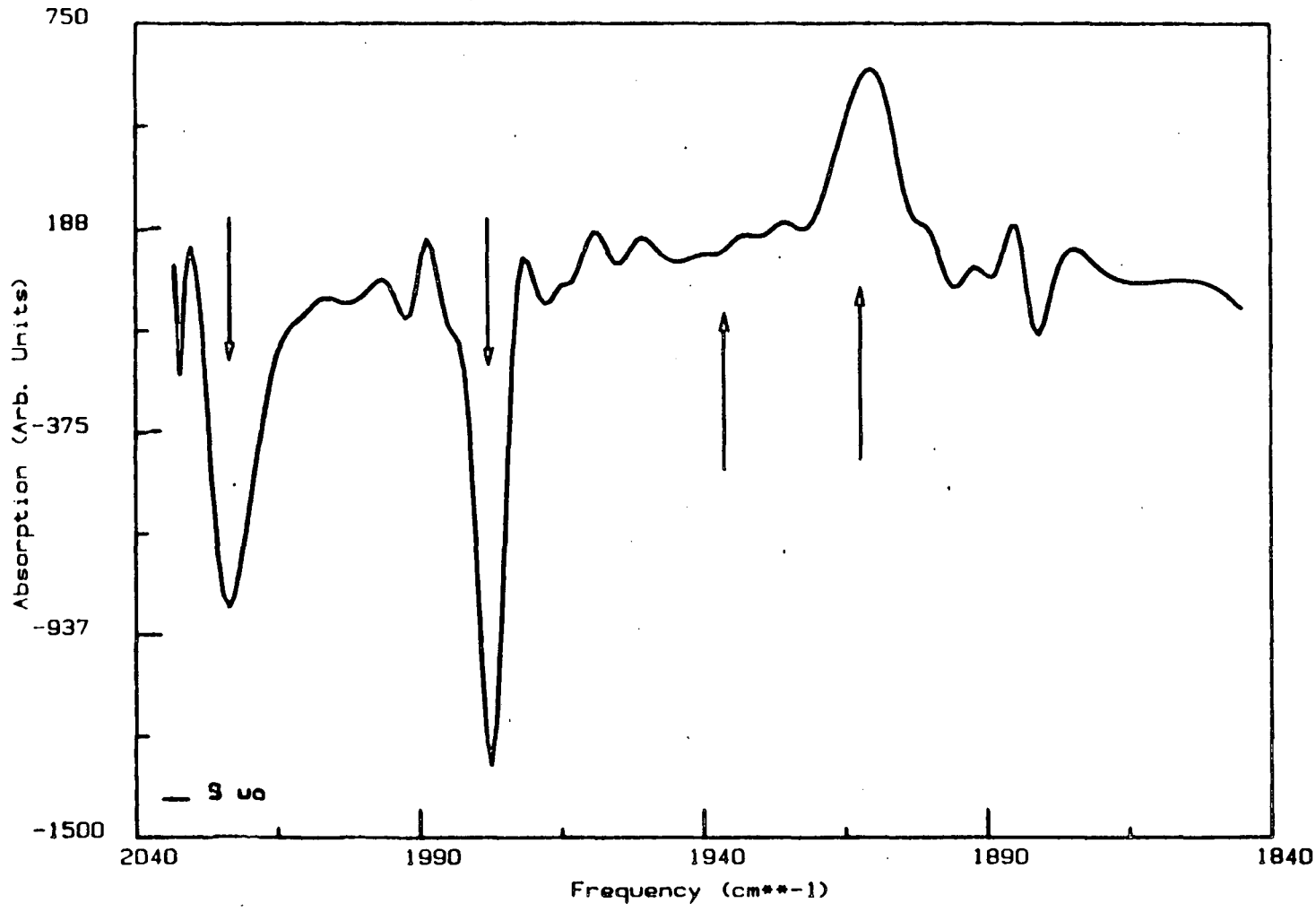

Figure 4.19. A spectrum assembled at 5 μs after the laser pulse of $Mn(NO)(CO)_4$ in a 3 x 10^{-3} M solution of $P(C_6H_{11})_3$ in cyclohexane. Arrows indicate positive and negative bands. The spectrum has been smoothed.

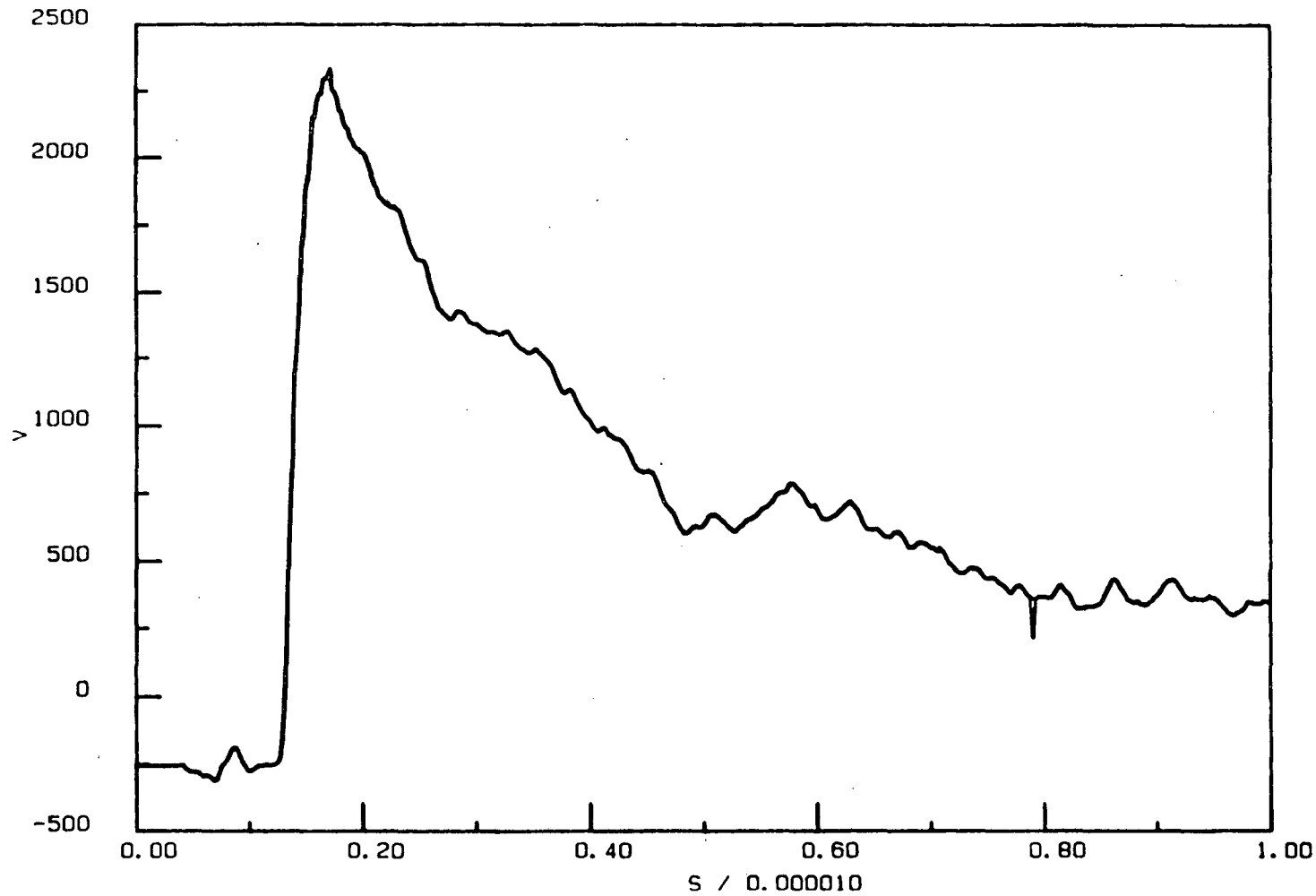

Figure 4.20. A kinetic trace taken at 1951 cm^{-1} showing the temporal behavior of a transient produced upon flash photolysis of $Mn(NO)(CO)_4$ in the presence of 1.4×10^{-3} M $P(C_6H_{11})_3$. The rate, as determined by an exponential fit to the trace, is 4.2×10^5 s^{-1}.

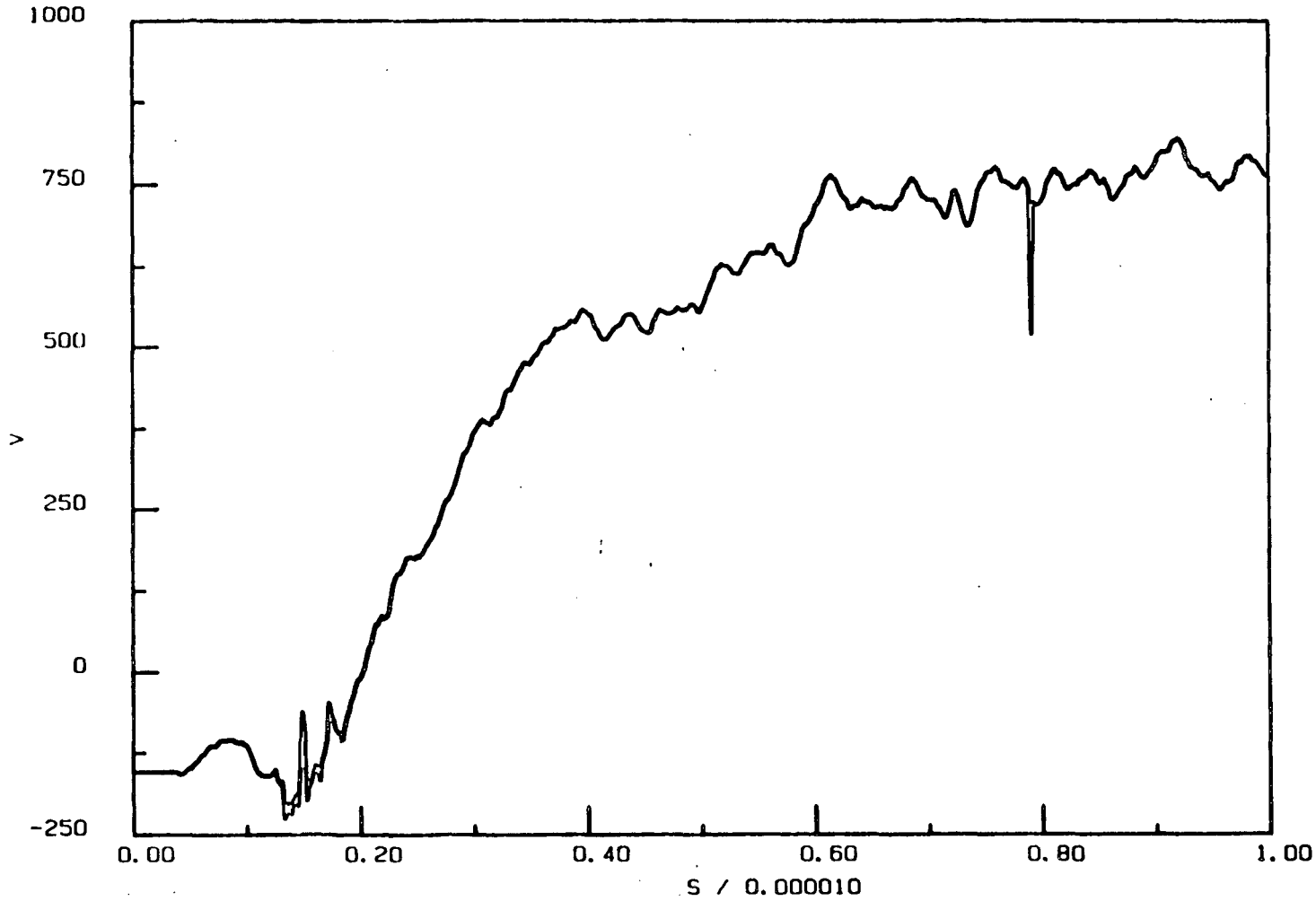

Figure 4.21. A kinetic trace taken at 1907 cm^{-1} showing the appearance of a new band over 10 μs in the flash photolysis of $Mn(NO)(CO)_4$ in the presence of 1.4×10^{-3} M $P(C_6H_{11})_3$. The rate, as determined by an exponential fit to the trace, is 5.4×10^5 s^{-1}.

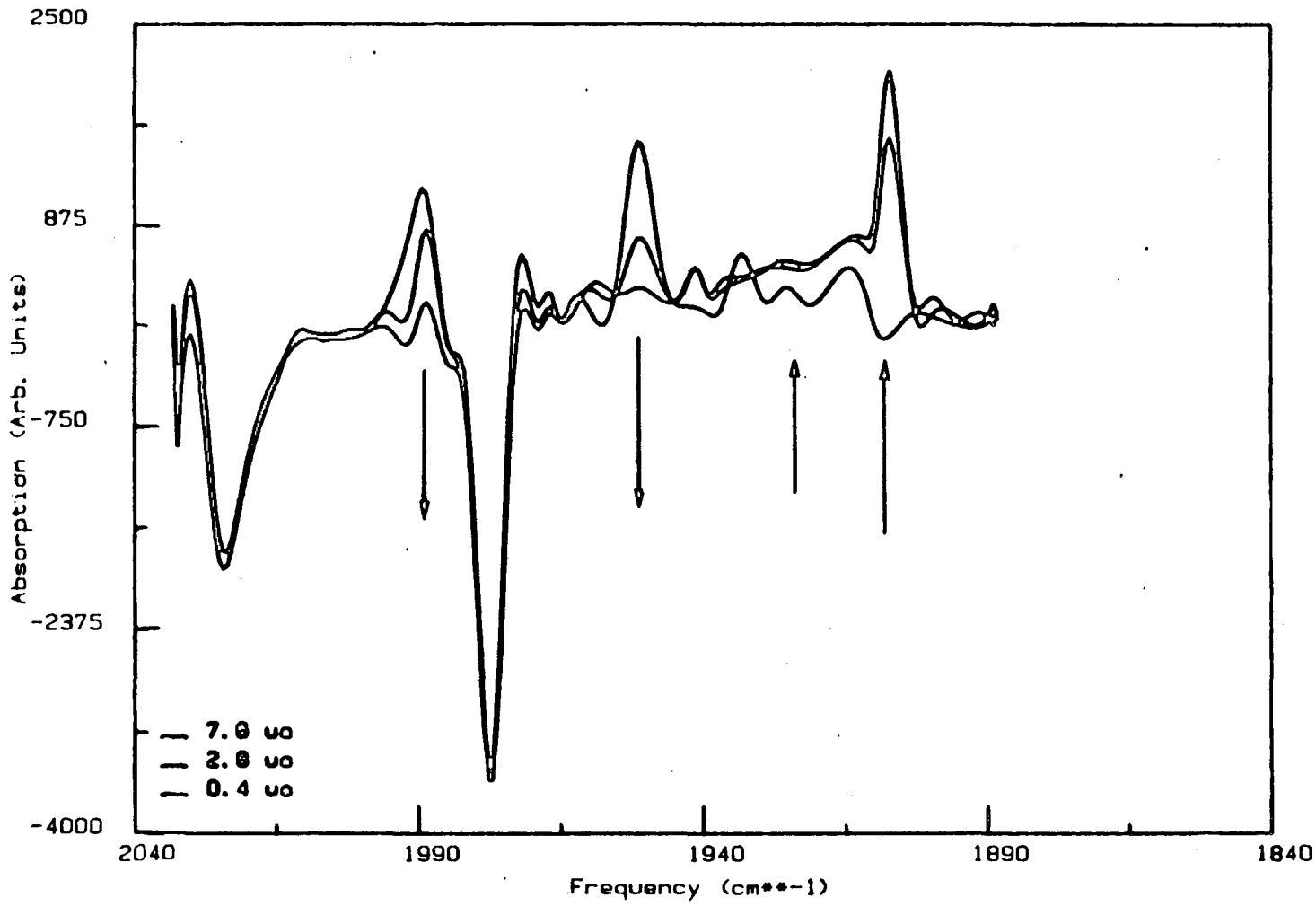

Figure 4.22. Spectra assembled at 0.4, 2.8, and 7.6 μs after the laser pulse of $Mn(NO)(CO)_4$ in a 1.4 x 10^{-3} M solution of $P(C_6H_{11})_3$ in cyclohexane. Arrows indicate bands increasing and decreasing in intensity. Spectra have been smoothed.

Although the assignment of the bands seen in the presence of phosphine will require further experimentation, we can speculate about what we might expect to see. In Basolo's study of the substitution mechanism, an intermediate with a lifetime on the order of minutes was observed (by UV-VIS spectroscopy) which eventually went on to form the final product $Mn(NO)(CO)_3(PR_3)$. It is reasonable to speculate that this intermediate was $Mn(CO)_4(^*NO)(PR_3)$ formed by ligand attack on $Mn(^*NO)(CO)_4$. This species should be infinitely stable on our timescale. This compound should have the same number of CO absorbances as $Mn(CO)_4(^*NO)$, but they should be shifted slightly to lower frequency. The other product, of course, should be the phosphine substitution product formed via pathway **A** which should have IR absorbances at lower frequency than $Mn(CO)_3(NO)$. Unfortunately the broadness of the bands seen in the presence of phosphine presently make assignments difficult. We will need to prepare $Mn(CO)_3(NO)(PR_3)$ to assign its IR bands. It does appear, however, that $Mn(NO)(CO)_4$ has a rich photochemistry which will be considerably easier to understand after we modify our apparatus to allow the observation of M-NO stretching bands.

Conclusion

While much remains to be done to complete the studies described above, we have now demonstrated the potential of time-resolved infrared spectroscopy in solution. The study of bimolecular reactions appears to be particularly amenable to the use of this technique, as the concentrations may be varied so that the reaction occurs within our observable time frame. The systems we can study are limited. First, compounds with low quantum yields of less than ca. 0.5 have proven difficult to study. In theory, one could simply use a more powerful laser, but we have observed that strong focusing of the UV laser beam frequently results in the production of shock waves which obscure the results. Second, many potential ligands and radical traps cannot be used as they absorb strongly in the UV, again creating shock waves. Organometallic compounds which can be irradiated

in the visible region will thus be easier to study, as longer wavelength lasers producing light not absorbed by ligands, radical traps, and common solvents can be used. Finally we have not yet begun to tackle the difficult problem of the identification of compounds with several bands in the IR spectrum. This may require matrix isolation work to supplement our flash kinetic experiments.

Experimental

General manipulations of air-sensitive compounds was carried out as described in Chapter 2 of this Thesis. The flash kinetic experimental setup is described in detail in the text.

Cyclohexane and hexane were spectroscopic grade and were distilled from $LiAlH_4$. $P(C_6H_{11})_3$ and P-*n*Bu_3 were purchased from Aldrich Chemical Co., and were used as received. $W(CO)_6$ and $CpMn(CO)_3$ were purchased from Strem Chemical Co. and was used as received. $Cp(CO)_2Re(CH_3)_2$[46] and $Mn(NO)(CO)_4$[47] were prepared by published procedures.

References

[1] Collman, J.P.; Hegedus, L.S.; Norton, J.R.; Finke, R.G. *Principles and Applications of Organotransition Metal Chemistry*; University Science Books: Mill Valley, CA, 1987.

[2] Langford, C.H.; Gray, H.B. *Ligand Substitution Processes*, W.A. Benjamin, Inc.: Reading, Mass., 1974.

[3] (a) Parshall, G.W. *Homogeneous Catalysis*, Wiley: New York, 1980. (b) reference 1.

[4] For recent reviews, see: (a) Burdett, J.K. *Coord. Chem. Rev.* **1978**, *27*, 1. (b) Hitam, R.B.; Mahmoud, K.A.; Rest, A.J. *Coord. Chem. Rev.* **1984**, *55*, 1. (c) Perutz, R.N. *Annu. Rep. Prog. Chem., Sect. C* **1985**, *82*, 157.

[5] (a) Hepp, A.F.; Wrighton, M.S. *J. Am. Chem. Soc.* **1983**, *105*, 6249. (b) Hepp, A.F.; Blaha, J.P.; Lewis, C.; Wrighton, M.S. *Organometallics* **1984**, *3*, 174. (c) Hooker, R.H.; Mahmoud, K.A.; Rest, A.J. *J. Chem. Soc., Chem. Comm.* **1983**, 1022.

[6] See for example: (a) Turner, J.J.; Simpson, M.B.; Poliakoff, M.; Waier, II., W.B. *J. Am. Chem. Soc.* **1983**, *105*, 3898. (b) Upmacis, R.K.; Gadd, G.E.; Poliakoff, M.; Simpson, M.B.; Turner, J.J.; Whyman, R.; Simpson, A.F. *J. Chem. Soc., Chem. Comm.* **1985**, 27.

[7] Poliakoff, M.; Weitz, E. *Adv. Organometallic Chem.* **1986**, *25*, 277 and references therein.

[8] (a) Simon, J.D.; Peters, K.S. *Chem. Phys. Lett.* **1983**, *98*, 53. (b) Simon, J.D.; Xie, X. *J. Phys. Chem.* **1986**, *90*, 6751. (c) Kelly, J.M.; Bent, D.V.; Hermann, H.; Schulte-Frohlinde, D.; Koerner von Gustorf, E. *J. Organomet. Chem.* **1974**, *69*, 259. (d) Hermann, H.; Grevels, F-W.; Henne, A.; Schaffner, K. *J. Phys. Chem.* **1982**, *86*, 5151.

[9] Kelly, J.M.; Long, C.; Bonneau, R. *J. Phys. Chem.* **1983**, *87*, 3344.

[10] Lees, A.J.; Adamson, A.W. *Inorg. Chem.* **1981**, *20*, 4381.

[11] See for example: *Time Resolved Vibrational Spectra*, Atkinson, G.H., Ed.; Academic: New York, 1983.

[12] For a recent review see: Poliakoff, M.; Weitz, E. *Adv. Organometallic Chem.* **1986**, *25*, 277.

[13] (a) Moore, B.D.; Simpson, M.B.; Poliakoff, M.; Turner, J.J. *J. Chem. Soc., Chem. Comm.* **1984**, 972. (b) Dixon, A.J.; Healy, M.A.; Poliakoff, M.; Turner, J.J. *J. Chem. Soc., Chem. Comm.* **1986**, 994.

[14] Dobson, G.R.; Hodges, P.M.; Healy, M.A.; Poliakoff, M.; Turner, J.J.; Firth, S.; Asali, K.J. *J. Am. Chem. Soc.* **1987**, *109*, 4218.

[15] For recent reviews of C-H bond activation, see: (a) Halpern, J. *Inorg. Chim. Acta.* **1985**, *100*, 41. (b) Aktogu, N.; Baudry, D.; Cox, D.; Ephritikhine, M.; Felkin, H.; Holmes-Smith, R.; Zakrzewski, J. *Bull. Soc. Chim. France* **1985**, 381. (c) Green,

M.L.H.; O'Hare, D. *Pure & Appl. Chem.* **1985**, *57*, 1897. (d) Crabtree, R.H. *Chem. Rev.* **1985**, *85*, 245.

[16] For general reviews of lasers aimed at the non-physical chemist, see: (a) Findsen, E.W.; Ondrias, M.R. *J. Chem. Ed.* **1986**, *63*, 479. (b) Moore, C.B.; Leone, S.R. in *Chemical and Biochemical Applications of Lasers* (C.B. Moore, Ed.) Publisher: New York, 1974, p. 1. For a more complete review, see: Demtroder, W. *Laser Spectroscopy*, Springer-Verlag: New York, 1982.

[17] Faster flash lamps have been developed, but these frequently have insufficent power, especially when a narrow frequency range is used.

[18] Use of solvents or ligands which absorb significant amounts of light not only lower the amount of transient produced, but generate shock waves which cause the IR beam to waver producing artifacts obscuring the signal due to the actual transients.

[19] Ouderkirk, A.J. Ph.D. Dissertation, Northwestern University, 1983.

[20] See, for example: (a) Patel, C.K.N. *Phys. Rev.* **1966**, *141*, 140. (b) Yardley, J.T. *J. Mol. Spect.* **1970**, *35*, 314. (c) Bhaumik, M.L. in *High Power Gas Lasers* (Pake, E.R., Ed.) Institute of Physics: London, 1976, p. 243.

[21] Gratings are reflective when the following condition is met: $2d(\sin \alpha) = m \lambda$, where d = separation of the groves on the grating, α = the angle of the incident light, and m = order of the grating (an integer). Gratings are thus scored for a specific frequency; deviating substantially from this substaintially will result in very small or very large angles α.

[22] Ho, Pauline Ph.D. Dissertation, University of California, Berkeley, 1981.

[23] For general reviews of infrared detectors, see: (a) *Optical and Infrared Detectors* Keyes, R.J., Ed., Springer-Verlag: New York, 1980.

[24] This effectively means that the detector cannot be used to measure reactions which occur in less than 200 ns or over more than 2 ms.

[25] Young, L. Ph.D. Dissertation, University of California, Berkeley, 1981.

[26] Immediately, as used here, means that the transient was produced in less than the response time of the detector (< 200 ns).

[27] Darensbourg, D.J.; Graves, A.H. *Inorg. Chem.* **1979**, *8*, 1257.

[28] (a) Kafafi, Z.H.; Hauge, R.H.; Margrave, J.L. *J. Am. Chem. Soc.* **1985**, *107*, 7550. (b) Stoutland, P.O.; Bergman, R.G. chapter 4 of this Thesis.

[29] (a) Cracknell, R.B.; Orpen, G.A.; Spencer, J.L. *J. Chem. Soc., Chem. Comm.* **1984**, 326. (b) Brookhart, M.; Green, M.L.H. *J. Organomet. Chem.* **1983**, *250*, 395. (c) Schmidt, G.F.; Brookhart, M. *J. Am. Chem. Soc.* **1985**, *107*, 1443 and references therein.

[30] Buchanan, J.M.; Stryker, J.M.; Bergman, R.G. *J. Am. Chem. Soc.* **1986**, *108*, 1537.

[31] For a general review of the substitution chemistry of $CpMn(CO)_3$ and $CpRe(CO)_3$ see: Caulton, K.G. *Coor. Chem. Rev.* **1981**, *38*, 1.

[32] (a) Wenzel, T.T.; Bergman, R.G. *J. Am. Chem. Soc.* **1986**, *108*, 4856. (b) Hoyano, J.K.; Graham, W.A.G. *J. Am. Chem. Soc.* **1982**, *104*, 3723. (c) Hoyano, J.K.; McMaster, A.D.; Graham, W.A.G. *J. Am. Chem. Soc.* **1983**, *105*, 7190.

[33] Giordano, P.J.; Wrighton, M.S. *Inorg. Chem.* **1977**, *16*, 160.

[34] Black, J.D.; Boylan, M.J.; Braterman, P.S. *J. Chem. Soc. Dalton Trans.* **1981**, 673.

[35] Anderson, W.P.; Brill, T.B.; Schoenberg, A.R.; Stanger, Jr., C.W. *J. Organomet. Chem.* **1972**, *44*, 161.

[36] At 0.4 M the phosphine is beginning to constitute a significant part of the solution (1:9 by volume); we did not wish to use higher concentrations as the properties of the solution would change (viscosity for example).

[37] Buchanan, J.M.; Stryker, J.M.; Bergman, R.G. *J. Am. Chem. Soc.* **1986**, *108*, 1537.

[38] Stephen, K.; Lucas, K. *Viscosity of Dense Fluids; Plenum*: New York, 1979.

[39] Chetwynd-Talbot, J.; Grebenik, P.; Perutz, R.N.; Powell, M.H.A. *Inorg. Chem.* **1983**, *22*, 1675.

[40] Literature values ν(CO) 2082, 1958, 1932 cm^{-1}. Reference 14.

[41] Woodward, S.S.; Angelici, R.J.; Dombek, B.D. *Inorg. Chem.* **1978**, *17*, 1634.

[42] Goldberg, K.I.; Bergman, R.G. *Organometallics* **1987**, *6*, 430.

[43] Stiegman, A.E.; Tyler, D.R. *Comments Inorg. Chem.* **1986**, *5*, 215 and reference therein.

[44] Keeton, D.P.; Basolo, F. *Inorg. Chim. Acta.* **1972**, *6*, 33.

[45] Crichton, O.; Rest, A.J. *J. Chem. Soc. Dalton Trans.* **1978**, 208.

[46] Hoyano, J.K.; Graham, W.A.G. *Organometallics* **1982**, *1*, 783.

[47] King, R.B. in*Organometallic Synthesis*, vol. 1 (J.J. Eisch and R.B. King, ed.), Academic Press: New York, 1965.

LAWRENCE BERKELEY LABORATORY
TECHNICAL INFORMATION DEPARTMENT
UNIVERSITY OF CALIFORNIA
BERKELEY, CALIFORNIA 94720